PROCEEDINGS OF THE 2021 ISGP MEETING

Texas A&M University, College Station, USA, 24 - 27 May 2021

frontiers Event Abstracts

PROCEEDINGS OF THE 2021 ISGP MEETING

ISBN: 978-2-88971-011-9
DOI: 10.3389/978-2-88971-011-9
Citation: Pooneh Bagher, Susan Bloomfield, Ana Diaz Artiles, Marc-Antoine Custaud. (2021). Proceedings of the 2021 ISGP Meeting.

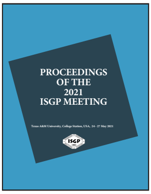

May 24-27, 2021, Texas A&M University, College Station, USA

Table of Contents

Welcome to the Proceedings of the 2021 ISGP Meeting

ISGP, the International Society of Gravitational Physiology holds his annual meeting that allows the presentation of original experimental research and reviews of current topics. The broad scientific spectrum of ISGP emphasizes gravity, life and physiology as its anchors. We were very happy to organize our 41st annual meeting in 2021, as a virtual meeting, with Texas A&M University, USA.

LIST OF ORGANIZERS

Pooneh Bagher
Susan Bloomfield
Ana Diaz Artiles
Marc-Antoine Custaud

ORGANIZING COMMITTEE

ISGP President
Pooneh Bagher

ISGP Council
Jeffrey Alberts
Alexander Choukér
Marc-Antoine Custaud
Michael Delp
Charles Fuller
Alan Hargens
Martina Heer
Richard Hughson
Dag Linnarsson
Alain Maillet
Tadaaki Mano
Peter Norsk
Yoshinobu Ohira
Elena Tomilovskaya
Olga Vinogradova

Local Organizers
Susan Bloomfield
Ana Diaz Artiles

Administrator
Tina Mendoza

Registration
Kathryn Giordano

Design
Ray Mitchell


ISGP
2021
Virtual Annual Meeting | 24 – 27 May 2021
International Society for Gravitational Physiology
INTERNATIONAL SOCIETY FOR GRAVITATIONAL PHYSIOLOGY
ISGP
1991

Sponsors

TEXAS A&M UNIVERSITY
College of Medicine

TEXAS A&M UNIVERSITY
Division of Research

TEXAS A&M UNIVERSITY
Engineering

TEXAS A&M UNIVERSITY
Education & Human Development

TEXAS A&M UNIVERSITY
Health & Kinesiology

TEXAS A&M UNIVERSITY
Medical Physiology

FLORIDA STATE UNIVERSITY
College of Human Sciences

Dear Colleagues,

It has been a tremendous honor and privilege to be the president of the International Society for Gravitational Physiology (ISGP) and a real pleasure to organize the ISGP annual meeting (twice!).

I originally organized the ISGP 2020 to take place in-person in College Station, Texas, on the campus of Texas A&M University in May 2020. Texas A&M University is the only Texas university to be designated a land-grant, sea-grant, and space-grant institution, so it was the perfect location to bring together gravitational physiology researchers from around the world. Our designation as a space-grant university further highlights Texas A&M's strength in space research and dedication to the advancement of the exploration of space. The ISGP conference had the strong support from the local community and from colleges and departments across The Texas A&M University System.

As the COVID-19 pandemic affected the lives of us all, it also led the local organizers and the Board of Directors to make the difficult decision to postpone the ISGP conference. With the pandemic and the associated travel restrictions worldwide, it was decided that the safest way to move forward would be via a virtual conference to take place May 24–27, 2021.

Each day consisted of two plenary lectures, followed by a themed session organized from submitted abstracts. In lieu of a traditional poster session, mini-talks were recorded by presenting authors, and these mini-talks were made available to registrants for on-demand viewing. I am very pleased that despite the challenges, the ISGP 2021 meeting had many outstanding, internationally renowned speakers representing a multitude of space agencies, universities, and research institutions. Students and trainees were well represented in the themed sessions and in the on-demand mini-talks, and eight of these presenters were selected for young investigator awards.

I would like to thank the local organizers, the ISGP Board of Directors, and the Texas A&M community for the support of this event. Finally, I would like to thank Texas A&M University Division of Research, College of Medicine, College of Education & Human Development, College of Engineering, Department of Health & Kinesiology, and Department of Medical Physiology, as well Florida State University College of Human Sciences for their support. I wish you all health, happiness, and success in your research endeavors.

Best Wishes,

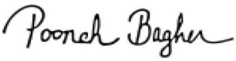

Pooneh Bagher, Ph.D.

Department of Medical Physiology

Texas A&M University College of Medicine

The Nello Pace Award 2021

Martina Heer

Martina Heer graduated with a PhD in Nutritional Sciences in 1996. She started her career at the Institute of Aerospace Medicine of the German Aerospace Center (DLR) of Cologne (Germany), in 1989 where she headed the Space Physiology Division from 2003 to 2009. From 2009 until 2014 she Director Nutritional Sciences at Profil, Neuss Germany and from 2014 until 2016 Senior Research Manager Nutritional Health at the Waltham Center for Pet Nutrition, Waltham, UK. Since 2018 she is a Professor and Program Director at the IUBH International University, Bad Reichenhall, Germany. She is also an affiliated Professor in Nutrition Physiology at the University of Bonn in Germany. She is an expert in Nutrition in Space carrying out research in that area since 1989. She has been involved in human space experiments since 1992. She was and still is Principal- and Co-Investigator of several spaceflight and ground-based analogue experiments. She has been the representative of ESA in the Multilateral Medical Operation Panel-Nutrition Working Group (MMOP-NWG) since 1999. From 2011 until 2020 she was Chair of the International Society for Gravitational Physiology (ISGP). She has published more than 135 papers in peer reviewed journals.

In recognition of Martina's outstanding contributions to the field of Gravitational Physiology and to ISGP, we are very pleased to give her the 2021 Nello Pace Award!

First Announcement - 42nd ISGP annual Meeting in Kazan - Russia

https://www.isgp-space.org/annual-meetings/

May 22 – 27, 2022
Kazan Federal University, Kazan, Tatarstan, Russia

We cordially invite you to participate in the 42nd Annual Meeting of ISGP to be held at Kazan Federal University, Kazan in Russia.

Active space exploration, including utilization of ISS now provides a platform for long-term microgravity exposure, allowing study of responses to long-term exposure to the spaceflight environment. Among other topics, the meeting will examine the effects of long-term residence on the International Space Station, including orthostatic hypotension, osteoporosis, muscle atrophy, the influence of cosmic radiation on living systems on different levels, including genetics, and the influence of the closed environment on various aspects of psychology. Countermeasures to these responses and their usefulness in ground medicine will also be discussed.

The conference will provide an excellent opportunity for researchers from different fields in physiology, genetics and molecular biology, space biology and biomedicine to discuss recent advances, share innovative ideas, and promote international collaborations.

A specific program with sessions dedicated for students and young researchers will be organized.

Venue

Founded in 1804, Kazan Federal University is the second oldest university in the Russian Federation. An internationally acknowledged center of academic excellence, it is listed among the 5 to 10 best institutions of higher education in the country. The history of KFU is associated with many world-renowned figures, like the father of non-Euclidian geometry, Nikolai Lobachevsky; the writer, Leo Tolstoy; the discoverer of the Antarctic, Ivan Simonov; the founder of organic chemistry, Alexander Butlerov; a father of modern linguistics, Ivan Baudouin de Courtenay; the discoverer of electron spin resonance, Evgeniy Zavoisky.

The University stands out as one of the architectural diamonds in the center of the 1,000 year-old city of Kazan, the capital of the Republic of Tatarstan and a city populated by 1.2 million people, mostly Russians and Tatars. While in the same time zone as Moscow, Kazan straddles Europe and Asia on the left bank of the great Volga River, some 500 miles east of Russia's capital. To reach the city from Moscow takes an hour by plane, overnight by train or four-days by a leisurely boat ride down the main waterway of Russia's heartland.

The organizers will be happy to provide Russian visa preparation support

This meeting will be also organized as a hybrid event both "face to face" and "online"

Second announcement + opening registration & submission: mid-January 2022

Local Organizing Committee

Oleg Gusev - Chair Kazan Federal University, Russia Juntendo University, Japan	Elena Shagimardanova - Secretary Kazan Federal University, Russia

Web site : https://www.isgp-space.org/annual-meetings/

Contact : extreme.biology.lab@gmail.com

Sponsors

MEGA GRANTS

МИНИСТЕРСТВО НАУКИ
И ВЫСШЕГО ОБРАЗОВАНИЯ
РОССИЙСКОЙ ФЕДЕРАЦИИ

About ISGP

The broad scientific spectrum of the **International Society of Gravitational Physiology emphasizes gravity, life and physiology as its anchors.** Gravitational physiology is considered to include the effects of the magnitude and direction of the gravitational force environment on cells, integrated physiological systems and behavior/performance of humans, animals and plants.

Benefits of Membership

- Discover student and post-doctoral opportunities
- Connect with experts in the field
- Get news on upcoming and recent space events
- Find out about new gravitational physiology publications
- Be notified first about upcoming meetings

Join today! www.isgp-space.org

In proud collaboration with frontiers

2021 ISGP Meeting Program

Monday, May 24, 2021

8:00 – 8:15 am **Introductions and Announcements**

8:15 – 9:15 am **Current Concepts in Gravitational Physiology**

Moderator: Marc-Antoine Custaud, MD, PhD and Martina Heer, PhD

Space anemia, same old or are we making progress?

Guy Trudel, MD
Professor of Medicine, Surgery and Biochemistry
University of Ottawa, Ottawa, ON, Canada
Bone and Joint Research Laboratory
The Ottawa Hospital Rehabilitation Centre, Ottawa, ON, Canada
MARROW Space Research
International Space Station Payload, Ottawa, ON, Canada

Self-organized criticality of cardiovascular function in the standing position

Jacques-Olivier Fortrat, MD, PhD
UMR CNRS Inserm, Biologie Neurovasculaire et
Mitochondriale Intégrée
Laboratoire d'Explorations Fonctionnelles Vasculaires
Centre Hospitalier Universitaire d'Angers, Angers, France

9:15 – 9:20 am **Break**

9:20 – 10:40 am **Effects of Spaceflight on Physiological Systems**

Moderators: Pooneh Bagher, PhD, and Susan Bloomfield, PhD

Decreasing exhaled nitric oxide before and during prolonged space flight
D Linnarsson

Characteristics of locomotion on the passive-mode treadmill at the on ground and space experiments
E Fomina

Impact of a four-hour leg cuff session on internal jugular vein distention during spaceflight
C Patterson

Effects of microgravity on ocular artery hydrodynamics
S Tsai

Middle cerebral jugular and portal vein adaptation to six months ISS spaceflight at rest and with LBNP
P Arbeille

Maintenance of central venous pressure and cardiovascular baroreflexes in astronauts tested within hours of return from the international space station
C Mastrandrea

Space flight cultivation for radish (raphanus sativus) in the advanced plant habitat
S John

Tuesday, May 25, 2021

8:00 – 9:00 am **Nutrition and Food**
Moderator: Scott Smith, PhD

Food system development for space exploration: Challenges and integrative solutions

Grace Douglas, PhD
Lead Scientist, Advanced Food Technology
NASA Johnson Space Center, Houston, TX, USA

Energy requirements of the astronauts onboard the ISS: The ENERGY protocol

Audrey Bergouignan, PhD
Institut Plurisdiciplinaire Hubert Curien, Département d'Écologie, Physiology, Éthologie
Unistra, Université de Strasbourg, Strasbourg, France

9:00 – 9:10 am **Break**

9:10 – 9:20 am **ISGP Announcements and Updates**

9:20 – 10:40 am **Effects of Spaceflight and Ground-Based Analogs on Bone and Muscle**

Moderator: Ruth Globus, PhD

Bone loss due to long-duration spaceflight and the effects of exercise and bone metabolism

L Gabel

Characterizing the role of exercise, recovery, and CDKN1a/p21 in mitigating the effect of simulated spaceflight on systemic tissue degeneration

A Kubik

The effect of weightlessness on the skeletal bones of amphibians and reptiles in the context of research on the ultimobranchial gland: Results and prospects

V Gulimova

Pretreatment with anabolic countermeasures enhances cancellous bone in the distal femur of male rats exposed to subsequent unloading

J Elizondo

21-days of head-down-tilt bed rest result in increased concentrations of cartilage degradation marker CTX-II

AM Liphardt

Foot-ground reaction force during short-radius centrifugation

A Saveko

Progestin-only contraception implants did not exacerbate simulated microgravity induced bone changes

H Allaway

Wednesday, May 26, 2021

8:00 – 9:00 am

Spaceflight Associated Neuro-ocular Syndrome and Cardiovascular

Moderator: Steven Laurie, PhD

Cerebral and Ocular Results from the SPACE-CENT study: A part of AGBRESA (Artificial Gravity Bed Rest Study)

Eric Bershad, MD

Associate Professor of Neurology, Neurosurgery and Space Medicine

Section of Neurocritical Care and Vascular Neurology

Baylor College of Medicine, Houston, Texas, USA

What are the risks to cardiovascular health in human spaceflight?

Richard Hughson, PhD, FCAHS

Schlegel Research Chair in Vascular Aging and Brain Health

Senior Director of Research

Schlegel-University of Waterloo Research Institute for Aging, Waterloo, ON, Canada

9:00 – 9:10 am	**Break**
9:10 – 9:20 am	**ISGP Announcements and Updates**
9:20 – 10:40 am	**Cardiovascular Function and Cognition: Examination Using Analog Models**

Moderator: Aleksandra Stankovic, PhD

Role of the external carotid artery in maintaining cerebral blood flow in the event of a sudden increase in central blood volume following a change in gravity stress

D Lanéelle

Head down tilt bed rest and arterial stiffness-results from a multi-method approach

S Möstl

A closed loop approach to the study of the baroreflex dynamics during fast tilt in humans

A Taboni

Effects of short-term isolation and chronic sleep deprivation on cognitive performance

K Brauns

1-week galvanic vestibular stimulation improves arterial pressure control at the onset of postural change

K Tanaka

Trapped between gravities: The influence of different gravity levels on brain cortical activity

C Badali

A computational tool for real-time detection of astronaut spatial disorientation during gravitational transitions and piloted landings

J Dixon

Thursday, May 27, 2021

8:00 – 9:00 am

Effects of Gravity and Spaceflight on Neurovestibular and Sensorimotor Systems

Moderator: Ana Diaz Artiles, PhD

Countermeasures for treating sensorimotor disturbances in astronauts and cosmonauts after long-duration space flights: Atonomous landings

Millard Reschke, PhD
Chief, NASA Neuroscience
NASA Johnson Space Center, Houston, TX, USA

Dry immersion model: Overview of unique experiments 2018-2020

Elena Tomilovskaya, PhD
Senior Researcher,
Head of the Laboratory of Gravitational Physiology of Sensory-motor System,
Head of the Department of Sensory-Motor Physiology and Countermeasures,
Russian Federation State Scientific Center Institute of Biomedical Problems of the Russian Academy of Sciences, Russia, Moscow

9:00 – 9:10 am

Break

9:10 – 10:30 am

Modeling Microgravity: Insights from Dry Immersion Studies

Moderators: Marc-Antoine Custaud, PhD and Elena Tomilovskaya, PhD

Changes in response of hemodynamics to head up tilt in healthy people during "dry" immersion and in patients suffering from vasovagal syncope

O Vinogradova

Effect of 21-day support unloading on the characteristics of postural correction responses

N Shishkin

Cardiovascular and fluid changes induced by the acute phase of dry-immersion
A Robin

Microgravity disturbs iron metabolism and hepcidin regulation: Lessons from ground-based models in humans and rodents
F Derbré

Effects of thigh-cuffs on bone remodeling unbalance induced by short-term dry immersion and the associated metabolic markers
MT Linossier

Early de-conditioning of human skeletal muscles and effects of a thigh cuff as a cardiovascular countermeasure
T Fovet

Stimulus-reaction tasks in subjects with Parkinson's disease under repetitive sessions of "dry" immersion: Issues of rehabilitation and modeling of interplanetary missions
A Meigal

10:30 – 10:40 am **Closing Remarks**

Mini-Talks

On-Demand Online Presentation

Effects of Spaceflight on Physiological Systems

Index of reflectivity of ultrasound radiofrequency signal from the carotid artery wall increases in astronauts after a 6-month spaceflight
P Arbeille

Central and peripheral pulse wave velocity changes in astronauts on ISS and up to one-year post-landing follow-up

D Greaves

Repeated long-term space flights: Proteomic investigations of cosmonauts' blood

D Kashirina

Effect of the exercise countermeasure to prevent the metabolic alterations induced by microgravity: Evidence from ground-based and in-flight studies

E Le Roux

Risk factors for the onset of cardiac arrhythmias in astronauts during long-term spaceflights

R Parisi

Lower dampening of carotid artery wave intensity following 6 months on the International Space Station: A Vascular Echo study

A Robertson

Effects of Spaceflight and Ground-Based Analogs on Bone and Muscle

Muscle tone - Research in space and ground models. A summary of the results and possible horizons

L Amirova

Tissue-specific sex differences in physiological reactions to simulated microgravity in mice

A Andreev-Andrievskiy

Whole-body reaching movements in micro- and hyper-gravity highlight distinct adaptive processes

L Chomienne

Microgravity-induced effects on motor system: Influence of spinal cord stimulation and support afferentation

A Fedianin

Whole-body vibration: An 18-month countermeasure evaluation of postmenopausal women

P Fernandez

Dynamics of functional performance indicators under conditions of a one-year wintering at the Antarctic station "Vostok"

N Osetskiy

Thermoneutral temperature mitigates hind-limb unloading-induced bone loss by preserving energetic metabolism

L Peurière

Denosumab as a potential pharmacological countermeasure against microgravity-induced osteopaenia in long duration space flight – a review and proposal

A Rengel

Role of neuronal control in development of immobilization osteoporosis

D Shcherbakov

Cardiovascular Function, Psychological Factors, and Cognition: Examination Using Analog Models

Effects of two months of bed rest and antioxidant supplementation on attentional processing
K Brauns

Cognitive performance during 60 days of head-down tilt bedrest with and without artificial gravity (AGBRESA)
L Braunsmann

To study the temporal changes in cardiovascular and cerebrovascular variables during acute exposure to simulated microgravity
S Chauhan

The influence of perceptual constraints on bimanual force coordination in simulated microgravity
M Davis

Analysis of the autonomous nervous system during simulated disorientation test in Italian Air Force pilots
GS Grasso

Sexual Wellbeing & sexual security in Isolation & Confinement Environments (SWICE)
D Grevers

Recent and remote memories are not affected by hypergravity in normotensive and hypertensive rats
A Gros

Assessment of systemic sclerosis patients treated with gravitational therapy
E Isasi

The influence of altered-gravity on bimanual force coordination

D Kennedy

Near-infrared coded hemodynamic imaging tracks changes in venous pressure during head-down tilt and lower body negative pressure

C Patterson

Emotion in space analog environments: Detection of affective changes in response to a stressful condition in situation of confinement

J Pauly

Lower body negative pressure an integrative countermeasure during spaceflight

L Petersen

Improved human performance through control response type for a piloted lunar lander

C Pinedo

Assessment of the relationship between the cardiovascular system during 6-degrees head down tilt using conditional entropy: A terrestrial based microgravity study

V Shankhwar

Cardiovascular effects during parabolic flight: Literature review

H Vellore

Integrated feedback displays to facilitate bimanual coordination in simulated microgravity

Y Wang

Acute gravitational dose-response curves in hemodynamic and ocular variables induced by tilt

R Whittle

Diagnostic Tests and Sensors

Smartphones motion-fingerprint in spaceflight: Motion tracking of astronauts on long duration missions for health monitoring

S Iliev

Space-inspired: E-Nose technology for detection of pneumonia in patients

F Pfeiffer

Effects of Radiation, Simulated Microgravity, or Hypergravity on Physiological Systems

Phosphatase inhibitors have different effects on the motility of fly and mouse spermatozoa under microgravity modeling

M Golubkova

Impact of extreme physical inactivity and low-dose testosterone treatment on iron distribution in male rats

M Horeau

Hypergravity suppresses allergic lung inflammation by attenuating JAK2-STAT3 pathway via Type 2 innate lymphoid cell

YH Kim

Central compensation of x-Irradiation on locomotion: Preliminary study for space radiation

G Kim

A review of ambulation energy expenditure in hypogravity analogs

L Kluis

Morphological and functional changes in murine intestine during 30-d hindlimb suspension: A dynamics

E Lagereva

Hypergravity and whole-body vibration affect distinct compartments of mouse bones, with opposite effects in osteopontin or bone sialoprotein knock-outs

M Maalouf

Resolution of inflammation is altered under simulated microgravity conditions

M Maccarrone

Neurobehavioural evaluation of C57BL/6 mice exposed to the hindlimb unloading model

A Racca

The Mouse Drawer System (MDS) in the Long Diameter Centrifuge (LDC): Neurobehavioral response to altered gravity exposure

D Santucci

Molecular basis of hypergravity-induced wheat root growth phenotype

M Sathasivam

Modeling the effect of curcumin on cancer and healthy breast cells under lunar surface radiation and microgravity conditions

S Sharma

Hypergravity-induced wheat root growth phenotype and associated physio-biochemical parameters

B Swamy

Organization of the cytoskeleton in mouse oocytes under modelling microgravity

M Usik

Effect of centrifuge generated altered-gravity on bimanual coordination

R Woodruff

Modeling Microgravity: Insights from Dry Immersion Studies

Study of postural stability after 5-day dry immersion with two posturology methods: Comparative analysis of video motion capture and inertial motion sensors

N Abu Sheli

Increased the REM sleep stage and blood pressure changes during 21-day dry immersion

E Bersenev

Evaluation of cardiovascular reactions in Parkinson's disease patients underwent repetitive short-term sessions of "dry" immersion for rehabilitation

L Gerasimova-Meigal

5 days of simulated microgravity promote ectopic adiposity development and ECM remodeling in skeletal muscle

C Guilhot

Prospects for using different classes of otoacoustic emission for intracranial pressure monitoring in astronauts during spaceflight

L Marchenko

Vertebral dysfunctions and viscoelastic properties after 5d Dry Immersion simulating microgravity

C Ple

MRI study of the spinal canal during dry immersion

A Robin

Molecular markers and functional characteristics of human skeletal muscle deconditioning after short-term dry immersion

L Stevens

DI-5-Cuffs. Intervertebral disc content increased after 5-day dry immersion

L Treffel

Parameters of vascular hemodynamics and body fluids redistribution in female volunteers during staying in 3-day "dry" immersion

I Vasilev

Extended Abstracts

Muscle tone research in space and ground models: Review and horizons

Liubov Amirova[1]*, Ilya Rukavishnikov[2], Alina Saveko[1], Anastasija Plehuna[1,3], Inna Nosikova[1], Tatiana Shigueva[1], Nikita Shishkin[1], Inna Zelenskaya[1], Nastassia Navasiolava[4], Loïc Treffel[5,6], Claude Gharib[5], Marc-Antoine Custaud[4], Elena Tomilovskaya[1]

[1]Department of Gravitational Physiology, Institute of Biomedical Problems, Russian Academy of Sciences, Moscow, Russia
[2]Department of Medical Support for Spaceflight, Institute of Biomedical Problems of Russian Academy of Sciences, Moscow, Russia
[3]King's College London, Center of Human & Applied Physiological Sciences, London, United Kingdom
[4]Univ Angers, CHU Angers, CRC, INSERM, CNRS, MITOVASC, Equipe CarMe, SFR ICAT, Angers, France
[5]Institut NeuroMyogène, Université Claude Bernard Lyon, Lyon, France
[6]Institut Toulousain d'Ostéopathie, IRF'O, Toulouse, France
**lyubove.dmitrieva@gmail.com*

INTRODUCTION

The first human spaceflight (SF) has initiated comprehensive muscle tone research in space medicine, yet numerous unsystematized studies have been accumulated to date. This short review is intended to summarize existing studies, mainly focusing on Soviet and Russian researches that are less accessible to the global community. Additionally, we are proposing possible development ways for muscle tone research.

MATERIALS AND METHODS

The current review examined 20 papers focusing on hardware-based, non-invasive studies of human muscle tone/transverse stiffness changes induced by the SF or its analogs: parabolic flights (PF), bed rest (BR), head-down bed rest (HDBR), dry immersion (DI), confinement. The comparative data are shown in Table 1.

Table 1: Muscle tone research in microgravity and its analogs: summary

Ref	Exposure	n, (CM)	Method	Parameter, unit	Measurement points	Main findings
(Yuganov et al., 1962)*	PF	22	EMG	Integrated EMG amplitude, mV	*m. trapezius*	Almost 2-fold decrease in EMG activity; in some cases "bioelectrical silence"
(Cherepakhin, 1968)*	62-d BR	6 (3 control, 3 RE)	Sirmai myotonometer	Hardness, a.u.	*m. tibialis anterior* *m. quadriceps femoris* *m. biceps brachii*	Progressive reduction in muscle tone throughout BR, both in Controls & RE
(Kakurin et al., 1971)*	2-5-d SF (Soyuz-3-8)	12	Sirmai myotonometer	Hardness, a.u.	*m. tibialis anterior* *m. quadriceps femoris* *m. biceps brachii*	Leg muscles: decrease; Arm muscle: unchanged; Observed changes are non-pathological
(Petukhov and Purakhin, 1971)*	120-d BR	10 (4 control, 6 drug support: 3 pituitrin & deoxy-corticosterone; 3 methandrostenolone)	EMG	EMG amplitude, mV	*m. tibialis anterior* *m. gastrocnemius*	Decrease in EMG activity of both muscles on day 3-4 post BR; no effect of CM
(Gevlich, 1984)* Data partially published (Kozlovskaya et al., 1988)	7- d SF (Soyuz-6)	6	Electromyotonometer	Transverse stiffness, kPa or g/mm^2	*m. tibialis anterior* *m. gastrocnemius* *m. soleus*	The most pronounced decrease in transverse stiffness was in tibialis extensors. The relationship of the detected abnormalities with the degree of unloading was shown: the greatest changes were registered after DI, the smallest - in SF with CM
	Combined 7- d DI (day) & 4° HDBR (night)	4				
	14-d 4° HDBR	7				
	120-d 4° HDBR	6				
	7-d DI	10				

(Continued)

(Vinogradova et al., 2002) (Kozlovskaya et al., 2007a) (Kozlovskaya et al., 2007b)	7-h DI	8 crossover (DI without CM; DI+stimulation of foot support zones)	Resonance vibrography (Viscoelastograph) EMG	Transverse stiffness, kPa EMG amplitude, mV	*m. tibialis anterior* *m. soleus*	DI without CM led to trends of decreased transverse stiffness and EMG activity for *m. soleus* and increased – for *m. tibialis* anterior in the first 24h. Foot support zones stimulation CM reversed these tendencies
	7-d DI	10 crossover (*idem* previous)				
(Rukavishnikov et al., 2017)	6-h DI 3-d DI	5 7	Resonance vibrography (Viscoelastograph)	Transverse stiffness, kPa	*m. erector spinae*	Decrease in tone of dorsal extensors was maximal at the first hours of DI (60% of baseline), then stabilized at 60-85% of baseline
(Schneider et al., 2015)	PF	12	MyotonPro	Oscillation frequency, Hz Dynamic stiffness, N/m Logarithmic decrement Mechanical stress relaxation time, ms	*m. erector spinae* *m. gastrocnemius* *tendo Achillis*	Immediate reduction in measured parameters when transiting to 0G
(Treffel et al., 2016) (Demangel et al., 2017)I (de Abreu et al., 2017)	3-d DI	12	MyotonPro	Oscillation frequency, Hz Dynamic stiffness, N/m Mechanical stress relaxation time, ms	*m. masseter* *m. sternocleido-mastoideus* *m. splenius* *m. trapezius* *m. longissimus cervicis* *m. longissimus thoracis* *m. multifidus* *m. rectus femoris* *m. tibialis anterior* *m. gastrocnemius lat.* *m. soleus*	The strongest decrease in tone was in the paravertebral muscles of the upper back (-12% for *m. longissimus cervicis*) and anterior surface of the leg (-10% for *m. rectus femoris*)

(Schoenrock et al., 2018)	60-d 6° HDBR	24 (12 control, 12 jump CM)	MyotonPro EMG	Oscillation frequency, Hz Dynamic stiffness, N/m Logarithmic decrement, Log_2 Mechanical stress relaxation time, ms	*m. trapezius* *m. deltoideus anterior* *m. longissimus dorsi* *m. multifidus* *m. rectus femoris* *infrapatellar tendon* *m. tibialis anterior* *m. gastrocnemius* *m. soleus* *tendo Achillis* *aponeurosis plantaris* *m. flexor digitorum brevis*	Significant tone decrease in Controls. Lesser tone decrease and faster recovery in Jump CM group compared to Controls
(Nistorescu et al., 2019)	21-d DI	6	MusTone	Oscillation frequency, Hz	*m. soleus*	Consistent increase in tone over 21 days of immersion
(Yuan et al., 2019)	180-d confinement	4	MyotonPro	Oscillation frequency, Hz	*m. erector spinae*: lumbar, thoracic & cervical levels *m. masseter* *m. rectus femoris*	Masseter tone increased by 6-14% at M5; Paravertebral tone decreased, with a drop in M1 of 10±6% in average for totality of *m. erector spinae* (15-20% for cervical, 15-25% for thoracic, and 3-6% for lumbar erector spinae), followed by steady state for M2-M6; *m. rectus femoris* tone largely unchanged

(Amirova et al., 2020b)*	21-d DI	10	MusTone MyotonPro	Oscillation frequency, Hz	*m. erector spinae* *m. rectus femoris* *m. tibialis anterior* *m. gastrocnemius*	Decreased tone of *m. rectus femoris* and *m. tibialis anterior* recorded by both instruments. Tone of *m. erector spinae* and *m. gastrocnemius* showed an upward trend over 21 days of DI
(Amirova et al., 2020a)	5-d DI	34 (18 control, 16 electromyostimulation CM)	MyotonPro	Oscillation frequency, Hz	*m. tibialis anterior* *m. gastrocnemius* *m. soleus*	Decrease in leg muscle tone in both groups. Myostimulation CM slightly reduced tone drop, but did not prevent it
(Amirova et al., 2021a)	2-h DI	12	MyotonPro	Oscillation frequency, Hz	*m. trapezius* *m. deltoideus posterior* *m. erector spinae* *m. rectus femoris* *m. biceps femoris* *m. tibialis anterior* *m. gastrocnemius* *m. soleus* *tendo Achillis* *m. flexor digitorum brevis* *aponeurosis plantaris*	Immediate decrease in tone of m. erector spinae, *m. biceps femoris, m. soleus, m. tibialis anterior* and *tendo Achillis* at the onset of immersion, followed by an even greater decrease in the first two hours of DI. Increase in *m. gastrocnemius* tone

SF – spaceflight, PF – parabolic flight, BR - bed rest, HDBR – head-down bed rest, DI – dry immersion, CM – countermeasure, RE – resistive exercise, d – day, h - hour

* In Russian

RESULTS

Spaceflights

In the late 1960s, Kakurin et al. (1971) described neuromuscular state of 12 cosmonauts after 2- to 5-day spaceflights, demonstrating a significant decrease in the "hardness" (hereafter terminology from the reviewed studies) of *m. tibialis anterior* (-7.4%) and *m. quadriceps femoris* (-10.7%) (Figure 1A). The hardness of the flexor *m. biceps brachii* did not change significantly. Circumferences of the shin, thigh, and shoulder showed a tendency to decrease, yet high variability within the group was observed (Figure 1B).

Extension of SFs to 7 days has led to a significant decrease in transverse stiffness of *m. soleus* (-15%) and *m. gastrocnemius lat.* (-12%) recorded on day 1 and 2 post-flight (Figure 2) (Gevlich, 1984). Reduction in stiffness of *m. gastrocnemius med.* was not significant. Interestingly, in contrast to the previous study, stiffness of *m. tibialis anterior* remained nearly unchanged.

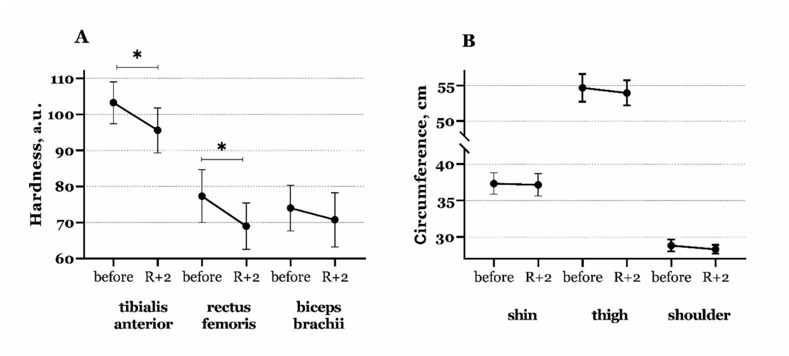

FIGURE 1: Hardness of *m. tibialis anterior, m. quadriceps femoris* and *m. biceps brachii* as measured using "Sirmai" myotonometer (**A**) and Circumferences of the shin, thigh and shoulder (**B**) pre- and post 2-5-day spaceflight (n=12). Mean±SD. * p<0.05 vs. Before. Adapted from Kakurin et al. (1971).

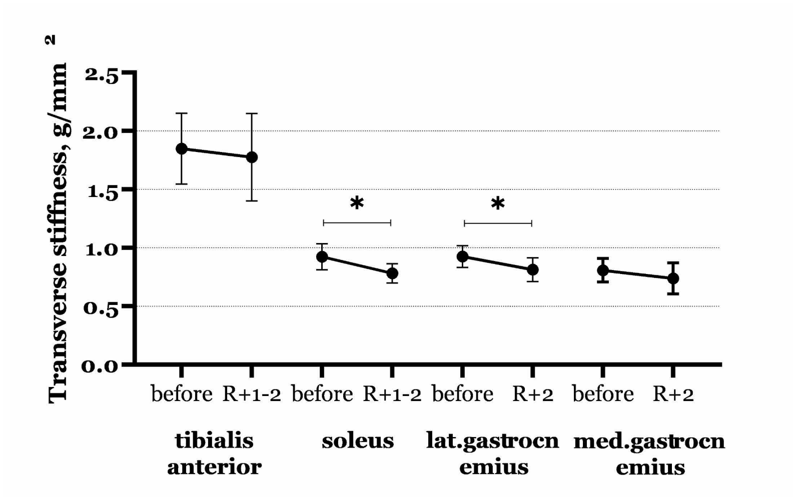

FIGURE 2: Muscle transverse stiffness as measured using electromyotonometer pre- and post 7-day spaceflight (n=6). Mean±SD. * p<0.05 vs. Before. Adapted from Gevlich (1984).

Parabolic flights

Early experiments with parabolic flights have demonstrated an immediate decrease in electromyographic (EMG) activity of *m. trapezius* from 40 to 25 mV, moreover some sessions recorded almost "bioelectrical silence" (Yuganov et al., 1962). Recent studies by Schneider et al. (2015) showed a significant decrease in tone and stiffness of *m. erector spinae*, *m. gastrocnemius*, and *tendo Achillis* immediately after transition to 0G.

Bed rest experiments

In 62-day BR study, Cherepakhin (1962) showed a consistent decline in the tone of all examined muscles, peaking towards the last day: 15% in *m. tibialis anterior*, 4.1% in *m. quadriceps femoris*, and 15.6% in *m. biceps brachii*. A 120-day BR study by Petukhov & Purakhin (1971) showed a reduction in EMG activity of lower leg muscles, which indicated the tonic activity of postural muscles, on days 3-4 post-BR. It is important to note, that *m. gastrocnemius* showed more than a twofold decrease in EMG activity, from 28 to 11 mV (Figure 3), indicating the high physiological cost of upright posture.

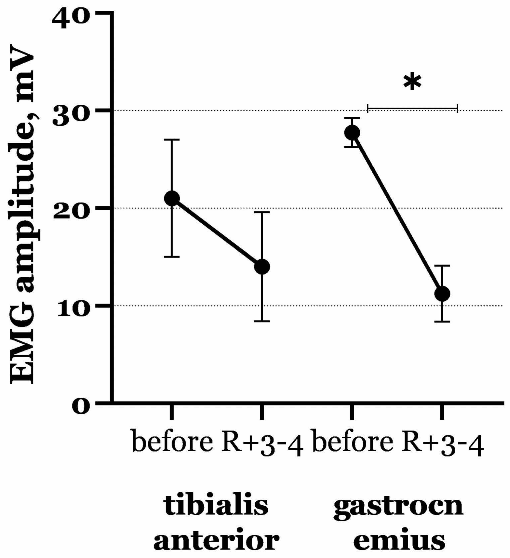

FIGURE 3: EMG amplitude for *m. tibialis anterior* and *m. gastrocnemius* in a calm standing posture with eyes open pre- and post 120-day horizontal bed rest (n=4). Mean±SD. * $p<0.05$ vs. Before. Adapted from Petukhov & Purakhin (1971).

A 120-day HDBR (-4°) has triggered a 20-40% reduction of *m. gastrocnemius* and *m. soleus* transverse stiffness on the 6th day (Gevlich, 1984), with further stiffness decrease up to the 31st day of exposure (Kozlovskaya et al., 1988). Further, the transverse stiffness tended to increase on the 90th and 120th days of HDBR. The authors have linked those changes to either connective tissue overgrowth or compensation of tonic reflexes (Gevlich, 1984).

Recent extensive study by Schoenrock et al. (2018) on the properties of skeletal muscles under 60-day HDBR (-6°) showed drop in tone and stiffness in all muscle groups examined. The most significant changes were observed in leg muscles - *m. rectus femoris, m. tibialis anterior, m. gastrocnemius, m. soleus*, as well as in Achilles tendon.

Immersion experiments

Early studies on transverse stiffness of shin muscles under DI (Kozlovskaya et al., 1988, 2007b, 2007a) demonstrated a more rapid and profound decrease of extensor stiffness in DI compared to HDBR - by 40-50% in the first 2 hours. This drop in stiffness lasted for the following 6 days in DI. The shin flexors showed a slight (5-7%) increase in stiffness after the first hours in DI, followed by a decrease (-10%) on the following days. In contrast, recent DI studies showed a trend to decrease in the tone of *m. tibialis anterior* (de Abreu et al., 2017; Amirova et al., 2020a). This discrepancy could be explained by the difference in the study protocols – previous studies of *m. tibialis anterior* stiffness have been performed with 90° in the ankle joint, thus potentially could lead to muscle activation.

Recent studies by Treffel et al., 2016, de Abreu et al., 2017, and Demangel et al., 2017 with 3-day DI also showed alterations in muscle viscoelasticity. Global leg muscle tone, proxy measured by "oscillation frequency" parameter, immediately decreased by ~8-10% under immersion. Changes were especially pronounced for *m. rectus femoris*: the first 6 hours in DI decreased tone by 10%, whereas elasticity increased by 31% after 3 days of DI. The tone of superficial muscles of the neck and upper trunk (*m. trapezius* and *m. splenius)* was unmodified. Deep back tone behavior had cervico-lumbar gradient - tone immediately dropped in the upper part (12% for *m. longissimus cervicis*), tended to slight decrease on D3 in the middle (*m. longissimus thoracis*) and was not modified in the lower part (lumbar portion of *m. multifidus*). Six hours following the end of DI, muscle tone was completely restored, except for *m. masseter* (tone unchanged under DI, but increased at recovery, probably in link with post-immersion postural disturbance).

The study by Amirova et al. (2021a) performed with MyotonPro showed that a decrease in muscle tone occurred instantly once exposed to DI for *m. erector spinae* (-10-12%), *m. biceps femoris* (-5,8%), *m. soleus* (-6-8%), *m. tibialis anterior* (-4,8%), and *tendo Achillis* (-11,4%), showing deterioration in the first two hours of DI. Interestingly, an extension of DI to 21 days did not further exacerbate a decrease in muscle tone (Amirova et al., 2020b), and in some cases muscle tone increased (Nistorescu et al., 2019). The most profound decrease in muscle tone occurs in the first hours and days of DI (de Abreu et al., 2017; Rukavishnikov et al., 2017; Amirova et al., 2021a).

Confinement experiments

MyotonPro measurements of 4 subjects, confined for 180 days in a closed-loop controlled ecological life support system, revealed muscle tone increase for *m. masseter* (probably in relation with stress), decrease - for paravertebral muscles, and no substantial change – for lower limb muscles (Yuan et al., 2019). Of note, in this confinement study daily routine included sustained physical work in greenhouses and life support systems.

DISCUSSION

Studies carried out over a prolonged period and conducted with different methods demonstrated a decrease in muscle tone and stiffness for most muscle groups examined. Most significant changes were observed in back and leg muscles, being directly involved in postural stability and locomotion.

Numerous studies revealed a significant decrease in muscle tone immediately upon exposure to support unloading - in transition to microgravity (Yuganov et al., 1962; Schneider et al., 2015) or immersion (de Abreu et al., 2017; Rukavishnikov et al., 2017; Amirova et al., 2021a). The reflex nature of the decrease in muscle tone is confirmed by PF studies, the short time of which (about 20 seconds) excludes any structural changes (Yuganov et al., 1962; Schneider et al., 2015). This fact suggests reflex mechanisms of muscle tone decrease, where support unloading plays a triggering role (Grigor'ev et al., 2004), activating further neuromuscular impairment (Shenkman et al., 2021). A similar observation was also noted in the earlier study performed by Gevlich (1984), who focused on comparing changes in the transverse stiffness of muscles by exposing them to varying degrees of support unloading. A decrease in transverse stiffness of both *m. tibialis anterior* and *m. soleus* was recorded predominantly following DI (Figure 4A,B). It is important to note that the decrease in transversal stiffness after 7-day SF was the least profound among the impacts, probably related to extensive countermeasures program during the flight.

It should be noted that the degree of muscle tone reduction depended not only on the degree of support unloading but also on the muscle group being examined. Slow postural muscles, in particular *m. soleus,* are of great interest to researchers. Early studies by Gevlich (1984) and Kozlovskaya et al. (1988) showed a two-fold reduction in *m. soleus* transverse stiffness induced by

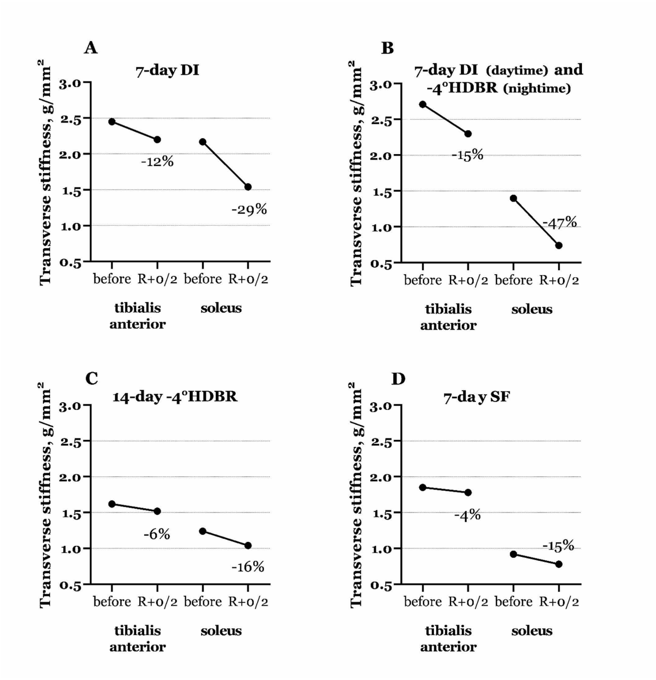

FIGURE 4: Transverse stiffness of *m. tibialis* anterior and *m. soleus* as measured using electromyotonometer before and after 7-day DI (**A**), 7-day combined DI and HDBR (**B**), 14-day HDBR (**C**) and 7-day SF (**D**). Average values. Adapted from Gevlich (1984).

support unloading. Latest experiments carried out using modern equipment also demonstrate a reduction in *m. soleus* tone, but the degree of this reduction is 5-15% of the initial values (de Abreu et al., 2017; Schoenrock et al., 2018; Amirova et al., 2020a). There is also evidence of increased *m. soleus* tone by the end of 21 days DI (Nistorescu et al., 2019). A similar phenomenon was observed by Gevlich during the late phases of 120-day HDBR. It remains unclear whether this phenomenon is due to reflex adaptation to new conditions or to the fact that alternative mechanisms, such as fascial contractility, are activated to maintain homeostasis (Schleip, 2020).

The use of different methods for assessing muscle tone can also lead to different results. This review alone presents six different approaches to the determination of muscles' viscoelastic properties (Table 1). They are based on determining muscle tissue resistance by an indentation of a mechanical probe (Sirmai, electromyotonometer), vibrating probe (viscoelastograph), by short impact (MusTone, MyotonPro), as well as determination of tone by EMG activity levels. Various devices have different units of measurement and mathematical principles, preventing direct comparison of the data obtained.

Further improvement of muscle tone research undoubtedly requires the development of a unified approach to prevent pathological changes and unified measurement protocol that currently is absent in space medicine. Introduction of the myotonometric test to the International Space Station on-board program would not only allow determining reference values, but would also provide a rapid and non-invasive assessment of muscle tonic properties in future. We suggest that such protocol can be based on the ones described in Schoenrock et al., (2018), Amirova et al., (2021b).

CONCLUSION

Support unloading causes a sharp reduction in back and shin muscle tone, which can persist for several hours/days afterwards, and is dependent on the duration and degree of exposure. Countermeasures fail fully eliminate this decrease in muscle tone in most studies analyzed (Table 1).

FUNDING

This study was carried out as part of the RAS basic research topic 63.1.

ACKNOWLEDGMENTS

The authors remember and honor the contribution of Prof. Inesa B. Kozlovskaya to the gravitational physiology development and particularly – in muscle tone research under microgravity conditions.

The authors are grateful to Yulia V. Komarova for the syntax review.

Keywords: muscle tone, muscle stiffness, spaceflight, bed rest, dry immersion, confinement

REFERENCES

Amirova, L. E., Osetskiy, N. Y., Shishkin, N. V., Ponomarev, I. I., Rukavishnikov, I. V., Kozlovskaya, I. B., et al. (2020a). Comparative Study of the Lower Limb Muscle Tone under the Conditions of Five-day Support Unloading Coupled with Different Regimens of Electromyostimulation. Hum. Physiol. 46, 391–400. doi:10.1134/S0362119720040027.

Amirova, L. E., Plehuna, A., Rukavishnikov, I. V., Saveko, A. A., Peipsi, A., and Tomilovskaya, E. S. (2021a). Sharp Changes in Muscle Tone in Humans Under Simulated Microgravity. Front. Physiol. 12. doi:10.3389/fphys.2021.661922.

Amirova, L. E., Plehuna, A., Rukavishnikov, I. V., Saveko, A. A., Peipsi, A., and Tomilovskaya, E. S. (2021b). Sharp Changes in Muscle Tone in Humans Under Simulated Microgravity. Front. Physiol. 12, 1–12. doi:10.3389/fphys.2021.661922.

Amirova, L. E., Saveko, A. A., Rukavishnikov, I. V., Nistorescu, A., Dinculescu, A., Valeanu, V., et al. (2020b). [Effects of 21-Day Support Unloading on Characteristics of Transverse Stiffness of Human Muscles. Estimation of Efficiency of New Myotonometric Approaches]. Aerosp. Environ. Med. 54, 15–22. doi:10.21687/0233-528x-2020-54-4-15-22.

Cherepakhin, M. A. (1968). [Effect of prolonged bed rest on the muscular tone and proprioceptive reflex of man]. Kosm. Biol. Med. 2, 43–47.

de Abreu, S., Amirova, L., Murphy, R., Wallace, R., Twomey, L., Gauquelin-Koch, G., et al. (2017). Multi-system deconditioning in 3-day dry immersion without daily raise. Front. Physiol. 8. doi:10.3389/fphys.2017.00799.

Demangel, R., Treffel, L., Py, G., Brioche, T., Pagano, A. F., Bareille, M. P., et al. (2017). Early structural and functional signature of 3-day human skeletal muscle disuse using the dry immersion model. J. Physiol. doi:10.1113/JP273895.

Gevlich, G. I. (1984). [Mechanisms of muscle tone disorders with a decrease in gravitational loads]. PhD thesis. Moscow. 132 p.

Grigor'ev, A. I., Kozlovskaia, I. B., and Shenkman, B. S. (2004). [The role of support afferents in organisation of the tonic muscle system]. Ross. Fiziol. Zh. Im. I. M. Sechenova 90, 508–521.

Kakurin, L. I., Cherepakhin, M. A., and Pervushin, V. I. (1971). [Effect of short-term flights on the state of the neuromuscular system of man]. Kosm. Biol. Med. 5, 53–56.

Kozlovskaya, I. B., Sayenko, I. V., Sayenko, D. G., Miller, T. F., Khusnutdinova, D. R., and Melnik, K. A. (2007a). Role of support afferentation in control of the tonic muscle activity. Acta Astronaut. 60, 285–294. doi:10.1016/j.actaastro.2006.08.010.

Kozlovskaya, I. B., Sayenko, I. V., Miller, T. F., Khusnutdinova, D. R., Melnik, K. A., Popov, D. V., et al. (2007b). Erratum to: New approaches to countermeasures of the negative effects of micro-gravity in long-term space flights. Acta Astronaut. 60, 783–789. doi:10.1016/j.actaastro.2006.09.038.

Kozlovskaya, I., Dmitrieva, I., Grigorieva, L., Kirenskaya, A., and Kreidich, Y. (1988). Gravitational Mechanisms in the Motor System. Studies in Real and Simulated Weightlessness. Stance and Motion, 37–48. doi:10.1007/978-1-4899-0821-6_4.

Nistorescu, A., Dinculescu, A., Vizitiu, C., Marin, M., and Mandu, M. (2019). Soleus muscle assessment during 21 day dry immersion study using mustone device. in 2019 7th E-Health and Bioengineering Conference, EHB 2019 doi:10.1109/EHB47216.2019.8970052.

Petukhov, B. N., and Purakhin, Y. N. (1971). [Electric activity of muscles during standing after a 120-day bed rest experiment]. Kosm. Biol. Med. 5, 64–68.

Rukavishnikov, I. V., Amirova, L. E., Kukoba, T. B., Tomilovskaya, E. S., and Kozlovskaya, I. B. (2017). Effects of gravitational unloading on back muscles tone. Hum. Physiol. 43, 291–300. doi:10.1134/S0362119717030173.

Schleip, R. (2020). Fascia, Function, and Medical Applications. , eds. D. Lesondak and A. M. Akey First edition. | Boca Raton : CRC Press, 2020.: CRC Press doi:10.1201/9780429203350.

Schneider, S., Peipsi, A., Stokes, M., Knicker, A., and Abeln, V. (2015). Feasibility of monitoring muscle health in microgravity environments using Myoton technology. Med. Biol. Eng. Comput. 53, 57–66. doi:10.1007/s11517-014-1211-5.

Schoenrock, B., Zander, V., Dern, S., Limper, U., Mulder, E., Veraksitš, A., et al. (2018). Bed Rest, Exercise Countermeasure and Reconditioning Effects on the Human Resting Muscle Tone System. Front. Physiol. 9. doi:10.3389/fphys.2018.00810.

Shenkman, B. S., Tsaturyan, A. K., Vikhlyantsev, I. M., Kozlovskaya, I. B., and Grigoriev, A. I. (2021). Molecular Mechanisms of Muscle Tone Impairment under Conditions of Real and Simulated Space Flight. Acta Naturae 13, 85–97. doi:10.32607/actanaturae.10953.

Treffel, L., Dmitrieva, L., Gauquelin-Koch, G., Custaud, M. A., Blanc, S., Gharib, C., et al. (2016). Craniomandibular system and postural balance after 3-day dry immersion. PLoS One 11. doi:10.1371/journal.pone.0150052.

Vinogradova, O. L., Popov, D. V., Saenko, I. V., and Kozlovzkaya, I. B. (2002). Muscle tranverse stifness and venous compliance under conditions of simulated supportlessness. Gravit Physiol 9, 327–329.

Yuan, M., Custaud, M.A., Xu, Z., Wang, J., Yuan, M., Tafforin, C., et al. (2019). Multi-System Adaptation to Confinement During the 180-Day Controlled Ecological Life Support System (CELSS) Experiment. Front. Physiol. 10:575. doi: 10.3389/fphys.2019.00575

Yuganov, E. M., Kasyan, I. I., Cherepahin, M. A., and Gorshkov, A. I. (1962). [On some human reactions under conditions of reduced weight, in Problems of space biology, 206–2014.

Trapped between gravities: The influence of different gravity levels on brain cortical activity

Constance Badalì[1]*, Petra Wollseiffen[1], Stefan Schneider[1,2,3]

[1]*Institute of Movement and Neurosciences, German Sport University Cologne, Köln, Germany*
[2]*School of Health and Sport Sciences, University of the Sunshine Coast, Maroochydore, Australia*
[3]*School of Maritime Studies, Offshore Safety and Survival Centre, Marine Institute, Memorial University of Newfoundland, Canada*
**c.badali@dshs-koeln.de*

INTRODUCTION

Beside the Space Flight Associated Neuro-ocular Syndrome (SANS), specifically visual impairments reported during and after long duration space flight, also other neurological issues such as motor control and coordination, neuromuscular drive and neuro-cognitive performance have been described to be impaired during long-term spaceflight. Interestingly the SAN syndrome seems to manifest itself mainly in well-established neuronal communication processes like vision, motor or the vestibular system but not cognitive performance (Lee et al., 2018). Previous results showed a positive impact of microgravity on cognitive performance and its underlying neurophysiological equivalent. Reaction time decreased in microgravity but interestingly the accuracy of the performance remained the same (Wollseiffen et al., 2019). This effect was independent of flight experience as well as space flight medication (scopolamine) but was also dependent on task complexity, whereby more complex tasks were more positively affected by microgravity (Wollseiffen et al., 2016). It might be, that cognitive performance is extremely complex and underlies numbers of influencing factors such as arousal, boredom, excitement, and stress. Humans, especially well-trained astronauts, are able to compensate these by allocating additional resources. In contrast, the visual, motor, and vestibular neural communication underlies relatively simple, but well-established neuronal communication sequences, so called engrams. Although engrams are extremely stable over time, external influences like fluid shifts as they occur during microgravity, might affect the recall of information. These observations are consistent with the model of Kohn and Ritzmann, which was developed from observations of in vitro and in vivo data and can explain changes in neural communication in weightlessness (Kohn et al., 2018). Based on the model, it was considered that the increase in intracranial pressure (ICP) during microgravity might affect these neural processing. Regarding the rationale mentioned afore, we hypothesized that either there is a graded response with respect to different levels of gravity, or that documented changes in cortical activity are dependent on a specific threshold of gravity.

MATERIAL AND METHODS

Parabolic flights take place from Merignac Airport, Bordeaux, France and carried under the lead of the European Space Agency (ESA) and the German Aerospace Centre (DLR). A parabolic flight is a specific flight manoeuvre flown by three trained pilots to induce different levels of gravity. A parabola consists of three flight phases which include two hyper-G-phases and one phase with microgravity condition. Depending on the pitch angle of the aircraft, it is possible to simulate different gravity levels. Here the results of three campaigns are presented. The first one took place in 2018 and exposed participants (n=6) to 0.25G, 0.5G, 0.75G and 1G. The second one (n=6) was carried out later in 2018, with participants performing under 0G and 1G conditions. Data of a third campaign (n=6) was recorded in November 2020 comparing 1.8G and normal gravity (1G). Prior, the experimental design of the study was approved by the Ethics Committee of the University of Caen, in accordance with the Declaration of Helsinki. Within the reduced gravity phases, the 1.8G phase as well as the steady flight, participants performed a neuro-cognitive task. This task consisted of a classic auditive oddball-paradigm and a mental arithmetic task. During the oddball-paradigm, the participants had to distinguish between high and low tones. The low tones (70% of all tones) are irrelevant, however, if a high-pitched tone occurs (30% of all tones, relevant), the participants had to react and press the space bar on their keyboard as quickly as possible. At the same time, the participants were presented with a mental arithmetic task on a screen in front of them. They had to decide between two equations displayed on the left and right side of the screen, which yields the larger result. The participants had to press the right or left arrow key on their keyboard indicating the higher value as quickly as possible. An electroencephalogram (EEG) was continuously recorded during the entire flight.

Data analysis

EEG data were processed using Brain Vision Analyzer 2.0 (Brain Products, Munich, Germany). After pre-processing the data, the integrated (Bai et al., 2007; Grech et al., 2008) module in the Brain Vision Analyzer was used to determine cortical activity. Cortical activity was defined as cortical current density and describes the amount of current in a pre-defined area. This value was calculated for the frontal lobe, parietal lobe, occipital lobe, and the region supplied by the middle cerebral artery. The data presented here are currently on a descriptive level, as the number of subjects is too low for a proper statistical analysis.

RESULTS

Comparing the 1G and 0G condition, a clearly lower cortical activity during the 0G condition can be shown (Figure 1). Comparing 1G and 1.8G (Figure 2)

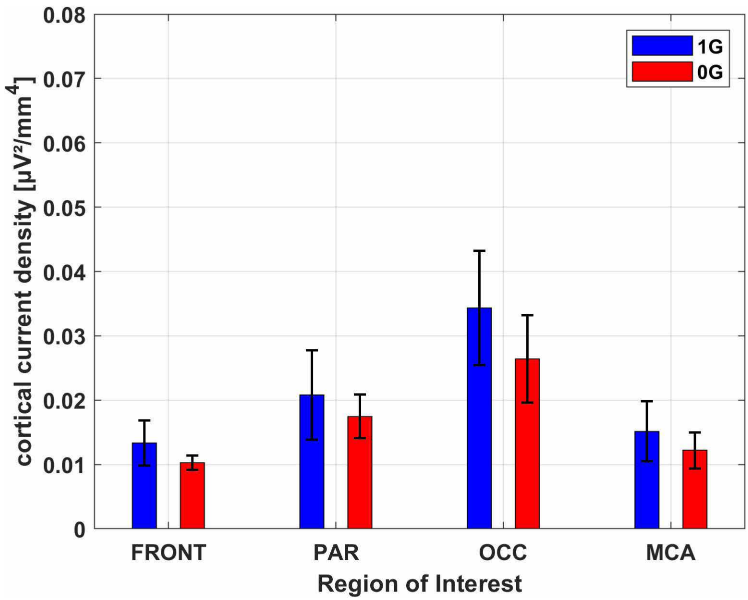

FIGURE 1: Averaged cortical activity within the frontal (FRONT), the parietal (PAR), the occipital (OCC) lobe, and the region supplied by the middle cerebral artery (MCA) in the 1G condition (blue) and 0G condition (red) for all participants (n=6). The mean values and standard deviations are shown. Data revealed a clear decrease of cortical activity in the lower gravity condition.

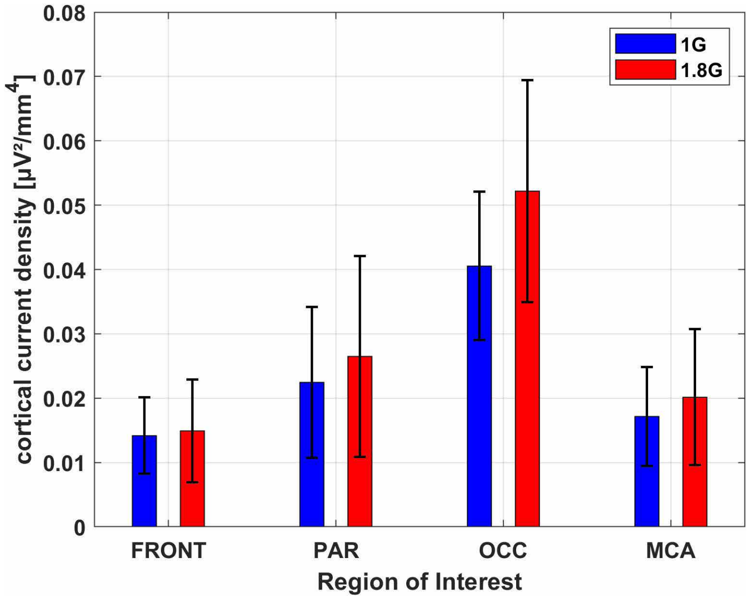

FIGURE 2: Averaged cortical activity within the frontal (FRONT), the parietal (PAR), the occipital (OCC) lobe, and the region supplied by the middle cerebral artery (MCA) in the 1G condition (blue) and 1.8G condition (red) for all participants (n=6). The mean values and standard deviations are shown. Data revealed a clear decrease of cortical activity in the lower gravity condition.

a clear decrease of cortical activity is seen in the lower gravity conditions. For the data under partial-G conditions 0.25G, 0.5G, 0.75G, 1G (Figure 3) cortical activity revealed a nearly linear relation between gravity levels and cortical activity. With decreasing gravity levels, cortical activity in the before mentioned regions decreased.

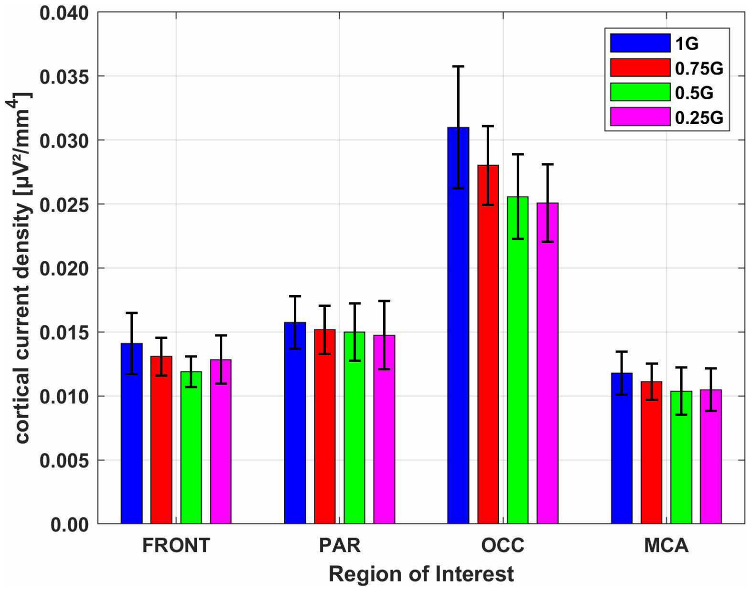

FIGURE 3: Averaged cortical activity within the frontal (FRONT), the parietal (PAR), the occipital (OCC) lobe, and the region supplied by the middle cerebral artery (MCA) in the 1G condition (blue), 0.75G condition (red), 0.5G condition (green) and 0.25G condition (purple) for all participants (n=6). The mean values and standard deviations are shown. Data showed a nearly linear decrease of cortical activity with lower gravity level.

DISCUSSION

This experiment was designed to investigate changes in cortical activity to different gravity levels and to identify if the observed changes are dependent on a threshold of gravity or if there is a linear relationship between gravity levels and cortical activity. The data displayed a decrease of cortical activity in the frontal lobe, parietal lobe, occipital lobe, and the region supplied by the middle cerebral artery of the brain with decreasing gravity levels. Previous studies showed that microgravity has an effect on neural processing. These results are in line with the in vitro data from Sieber et al. (2016) reporting an increased excitability of neurons under microgravity (Sieber et al., 2016). On a cellular level changes in the neuronal communication under microgravity are described by Kohn and Ritzmann (Kohn et al., 2018). Due to the fluid shift in microgravity, the intracranial pressure increases which correspondingly generate an increase in the lateral pressure on the neuronal cells in the brain. This increase leads to a decreased membrane viscosity and that means the membrane becomes more fluid as a result. Hanke and Schluhe (1993) further described in non-space related experiments a decrease in the open state probability of ion channels (Hanke et al., 1993), which defines the proportion of the total recording time a channel is in its open state. This leads to a slight increase in the resting membrane potential of neurons by about 3 mV and therefore makes it easier to exceed the threshold that must be reached to trigger an action potential. Due to the slightly depolarized resting membrane potential of the neuronal cells, the amplitude and regarding that, the voltage difference between the resting membrane potential and the peak of the triggered action potential is also lower. This reduction of voltage difference could explain the lower cortical activity measured during microgravity. Furthermore, the lower activity needed to trigger an action potential might be the reason of the reduction in reaction time. (Figure 4)

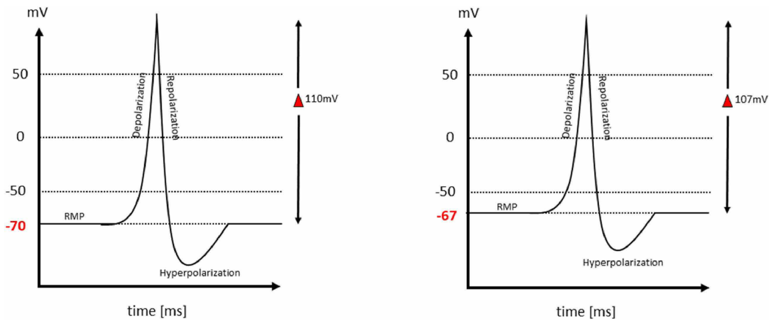

FIGURE 4: On the left side, a classic action potential of a nerve cell is shown. The resting membrane potential (RMP) is about -70mV and the voltage difference between the RMP and the peak of the action potential is 110 mV. On the right side, an action potential under microgravity is shown. Due to the fluid shift in microgravity, the intracranial pressure increases which leads to a slight increase in the resting membrane potential of about 3mV. As a result of the slightly depolarized RMP of the neuronal cells, the amplitude and the voltage difference between the RMP and the peak of the triggered action potential is also lower. This reduction of voltage difference could explain the lower cortical activity measured during microgravity.

CONCLUSION

Previous studies on neurons show an influence of microgravity on the neurophysiological properties of the cell membrane (Hanke et al., 1993; Meissner et al., 2005; Wollseiffen et al., 2019). Increased intracranial pressure due to altered fluid distribution in lower gravity changes membrane properties. However, so far these observations have been made exclusively in 0G, 1G, and 1.8G. The data presented here suggest that there is a linear relationship between gravity level and cortical activity. With decreasing gravity level cortical activity decreases as well in all brain regions. Based on this, we assume a linear, graded response of neural activity to gravity. But obviously, further data is necessary to present a sound statistical model. Microgravity in this study, however, was only present in repetitive intervals of about 20 seconds. Further studies should investigate the effect of long-term microgravity on the neurophysiological properties of observed lower cortical activity. Moreover, it needs to investigate whether these changes on a cellular level have an impact on the behavioural level like mental performance or reaction time, which would be in contrast to previous studies reporting deficits in sensorimotor performance/cognitive performance in weightlessness.

ACKNOWLEDGMENTS

The authors would like to thank all the participants that have been involved and contributed with their valuable time to this experiment. A special thank goes to the team at NOVESPACE for a great support, on earth as well as in space. This study would not have been possible without financial support from German Space Agency (DLR 50WB2020 and 50WB1561).

Keywords: Parabolic flight, EEG, cortical activity, electro-cortical processing, neurophysiology

REFERENCES

Bai, Xiaoxiao; Towle, Vernon L.; He, Eric J.; He, Bin (2007): Evaluation of cortical current density imaging methods using intracranial electrocorticograms and functional MRI. In *NeuroImage* 35 (2), pp. 598–608. doi: 10.1016/j.neuroimage.2006.12.026.

Grech, Roberta; Cassar, Tracey; Muscat, Joseph; Camilleri, Kenneth P.; Fabri, Simon G.; Zervakis, Michalis et al. (2008): Review on solving the inverse problem in EEG source analysis. In *Journal of neuroengineering and rehabilitation* 5, p. 25. doi: 10.1186/1743-0003-5-25.

Hanke, Wolfgang; Schlue, W.-R. (1993): Planar lipid bilayers. Methods and applications. London, New York: Academic Press (Biological techniques). Available online at http://site.ebrary.com/lib/alltitles/docDetail.action?docID=10665766.

Kohn, Florian P. M.; Ritzmann, Ramona (2018): Gravity and neuronal adaptation, in vitro and in vivo-from neuronal cells up to neuromuscular responses: a first model. In *European biophysics journal : EBJ* 47 (2), pp. 97–107. doi: 10.1007/s00249-017-1233-7.

Lee, Andrew G.; Mader, Thomas H.; Gibson, C. Robert; Brunstetter, Tyson J.; Tarver, William J. (2018): Space flight-associated neuro-ocular syndrome (SANS). In *Eye (London, England)* 32 (7), pp. 1164–1167. doi: 10.1038/s41433-018-0070-y.

Meissner, Klaus; Hanke, Wolfgang (2005): Action potential properties are gravity dependent. In *Microgravity Sci. Technol.* 17 (2), pp. 38–43. doi: 10.1007/BF02870977.

Sieber, Michaela; Kaltenbach, Stefan; Hanke, Wolfgang; Kohn, Florian P. M. (2016): Conductance and Capacity of Plain Lipid Membranes under Conditions of Variable Gravity. In *JBiSE* 09 (08), pp. 361–366. doi: 10.4236/jbise.2016.98031.

Wollseiffen, Petra; Klein, Timo; Vogt, Tobias; Abeln, Vera; Strüder, Heiko K.; Stuckenschneider, Tim et al. (2019): Neurocognitive performance is enhanced during short periods of microgravity-Part 2. In *Physiology & behavior* 207, pp. 48–54. doi: 10.1016/j.physbeh.2019.04.021.

Wollseiffen, Petra; Vogt, Tobias; Abeln, Vera; Strüder, Heiko K.; Askew, Christopher D.; Schneider, Stefan (2016): Neuro-cognitive performance is enhanced during short periods of microgravity. In *Physiology & behavior* 155, pp. 9–16. doi: 10.1016/j.physbeh.2015.11.036.

Role of neuronal control in development of immobilization osteoporosis

Tatyana Baltina[1]*, Daniel Shcherbakov[1], Artur Fedyanin[2], Maxim Baltin[2], Nikita Kharin[2,3], Oleg Gerasimov[3], Oskar Sachenkov[3]

[1]Department of Human and Animal Physiology, Institute of Fundamental Medicine and Biology, Kazan Federal University, Kazan, Russia
[2]Laboratory of Neurobiology, Institute of Fundamental Medicine and Biology, Kazan Federal University, Kazan, Russia
[3]Department of Theoretical Mechanics, N.I. Lobachevsky Institute of Mathematics and Mechanics, Kazan Federal University, Kazan, Russia
**tvbaltina@gmail.com*

INTRODUCTION

Osteoporosis is a musculoskeletal system disorder characterized by loss of bone mass, alteration of mechanical properties of bone, and disruption of the balance between osteogenesis and bone resorption (Frost, 2003; Sugiyama et al., 2012). Modern lifestyle shows the prevalence of loss of mobility for an average person, both in workplaces and everyday life thus making immobilization osteoporosis a high-risk disease for everybody regardless of social status or age (Sözen et al., 2017; Rolvien et al., 2020).

There are different factors that contribute to the stable functioning of the musculoskeletal system: gravitational pull (Fitts et al., 2010; Peres-Ueno et al., 2017), bearing area (De-Doncker et al., 2000; Kyparos et al., 2005), physical activity (McLaughlin, Jacobs, 2017) and innervation (Elefteriou et al., 2008; Ko et al., 2017; Ishimaru et al., 2018; Brent et al., 2020). Immobilization disrupts all factors simultaneously which could be observed in changing of different parameters of bone and muscle. Effects of these changes combine into the overall pathological state (McGee-Lawrence et al., 2008; Bettis et al., 2018; Rolvien, Amling, 2021).

The aim of this study is to evaluate the contribution of effects from disruption of different factors utilizing different techniques that simulate immobilization osteoporosis.

MATERIAL AND METHODS

The research was carried out on the no-linear rats weighing 180-200 grams. All experiments were performed in compliance with bioethical standards and approved by the Local Ethics Committee of the Kazan Federal University Protocol No. 2 of 05/29/2018.

Combined intramuscular anesthesia with zoletil used for painkiller. («Zoletil 50» «Virbac», France), 0.5 ml / kg and xylazal injection (Xylazalum, « Biogel », Belarus) 0.05 ml / kg – 0.5ml/kg. The dosage of the drug was chosen based on the weight of the experimental animal.

Animals were divided into four experimental groups:
Intact ("Con", n=6),
tenotomy only ("T", n=8),
denervation only ("D", n=10),
Hindlimb unloading+tenotomy ("HUT", n=8),
Hindlimb unloading+denervation ("HUD", n=12).

Experiment duration in days indicated by a digit after type model, e.g. HUD7 means hindlimb unloading plus denervation during 7 days.

Hindlimb unloading was performed as in Morey-Holton (1979) with custom modifications by Ilyin and Novikov (1980) (Morey-Holton et al., 1979; Ilyin, Novikov, 1980). Denervation was performed as described in Angelis et al. (1994). Animals were subjected to sciatic nerve dissection with subsequent nerve compression by a "mosquito" forceps for forty seconds (De Angelis et al., 1994). Tenotomy was performed after anesthetization in aseptic conditions. The achilles' tendon was dissected at the site of attachment to the foot. After bone extraction geometric parameters, weight and volume were measured. In order to determine the mechanical properties of bones, three-point bending tests were carried out in a specially prepared experimental setup (Baltina et al., 2017). Additionally, bones were scanned by CT to get structural data (Semenova et al., 2019; Kharin et al., 2019) and to provide numerical simulations (Sachenkov et al., 2018; Gerasimov et al., 2019).In the article results for mechanical parameters (ultimate strength and Young's modulus) are presented.

MATLAB software was used for data analyses and visualization. For determining the mean in the dataset used N-variant analysis of variance by groups of several factors. Differences are significant if $p < 0.05$. The result is presented as M ± SE (mean ± standard error of the mean).

The results in the figures are presented by boxplots, where redline – median, blue box - the first and the third quartiles, black dashes – minimum and maximum.

RESULTS

In the groups with denervation and tenotomy for 50 days, the following changes in the mechanical properties of bones were found. The ultimate strength of femoral (Figure 1) and tibial (Figure 2) bones were significantly decreased from 97 ± 1 MPa to 71 ± 2 MPa and 63 ± 1 MPa and from 190 ± 12 MPa to 147 ± 9 MPa and 113 ± 3 MPa respectively. Also the femoral (Figure 1) and tibial (Figure 2) Bones have a significant increase in Young's modulus compared to the control group (femoral: from 1219 ± 38 MPa to 2079 ± 229 MPa and 1745 ± 80 MPa; tibial: from 2293 ± 155 MPa to 3085 ± 87 MPa) excluding Young's modulus for the tibia after tenotomy.

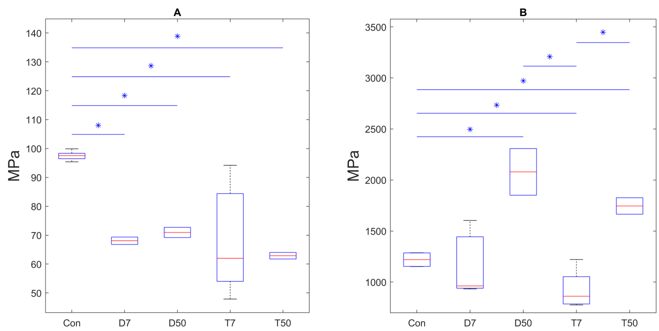

FIGURE 1: Femur mechanical properties: **A** – ultimate strength **B** – Young's modulus in different models, * - p<0.05, where Con – intact animal, D and T – denervation and tenotomy models respectively, digit after letter – experiment duration in days.

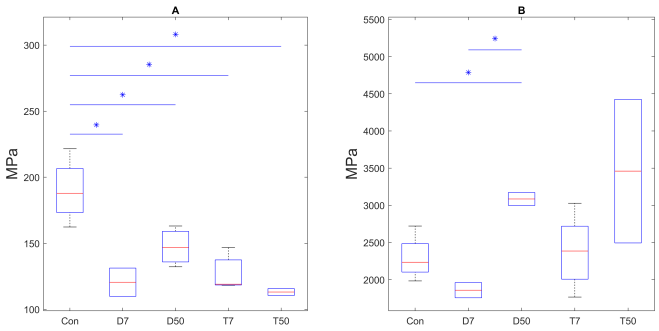

FIGURE 2: Tibia mechanical properties: **A** – ultimate strength **B** – Young's modulus in different models, * - p<0.05, where Con – intact animal, D and T – denervation and tenotomy models respectively, digit after letter – experiment duration in days.

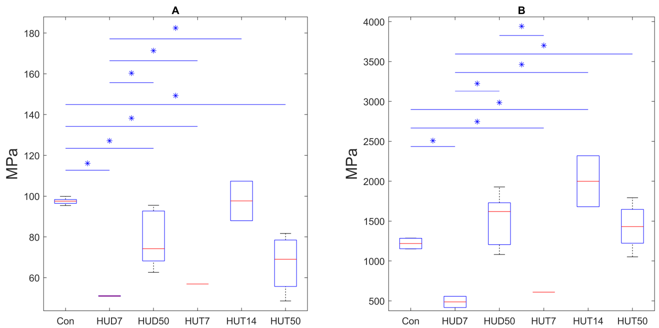

FIGURE 3: Femur mechanical properties: **A** – ultimate strength **B** – Young's modulus in different models, * - p<0.05, where Con – intact animal, HUD and HUT – hindlimb unloading with denervation and tenotomy models respectively, digit after letter – experiment duration in days.

Combining hanging rats with denervation and tenotomy, it was shown that after 50 days Young's modulus of the hind limbs decreases, the femoral (Figure 3) (from 97 ± 1 MPa to 79 ± 5 MPa and 67 ± 7 MPa) and tibial (Figure 4) (from 190 ± 12 MPa to 101 ± 4 MPa and 97 ± 7 MPa). For the femur, Young's modulus in the case of denervation did not change significantly, and in the case of tenotomy, it insignificantly increased (Figure 3). The Young's modulus

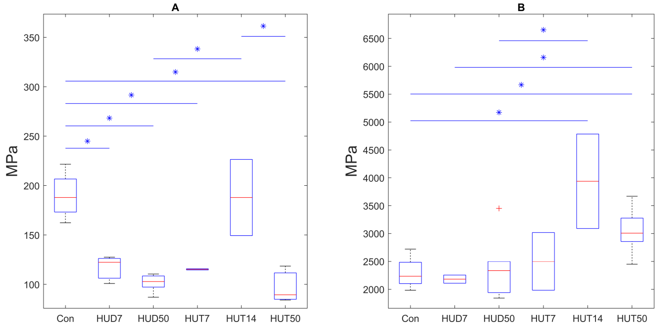

FIGURE 4: Tibia mechanical properties: **A** – ultimate strength **B** – Young's modulus in different models, * - $p<0.05$, where Con – intact animal, HUD and HUT – hindlimb unloading with denervation and tenotomy models respectively, digit after letter – experiment duration in days.

of the tibia, which has been exposed to the combined technique, increased in both cases (Figure 4).

Compared Group "HUD" didn't show significant alterations of ultimate strength in femur and forearm. Tibia and humerus show significantly lesser loss of ultimate strength than in "D" group. According to Young's modulus assessment, stiffness was significantly higher in the femur, forearm, and humerus in "HUD" group than in "D" group. The Young's modulus of the tibia was not significantly changed between groups. There were no significant changes in rigidity and Young's modulus between groups "HUD" and "T".

DISCUSSION

Through the use of a combined research technique on one object, it is possible to obtain the dependence of the influence of several factors simultaneously. The mechanical properties of bone were compared in different models, unlike other authors who usually use one method in the development of muscle disuse model. (Caron et al., 2009; Du et al., 2011; Sørensen et al., 2020). The results of the research are comparable to similar research when the mechanical properties of the hind limb bones deteriorate over time in muscle disuse models. (Yarrow et al., 2014; Cunningham et al, 2018; Friedman et al., 2019).

Results showed that factors such as muscle activity, gravity, and support afferentation have the other influence on the stiffness and ultimate strength of hind limb bone of rats. Comparing with the research by other authors shows similarities and differences with our results. In research, where immobilization was achieved by reducing the volume of the animal's cell, it was shown that the most significant effect was exerted not by the immobilization factor itself, but by the length of time during which the rats remained immobilized. (Marmonti et al., 2017). On the other hand, research, where plaster immobilization was used, showed that total immobilization time was the main factor from day 21. It has been shown that there is a significant negative correlation between immobilization time and a decrease in bone mineral density for the calcaneus and femur upon suspension (Ceroni et al., 2015). These results are consistent with the conclusion about the role of muscle loading - is to maintain the strength of the bones of the hind limbs through the action of different mechanical factors on different bones.

A significant of the study is the data obtained, which will be further used for fundamental research in the field of immobilization osteoporosis. The research has shown that maintaining the strength and stiffness of the rat hind limb bones during gravitational unloading and impaired muscle activity is due to changes in neuronal control. This fact suggests that it is necessary to additionally check the bone innervation and the interaction of the higher centers that regulate osteogenesis.

CONCLUSION

Therefore, the results show that hindlimb unloading worsens strength and stiffness in combination with denervation more than in combination with tenotomy. Hindlimb unloading by itself did not alter bone properties in combination with tenotomy. With that in mind, stiffness and strength are lower after pure tenotomy than after pure denervation. Thus, denervation effects on bone during osteoporosis are lesser than those of tenotomy. Alterations of bone properties during hindlimb unloading are dependent upon changes in neuronal control.

ACKNOWLEDGMENTS

This work was supported by the Russian Foundation for Basic Research (RFBR grant No. 20-01-00535)

Keywords: bone, hindlimb unloading, denervation, tenotomy, osteoporosis

REFERENCES

Baltina, T.V., Ahmetov, N. F., Sachenkov, O. A., Fedyanin, A. O., Lavrov, I. A. (2017). The Influence of Hindlimb Unloading on Bone and Muscle Tissues in Rat Model. Bionanoscience. 7, 67–69.

Bettis, T., Kim, B.J., Hamrick, M.W. (2018). Impact of muscle atrophy on bone metabolism and bone strength: implications for muscle-bone crosstalk with aging and disuse. Osteoporos Int. 29, 1713-1720.

Brent, M. B., Lodberg, A., Thomsen, J. S., and Brüel, A. (2020). Rodent model of disuse-induced bone loss by hind limb injection with botulinum toxin A. MethodsX. 7: 101079. doi: 10.1016/j.mex.2020.101079.

Caron, A. Z., Drouin, G., Desrosiers, J., Trensz, F., Grenier, G. (2009). A novel hindlimb immobilization procedure for studying skeletal muscle atrophy and recovery in mouse. Journal of applied physiology. 106, 2049–2059.

Ceroni, D., Martin, X., Kherad, O., Salvo, D., Dubois-Ferrière, V. (2015). Factors affecting bone mineral mass loss after lower-limb fractures in a pediatric population. Journal of Pediatric Orthopaedics. 35, 345–351.

Cunningham, H. C., West, D. W., Baehr, L. M., Tarke, F. D., Baar, K., Bodine, S. C., Christiansen, B. A. (2018). Age-dependent bone loss and recovery during hindlimb unloading and subsequent reloading in rats. BMC musculoskeletal disorders. 19: 223. doi: 10.1186/s12891-018-2156-x.

De Angelis, C., Scarfo, C., Falcinelli, M., Perna, E., Reda, E., Ramacci, M.T., Angelucci, L. (1994). Acetyl-L-carnitine prevents agedependent structural alterations in rat peripheral nerves and promotes regeneration following sciatic nerve injury in young and senescent rats. Exp. Neurol. 128, 103–114.

De-Doncker, L., Picquet, F., Falempin, M. (2000) Effects of cutaneous receptor stimulation on muscular atrophy developed in hindlimb unloading condition. Journal of Applied Physiology. 89, 2344–2351.

Du, F., Wang, J., Gao, Y., Wang, H., Wang, Q., Jiang, S., Goswami, N. (2011). A hind limb disuse model inducing extensor digitorum longus atrophy in rats: tail suspension-immobilization. Aviation, space, and environmental medicine. 82, 689–693.

Elefteriou, F. (2008). Regulation of bone remodeling by the central and peripheral nervous system. Archives of biochemistry and biophysics. 473, 231–236.

Fitts, R. H., Trappe, S. W., Costill, D. L., Gallagher, P. M., Creer, A. C., Colloton, P. A., Riley, D. A. (2010). Prolonged space flight-induced alterations in the structure and function of human skeletal muscle fibres. The Journal of physiology. 588, 3567–3592.

Friedman, M. A., Zhang, Y., Wayne, J. S., Farber, C. R., Donahue, H. J. (2019). Single limb immobilization model for bone loss from unloading. Journal of biomechanics. 83, 181–189.

Frost, H. M. (2003). Bone's mechanostat: a 2003 update. Anat. Rec. A Discov. Mol. Cell Evol. Biol. 275, 1081–1101.

Gerasimov, O.V., Berezhnoi, D.V., Bolshakov, P.V., Statsenko, E.O., Sachenkov, O.A. (2019). Mechanical model of a heterogeneous continuum based on numerical-digital algorithm processing computer tomography data. Russian Journal of Biomechanics. 23, 87–97.

Ilyin, E.A., Novikov, V.E. (1980). Stand for modelling the physiological effects of weightlessness in laboratory experiments with rats. Kosmicheskaya biologiya i aviakosmicheskaya meditsina.24, 79–80.

Ishimaru, Y., Oshima, Y., Imai, Y., Iimura, T., Takanezawa, S., Hino, K., Miura, H. (2018). Raman spectroscopic analysis to detect reduced bone quality after sciatic neurectomy in mice. Molecules. 23: 3081. doi: 10.3390/molecules23123081.

Ko, H. Y., Chang, J. H., Shin, Y. B., Shin, M. J., Shin, Y. I., Lee, C. H., Hong, J. W. (2017). Changes of lower–limb trabecular bone density after sciatic nerve transection in immature rats. Biomedical Research. 28, 8079-8084.

Kyparos, A., Feeback, D. L., Layne, C. S., Martinez, D. A., Clarke, M. S (2005). Mechanical stimulation of the plantar foot surface attenuates soleus muscle atrophy induced by hindlimb unloading in rats. Journal of Applied Physiology. 99, 739–746.

Marmonti, E., Busquets, S., Toledo, M., Ricci, M., Beltrà, M., Gudiño, V., Argilés, J. M. (2017). A rat immobilization model based on cage volume reduction: a physiological model for bed rest? Frontiers in physiology. 8: 184. doi: 10.3389/fphys.2017.00184.

McGee-Lawrence, M.E., Carey, H.V., Donahue, S.W. (2008). Mammalian hibernation as a model of disuse osteoporosis: the effects of physical inactivity on bone metabolism, structure, and strength. Am. J. Physiol. Regul. Integr. Comp. Physiol. 295, 1999-2014.

McLaughlin, M. and Jacobs, I. (2017). Exercise is medicine, but does it interfere with medicine? Exercise and sport sciences reviews. 45, 127–135.

Morey-Holton, E.R., Sabelman, E.E., Turner, R.T. and Baylink, D.J. (1979). A new rat model simulating some aspects of space flight. Physiologis. 22, 523–524.

Kharin, N.V., Gerasimov, O.V., Bolshakov, P.V., Khabibullin, A.A., Fedyanin, A.O., Baltin, M.E., Baltina, T.V., Sachenkov, O.A. (2019). Technique for determining the orthotropic properties of the bone organ according to computer tomography. Russian Journal of Biomechanics. 23, 460–468.

Peres-Ueno, M. J., Stringhetta-Garcia, C. T., Castoldi, R. C., Ozaki, G. A. T., Chaves-Neto, A. H., Dornelles, R. C. M., and Louzada, M. J. Q. (2017). Model of hindlimb unloading in adult female rats: Characterizing bone physicochemical, microstructural, and biomechanical properties. PloS one. 12: 0189121. doi: 10.1371/journal.pone.0189121.

Rolvien, T. and Amling, M. (2021). Disuse Osteoporosis: Clinical and Mechanistic Insights. Calcif Tissue Int. doi: 10.1007/s00223-021-00836-1.

Rolvien, T., Milovanovic, P., Schmidt, F. N., von Kroge, S., Wölfel, E. M., Krause, M., Busse, B. (2020). Long-term immobilization in elderly females causes a specific pattern of cortical bone and osteocyte deterioration different from postmenopausal osteoporosis. Journal of Bone and Mineral Research. 35, 1343–1351.

Sachenkov, O.A., Gerasimov, O.V., Koroleva, Y.V., Mukhin, D.A., Yaikova, V.V., Akhtyamov, I.F., Shakirova, F.V., Korobeynikova, D.A., Chzhi K.K. (2018). Building the inhomogeneous finite element model by the data of computed tomography. Russian Journal of Biomechanics. 22, 291–303.

Semenova, E., Gerasimov, O., Koroleva, E., Ahmetov, N., Baltina, T., Sachenkov, O. (2019). Automatic processing and analysis of the quality healing of derma injury. Advances in Intelligent Systems and Computing. 831, 107–113.

Sørensen, T. G., Brent, M. B., Thomsen, J. S., Brüel, A.(2020). Disuse-induced loss of bone mineral density and bone strength is attenuated by post-lactational bone gain in NMRI mice. Bone. 131: 115183. doi: 10.1016/j.bone.2019.115183.

Sözen, T., Özışık, L., Başaran, N. Ç. (2017). An overview and management of osteoporosis. European journal of rheumatology. 4, 46-56.

Sugiyama, T., Meakin, L. B., Browne, W. J., Galea, G. L., Price, J. S., Lanyon, L. E. (2012). Bones' adaptive response to mechanical loading is essentially linear between the low strains associated with disuse and the high strains associated with the lamellar/woven bone transition. Journal of bone and mineral research. 27, 1784–1793.

Yarrow, J. F., Ye, F., Balaez, A., Mantione, J. M., Otzel, D. M., Chen, C., Vandenborne, K . (2014). Bone loss in a new rodent model combining spinal cord injury and cast immobilization. J. Musculoskelet. Neuronal. Interact. 14, 255–266.

Ultimobranchial gland and mineral metabolism of amphibians and reptiles after the long space flights

Nadezhda V. Besova, Victoria I. Gulimova*, Alexandra E. Proschina, Sergey V. Saveliev

Laboratory of nervous system development, A.P. Avtsyn Research Institute of Human Morphology, Ministry of Science and Higher Education, Moscow, Russia

**gulimova@yandex.ru*

INTRODUCTION

During a long stay in weightlessness (G0), humans and many experimental animals exhibit site-specific changes in the structure and mineral composition of the extracellular matrix of bone tissue (Coulombe et al., 2020; Giuliani et al., 2018; Besova et al., 1993; Vico, Hargens, 2018). The causes of these processes, which may be associated with hormonal regulation of calcium metabolism, have been studied most poorly. In vertebrates, this regulation is based on the balance of synthesis and secretion of calcitonin (CT) and parathyroid hormone (PTH). CT is produced by C-cells of the thyroid gland and promotes active binding of Ca and P in the bone mineral composition. PTH is produced by cells of the parathyroid gland and causes demineralization of the skeleton. The study of the effect of G0 on these endocrine glands is of great interest, but in mammals both types of cells are incorporated into the thyroid gland, which makes their study extremely difficult. The advantage of amphibians and reptiles is that in them CT-secreting cells are combined into follicular ultimobranchial glands (UBG) (Besova, Savel'ev, 1993). We suggested that such animals could be an interesting model object for space research.

MATERIAL AND METHODS

UBG was studied histologically and immunohistochemically in urodelous amphibia, young mature ribbed newts (RN, *Pleurodeles waltl*), after 10-14 days of space flight. In some animals, the limbs were removed before the flight and the retina was damaged for additional load on the mineral metabolism (Besova, Savel'ev, 1993). 32 animals after 7 space flights and 79 animals from control groups were examined. After using of traditional histological methods, we counted the number of follicles, the number of secreting and dead cells. The activity of C-cells was determined using monoclonal antibodies to CT.

The bones and cartilaginous elements of the skeleton were analyzed in the same RN. The focus was on hypobranchiale, ceratobranchiale I-III basibranchiale, humerus, radius, ulna, coracoideum, protocoracoideum, scapula, sternum, ceratohyale, hypohyale. They were studied histologically, as well as using a KEVEX-S100 X-ray microspectrometer (USA) installed on a Hitachi S-500 scanning electron microscope (Japan). The ratio of elements of the entire mineral composition of the skeleton was evaluated both in the experiment and in the control.

In thick-toed geckos (TTG, *Chondrodactylus turneri*, Reptilia), UBG was not studied, but some bones of the skeleton were analyzed by X-ray microtomography. These were femur, humerus, tibia, fibula, phalangeal bones, mandibular bones and proximal tail vertebrae. We examined them by 3D-X-ray microtomography (Asadchikov et al., 2012). For chemical analysis Oxford Instruments JEOL JSM 646 OLV Scanning Electron Microscope with energy dispersion X-ray spectroscope INCA x-sight was used. 25 animals after 3 space flights (12-30 day) and 50 animals from control groups were examined. All procedures were approved by the Commission on Biomedical Ethics of the Institute of Biomedical Problems.

RESULTS

The death of C-cells in the UBG of RN during the flight was 40-60%. Mass death was accompanied by a very high synthesis and secretion of CT, which led to a 5-8-fold increase in follicle size (Figure 1, A). Thus, in G0, hypertrophy of the UBG and active secretion of CT were observed.

However, the retention of the secreted CT led in operated animals to calcification of UBG and prevented the transport of CT to target organs (Figure 1, B).

The skeleton of the limbs and the visceral skeleton of RN changed greatly in weightlessness. Resorption of both bone and cartilaginous elements occurred (Figure 2). The ossification of limbs skeleton was disturbed and the mineral composition of bones changed. Thus, in flight (F) amphibians, osteoporosis of the skeleton was stimulated and its demineralization began. Impaired proliferation of chondrocytes and osteoclasts activation led to resorption

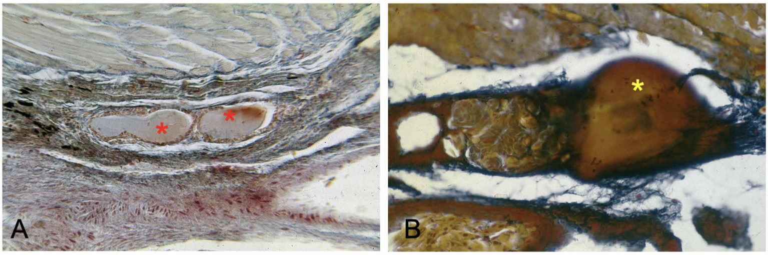

FIGURE 1: UBG of flight newts, Mallory stain. Hypertrophied follicles of intact RN are indicated by red asterisks (**A**), a calcified sarcophagus around UBG follicles of operated RN is indicated by a yellow asterisk (**B**). Magnification - 380x.

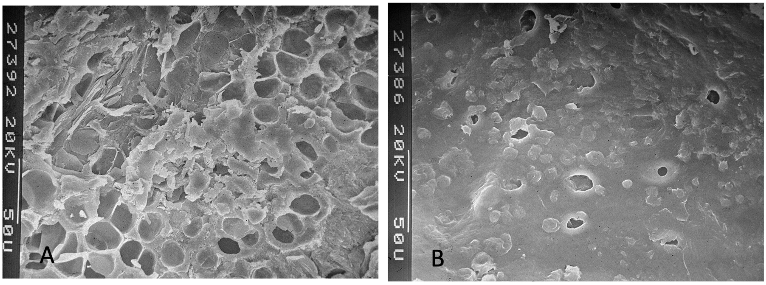

FIGURE 2: Cartilage of newts' hypobranchiale, scanning electron microscopy: flight (**A**) and control (**B**). Scale bar on the left of both photos – 50 mkm.

of trabeculae of the endochondral bone of the limbs. A mineral imbalance occurred, resulting in the loss of Ca, P, S and the accumulation of K in the cartilage and bone matrix. During the 72 day readaptation period, bones and UBG were not completely restored, and the regenerated bones had an atypical lamellar structure.

For TTG no significant differences were found between the skeletal elements of F and delayed synchronous control (DSC) groups (Figure 3).

At the same time, the bone loss that was detected for femur and tibia in groups F and DSC compared to the basal control (animals kept in vivarium) indicates that the observed demineralization was caused by the housing, and

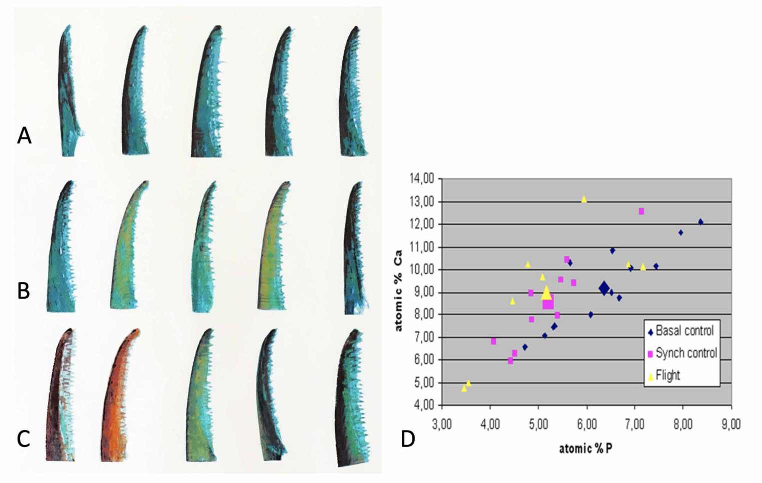

FIGURE 3: Analysis of mandibular bone tissue of TTG by X-ray microtomography and X-ray spectroscopy: flight (**A**), delayed synchronous control (**B**), basal control group (**C**). A diagram demonstrates the distribution of calcium and phosphorus in the surface layers of the bone (**D**). Magnification (**A-C**) – 2.7x.

not the influence of G0. A similar trend, but without statistically significant differences was found for mandibular bones. (Figure 3).

DISCUSSION

The available data on changes in the thyroid gland, parathyroid glands, and calcitonin-secreting cells under the influence of space flight factors are few and contradictory, and the relevance of such information is obvious. In rats that were in weightlessness for 19.5 days (biosatellite Kosmos-782), no significant structural abnormalities in the thyroid gland and the number of parafollicular cells were found in comparison with ground controls (Plakhuta-Plakutina, 1979). However, later the studies of the mouse thyroid gland after a 91-day orbital experiment on the ISS (Masini et al. 2012; Albi et al. 2017) showed that a reduction of follicular calcitonin-producing cells (C-cells) occurred in a wild-type mouse in weightlessness.

Being an anatomically separate and asymmetric organ that unites C-cells at different stages of differentiation, UBG of amphibians and reptiles is an optimal model for analyzing changes in CT secretion during the space flight. In weightlessness, UBG hypertrophy and active secretion of CT occurred in intact RN. The retention of the secreted CT was maximal in the operated flight newts during the calcification of UBG, but to a lesser extent it was also observed in intact flight newts.

The demineralization of the skeletal bones of amphibians caused by the effect of G0 may be associated with the changes found in the UBG of flight newts (Besova et al., 1993). We believe that the absence of bone loss in TTG after prolonged space flight is due to their ability to maintain adhesion to the surfaces and normal locomotion in G0; however, the mechanisms that ensure the preservation of the skeletal bones of flight geckos remain unclear.

CONCLUSION

Thus, amphibians and reptiles with C-cells isolated in the UBG are unique models for studying the hormonal regulation of mineral metabolism. Their investigation can contribute to the development of ways to preserve the health of astronauts during long space flights. Studies of the UBG and the skeleton of geckos after long-term orbital experiments are needed to determine the possible mechanisms of their interaction in weightlessness.

ACKNOWLEDGEMENTS

The study was supported by the State Scientific Center of Russian Federation Institute of Biomedical Problems of the Russian Academy of Sciences (SSCRF–IBMP RAS) and the Ministry of Science and Higher Education within the State assignment FSRC «Crystallography and Photonics» RAS.

Keywords: Bone, Ultimobranchial gland, Space flight, Amphibians, Reptiles

REFERENCES

Albi, E., Krüger, M., Hemmersbach, R. et al. (2017). Impact of Gravity on Thyroid Cells. Int. J. Mol. Sci. 18(5), 972. doi:10.3390/ijms18050972

Asadchikov, V.E.; Senin, R.A.; Blagov, A.E. et al. (2012) Comparison of the Data of X-Ray Microtomography and Fluorescence Analysis in the Study of Bone-Tissue Structure. Crystall. Rep. 57, 700–707.

Besova, N.V., Savel'ev, S.V. (1993) The influence of weightlessness of amphibians: Ultimobranchial body. Bull. Exp. Biol. Med. 7, 87-89.

Besova, N.V., Savel'ev, S.V., Chernikov V.P. (1993) The influence of weightlessness of amphibians: Skeleton and mineral metabolism. Bull. Exp. Biol. Med. 7, 90-92.

Coulombe, J.C.; Senwar B., Ferguson V.L. (2020). Spaceflight-Induced Bone Tissue Changes that Affect Bone Quality and Increase Fracture Risk. Curr. Osteoporos. Rep., doi:10.1007/s11914-019-00540-y

Giuliani, A., Mazzoni, S., Ruggiu, A. et al. (2018). High-resolution X-ray tomography: a 3D exploration into the skeletal architecture in mouse models submitted to microgravity constraints. Front. Physiol., 9, 181. doi:10.3389/fphys.2018.00181

Masini, M.A.; Albi, E.; Barmo, C. et al. The Impact of Long-Term Exposure to Space Environment on Adult Mammalian Organisms: A Study on Mouse Thyroid and Testis. PLoS ONE. 2012, 7, e35418.

Plakhuta-Plakutina, G.I. (1979). Morphological characteristics of the thyroid and parathyroid glands of rats after prolonged space flights. Kosm. Biol. Aviakosm. Med. 13, 80–84.

Vico, L., & Hargens, A. (2018). Skeletal changes during and after spaceflight. Nat. Rev. Rheumatol., 14(4), 229–245. doi:10.1038/nrrheum.2018.37

5 days of simulated microgravity promote ectopic adiposity development and ECM remodeling in skeletal muscle

Corentin Guilhot, Théo Fovet, Manon Dargegen, Manon Faedy, Rémi Roumanille, Thomas Brioche, Angèle Chopard, Guillaume Py*

INRAE, UMR Dynamique Musculaire et Métabolisme, Place Pierre Viala, Montpellier, Université de Montpellier, France

**guillaume.py@umontpellier.fr*

INTRODUCTION

Space flight involves extreme conditions to human musculoskeletal system. During these flights hypokinesia and hypoactivity lead to muscle deconditioning, characterized by a loss of muscle mass, strength and increased fatigability (Shenkman & Kozlovskaya, 2019; Vilchinskaya et al., 2015). Space flight-induced muscle deconditioning is strongly link with Inter-muscular adipose tissue (IMATs) appearance. IMATs are now well recognized as a irreversible consequence of muscle deconditioning (MD) also reported in some myopathies or even aging situation. Only few studies have documented today the kinetic of IMAT appearance during space flight or in ground-based models of microgravity. Increased IMATs contents leads to muscle dysfunctions, altering both metabolism and muscle stem cell microenvironment. Even if their accumulation is linked to muscle disuse, the precise underlying mechanisms of their origin and development are still poorly understood. Uezumi et al., 2010 described a muscle resident stem cells population positive for PDGFRα surface markers as IMATs progenitors called Fibro adipogenic progenitors (FAPs). FAPs are located between muscle fibers in muscle Extra Cellular Matrix (ECM) and have the capacity to adopt at least two different lineage (A. Uezumi et al., 2011). Indeed, FAPs could differentiate into adipocytes or myofibroblasts depending on the context. This cell population is very sensitive to muscle local environment which seems to strongly influence their fates/behaviour (Lukjanenko et al., 2019). Microenvironment is defined as the local environment surrounding cells, which contains the material and chemical signalling influencing resident cells where the major component is ECM. ECM is a network composed of several collagens isoforms, glycoproteins, proteoglycans which forms a mesh serving as both cell-binding support and factors reservoir. Therefore, ECM act on the biodisponnibility of factors and directly impact local signalling. Altered ECM becomes more permeable to harmful signals and promotes degradated microenvironment (Chen et al., 2021; Stearns-Reider et al., 2017).

The direct link established between ECM and muscle fibers, resident stem cells and local factors/pathways, seems to support a sensitive and well organize crosstalk (Lin et al., 2020; Stearns-Reider et al., 2017). It was shown during hypertrophy or aging that muscle progenitors satellite cells interact with interstitial fibrogenic cells leading to ECM remodelling (Fry et al., 2017; Mann et al., 2011) . The deregulation of this crosstalk, as can be found in MD, could have major impact on muscular function (Biferali et al., 2019).

We hypothesized that alterations of ECM structure and composition during space flight or in ground-based models of microgravity lead to altered muscle local environment and could participate to adipogenic progenitors' fate/behaviour.

The aim of this study was to decipher the role of ECM remodelling in a model of MD. Accumulating knowledge into the role of each resident cells interacting with ECM is still needed to consider further design of efficient countermeasures to prevent IMAT development. Thigh cuff, currently used to counteract microgravity-induced cardiac/ocular alterations, was tested in the present ground-based model allowing to test its potential effects on muscle homeostasis.

MATERIALS AND METHODS

This study took place in the space clinic (MEDES, Toulouse) and use the Dry Immersion (DI) model, known to generate rapid and severe MD, caused by drastic hypoactivity without mechanical stress during a short period, i.e 5 days. DI protocol involve 18 healthy men randomly assigned in two groups (Ctrl=9; age=33,8 $\pm$ 4, Thigh Cuff=9; age=33,4 $\pm$ 7) strictly lay in supine position and immersed in thermo-neutral water bath. Food intake and health status was fully monitored. Thigh cuff group wore a cuff placed in the upper tight (30-50 mmHg, 10h/days). Vastus lateralis biopsies were obtained before/after 5 days of immersion for each subject. Muscle samples were divided into several pieces to perform the following analysis. Transverse serial cross sections were used to determine both cross sectional area, PDGFRα^+ population and ECM surface area by immunohistochemistry. Protein content and gene expression were respectively assessed by Western blotting and qPCR.

Tight cuff countermeasure used in this multi-team project, was develop to limits cardio-vascular and ophthalmic but not initially to limit muscular MD. Indeed, because no differences on functional test between thigh cuff group and control group was seen at the end of DI protocol, and in order to gain statistical power, we have made the decision to pool all subjects and present "Pre-DI" vs "Post-DI" results.

RESULTS

We first confirmed that only 5 days of DI are able to impaired muscle thigh mass (-2,4%, p<0,05). Myofiber cross-sectional area was also significantly decrease after immersion (-18%, p<0,05) (Figure 1). This observation was associated to an increase in protein degradation levels and lower protein synthesis (+ 32% and-28% respectively, p<0,05). Moreover, several markers involved in development, accumulation and maturation of IMATs were significantly up-regulated after 5 days of DI. Protein level of C/EBPa, C/EBPb and PPARg were increased (Figure 2), indicating an early and later adipogenic process commitment. Perilipin-1 (PLIN-1) and fatty acid binding protein 4 (FABP4), key

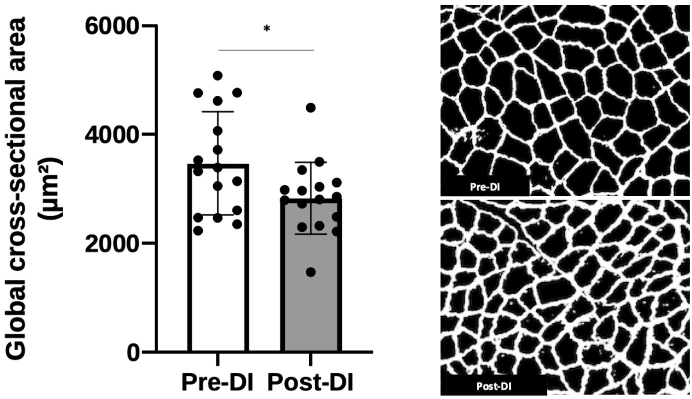

FIGURE 1: Changes in cross-sectional area (CSA) measurement after 5 days of dry immersion. CSA measurement of all vastus lateralis fibers before (Pre-DI) and after (Post-DI) 5 days of dry immersion (DI). * P<0,05.

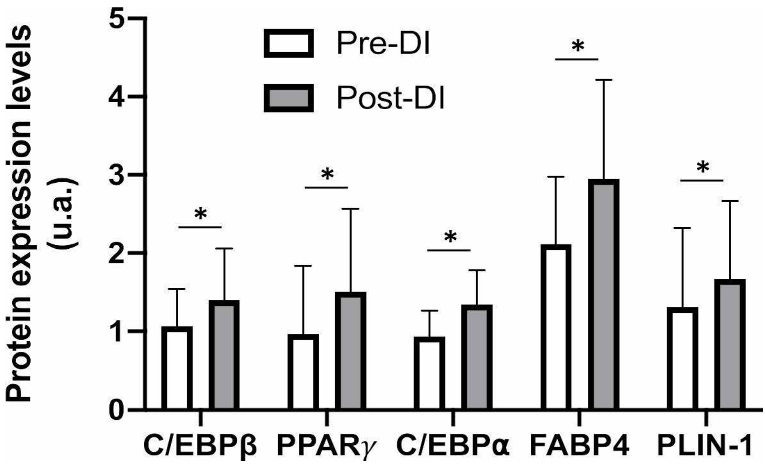

FIGURE 2: Changes in protein levels of key adipogenic markers before (Pre-DI) and after (Post-DI) 5 days of dry immersion. * P<0,05.

markers of mature adipocytes were also significantly up-regulated (+34%, +29% respectively p<0,05) (Figure 2). Both protein level (WB) and stained positive cells (IHC) for PDGFRα, a specific fibro-adipogenic progenitor (FAPs) surface marker, were increased after 5 days of DI (Figure 3).

We then focused on local muscle environment degradation. First, we showed a disorganisation in ECM structure with a decrease in both colagen1a (p=0,1), 3a, 4, fibronectin and CTGF (p<0,001) content (Figure 4). These results were reinforced by a decrease of ECM relative surface area (-37%; p<0,05) observed with Red Sirius staining (Figure 4). Moreover, our results also indicated a degradation in local signalling with a decrease in IGF1, VEGF (p<0,01) and an increase in myostatin and FGF2 (p<0,01) genes expressions (Figure 5).

As expected analysing separate groups, thigh cuff countermeasure had no preventive effect on muscle loss, IMATs development or ECM remodelling.

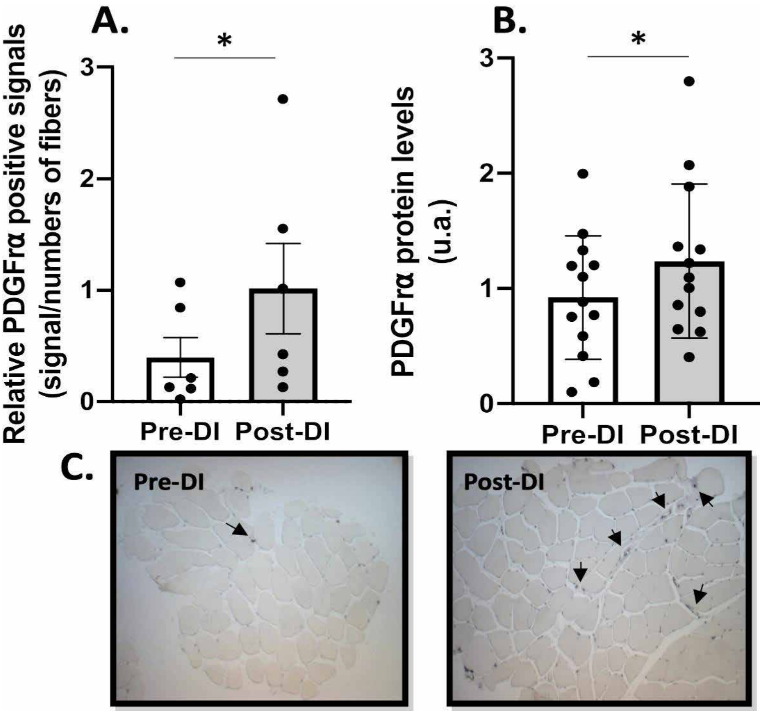

FIGURE 3: Changes in the fibro-adipogenic progenitor cells surface markers PDGFRα before (Pre-DI) and after (Post-DI) 5 days of dry immersion (DI). (**A**) Changes in relative PDGFRα-positive signals following immunosainting on transversal paraffin-embedded vastus lateralis sections after 5 days of DI. (**B**) Changes in protein levels of PDGFRα markers before and after 5 days of dry immersion. (**C**) Representative histological transversal paraffin-embedded vastus lateralis muscle sections immunostained with PDGFRα antibody, arrrows showing the staining localization. * P<0,05.

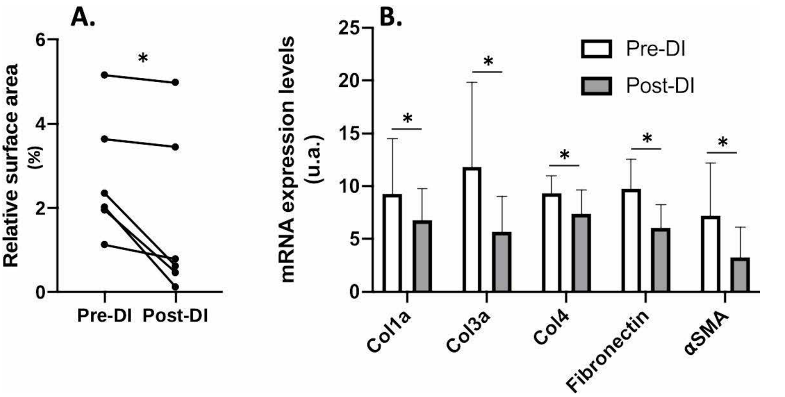

FIGURE 4: Changes in extracellular matrix structure/components before (Pre-DI) and after (Post-DI) 5 days of dry immersion (DI). (**A**) Changes in relative red sirius staining surface area in vastus lateralis after 5 days of dry immersion. (**B**) Changes in mRNA levels of key fibrotic markers before and after 5 days of dry immersion. * P<0,05.

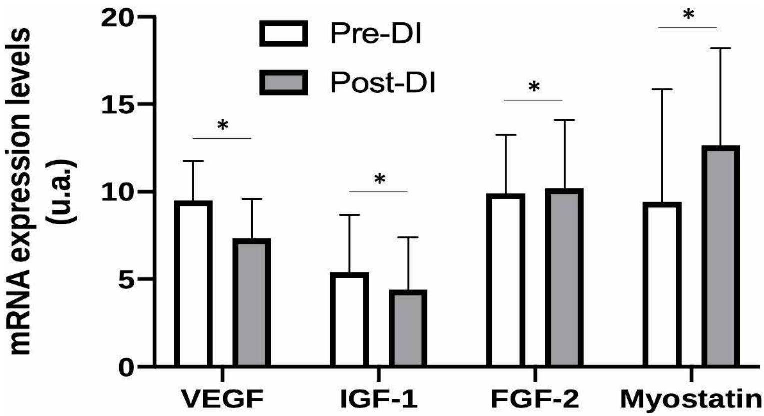

FIGURE 5: Changes in mRNA levels of key microenvironement signalling protein before (Pre-DI) and after (Post-DI). * P<0,05.

DISCUSSION

The purpose of this study aim to characterized the ectopic adipogenesis process after 5 days of DI induced DM and then decipher the mechanisms leading to development of this process in relation to muscle environment. Skeletal loss of mass is rather well characterized during space flight or microgravity models. Edgerton et al., (1985) already showed during five days of flight a decrease in CSA mean of type I and II fibers (11% and 24%). Shenkman et al., 2004 also showed a decrease of 5-9% in only three days of flight, when Widrick et al. (1999) showed a 15% to 26% diminution on both type I and Type II fiber respectively after 17 days of flight. Our results are in line with these observations with a decrease of 18% in 5 days of dry immersion. As mentioned above, IMATs appearance is strongly linked to muscle atrophy, however few studies have focused on IMATs appearance in microgravity context. A previous study, conducted by Pagano et al., (2018) on 3 days of DI showed an up-regulation of adipogenic process. Indeed, they showed a massive increase of PDGFRα signaling (+80%) following of an up regulation of C/EBPa, PPARg and mature adipocyte markers. These observations are consistent with our results and showed that proliferation of PDGFRα positive cells as well as adipogenic process is still up-regulated after 5 days of DI. We further investigated the local muscle environment remodeling and particularly ECM composition and anabolic/catabolic signaling. We showed that ECM is very responsive to external constraint, therefore 5 days of unloading seems to lead to ECM disorganization. A downregulation of ECM gene expression has been shown in soleus of sarcopenic rat (Pattison et al., 2003). We showed an downregulation of proangiogenic and anabolic growth factors VEGF an IGF-1 gene expression after DI, a result previously retrieved in other deconditioning contexts as inactivity (Lammers et al., 2013), unloading, denervation or immobilization (Timmer et al., 2018). This anabolic growth factors decrease seems to be concomitant with an up-regulation in FGF-2 and myostatin levels which could lead to decrease muscle mass. (Chakkalakal et al., 2012; Wall et al., 2014)

We showed that only 5 days of DI were sufficient to alter ECM structure and signalling in favour of catabolic process, concomitantly with a decrease muscle mass and an increase in adipogenic process.

CONCLUSIONS

Our results complete a previous similar but shorter study (3 days of DI, Pagano et al., 2018) on the concomitant early activation of atrophic process and muscle ectopic adipogenesis. This study also reveals that resident mesenchymal FAPs are the main cell population involved in muscle adiposity in human during a short period of severe inactivity. Interestingly, all these events are concomitant of an early ECM remodelling. We propose that ECM remodelling promotes FAPs proliferation/differentiation leading to an IMATs accumulation. Further experiments are needed to explore the link between muscle microenvironment and FAPs fate/behaviour.

ACKNOWLEDGMENTS

We would thank all the team of Space clinic of the institute of Space Medicine and Physiology (Medes-IMPS) in Toulouse for having organized and allowed the perfect running of the protocol. Then we would also like to thank both 'Réseau d'Histologie Expérimentale de Montpellier' (RHEM) and 'Montpellier resource imagerie' (MRI) respectively for histology (paraffin process) and microscopy (fluorescent or polarized slide scan) facilities and expertise. Thus, we would particularly acknowledge the subjects for their participations in this project.

This work was supported by the "Centre National d'Etudes Spatiales" (CNES).

Keywords: Muscle deconditioning, extracellular matrix, ectopic adiposity, stem cells, muscle progenitor's crosstalk

REFERENCES

Biferali, B., Proietti, D., Mozzetta, C., & Madaro, L. (2019). Fibro–Adipogenic Progenitors Cross-Talk in Skeletal Muscle : The Social Network. *Frontiers in Physiology*, *10*, 1074. https://doi.org/10.3389/fphys.2019.01074

Chakkalakal, J. V., Jones, K. M., Basson, M. A., & Brack, A. S. (2012). The aged niche disrupts muscle stem cell quiescence. *Nature*, *490*(7420), 355-360. https://doi.org/10.1038/nature11438

Chen, W.-J., Lin, I.-H., Lee, C.-W., & Chen, Y.-F. (2021). Aged Skeletal Muscle Retains the Ability to Remodel Extracellular Matrix for Degradation of Collagen Deposition after Muscle Injury. *International Journal of Molecular Sciences*, *22*(4), 2123. https://doi.org/10.3390/ijms22042123

Edgerton, V. R., Zhou, M. Y., Ohira, Y., Klitgaard, H., Jiang, B., Bell, G., Harris, B., Saltin, B., Gollnick, P. D., Roy, R. R., & et, al. (1995). Human fiber size and enzymatic properties after 5 and 11 days of spaceflight. *Journal of Applied Physiology*, *78*(5), 1733-1739. https://doi.org/10.1152/jappl.1995.78.5.1733

Fry, C. S., Kirby, T. J., Kosmac, K., McCarthy, J. J., & Peterson, C. A. (2017). Myogenic Progenitor Cells Control Extracellular Matrix Production by Fibroblasts during Skeletal Muscle Hypertrophy. *Cell Stem Cell*, *20*(1), 56-69. https://doi.org/10.1016/j.stem.2016.09.010

Lammers, G., van Duijnhoven, N. T. L., Hoenderop, J. G., Horstman, A. M., de Haan, A., Janssen, T. W. J., de Graaf, M. J. J., Pardoel, E. M., Verwiel, E. T. P., Thijssen, D. H. J., & Hopman, M. T. E. (2013). The identification of genetic pathways involved in vascular adaptations after physical deconditioning *versus* exercise training in humans : Vascular changes and gene expression after (in)activity. *Experimental Physiology*, *98*(3), 710-721. https://doi.org/10.1113/expphysiol.2012.068726

Lin, Y., Wen-jie, Z., Chang-qing, L., Sheng-xiang, A., & Yue, Z. (2020). Mir-22-3p/KLF6/MMP14 axis in fibro-adipogenic progenitors regulates fatty infiltration in muscle degeneration. *The FASEB Journal*, *34*(9), 12691-12701. https://doi.org/10.1096/fj.202000506R

Lukjanenko, L., Karaz, S., Stuelsatz, P., Gurriaran-Rodriguez, U., Michaud, J., Dammone, G., Sizzano, F., Mashinchian, O., Ancel, S., Migliavacca, E., Liot, S., Jacot, G., Metairon, S., Raymond, F., Descombes, P., Palini, A., Chazaud, B., Rudnicki, M. A., Bentzinger, C. F., & Feige, J. N. (2019). Aging Disrupts Muscle Stem Cell Function by Impairing Matricellular WISP1 Secretion from Fibro-Adipogenic Progenitors. *Cell Stem Cell*, *24*(3), 433-446.e7. https://doi.org/10.1016/j.stem.2018.12.014

Mann, C. J., Perdiguero, E., Kharraz, Y., Aguilar, S., Pessina, P., Serrano, A. L., & Muñoz-Cánoves, P. (2011). Aberrant repair and fibrosis development in skeletal muscle. *Skeletal Muscle*, *1*(1), 21. https://doi.org/10.1186/2044-5040-1-21

Pagano, A. F., Brioche, T., Arc-Chagnaud, C., Demangel, R., Chopard, A., & Py, G. (2018). Short-term disuse promotes fatty acid infiltration into skeletal muscle : Short term muscle disuse promotes IMAT development. *Journal of Cachexia, Sarcopenia and Muscle*, *9*(2), 335-347. https://doi.org/10.1002/jcsm.12259

Pattison, J. S., Folk, L. C., Madsen, R. W., Childs, T. E., & Booth, F. W. (2003). Transcriptional profiling identifies extensive downregulation of extracellular matrix gene expression in sarcopenic rat soleus muscle. *Physiological Genomics*, *15*(1), 34-43. https://doi.org/10.1152/physiolgenomics.00040.2003

Shenkman, B. S., & Kozlovskaya, I. B. (2019). Cellular Responses of Human Postural Muscle to Dry Immersion. *Frontiers in Physiology*, *10*, 187. https://doi.org/10.3389/fphys.2019.00187

Stearns-Reider, K. M., D'Amore, A., Beezhold, K., Rothrauff, B., Cavalli, L., Wagner, W. R., Vorp, D. A., Tsamis, A., Shinde, S., Zhang, C., Barchowsky, A., Rando, T. A., Tuan, R. S., & Ambrosio, F. (2017). Aging of the skeletal muscle extracellular matrix drives a stem cell fibrogenic conversion. *Aging Cell*, *16*(3), 518-528. https://doi.org/10.1111/acel.12578

Timmer, L. T., Hoogaars, W. M. H., & Jaspers, R. T. (2018). The Role of IGF-1 Signaling in Skeletal Muscle Atrophy. In J. Xiao (Éd.), *Muscle Atrophy* (Vol. 1088, p. 109-137). Springer Singapore. https://doi.org/10.1007/978-981-13-1435-3_6

Uezumi, A., Fukada, S., Yamamoto, N., Takeda, S., & Tsuchida, K. (2010). Mesenchymal progenitors distinct from satellite cells contribute to ectopic fat cell formation in skeletal muscle. *Nature Cell Biology*, *12*(2), 143-152. https://doi.org/10.1038/ncb2014

Uezumi, A., Ito, T., Morikawa, D., Shimizu, N., Yoneda, T., Segawa, M., Yamaguchi, M., Ogawa, R., Matev, M. M., Miyagoe-Suzuki, Y., Takeda, S., Tsujikawa, K., Tsuchida, K., Yamamoto, H., & Fukada, S. -i. (2011). Fibrosis and adipogenesis originate from a common mesenchymal progenitor in skeletal muscle. *Journal of Cell Science*, *124*(21), 3654-3664. https://doi.org/10.1242/jcs.086629

Vilchinskaya, N. A., Mirzoev, T. M., Lomonosova, Y. N., Kozlovskaya, I. B., & Shenkman, B. S. (2015). Human muscle signaling responses to 3-day head-out dry immersion. *Journal of Musculoskeletal & Neuronal Interactions*, *15*(3), 286-293.

Wall, B. T., Dirks, M. L., Snijders, T., Senden, J. M. G., Dolmans, J., & van Loon, L. J. C. (2014). Substantial skeletal muscle loss occurs during only 5 days of disuse. *Acta Physiologica*, *210*(3), 600-611. https://doi.org/10.1111/apha.12190

Widrick, J. J., Knuth, S. T., Norenberg, K. M., Romatowski, J. G., Bain, J. L. W., Riley, D. A., Karhanek, M., Trappe, S. W., Trappe, T. A., Costill, D. L., & Fitts, R. H. (1999). Effect of a 17 day spaceflight on contractile properties of human soleusmuscle fibres. *The Journal of Physiology*, *516*(3), 915-930. https://doi.org/10.1111/j.1469-7793.1999.0915u.x

The influence of perceptual constraints on bimanual coordination in simulated microgravity

Madison M. Davis[1]*, Yiyu Wang[1], Renee Woodruff[2], Traver Wright[1], Bonnie J. Dunbar[2], Ana Diaz-Artiles[2], Deanna M. Kennedy[1]

[1]*Department of Health & Kinesiology, Texas A&M University, College Station, Texas*
[2]*Department of Aerospace Engineering, Texas A&M University, city, country*
**mdavis2798@tamu.edu*

INTRODUCTION

Understanding how individuals control and coordinate movement within their environment has been the focus of a large body of research for over 50+ years (Shea et al., 2016). The general results of this line of research have indicated only two inherently stable coordination patterns: in-phase (Φ = 0°) and anti-phase (Φ = 180°); while other phase relationships (e.g., Φ = 90°) have proved difficult or near impossible without extensive training (e.g., (Fontaine et al., 1997; Lee et al., 1995; Swinnen et al., 1997). Based on non-linear dynamics, the Haken-Kelso-Bunz (HKB) model provides a formal account of the stability properties associated with coordination dynamics in Earth gravity (Haken et al. 1985). In-phase and anti-phase coordination patterns are modeled as stable fixed-point attractors while other relative phase patterns represent repellers in the attractor landscape.

The difficulty of producing complex bimanual coordination patters, such as Φ = 90°, has been typically attributed to inherent constraints (e.g, structure and/or function of neuromuscular, visual, vestibular systems). For example, strong phase attraction to inherently stable coordination modes (i.e., in-phase and anti-phase) can be associated with the activation and associated proprioceptive signals of non-homologous muscles via crossed and uncrossed cortical pathways (Swinnen, 2002). However, evidence also suggest that the difficulty may be due, in large part, to incidental constraints (perceptual, attentional, and/or cognitive factors associated with the task or the environment) (Shea et al., 2016).

Research has indicated that much of the difficulty associated with complex bimanual coordination patterns can be circumvented with relatively simple visual feedback manipulations (e.g., Lissajous feedback) that reduce the perceptual and/or attentional constraints associated with the task or task environment (Panzer et al., 2018; Shea et al., 2016). Lissajous displays integrate the position of two limbs into a single point (cursor) in one plane with one limb moving the cursor in the horizontal direction while the other limb moves the cursor in the vertical direction, much like a videogame control system. That is, one avatar is often controlled with two effectors (i.e., thumbs). Lissajous displays have been used to successfully produce a variety of bimanual coordination patterns (e.g., Kovacs et al. 2020; Wang et al., 2021) in normal gravity. It is believed that Lissajous displays provide the central nervous system (CNS) an opportunity to override the perceptual and/or neurophysiological constraints acting on the system (Shea et al., 2016).

Advances in science and technology have altered the way billions of people interact with the environment. For example, the use of virtual and augmented reality is becoming more common in domains such as education, entertainment, healthcare, military, sport, and telecommunications (e.g., Oman et al., 2021). In addition, the use of virtual reality has become a popular tool for space exploration and astronaut training (e.g., Chen et al., 2017). Yet, it is unclear if altered environmental information changes the coordination landscape. To begin the process of understanding how constraints associated with altered environments (e.g., feedback, gravity) influence coordination dynamics, an experiment was designed to assess bimanual coordination performance in simulated microgravity when visual feedback was presented via headset goggles compared to traditional feedback displays.

MATERIAL AND METHODS

Right limb dominate subjects (N=8, mean age = 21.4 SD=2.3) participated in the experiment. A tilt table was used to simulate altered gravity using a head-up tilt (HUT)/head-down tile (HDT) paradigm to compare bimanual performance between Earth (90° HUT) and simulated microgravity (6° head-down HDT) conditions (Figure 1). Participants were required to produce a continuous 1:1 bimanual force pattern with a 90° relative phase offset. Lissajous feedback information was displayed via goggles or on a screen directly in front of the participant to guide performance (see Figure 2). Participants performed 14 trials in each feedback (goggles, no goggles) and gravity (Earth, microgravity) condition, counterbalanced across conditions. Each trial was 30 s.

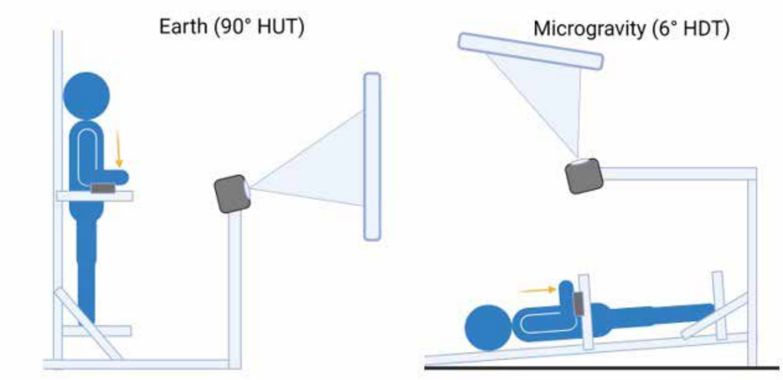

FIGURE 1: These illustrations display the position of subjects during the Earth (90° HUT) and simulated microgravity (6° HDT) condition.

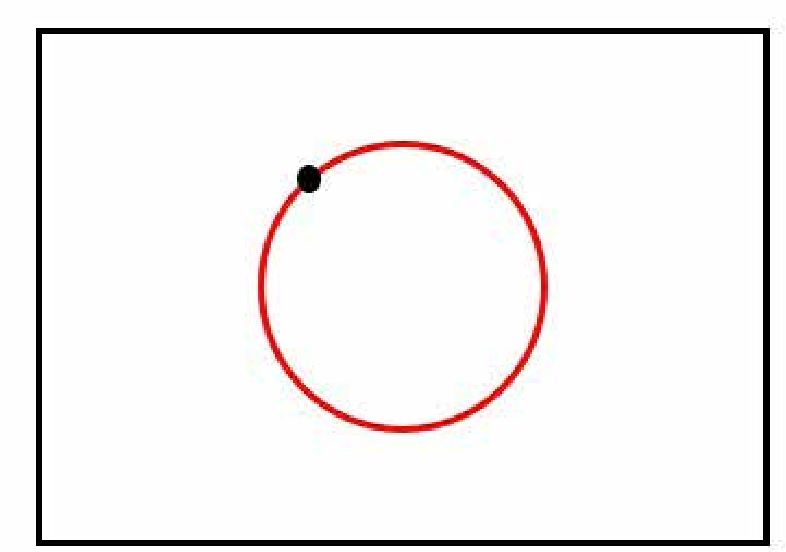

FIGURE 2: This figure represents the Lissajous plot displayed to subjects. The black cursor represents integrated feedback of the left and right limbs force output. The red circle represents the 90° relative phase coordination.

Absolute error (AE) of the continuous relative phase was used as a measure of the degree to which the required goal relative phase was achieved. Variable error (VE) was used as a measure of stability, and constant error (CE) was used as a measure of coordination bias.

RESULTS

The analysis of the relative phase AE (Figure 3) indicated a significant difference in simulated gravity environments for the no goggle condition (p=0.017). Thus, participants were more accurate (lower AE) in simulated microgravity than the Earth condition. However, differences in performance between the two gravity conditions were reduced when visual feedback was presented through goggles.

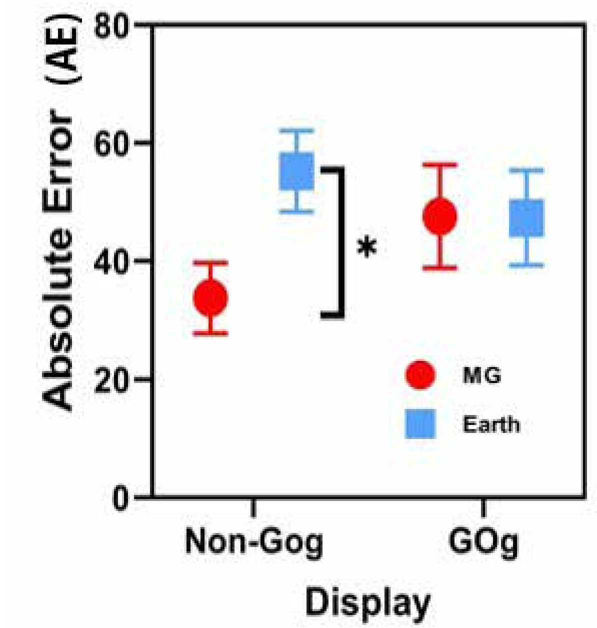

FIGURE 3: Absolute relative phase error (AE) for the Earth (90° HUT) and simulated microgravity (6° HDT) with headset goggles (GOg) and without headset goggles (Non-Gog).

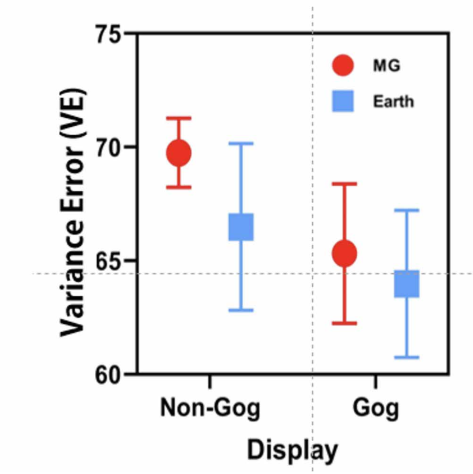

FIGURE 4: Variance error of relative phase (90°) for the Earth (90° HUT) and simulated microgravity (6° HDT) with headset goggles (Gog) and without headset goggles (Non-Gog).

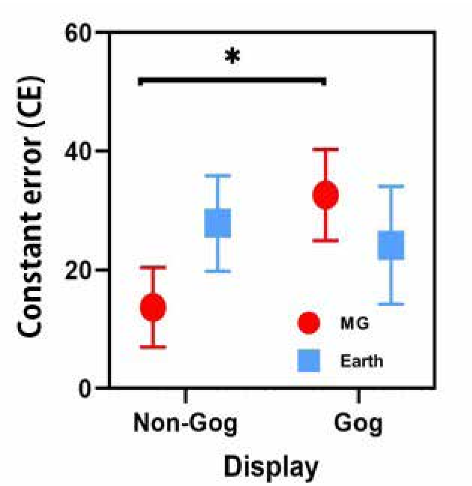

FIGURE 5: Constant relative phase error (CE) for the Earth (90° HUT) and simulated micro gravity (6° HDT) with headset goggles (Gog) and without headset goggles (Non-Gog).

The analysis of the relative phase VE (Figure 4) found no significant differences in stability between the goggle and non-goggle feedback conditions. However, the analysis of the relative phase CE (Figure 5) detected a significant difference between the two feedback conditions (goggle and non-goggle) for the simulated microgravity environment. Higher CE values, or less bias, was found for the goggle condition compared to the non-goggle condition in the microgravity environment. All other interactions were insignificant.

DISCUSSION

When participants were required to produce the goal coordination pattern using a traditional display (no-goggles) performance was more accurate in the microgravity condition than in the Earth condition. In terms of coordination dynamics, this result may suggest that neurophysiological constraints, such as neural crosstalk, are acting on the central nervous system (CNS). Neural crosstalk occurs during bimanual tasks when a mirror image of the motor command sent to one muscle group is also dispatched to the homologous muscles of the contralateral limb via crossed and uncrossed corticospinal pathways (Swinnen, 2002). Research has indicated that the effects of neural crosstalk is partially dependent on the force requirements of the task, with higher forces resulting in stronger crosstalk and lower forces in weaker crosstalk effects (Heuer et al., 2001; Kennedy et al., 2017). As such, it is possible that gravitational force acting on the body may influence an individuals' ability to effectively produce bimanual tasks. From this perspective, bimanual interference would be reduced in microgravity environments. This result may also have important implications regarding body position (supine vs. upright) during task performance.

Interestingly, there were no difference in performance accuracy when information was presented via the headset goggles during both gravity conditions. This result is consistent with previous research that has demonstrated the beneficial effects of removing vision of limbs when producing bimanual tasks (Kovacs et al., 2010). It is possible that the goggles reduce attentional demands of the task by removing non-salient environmental information during task performance while in a simulated microgravity environment. The results suggest that changes in environmental information can influence coordination dynamics. As such, researchers should recognize such limitations when using altered environments to make inferences regarding motor performance.

CONCLUSIONS

Results indicated that participants were more accurate in the microgravity condition than in the Earth condition when visual feedback was displayed on a screen directly in front of the participant. However, differences in performance accuracy between the two gravity conditions were reduced when visual feedback was presented through goggles. These results suggest that altered environmental information (gravity, display) can influence coordination dynamics. Future research should continue to explore constraints that influence coordination dynamics in altered environments.

ACKNOWLEDGMENTS

Work Supported by NASA 80NSSC20K1499

Keywords: Bimanual coordination, Simulated gravity, Augmented reality, Visual feedback

REFERENCES

Chen W.., Chao JG, Zhang Y, Wang JK, Chen XW, Tan C. Orientation Preferences and Motion Sickness Induced in a Virtual Reality Environment. Aerosp Med Hum Perform. 2017;88(10):903-910.

Fontaine R.J., Lee, T.D., Swinnen, S.P. (1997) Learning a new bimanual coordination pattern: reciprocal influences of intrinsic and to-be-learned patterns. Can J Psychol 51.

Haken, H., Kelso, J.A., Bunz, H., (1985) A theoretical model of phase transitions in human hand movements. Biol Cybern 51:347-356

Kelso, J.A.S., Scholz, J.P., Schoner, G. (1986). Nonequilibrium phase-transitions in coordinated biological motion - Critical fluctuations. Phys Lett A 118:279–284

Kovacs, A.J., Buchanan, J.J., Shea, C.H. (2010) Perceptual and attentional influences on continuous 2:1 and 3:2 multi-frequency bimanual coordination. J Exp Psychol Hum Percept Perform. Aug;36(4), 936-54. doi: 10.1037/a0019259.

Lee, T.D., Swinnen, S.P., and Verschueren, S. (1995). Relative Phase Alterations During Bimanual Skill Acquisition. J Mot Behav 27, 263-274.doi: 10.1080/00222895.1995.9941716

Oman, S. P., Magdi, Y., & Simon, L. V. (2021). Past Present and Future of Simulation in Internal Medicine. In StatPearls. StatPearls Publishing.

Panzer, P., Kennedy, D., Wang, C., Shea, C., (2017) The simplest acquisition protocol is sometimes the best protocol: performing and learning a 1:2 bimanual coordination task. Exp Brain Res 236:539-550

Shea, C.H., Buchanan, J.J., Kennedy, D.M. (2016). Perception and action influences on discrete and reciprocal bimanual coordination. Psychon. Bull. Rev. 23, 361–386.

Swinnen S.P., Lee, T.D., Verschueren, S., Serrien, D.J., Bogaerts, D. (1997) Interlimb coordination: learning and transfer under different feedback conditions. Hum Mov Sci 16:749-785

Microgravity-induced effects on motor system: Result of spinal cord stimulation and support afferentation

Artur Fedianin*, Tatiana Zaytseva, Maxim Baltin, Alexandr Eremeev, Tatiana Baltina, Anton Eremeev

Department of Human and Animal Physiology, Kazan Federal University, Kazan, Russia
**artishock23@gmail.com*

INTRODUCTION

The development of innovative therapeutic strategies aimed at preventing the consequences of unloading skeletal muscles during space missions is one of the main tasks of gravitational physiology. Mechanical unloading of skeletal muscles during space flights or its ground-based counterparts, such as bed rest and unloading of the hind endpoints in rodents, which causes skeletal muscle atrophy, which is especially related to the antigravity muscles of the lower extremities [Edgerton, Roy, 1996; Fitts, Riley, Widrick, 2000]. The effects of muscle atrophy have serious implications for different populations. As a gravitationally-dependent functional system, the human muscular system undergoes hypotrophy while being in zero gravity and under conditions of modeling its action. Astronauts must maintain optimal physical performance while performing resource-intensive and unexpected activities. Finding new training methods can help find effective ways to prevent the negative effects of decreased muscle activity.

MATERIAL AND METHODS

The experiments were carried out on Wistar rats weighing 190-210 g in compliance with all bioethical standards. We are used the rat hindlimb unloading model to simulate microgravity according to the method of Morey-Holton, Globus, 2002. Depending on the experimental conditions, the animals were randomly divided into the following groups: "HU" - animals with hindlimb unloading (n=14); "HU+ES" - animals with hindlimb unloading, combined with electrical stimulation of the spinal cord (n=9); "HU+MS" - animals with hindlimb unloading, combined with magnetic stimulation of the spinal cord (n=12); "HU+SA" - animals with hindlimb unloading, combined with the activation of supporting receptors (afferentation) (n=12). After 7, 14 and 35 days of exposure to the experimental conditions, the functional state of the central (spinal motoneurons) and peripheral (muscle fibers, neuromuscular synapse) structures of the neuro-motor apparatus of the antigravity (postural) m. soleus. For this, H-reflex, M-wave were recorded, H/M ratio, M-wave amplitude decrement during frequency stimulation, and wet and dry muscle weights were estimated. The data obtained in the study of intact animals (n=5) were used as controls. The method of video analysis of locomotor activity [Moeslund, Granum, 2001; Krishnan et al., 2015] studied the kinematic characteristics of movements. A high-precision marker system for capturing movements with 6 Vicon optical cameras (Culver City, California, USA) was used in the experiments. Passive reflective markers were placed in the projections of the hind limb joints of the rat. When the animal moves along the horizontal surface of the plane, the phases of the locomotor cycle with timestamps of events - the separation of the foot and the resumption of contact with the surface, in the joints. Kinematic analysis was performed for the complete locomotor cycle. The time of all experimental influences remained the same throughout the entire experiment. Prior to the analysis of the research results, the belonging of the animal to a particular experimental group remained coded. The control data were the data obtained in the group of intact animals (n = 7). All experimental data are presented as mean ± se. Statistical processing was performed using analysis of variance ANOVA and Student’s t-test. Significance level: * $p < 0.05$.

RESULTS

After 7 days of exposure to experimental conditions, an increase in the reflex excitability of motoneurons of the spinal motor center of m. soleus in the HU and HU+MS groups was observed, an increase in the rate of propagation of excitation along the reflex arc in the HU+ES and HU+MS groups; decrease in the reliability of neuromuscular transmission in the HU and HU+MS groups, increase in the rate of generation of the action potential of motor units m. soleus in the HU+MS group, increased synchronization of motor unit recruitment in the HU+ES and HU+MS groups, the development of atrophy in the HU, HU+ES, and HU+MS groups. After 14 days of exposure to experimental conditions, no significant changes in the recorded indicators were found in comparison with the data obtained at the previous stage of the study. However, in comparison with the control, a significant increase in the reflex excitability of the motor centers and a significant atrophy of m. soleus was found in all experimental groups. After 35 days of simulated microgravity, an increase in the reflex excitability of the spinal motor center m. soleus was record in all experimental groups; a decrease in the M-wave threshold in the HU group, a decrease in the number of activated motor units, a decrease in the reliability of neuromuscular transmission and a significant atrophy of muscle fibers was recorded in all experimental groups too. As a result of the analysis of locomotor motor activity at various periods of simulated gravitational unloading (7, 14, 35 days), changes in the angular ranges in the joints of the hind limbs were found. On average, the angle in the knee joint after the simulated gravitational unloading decreased almost twice, while jumps in the values of the angles appeared, which is associated with the sharp / "jerky" nature of the movement. In control animals, the range of angles in the hip joint was from 131° ± 2° to 142° ± 3°, for the knee joint - from 102° ± 4° to 127° ± 4°. After simulating gravitational unloading, the range of angles in the hip joint was from 154° ± 2° to 168° ± 7° ($p < 0.05$), for the knee joint - from 66° ± 16° to 168° ± 7° (p <0 , 05). Differences for the upper and lower joint angle thresholds were assessed. All values were found to be reliably distinguishable. For the hip joint, after simulating gravitational unloading, the range of angles increased by 18%, and for the knee joint, the lower threshold decreased by 35%, and the upper one increased by 31%. The movements in the hip joint remained about the same volume, but the angle of maximum extension increased. The nature of movements in the knee joint also changed - the range of motion increased and an extensor set was formed in the joint.

DISCUSSION

Electrical, but not magnetic, stimulation of the spinal cord during short-term microgravity prevents changes in reflex excitability of motor neurons and does not affect peripheral microgravitational transformations. The activation of support afferents completely excludes the effects of 7 days of simulated microgravity, but does not exclude changes in the functional state of postural neuro-motor systems under prolonged exposure to microgravity. The results obtained for assessing the kinematics of walking after gravitational unloading in the form of an extensor installation are consistent with the literature data. With a decrease in the activity of primary afferents from the corresponding extensor muscles in a state of contraction, hyperexcitability of extensor motoneurons and a discrepancy in the length of extensors and flexors [Canu, Falempin, 1997] occur, which, in turn, leads to hyperextension due to the forced position of the foot during suspension. Thus, under conditions of limiting the action of the support reaction force and axial loads and, as a consequence, changes in the intensity of peripheral afferentation, including the support one, there is a change in the functional state of the motor centers and the peripheral structures of the neuromotor systems controlled by them. The processes of gravitational-dependent motor reorganization are, first of all, and to a greater extent expressed in the tonic "anti-gravity" muscles.

CONCLUSION

Simulated microgravity initiates changes in motor systems at all levels of their organization.

ACKNOWLEDGMENTS

The reported study was funded by RFBR according to the research project No. 19-04-01067.

Keywords: stimulation, microgravity, spinal cord, soleus muscle, support afferentation

REFERENCES

Edgerton V. R., Bethesda M. D., Roy R. R. Neuromuscular adaptations to actual and simulated spaceflight//Handbook of Physiology. Environmental Physiology. – 1996. – V.1, No32. – P.721–763.

Fitts R. H. Riley D. R., Widrick J. J. Physiology of a microgravity environment invited review: microgravity and skeletal muscle [Text] // J Appl Physiol. – 2000. – vol 89. – p 823–839.

Morey-Holton E. R., Globus R. K. Hindlimb unloading rodent model: technical aspects // J. Appl. Physiol. – 2002. – Vol. 92. – P. 1367–1377.

Moeslund T. B., Granum E. A survey of computer vision-based human motion capture//Computer Vision and Image Understanding. – 2001. - V.81, No3. – P.231-268.

Krishnan C., Washabaugh E. P., Seetharaman Y. A low cost real-time motion tracking approach using webcam technology//J. Biomech. – 2015. – V.48, No3. – P.544-548.

Canu M., Falempin M. Effect of hindlimb unloading on two hindlimb muscles during treadmill locomotion in rats//Eur J Appl Physiol Occup Physiol. – 1997. V.75, No4. – P.283-288.

Characteristics of locomotion on the passive-mode treadmill at the on ground and space experiments

Elena Fomina[1]*, Danil Ivanov[2], Uliana Monakhova[2], Natalya Senatorova[1], Roman Zhedyaev[1], Alexander Meigal[3]

[1]State Scientific Center of Russian Federation - Institute of Biomedical Problems, RAS, Moscow, Russia
[2]Federal Research Center - Keldysh Institute of Applied Mathematics, RAS, Moscow, Russia
[3]Petrozavodsk State University, Petrozavodsk, Russia
**fomin-fomin@yandex.ru*

INTRODUCTION

Currently, the search for the most effective countermeasures for flights to the Moon and Mars is underway. One possible means for such missions is a passive mode treadmill. Coordination between synergist and antagonist muscles appears important for efficient motor control, both during on-Earth locomotion and activities in the conditions of real microgravity. In the Mars-500 project, where microgravity was a missing factor, we observed a time gap between recruitment of the lower limb synergists during locomotion on the leg-driven (passive-mode) treadmill (Meigal, Fomina, 2016). Also, we reported that mean frequency of surface electromyogram (sEMG) of soleus muscle has decreased after 70 days of running on the passive-mode treadmill. In this study, we evaluated coordination among the lower limb muscles under the conditions of long duration space flight (SF) onboard ISS.

The aim of the study was to develop a design of a countermeasure system for lunar and interplanetary missions testing a support unloading compensator and a cycle ergometer as promising means of preventing hypogravitational disorders in cosmonauts during a long duration SF.

MATERIAL AND METHODS

The space experiment "Profilactika-2" was conducted in the conditions of the ISS missions lasting from 138 to 205 days. The assessment of physical performance was carried out based on the MO-3 locomotor test on the

BD-2 treadmill (IBMP, Russia) in the passive (leg-driven) mode of treadmill belt movement. The test consisted of walking and slow, medium and fast running. In zero gravity conditions, an axial load of 50-70% of the cosmonaut's bodyweight was created by means of a training-load suit attached to the treadmill via carabiners. During the test the parameters of the response of the cardiovascular and respiratory systems to physical activity were recorded. Integral for heartbeats number (Pulse sum) in MO-3 test normalized to load-to-bodyweight percent ratio (iHBn) was calculated throughout the test and for 2.5 minutes of the recovery period. The distance covered during the test was

Surface electromyogram (sEMG) was obtained via "Miograf" device (Biofizpribor, Russia) from vastus lat. (VL), tibialis ant. (TA), gastrocnemius lat. (G), and soleus (Sol) muscles during the test. In 2 cosmonauts, sEMG was obtained at 2 study points - before (preSF) and during SF (inSF, days 80-85), and in 4 cosmonauts, sEMG was evaluated within the days 40-50, 80-90 and 115-120 of SF. Samples of sEMG obtained during locomotion at MO-3 test were characterized with mean frequency (MNF, Hz) and average amplitude (aEMG, mV). Coordination between Sol and G was evaluated with sEMG as the time gap between moments of their recruitment in all step cycles (ΔSol/G, ms), as it was in Mars-500 experiment.

RESULTS

The aEMG has increased and MNF decreased specifically in Sol inSF in comparison with the preSF time point. aEMG amplitude tended to increase with the growth of flight duration (p=0,08), while for MNF this influence was not significant (p=0,2). Values of ΔSol/G were highly individual in all cosmonauts and they did not modify under the conditions of SF.

After using the KOR (n=5) and the cycle ergometer (n=5) Sol aEMG has increased (Figure 1). ΔSol/G value implied Sol first to be recruited at the stages of slow running and walking (Figure 2). The tendency to change in iHBn and a decrease in covered distance during MO-3 test was identified, but no significant changes were found (Figure 3).

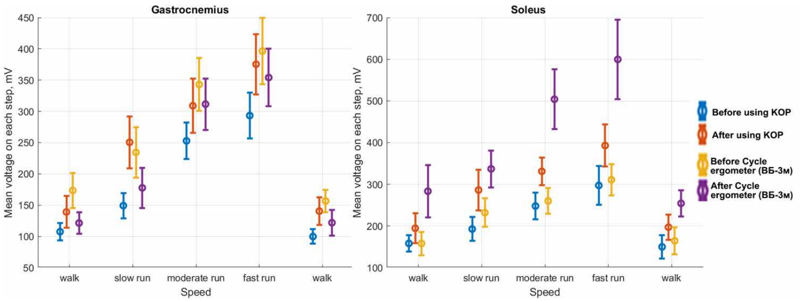

FIGURE 1: aEMG of soleus and gastrocnemius muscles at different stages of MO-3 test before and after KOR and cycle ergometer usage.

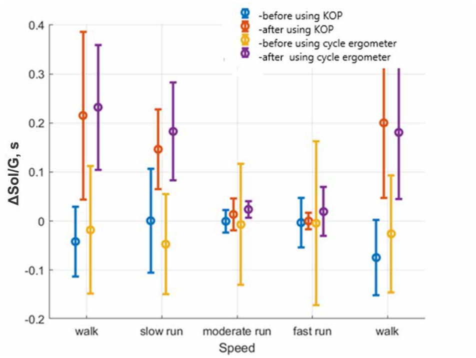

FIGURE 2: Time gap between Sol and G recruitment at different stages of MO-3 test before and after KOR and cycle ergometer usage.

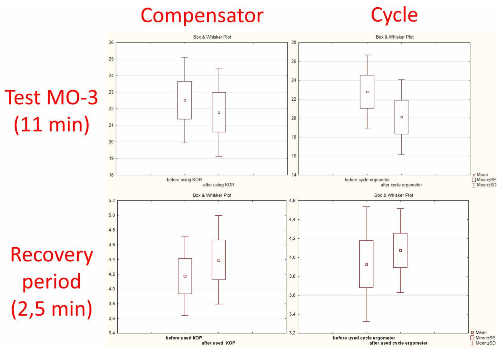

FIGURE 3: Normalized pulse sum before and after countermeasures usage.

DISCUSSION

Increased EMG amplitude during locomotion at SF was presumably produced by greater number of active motor units, supposedly to compensate for microgravity-induced atrophy. Change in muscular activation strategies after SF were shown previously (Layne et al., 1997). Current findings suggest that time spent in SF is an important factor in neuromuscular activation alterations.

CONCLUSION

An increase in the duration of zero gravity exposure leaded to an increase in the EMG amplitude and a decrease in EMG frequency. The iHBn and covered distance did not change significantly during the flight in the case of using standard countermeasure means. KOP and cycle ergometer effectiveness should be further studied as a countermeasure means.

ACKNOWLEDGMENTS

We wish to express our gratitude to cosmonauts participated in the study, flight surgeons, Russian academy of science and our international partners.

Keywords: electromyography, spaceflight, neuromuscular activation pattern, countermeasures, ISS

REFERENCES

Meigal, A., and Fomina, E. (2016). Electromyographic evaluation of countermeasures during the terrestrial simulation of interplanetary spaceflight in Mars500 project. Pathophysiology : the official journal of the International Society for Pathophysiology, 23(1), 11–18. https://doi.org/10.1016/j.pathophys.2015.10.001

Layne, C. S., McDonald, P. V., and Bloomberg, J. J. (1997). Neuromuscular activation patterns during treadmill walking after space flight. Experimental brain research, 113(1), 104–116. https://doi.org/10.1007/BF02454146

Evaluation of cardiovascular reactions in Parkinson's disease patients underwent repetitive short-term sessions of "dry" immersion for rehabilitation

Liudmila Gerasimova-Meigal[1,2]*, Alexander Meigal[1,2]

[1]Department of Human and Animal Physiology, Pathophysiology, Histology, Petrozavodsk State University, Petrozavodsk, Russian Federation

[2]Laboratory of Novel Methods in Physiology, Institute of Advanced Biomedical Technologies, Petrozavodsk State University, Petrozavodsk, Russian Federation

**gerasimova@petrsu.ru*

INTRODUCTION

"Dry" immersion (DI) is a widely recognized method for ground-based modeling of microgravity in humans, along with antiorthostatic hypokinesia (bed-rest) and parabolic flights (Pandiarajan, Hargens, 2020). In comparison to other methods, DI is considered as one of the most effective and sparing technique for microgravity modeling (Amirova *et al.,* 2020; Tomilovskaya *et al.,* 2019; Watenpaugh 2016). The knowledge from space physiology eventually has begun to be translated to the rehabilitation of patients with chronic diseases mostly to correct either increased muscle tone or elevated arterial blood pressure (BP) (Tomilovskaya *et al.,* 2019). In our earlier study, the course of seven 45-minute DI sessions exerted notable rehabilitation effect in Parkinson's disease (PD) patients (Meigal *et al*., 2020). Along with the typical motor disorders, autonomic dysfunction in PD also develops as a consequence of neurodegeneration of the central and peripheral autonomic nervous system (Jain, Goldstein, 2012; Palma, Kaufmann, 2018). Additionally, autonomic regulation largely contributes to the subjects' tolerance of DI.

This study was focused on evaluation of cardiovascular reactions and heart rate variability (HRV) in PD patients before and after a course of seven 45-minute DI sessions to assess its long-term effects on autonomic regulation.

MATERIAL AND METHODS

The study involved seven PD patients (five men and two women aged 51-66 years, staged 1-3 by H&Y scale) on the base of informative consent (Ethic committee of the Ministry of Health care of the Republic of Karelia and Petrozavodsk State University; Statement of approval No. 31, 18.12.2014). The study group met inclusion criteria for HRV analysis, such as sinus rhythm and no arrhythmia.

To induce DI condition, the "Medical facility of artificial weightlessness" (MEDSIM, Center for Aerospace Medicine and Technologies, State Scientific Center of Russian Federation "Institute of Biomedical Problems", Moscow, Russia) was used. The procedure of DI applied in this study is described in out earlier papers (Meigal *et al.*, 2018, 2020, 2021). One DI session lasted 45 minutes, the DI course comprised seven short-term DI sessions.

Blood pressure (BP) was monitored and ECG was recorded in standard lead II at a baseline test for five minutes, during deep controlled breathing (15 respiratory cycles of rate 6 min^{-1}), and during orthostatic test before (PreDI), one day (PostDI) and two weeks (2w-PostDI) after the DI course. ECG was recorded using "Poly-Spectr" device (Neurosoft, Russia). ECG records were visually inspected for stationarity, and artifacts were corrected manually. The analysis of HRV was performed in accordance with international Standards of measurement, physiological interpretation, and clinical use (Shaffer, Ginsberg, 2017). HRV analysis was performed with the help of Kubios HRV Standard (v3.4.3, Kubios Ltd., Kuopio, Finland) and included the assessment of linear (time-domain, geometric, frequency-domain) and non-linear (SD1 and SD2 of the Poincaré ellipse, ApEn, SampEn, indices $\alpha 1$ and $\alpha 2$ of DFA) parameters (Tarvainen *et al.,* 2014).

RESULTS

The data on heart rate and BP are presented on Figure 1. At baseline test before the DI course, the systolic and diastolic BP in PD patients ranged within normal values (122±14 and 73±9 mm Hg, respectively). At active orthostatic test, a modest change in systolic and diastolic BP was documented (126 ± 13 and 83 ± 7 mm Hg, respectively). Orthostatic hypotension was detected in none of the subjects.

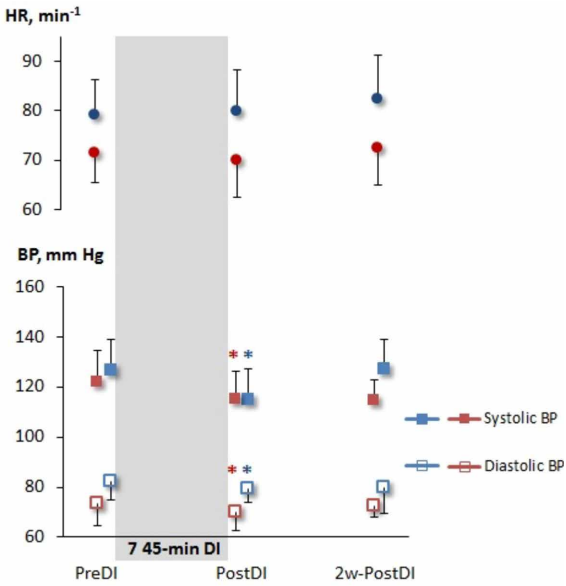

FIGURE 1: Heart rate (upper panel) and blood pressure (lower panel) at baseline (red) and orthostatic (blue) test in Parkinson's disease subjects along repetitive short-term sessions of "dry" immersion. Grey zone depicts the course of DI sessions.
The significance of differences in comparison to the baseline condition * - p<0.05.

HRV data are presented on Table 1. Low values of time- (SDNN, RMSSD, pNN50), geometric (TINN), and frequency-domain HRV parameters (total power (TP), LF- and HF-frequency bands) were characteristic of baseline and cardiovascular tests, what indicated on reduced autonomic neurogenic control of the heart rate in PD patients. Nonlinear HRV parameters during baseline and cardiovascular tests were indicative of lesser complexity of the mechanisms of heart rate regulation (Javorka *et al.*, 2002; Pursiainen *et al.*, 2002).

After the DI course, the parameters of BP have modestly decreased at baseline and orthostatic tests (p<0,05). The reactivity of the autonomic nervous system according to the HRV analysis in the deep breathing and in the active orthostatic tests did not differ significantly from the initial (PreDI) parameters.

Table 1: Results of the analysis of heart rate variability in patients with Parkinson's disease before (PreDI) and after a course of "dry" immersion (PostDI). Data are presented in format *Me* (0.25; 0.75)

Parameter	PreDI	PostDI
Baseline test		
RR, ms	857 (775; 911)	866 (767; 975)
SDNN, ms	15,3 (11,6; 32,3)	15,8 (13,5; 22,3)
HR_{mean}, min^{-1}	70 (66; 77)	69 (62; 78)
RMSSD, ms	14,5 (10,7; 25,0)	14,3 (10,3; 17,2)
pNN50, %	0,28 (0,00; 5,98)	0,28 (0,00; ,66)
TINN	91 (63; 150)	85 (70; 110)
SI	17,7 (14,0; 23,0)	20,2 (18,2; 22,1)
VLF, ms^2	11 (7; 32)	22 (10; 29)
LF, ms^2	214 (110; 995)	112 (69; 187)
HF, mc^2	70 (45; 315)	58 (43; 79)
TP, ms^2	286 (149; 1131)	198 (175; 282)
LF/HF	2,258 (1,577; 4,036)	2,269 (1,199; 3,425)
%VLF	4,21 (2,62; 6,56)	9,67 (5,07; 18,55)
%LF	67,50 (57,64; 74,57)	60,49 (46,23; 72,12)
%HF	29,27 (18,50; 36,55)	24,91 (20,65; 41,06)
LFn.u.	69,31 (61,18; 80,13)	69,38 (54,52; 77,40)
HFn.u.	30,69 (19,86; 38,79)	30,58 (22,60; 45,46)
SD1	10,3 (7,6; 17,7)	10,1 (7,7; 12,2)
SD2	19,7 (15,4; 43,1)	20,1 (15,6; 30,0)
SD2/SD1	2,011 (1,718; 2,631)	1,985 (1,832; 2,290)
ApEn	1,156 (1,108; 1,199)	1,179 (1,084; 1,204)
SampEn	1,680 (1,496; 1,757)	1,821 (1,551; 1,900)
DFA:α1	1,199 (0,980; 1,280)	1,097 (1,006; 1,278)
DFA:α2	0,303 (0,237; 0,391)	0,399 (0,326; 0,545)
Deep breathing		
RR, ms	846 (774; 885)	871 (777; 948)
SDNN, ms	43,2 (22,1; 80,7) **	47,3 (27,5; 62,9) ***

HR_{mean}, min^{-1}	71 (68; 78)	69 (63; 77)
RMSSD, ms	29,1 (16,1; 64,5)	39,3 (17,2; 55,7) **
pNN50, %	6,25 (0,56; 23,35)	12,82 (0,00; 23,38)
TINN	197 (121; 324) *	259 (116; 279) **
SI	9,4 (5,9; 17,0) *	8,0 (7,7; 17,3) **
SD1	20,60 (11,40; 45,80)	27,90 (12,20; 39,50) ***
SD2	59,00 (29,10; 100,10) **	61,00 (37,50; 80,00) ***
SD2/SD1	2,511 (2,186; 3,626) *	2,361 (2,186; 3,260) *
ApEn	0,745 (0,501; 0,759) ***	0,731 (0,658; 0,767) ***
SampEn	0,951 (0,554; 1,089) ***	0,943 (0,902; 1,044) ***
DFA:α1	1,559 (1,308; 1,649) ***	1,363 (1,254; 1,581) **
DFA:α2	0,094 (0,069; 0,169) ***	0,118 (0,093; 0,132) ***
Active orthostatic test		
RR, ms	793 (703; 819) **	756 (682; 824) **
SDNN, ms	18,0 (12,5; 22,4)	21,3 (12,0; 26,5)
HR_{mean}, min^{-1}	76 (73; 85) **	76 (73; 88) **
RMSSD, ms	11,3 (8,4; 15,3)	12,9 (7,4; 14,7)
pNN50, %	0,00 (0,00; 0,58)	0,00 (0,00; 0,57)
TINN	90,0 (64,0; 108,0)	107,0 (61,0; 138,0)
SI	19,2 (17,3; 20,7)	19,2 (15,5; 27,1)
VLF, ms^2	33 (16; 118)	38 (5; 73)
LF, ms^2	150 (92; 404)	337 (29; 554)
HF, mc^2	47 (11; 90)	48 (10; 55)
TP, ms^2	294 (156; 525)	439 (83; 714)
LF/HF	4,546 (3,874; 6,780)	9,613 (2,368; 11,303) *
%VLF	19,26 (8,45; 23,15) *	10,64 (6,10; 13,79)
%LF	66,17 (52,23; 74,76)	76,64 (62,82; 86,26) *
%HF	14,56 (10,65; 19,06)	9,32 (6,18; 26,53) *
LFn.u.	81,96 (79,48; 87,13) *	90,58 (70,30; 91,86) *
HFn.u.	18,03 (12,85; 20,52) *	9,42 (8,13; 29,69) *
SD1	8,0 (5,9; 10,8)	9,1 (5,2; 10,4)

SD2	22,0 (16,1; 29,9)	28,8 (13,8; 35,8)
SD2/SD1	2,843 (2,342; 3,101) **	3,471 (2,004; 3,774) **
ApEn	1,160 (1,138; 1,215)	1,110 (1,045; 1,183)
SampEn	1,574 (1,401; 1,745)	1,431 (1,265; 1,660) *
DFA:α1	1,453 (1,308; 1,520) **	1,556 (1,155; 1,703) *
DFA:α2	0,522 (0,380; 0,719) ***	0,455 (0,307; 0,593)

Significance of differences in comparison to the baseline test according to Wilcoxon, Mann-Whitney, Spearman criteria * - p <0.05; ** - p <0.01; *** - p <0.001.

Two weeks after the DI (2w-PostDI) course, systolic and diastolic BP at the baseline test remained at the level of 114 ± 9 and 72 ± 4 mm Hg, respectively, and the main characteristics of HRV were similar to those of PostDI (see Figure 1).

DISCUSSION

The decrease in baseline BP found in our study after the DI course allows to document the hypotensive effect of DI. According to a study (Ogoh *et al.*, 2019), the hypotensive effect in DI conditions is characterized by a decrease in BP by an average of 8-10 mm Hg. and usually it is observed during the first day of DI. Therefore, short-term DI sessions with duration of two hours and even shorter sessions (45 minutes) can be suggested as optimal for using DI in rehabilitation programs. The HRV analysis made before the DI course showed that patients with PD had significant deficit in autonomic neurogenic regulation of the heart rate. These features of HRV can be associated both with age-related changes (Shaffer, Ginsberg, 2017) and neurodegeneration in the central nervous system in PD (Jain, Goldstein, 2012; Palma, Kaufmann, 2018). Cardiovascular tests in patients with PD have revealed decreased autonomic neurogenic reactivity, what is in line with other studies. Thus, the data of the time-domain HRV analysis reflect decreased cardiorespiratory coupling at rest and during deep breathing due to a deficiency of parasympathetic (vagal) influences. The temporal structure of HRV in patients with PD, seen with non-linear parameters of HRV, has not change by the course of DI sessions; neither did it during baseline recording, nor during cardiovascular tests. Similar data were obtained in the study of Rocha *et al.* (2018) who assessed HRV with the same Kubios-based metrics after applying game-based methods for the rehabilitation of patients with PD. A similar discrepancy between the clinimetric and instrumental data was noted in the study of motor and cognitive functions in patients with PD during the course of DI (Meigal *et al.,* 2020).

CONCLUSION

Thus, the major outcome of our research was that repetitive short-term DI sessions produced modest hypotensive effect in patients with PD. The permanent autonomic failure associated with the neurodegenerative process, documented in PD subjects by means of HRV analysis, had not improved or been modulated by the DI course, unlike to some motor or cognitive functions (Meigal *et al*., 2020). Therefore, the reduced autonomic reactivity in PD patients requires, primarily, careful examining of subjects when using DI for the purpose of rehabilitation, and also monitoring their cardiovascular function during DI. Therefore, preliminary evaluation of the autonomic regulation in subjects is of great importance to predict his/her tolerance of DI. This would become even more important for older subjects, which are supposed to undergo the DI procedure or real space flight as tourists.

ACKNOWLEDGMENTS

This research was financially supported by the Ministry of Science and Higher Education of the Russian Federation (Theme No. 0752-2020-0007).

Keywords: Dry immersion, Parkinson's disease, Heart rate variability, Deep breathing, Active orthostatic test

REFERENCES

Amirova, L., Navasiolava, N., Rukavishvikov, I., Gauquelin-Koch, G., Gharib, C., Kozlovskaya, I., Custaud, M. A., and Tomilovskaya, E. (2020). Cardiovascular System Under Simulated Weightlessness: Head-Down Bed Rest vs. Dry Immersion. Front. Physiol. 11:395. doi: 10.3389/fphys.2020.00395.

Jain, S., Goldstein, D.S. (2012) Cardiovascular dysautonomia in Parkinson disease: from pathophysiology to pathogenesis. Neurobiol Dis. 46(3):572-580. doi: 10.1016/j.nbd.2011.10.025.

Javorka, M., Zila, I., Balhárek, T., & Javorka, K. (2002). Heart rate recovery after exercise: relations to heart rate variability and complexity. Braz J Med Biol Res. 35(8): 991–1000. doi: 10.1590/s0100-879x2002000800018.

Meigal, A.Y., Gerasimova-Meigal, L.I., and Saenko, I.V. (2020) Physiological reactions of patients with parkinsonism to simulated microgravity using "dry" immersion: a pilot study. Hum Physiol, 46:579–586. https://doi.org/10.1134/S0362119720050096.

Meigal, A., Gerasimova-Meigal, L., Saenko, I., and Subbotina, N. (2018). Dry immersion as a novel physical therapeutic intervention for rehabilitation of Parkinson's disease patients: a feasibility study. Phys. Med. Rehab. Kuror. 28:275–281. doi: 10.1055/a-0577-5139

Meigal, A.Y., Tretjakova, O.G., Gerasimova-Meigal, L.I. and Sayenko, I.V. (2021b). Program of Seven 45-min Dry Immersion Sessions Improves Choice Reaction Time in Parkinson's Disease. Front. Physiol. 11:621198. doi: 10.3389/fphys.2020.621198

Ogoh, S., A. Hirasawa, S. de Abreu, P. Denise and H. Normand (2017). Internal carotid, external carotid and vertebral artery blood flow responses to 3 days of head-out dry immersion. Experiml Physiol, 102(10):1278-1287. doi: 10.1113/EP086507.

Palma, J.A., Kaufmann, H. (2018) Treatment of autonomic dysfunction in Parkinson disease and other synucleinopathies. Mov Disord. 33(3):372-390. doi: 10.1002/mds.27344.

Pandiarajan, M., Hargens, A.R. (2020) Ground-Based Analogs for Human Spaceflight. Front. Physiol. 11:716. doi: 10.3389/fphys.2020.00716.

Pursiainen, V, Haapaniemi, TH, Korpelainen, JT, Huikuri, HV, Sotaniemi, KA, Myllylä, VV.. (2002). Circadian heart rate variability in Parkinson's disease. J Neurol, 249(11):1535–1540. doi: 10.1007/s00415-002-0884-0.

Rocha, R., De Oliveira Rocha, L. S., Pena, E., Caldas, LCP, Moreno, MA. (2018). Analysis of autonomic modulation of heart rate in patients with Parkinson's disease and elderly individuals submitted to game therapy training. Geriatr Gerontol Int 18(1):20–25. doi: 10.1111/ggi.13130.

Shaffer, F., Ginsberg, J.P. (2017) An overview of heart rate variability metrics and norms. Front Public Health, vol. 5. pp. 258. doi: 10.3389/fpubh.2017.00258.

Tarvainen, M. P., Niskanen, J. P., Lipponen, J. A., Ranta-Aho, P. O., and Karjalainen, P. A. (2014). Kubios HRV-heart rate variability analysis software. Comput Methods Programs Biomed. 113(1):210-20. doi: 10.1016/j.cmpb.2013.07.024.

Tomilovskaya, E., Shigueva, T., Sayenko, D., Rukavishnikov, I., and Kozlovskaya, I. (2019). Dry immersion as a ground-based model of microgravity physiological effects. Front. Physiol. 10:284. doi: 10.3389/fphys.2019.00284

Watenpaugh, D. E. (2016) Analogs of microgravity: head-down tilt and water immersion. J Appl Physiol (1985), 120: 904-914. doi: 10.1152/japplphysiol.00986.

Central compensation of x-irradiation on locomotion: Preliminary study for space radiation

Gyutae Kim[1,2]*, Mi-Hyun No[1,2], Nara Shin[1], Kyu-Sung Kim[1,2,3]

[1]*Research institute for Aerospace Medicine, Inha University, InCheon, Korea*
[2]*Medical Research Institute, Inha University, InCheon, Korea*
[3]*Department of Otolaryngology, Inha University Hospital, InCheon, Korea*
*kimg@inha.ac.kr

INTRODUCTION

The effects of irradiation are accumulated in the body during the exposure, and the effects last for some periods of time. Despite of the radial difference between x-rays and the ionizing radiation in the space (space radiation), x-ray has been widely adopted to assess its relevant biological effects due to its easy control [Kim et al., 2015; Miyahara et al., 2016; Kim et al., 2019]. Compared to the space radiation, the biological effects by x-ray were limited at low dose level [Miyahara et al., 2016]. Cell viability and apoptosis in the liver also showed the limited effects by x-irradiation depending on its total dose [Abdelrazzak et al., 2019]. The comparison of effects in x-irradiation indicated that the irradiated dose induced less cell viability and more apoptosis in the relatively higher (2Gy) than the other (10cGy) [Abdelrazzak et al., 2019]. In the experiment using 6000-7000R (same as 60-70Gy) x-irradiation, the physical damages of the peripheral sensory cells in the cristae ampullares were observed, but only half of animals (8/16) were reported to show postural instability during voluntary walking or upright standing [Winther et al., 1969]. As shown in the results, the effects even by the high-dose irradiation was unpredicted. Moreover, a recent report suggested these damages were temporary and appeared in delayed [da Silva et al., 2020]. Although a radiational technique has been widely used in medical treatments, the consequences in the high dose of x-irradiation (>10Gy) are still arguable. Especially, few studies have explored the effects on motor control by x-irradiation, and most relevant research focused on molecular and cellular responses [Tada et al., 2000; Kim et al., 2015; Miyahara et al., 2016; Shimura et al., 2016; Zhang et al., 2019]. In this study, we attempted to revisit the effects of x-irradiation, and this study tried to explain the arguments in the mismatched responses between the molecular and the kinetic responses.

MATERIAL AND METHODS

All experimental procedures and the laboratory animal care in this study were verified and approved by Inha University Animal Ethics Committee (INHA 200721-703). Rodents (SD rats, male) were used, and the animals were exposed to x-ray (dose rate : 2.46 Gy/min) by different total doses ranged from 10 to 50 Gy. As the dose rate was consistantly maintained, the total dose was determined by controling the exposing time to x-irradiation. To avoid the disturbance of x-ray transmission, the animals were placed in a transparent box (W×D×H : 38×22×18 cm), and it was wrapped by a a fabric mesh. Also, the number of animal was limited up to three at a time to allow the animals have a space for their movements during the x-irradiation. The kinetic function was assessed using rota-rod and foot pressure tests for the locotmoion and the postural balnce, respectively, which were closely related with the general vestibular functions. The rota-rod test measured the animals' maintaining time on the rolling rod (expected at least 5 minutes for the control group), and a well locomotion was evaluated based on the time (sec). The test of foot pressure allowed to quantify the postural balance by comparing the left and the right foot pressures (kPa). Especially, the moving velocity was also recorded during the foot pressure test, and a possibe effect by the velocity was minimized in the results of the foot pressure. All tests were repeated in 3-5 times, and the average and the standard deviation were calculated to compare the kinetic function before and after the x-irradiation. Using the isolated myofibers from the skeletal muscle, the mitochondrial function was examined, and the functional indicators were mainly estimated based on the oxygen (O_2) respiration, the hydrogen peroxide (H_2O_2) emission, and calcium ion (Ca^{2+}) retention. Of the skeletal muscles, the different types, type I and II, were separately examined, and the soleus muscle and the white gastrocnemius muscle were selected as a representative muscle for type I and II, respectively. To identify the damages in the central vestibular system, we examined the cell apoptosis through immunohistochemistry, showing the increase of caspase-3 enzyme activation and TUNEL assay analysis. The immunochemistry was conducted on the vestibular nucleus (VN), which was a core area in the central vestibular system. Three μm-thick slices of VN were proceeded to leave histochemical stains, and the images were prepared to count the relevant enzyme and DNA fregmentation in both methods before and after x-irradiation. The overall process was presented in Figure 1.

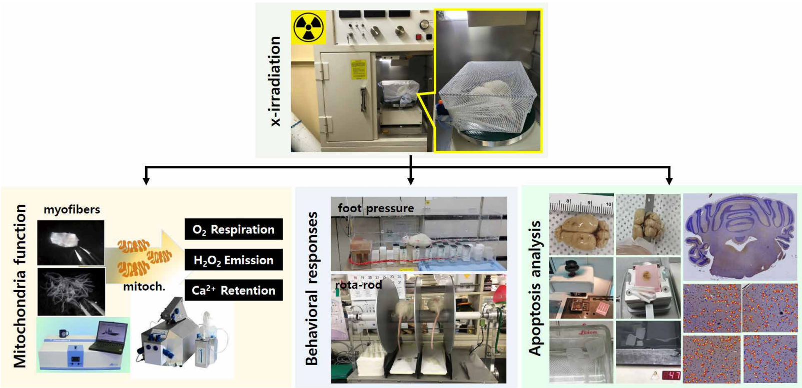

FIGURE 1: Overview of experimental process. Exposure to x-irradiation produced radiated animal models, and the models were used to assess mitochondria function, behavioral responses, and apoptosis. Total amounts of x-ray dose were three types, such as 10Gy, 25Gy, and 50Gy, and the behavioral test was initially applied to examine the effects on the controls for locomotion (rota-rod) and balance (foot pressure). The effects at a molecular level was investigated based on the mitochondrial function, and those at the central vestibular system was done by the cell apoptosis analysis.

RESULTS

Fourteen rats (SD, 363.3±6.9g, M) were used, and the same animals were used for the examination of the mitochondrial functions as they completed the kinetic tests. As explained, the kinetic performances were evaluated based on the locomotional control and the postural balance, and the rota-rod and the foot pressure were adopted, repectively. The group of controls reached the expected time (296.74±17.72 sec) with several training sessions in the rota-rod test (Figure 2A). On the other hand, the x-irradiated animals spent longer time to reach the expected time on the rod, indicating that the x-irradiation affected the locomotional control. However, the irradiated group to 25Gy showed few effects on the locomotion by showing the learning curve was not different from that of control group (Figure 2A). Considering the accumulation of x-irradiated effects, the outcomes of 25Gy could not be better than those of 10Gy, and the current results of the locomotional control hardly confirm the effects of x-irradiation well. The results of foot pressure also supported our current provision. The examination of the balance based on the foot pressure revealt no skewed pressure, which indicated there was no effect

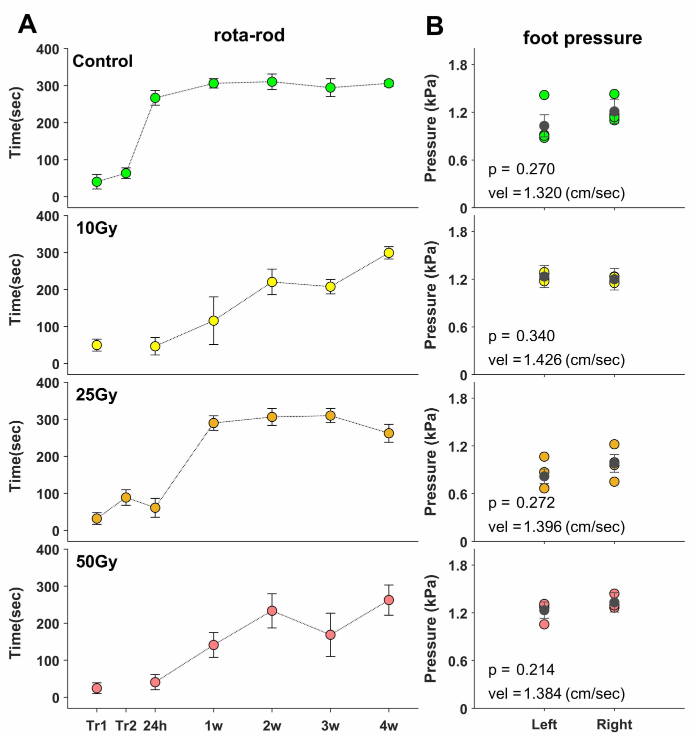

FIGURE 2: Locomotional responses (**A**) and postural balance (**B**) by rota-rod and foot pressure, respectively. Depending on the total amount of x-irradiation, animals were grouped as control (green), 10Gy (yellow), 25Gy (orange), 50Gy (red) during a long term (up to 4 weeks). Foot pressure was measured at 24 hours later after x-irradiation. The p-values showed the difference of pressure between the left and the right sides. During the repeated measurement, the moving velocity (cm/sec) was recorded, and the average was indicated in the figure.

on the postural balance by x-irradiation (Figure 2B). Unlike the results of the kinetic responses, the functional test in the mitochondria of the skeletal muscles showed some positive clues to show the damages by x-irradiation. Using different types of muscle fibers, two primary factors demonstrated that x-irradiation damaged the mitochondria functions. The responding O_2 respiration and Ca^{2+} retention capacity reduced their amounts depending on the total mount of x-irradiation in both types (Figure 3). The decrease

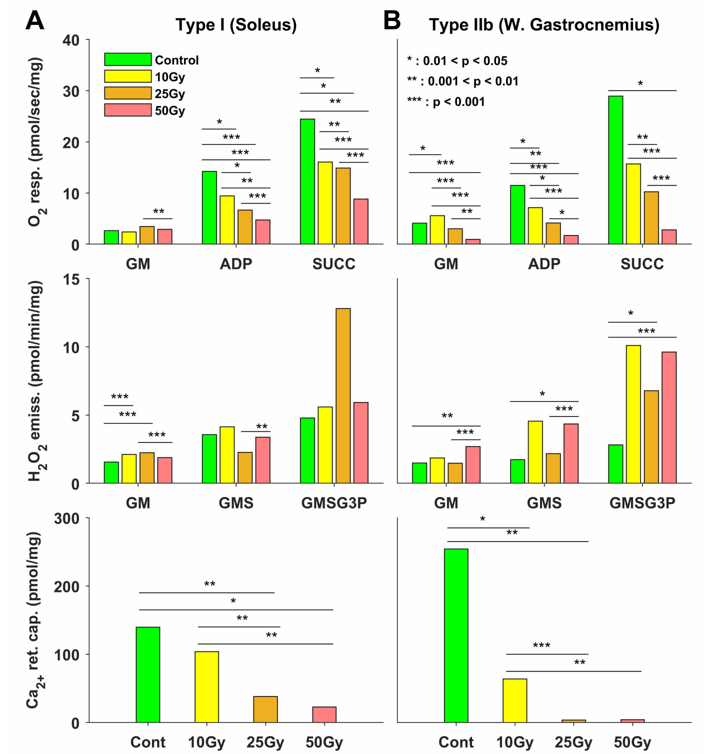

FIGURE 3: Functional test of mitochondria in the type I (Soleus) (**A**) and II (white Gastocnemius) skeletal muscles (**B**) For each type, three functions were evaluated in O_2 respiration, H_2O_2 emission, and Ca^{2+} retention capacity. Of the functions, O_2 respiration and Ca^{2+} retention capacity reduced the amounts depending on the total dose of x-irradiation while little relation was observed in H_2O_2 emission. The p-values were provided to specify the difference among the bars (* : 0.01<p<0.05, ** : 0.001<p<0.01, *** : p<0.001).

was more apparent in type IIb, which required a fast twitching muscular activity, and the biggest reduction was observed after the exposure to 25Gy x-ray (Figure 3B, bottom). In type I, the responding pattern was similar to that in type IIb, and it also demonstrated the radiation-induced functional damages in mitochondria of the skeletal muscles (Figure 3A). Based on these changes depending on the total amount of x-irradiation, the radiation-induced molecular damages were highly expected, but one of critical factor, H_2O_2 emission, indicated an inconsistent response to x-irradiation (Figure 3, middle).

Thus, a conclusion had deferred until an additional clue was revealt to clearly explain the normal kinetic responses under the functional decrease of the mitochondria.

DISCUSSION

A possible hypothesis to explain the mismatched results of the molcular and kinetic responses was the undamaged central vestibular system, which controled the given kinetic tests. The tests of rota-rod and foot pressure required a fine control initiated from the central vestibular system, which generally provided the neural infomaion related with a body position and a head spacitial orientation for a balance. If the x-irradiation failed to damage the central vestibular area, the initial functional decrease in the mitochondria of the skeletal muscle might be compensated to produce a normal performance in locomotion and postural balance. To prove this hypothesis, a cell apoptosis was examined in the vestibular nucleus. The investigation based on caspase-3 and TUNEL demonstrated that there was no difference between the control and 25Gy-exposed groups (p=0.53 for caspase-3 and p=0.08 for TUNEL), suggesting that the given x-irradiation caused no effects on the central vestibular area (Figure 4). Due to the poor performance in

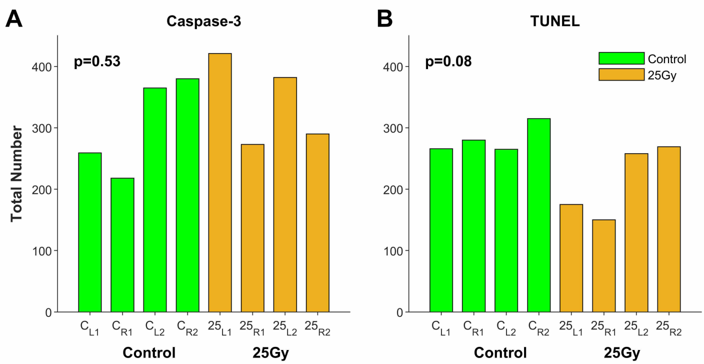

FIGURE 4: Apoptosis based on caspase-3 (**A**) and TUNEL (**B**). The counting was manually conducted separately, left (L) and right (R), to identify a unbalanced distribution before and after the radiation. The significance (t-test) was tested if two groups, control (C, green) and 25Gy (25, orange), were different in caspase-3 and TUNEL. The statistical analysis indicated there were no damages in the vestibular nucleus by 25Gy x-irradiation in both.

locomotion at 24-hour after x-irradiation, the apoptosis was also examined using the samples of VN at 24-hour after the radiation, but no cell apoptosis was verified. Thus, the given x-irradiation induced the funtional weakness in the mitochondria, but the kinetic performance was correctly conducted by the unmanaged central vestibular system.

CONCLUSION

From a molecular to a kinetic level, the wide range of biological effects were assessed using the different total doses of x-irradiation. Our results indicated that the mitochondrial function reduced as the total amount of x-irradiation increased. Under the same conditions, on the other hand, there was no functional reduction in locomotion and balance, causing the mismatching consequences between the mitochondrial function and the behavioral response. The normal behavioral responses under the mitochondrial malfunction was further examined through the apoptosis in VN, and the results identified that VN had no damages by x-irradiation. Therefore, the correct kintic responses under the mitochondrial malfunction were possibe by the neural compensation relevant to the central vestibular system.

ACKNOWLEDGMENTS

This research was supported by Basic Science Research Program through the National Research Foundation of Korea (NRF) funded partially by the Ministry of Education (2018R1A6A1A03025523 & 2019R1I1A1A01041450).

Keywords: x-irradiation, locomotion, balance, mitochondria function, apoptosis

REFERENCES

da Silva Santin, M., Koehler, J., Rocha, D.M., dos Reis, C.A., Omar, N.F., Fidler, Y., de Miranda Soares, M.A., Gomes, J.R. (2020) Initial damage produced by a single 15-Gy x-ray irradiation to the rat calvaria skin. European Radiology Experimental. 4 :32. doi : 10.1186/s41747-020-00155-4

Kim, CS., Seong, KM., Lee, BS., Lee, IK., Yang, KH., Kim, J. (2015) Chronic low-dose γ-irradiation of Drosophila melanogaster larvae induces gene expression changes and enhances locomotive behaviors. Journal of Radiation Research. 56(3), 475-484.

Abdelrazzak, A.B., El-Missiry, M.A., Ahmed, M.T., Elnady, B.F. (2019) Effect of low-dose X-rays on the liver of whole body irradiated rat. International Journal of Radiation Biology. 95(3), 264-273.

Kim, YJ., Jeong, J., Shin, SH., Lee, D., Sohn, KY., Yoon, S., Kim, J. (2019) Mitigating effects of 1-Palmitoyl-2-linoleoyl-3-acetyl-rac-glycerol (PLAG) on hematopoietic acute radiation syndrome after total-body ionizing irradiation in mice. Radiation Research. 192, 602-611.

Miyahara, N., Kokubo, T., Hara, Y., Yamada, A., Koike, T., Arai Y. (2016) Evaluation of X-ray doses and their corresponding biological effects on experimental animals in cone-beam micro-CT scans (R-mCT2). Radiological Physics and Technology. 9, 60-68.

Shimura, T., Kobayashi, J., Komatsu, K., Kunugita, N. (2016) Severe mitochondrial damage associated with low-dose radiation sensitivity in ATM-and NBS1-deficient cells. Cell Cycle. 15(8), 1099-1107.

Tada, E., Parent, J.M., Lowenstein, D.H., Fike, J.R. (2000) X-irradiation causes a prolonged reduction in cell proliferation in the dentate gyrus of adult rats. Neuroscience. 99(1), 33-41.

Winther, F.Ø. (1969) X-ray irradiation of the inner ear of the guinea pig: Early degenerative changes in the vestibular sensory epithelia. Acta oto-laryngologica. 68, 514-525.

Zhang, J., Tao, X., Sun, M., Ying, R., Su, W., Wei, W., Meng, X. (2019) A rat model of radiation vasculitis for the study of mesenchymal stem cell-based therapy. Biomed Research International. Art. ID. 3727635. doi : 10.1155/2019/3727635

Motion tracking of astronauts on long duration missions for health monitoring: The smartphone "Motion-Fingerprint" applicable spaceflight

Sergiu Petre Iliev[1]*, Alan Zhu[2], Audrey Zhang[3]

[1]*Mechanical Engineering, Carnegie Mellon University, Pittsburgh, PA, USA*
[2]*Statistics and Machine Learning, Dietrich College of Humanities and Social Sciences, Carnegie Mellon University, PA, USA*
[3]*Heinz College of Information Systems and Public Policy, Carnegie Mellon University, Pittsburgh, PA, USA*
**iliev@cmu.edu*

INTRODUCTION

Humankind aspires to transition towards a multiplanetary species. To achieve this goal, it is vital to understand the long-term effects of altered states of gravity on astronaut health. Future exploration missions to Mars, led by NASA, SpaceX, and other organizations across the globe, will involve a long period of microgravity (in the order of months), followed by a period of hypogravity (in the order of years), and finally a return to normal gravity levels. There is a research gap in our understanding of these effects, in devising effective countermeasures, and in establishing the best methods to promote long-term post-mission behavioral health (in accordance with NASA's BMed9 Gap in the 2021 Human Research Roadmap).

This student-led project proposes a method to address these challenges through minimally invasive continuous monitoring of astronaut body dynamics within the space habitat, on Earth and on extravehicular activities using a conventional smartphone. Over the course of a semester we have conducted a feasibility study on utilizing smartphones to capture gait data followed by machine learning encoding of it to learn a "motion fingerprint" specific to each test subject and their current gait style. Through ground based we validated the experimental methods and data analysis techniques that could be applied to space-based data collection. We propose that a comparison of multiple "fingerprints" at various points in time (before, during and after) spaceflight can reveal and quantify a deviance from nominal gain and its magnitude.

MATERIAL AND METHODS

Data for this analysis was collected by the research team using the following Android (OnePlus 7T Pro, Samsung Galaxy S20) and iOS (iPhone 12) smartphones. A standard motion-sensor application was used for data capture, with frequency set to 60 Hertz.

First, walking data were recorded from three subjects over varying lengths of time. subjects were requested to record their walking data using pre-specified smartphone applications while walking on mostly flat surfaces in an urban environment and indoors. The following data were captured: acceleration and rotation using the smartphone's accelerometer and gyroscope. Figure 1 shows the smartphone local coordinate system as well as the global system as defined with the Anterior Posterior (AP), Medial Lateral (ML) and Vertical (V) planes of motion. In total 12 walking trials were recorded.

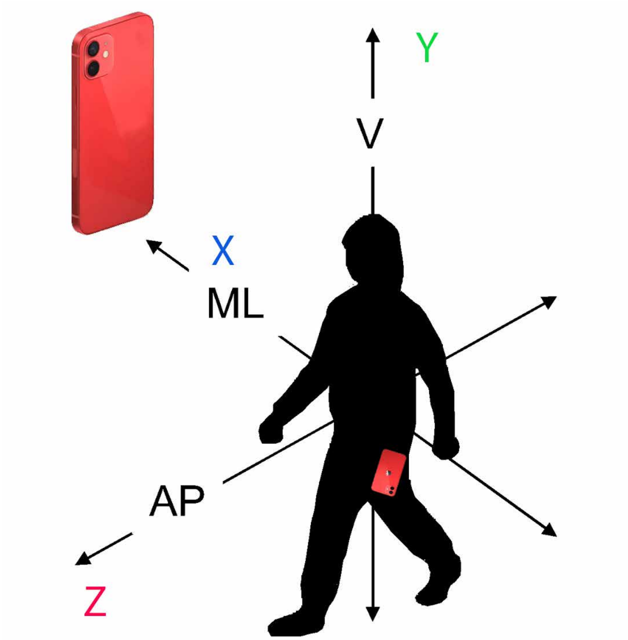

FIGURE 1: Coordinate systems definition.

A peak detection algorithm was implemented to identify steps walking. In total, 854 steps were captured. As each step varies in length, the frames of each step were resampled into 128 frames and combined into one sample to keep the dimensionality of the Machine Learning training data constant. Furthermore, the first and last 10 seconds of the data were discarded to ensure the input only contains steady-state walking data.

The team used a convolutional neural network (CNN) to generate an algorithmic encoding or "motion fingerprinting" of the subject's gait. Remarkable results have been achieved in the literature with the aim of authenticating a user based on their gait as encoded though a CNN & LSTM combination. Zou, Q. et al. (2018) achieved an authentication accuracy of 93.75% and work is a good example of such an implementation. Although this project involved time-series data, it was less important to develop an algorithm that could recognize individuals using long snippets of walking pattern (which could be achieved using recurrent neural network models). Notably, a subject's walking data is unarguably impacted by the environment, despite efforts to standardize the data capturing process. As such, an algorithm that 'remembers' historical information such as an RNN model could simply classify individuals based on differences in walking environments. Instead, the team focused on developing an algorithm that could identify gait using short snippets of motion data, such that the algorithm is generalizable to different walking environments. By using the kernel feature of CNNs, the algorithm is trained to recognize generalized patterns in motion fingerprinting instead of specific patterns in the data itself. Figure 2 presents the final version of the network architecture used in our work.

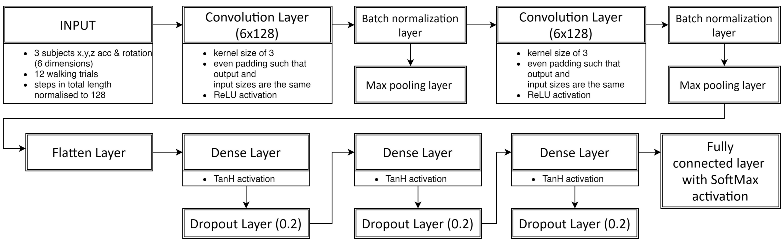

FIGURE 2: Network architecture.

RESULTS

Following data acquisition, representative acceleration and rotation data has been highlighted in Figures 3 A and B, respectively. The figures show the motions recorded in the global frame of refence following from the moment of starting the recoding process. The motion captured includes inserting the phone in the pocket and initial walking steps until a steady state is achieved. The repetitive nature of this data allows for peak detection algorithms to be used for segregating individual steps. The end result is a 6-dimensional matrix representing each step. The model architecture from Figure 2 was trained on 80% of the data and evaluated on the remaining 20%. After running for 15 epochs, the model achieved 100% cross-entropy accuracy in classifying the walking data to distinguishing between each test subject.

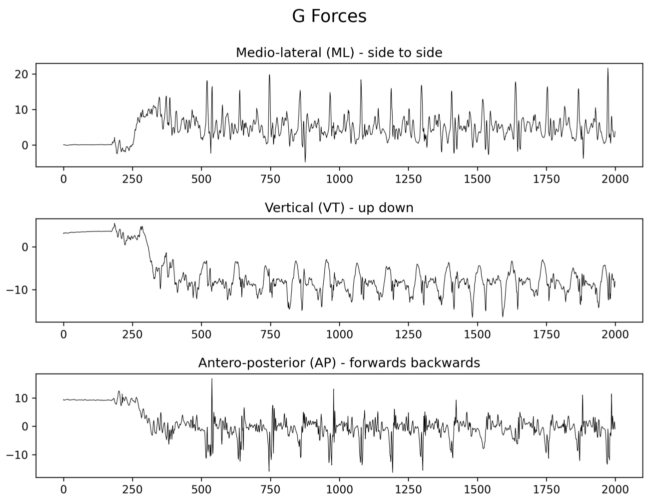

FIGURE 3A: Representative accelerometer data for 14 steps.

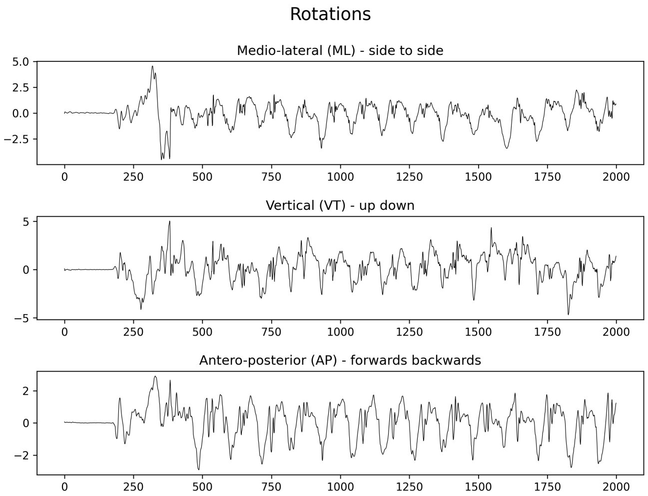

FIGURE 3B: Representative gyroscope data for 14 steps.

DISCUSSION

The field of musculoskeletal biomechanics has experienced a paradigm shift in the way data are being captured. Capabilities have expanded beyond using time-limited lab-scale optical motion-capture experiments to 'in the wild' motion-capture over using Inertial Measurement Units (IMUs) and highlighted by Shull, P. et al. (2014) and Porciuncula, F. et al. (2018). Machine Learning algorithms are further being leveraged to capture, analyze, and categorize natural behavior [Shull, P. et al. (2014), Porciuncula, F. et al. (2018)]. Now, IMUs can be embedded in smart watches and smart phones. Their sensor streams can further be combined with other devices, such as cortisol and pulse measurement flexible sensors, to collect biometric data [Torrente-Rodríguez, R. et al. (2020)]. The resulting sensor suite is non-intrusive and easy to wear, allowing a longitudinal study on astronaut body dynamics and stress levels during exercise and normal activities.

This work constitutes a preliminary test of the "motion fingerprint" proposed method. The results are promising although limited by the number of test subjects and data collection conditions. However, we have demonstrated it is possible to distinguish between individuals based on their walking style.

The natural progression would be to track the evolution of the gait signature of ground-based subjects following an actual or simulated injury affecting their walking style before proceeding to carrying on the analysis on astronaut data. This work provides the foundation of future analyses of changes in motion/gait patterns of astronauts during and after a space flight. Specifically, the model could be adapted to identify specific patterns in gait indicative of potential motion-impacting issues, such as an early-identification of muscle weakness or atrophy.

CONCLUSION

This work constitutes a feasibility study in using smartphones and deep learning to identify a person based on their specific gait “Motion-Fingerprint”. A basic use case would be to monitor the disease progression or recovery of patients that have suffered a disease or injury affecting their gait (e.g. broken leg, osteoarthritis). The technology also has exciting implications for monitoring the long-term musculoskeletal health of astronaut’s post-mission. It is the first step of a future project proposal for implementing novel wearable sensors on Earth-based analog astronaut missions followed by trials on the International Space Station, including testing on the COLBERT T2 treadmill and subsequent missions to the Gateway and the Mars Research Stations. The work has the potential to provide unprecedented insight into the evolution of astronaut musculoskeletal health in long-term exploration missions. The next steps for this analysis would be to utilize a larger dataset with more subjects and varied walking environments to further refine the model and improve generalizability.

ACKNOWLEDGMENTS

The authors would like to thank Greta Luo and Jack Chang from the Heinz College of Information Systems and Public Policy at Carnegie Mellon University for their contribution in acquiring the and cleaning the experimental data used in this study.

We would like to thank the Carnegie Mellon University Data Science Club for providing the context in which we collaborated on this piece of research.

Keywords (5 max): machine learning, bioastronautics, motion fingerprint, wearables, ISS

REFERENCES

HRR - Gap - BMed-107: What are the long-term changes and risks to astronaut health post-mission that, when using a continuity of care model, helps retrospectively identify and understand individual susceptibility (e.g., hereditary, dose, thresholds) to mitigate adverse CNS, cognitive, and behavioral health changes resulting from long-duration exploration missions, promoting the behavioral health of current and future crews? (2021). Available at: https://humanresearchroadmap.nasa.gov/Gaps/gap.aspx?i=706 (Published 26 March 2021, Accessed: 13 July 2021).

Shull, P. et al. (2014) "Quantified self and human movement: A review on the clinical impact of wearable sensing and feedback for gait analysis and intervention", Gait & Posture, 40(1), pp. 11-19. doi: 10.1016/j.gaitpost.2014.03.189.

Porciuncula, F. et al. (2018) "Wearable Movement Sensors for Rehabilitation: A Focused Review of Technological and Clinical Advances", PM&R, 10(9S2). doi: 10.1016/j.pmrj.2018.06.013.

Zou, Q. et al. (2018) Deep Learning-Based Gait Recognition Using Smartphones in the Wild, arXiv.org. Available at: https://arxiv.org/abs/1811.00338 (Accessed: 13 July 2021).

Torrente-Rodríguez, R. et al. (2020) "Investigation of Cortisol Dynamics in Human Sweat Using a Graphene-Based Wireless mHealth System", Matter, 2(4), pp. 921-937. doi: 10.1016/j.matt.2020.01.021.

Repeated long-term space flights: Proteomic investigations of cosmonauts' blood

Daria Kashirina[1]*, Kirill Kireev[2], Ludmila Pastushkova[1], Irina Larina[1]

[1]*Institute of Biomedical Problems of the Russian Academy of Sciences, Moscow, Russia*
[2]*Gagarin Research & Test Cosmonaut Training Center, Star city, Moscow region, Russia*
**daryakudryavtseva@mail.ru*

INTRODUCTION

The implementation of an increasing number of repeated flights poses new questions for space physiology: how does the state of health of cosmonauts who make repeated flights change, and how does their body's response to a repeated flight change (and whether it changes). Usually, repeated flights of Russian crew members are carried out 1.5–5 years after the previous one. It is known that the restoration of functioning of physiological systems of the human body occurs at different rates. Thus, it has been shown that, in skeletal system, the duration of recovery, as a rule, exceeds the duration of the flight itself (Oganov et al., 2010). At the same time, for many systems of the body, medical risks of long-term consequences of space missions have not been determined.

Approaches to the study of these issues are provided by studies of the protein composition of blood. The aim of the work was to compare the modifications of the proteome, ionogram, and other biochemical parameters of the blood plasma of cosmonauts who made their first or repeated long term space flight on the Russian segment of the International Space Station.

MATERIAL AND METHODS

The blood of 18 Russian cosmonauts (all men) was analyzed by mass spectrometry and routine biochemical methods. Of these, 11 cosmonauts completed their first space flight (1F) and 7 – the repeated flight (RF) 1.5–5 years after the previous one. By the age of the participants at the time of the flight, the groups 1F and RF did not differ significantly (M $\pm$ SD): 43 $\pm$ 5 years (from 36 to 52, 1F) and 48 $\pm$ 9 years (from 37 to 60, RF). The duration of their missions on the ISS was 160 ± 14 days in group 1F and 169 ± 27 days in group RF. Samples of their blood were collected before launch, on the 1st day (25.2 ± 0.1 h) after landing, and after 7 days of readaptation. More than 30 biochemical blood parameters were measured in each time point, using a routine biochemical techniques. A panel of 125 proteins in the blood plasma was quantitated by a well-established targeted mass spectrometry approach involving multiple reaction monitoring (MRM) in conjunction with stable isotope-labeled standards at the University of Victoria in Canada, as described earlier (Larina et al., 2017). Molecular functions, biological processes and paths were analyzed using DAVID database and ANDsystem program [http://www-bionet.sscc.ru/and/cell].

RESULTS AND DISCUSSION

Analysis of the post-flight dynamics of biochemical parameters and protein concentrations in the blood plasma of cosmonauts after the first (Table 1) and the repeated flights (Table 2) was performed. After the first flights, on the

Table 1: Analysis of the post-flight dynamics of biochemical parameters and protein concentrations in the blood plasma of cosmonauts after the first space flight

Blood parameter	Background	+1 day	+7 day
Total bilirubin	17,3±6,1	15,1±6,5	*11,0±2,7
Direct bilirubin	5,2±0,7	4,5±0,9	*4,4±0,6
Uric acid	300±40	#260±47	295±43,8
Urea	5,2±1,0	*6,7±1,7	5,6±1,2
C-reactive protein	0,41±0,19	*1,9±1,7	1,2±1,3
Albumin	45±2	44±2	*42±2
Alkaline phosphatase	156±27	186±51	*198±43
Potassium	3,9±0,1	*3,7±0,2	3,9±0,4
Magnesium	0,83±0,07	*#0,74±0,07	0,9±0,07
Iron	25,4±4,5	*17,2±4,8	*19,2±4,1
Transferrin	2,7±0,4	*2,4±0,3	*2,2±0,2

78kDa glucose-regulated protein	6,6±1,4	*4,7±1,2	*5,0±0,7
Apolipoprotein A-IV	1253±458	#1055±442	1481±326
Beta-2-microglobulin	110±16	#96±15	118±19
cDNA FLJ53327	1110±135	*#882±161	1031±118
Fibulin-1	147±25	#134±24	167±19
Gelsolin	829±208	*#629±127	745±67
Lumican	510±85	#457±83	539±55
Plasma serine protease inhibitor	90±16	#88±13	104±21
Protein S100-A9	2,5±0,7	*#6,2±4,2	3,2±1,1

Note: significance levels $p < 0.05$ - * - with the background, # - between +1 day and +7 days

first day, a significant change in 19 parameters was noted. On the + 7th day, only 7 of them remained different from the preflight values. However, since the dynamics of their changes repeated the dynamics of albumin, there were reasons to believe that hemodilution, which develops during the restoration of fluid volumes and the return of the body's water balance to the pre-flight state, made a significant contribution to post-flight dynamics and led to underestimated values of the concentration of blood components (Kashirina et al., 2019). An exception was an increase of alkaline phosphatase (ALP) on the seventh day. This enzyme is a recognized marker of bone remodeling (Siller et al., 2018), which is a rather slow responds to stimuli. That is, after the first flights most of biochemical parameters were restored 1 week after landing.

After the repeated space flights, changes in 17 parameters were revealed, while 8 of them did not return to background levels after 1 week, including alkaline phosphatase, triglycerides, lactate dehydrogenase, complement component C9, apolipoprotein E and mRNA for apolipoprotein E whose concentrations remained above background levels, despite the hemodilution. So, blood indices recovery from the first and the repeated missions reflected changes in the body systems and went at a various speed.

In view of the importance of the physiological effects of microgravity observed in the metabolism of bone tissue (Oganov et al., 2010), we analyzed the

Table 2: Analysis of the post-flight dynamics of biochemical parameters and protein concentrations in the blood plasma of cosmonauts after the repeated flights

Blood parameter	Background	+1 day	+7 day
Total cholesterol	4,6±0,4	*5,4±0,8	5,2±0,6
Triglycerides	0,98±0,30	#0,97±0,30	*1,7±0,7
Aspartate amino-transferase	21,3±5,4	*28,6±5,7	26,5±6,4
Alkaline phosphatase	150±26	181±24	*211±17
Creatine phosphoki-nase	126±31	*#305±79	139±76
Lactate dehydroge-nase	314±59	#342±39	*458±31
Iron	23,2±3,5	*#17,9±3,5	23,6±3,2
Alpha-2-HS-glycoprotein	157±47	*82±35	*84±46
Apolipoprotein A-II	5276±11344	*4100±667	4271±688
Apolipoprotein E	740±142	912±147	*1028±235
Complement component C9	189±43	*260±40	*248±36
Cystatin-C	76,6±21,3	*45,6±14,5	64,6±18,9
Fibulin-1	129±28	#121±9	162±36
Gelsolin	798±155	*583±140	725±152
Intercellular adhesion molecule 1	2,89±0,48	*1,86±0,34	2,59±0,54
Mannan-binding lec-tin serine protease 1	67,2±7,7	59,8±10,7	*55,6±7,8
mRNA for apolipo-protein E	634±137	798±154	*852±219

Note: significance levels p <0.05 - * - with the background, # - between +1 day and +7 days equations of multiple regression of changes in the alkaline phosphatase activity to determine the possible effect of blood proteins on it.

The ANDsystem program was used to construct networks of protein interactions that were significantly different on days 1 and 7 after the flights relative to the background and associated with ALP enzymes (ALPP, GCAP, and intestinal forms). It turned out that proteins with a significantly changed concentrations after space flight formed close and complex schemes of interactions with alkaline phosphatase (various enzymes of alkaline phosphatase are indicated on the left side of the figures) (Figure 1 and 2). Four significantly different proteins after the first space flight (GRP78, Transferrin, S100A9, Gelsolin) were associated with ALP enzymes through one node (Figure 1). As can be seen from the figure, the group of intermediary proteins was represented by proteins that were associated not only with significantly different proteins (and not only with one of them), but also with other intermediary proteins and ALP enzymes (and, as a rule, not with one isoform). Mediator proteins were united by participation in such biological processes as stress response, DNA reparation, apoptosis, catabolism and proteolysis. For proteins, concentrations of which significantly differed on the 7th day after the first space flights relative to the background, a similar pattern of bonds with ALP enzymes was

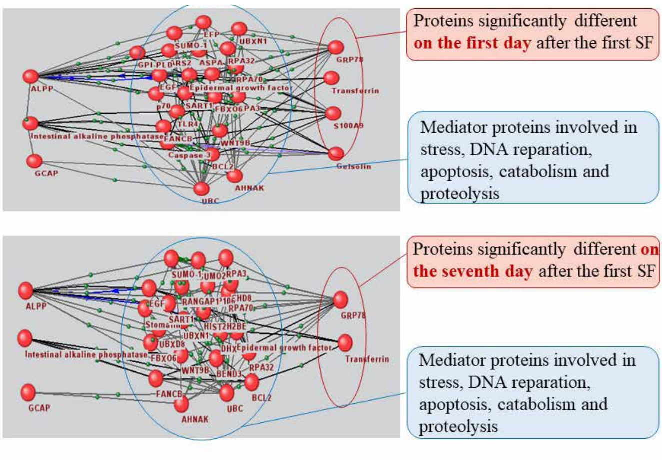

FIGURE 1: Interaction networks for proteins significantly different after the first space flight (SF) associated with alkaline phosphatase enzymes.

observed (Figure 1). Mediator proteins were linked by participation in stress response, DNA reparation, apoptosis, catabolism, and proteolysis.

After the repeated space flights, mediator proteins associated with alkaline phosphatase and significantly different proteins, were united by participation in such biological processes as bone remodeling, phosphorylation, angiogenesis and coagulation cascade (Figure 2). These processes could affect the level of alkaline phosphatase in the blood. These findings make it possible to propose a hypothesis about a more active, urgent activation of the processes of readaptation of the structure of bone tissue and its mineralization after the repeated flights.

It should be noted that a change in the concentrations of proteins (on the right side of the figures) and ALP enzymes (on the left side) does not exclude the possibility of synchronous changes in intermediary proteins (in the middle of the figures), with which the changed proteins form close and complex interaction schemes. It is possible that the concentrations of these proteins

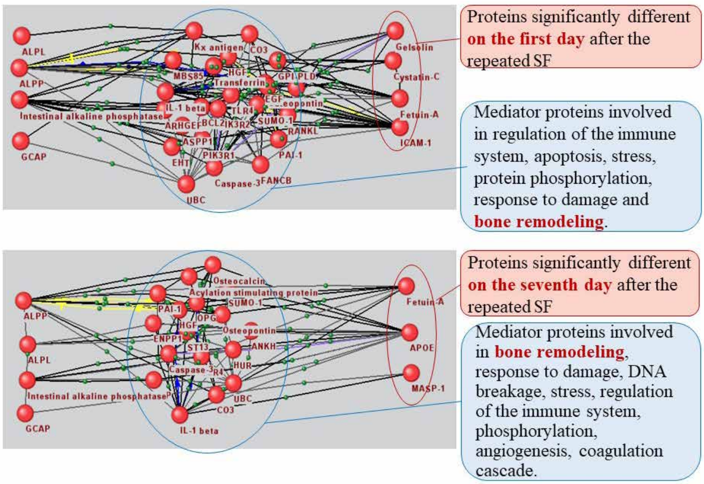

FIGURE 2: Interaction networks for proteins significantly different after the repeated space flight (SF) associated with alkaline phosphatase enzymes.

are below the sensitivity threshold of the mass spectrometer and therefore have not been recorded. This assumption is also supported by the list of biological processes that combine mediator proteins, since these are processes that are subject to changes under the influence of SF factors.

CONCLUSION

It was shown that blood indices recovery from the first and the repeated missions reflected changes in the body systems and went at a various speed. The results of measurements made prior to launch and on day 7 after landing were dependent on the number of flights. The post-flight dynamics of the level of alkaline phosphatase in the blood of cosmonauts did not depend on the number of flights. In both groups of cosmonauts, an increase on the + 7th day after space flight of alkaline phosphatase, a recognized marker of bone remodeling, was revealed. It turned out that proteins with a significantly changed level after space flight formed close and complex schemes of interactions with alkaline phosphatase, however, in the study of the first and the repeated flights, these networks were associated with different processes. The revealed differences in the processes indicated a pronounced and more relevant inclusion of the processes of readaptation of the structure of bone tissue and its mineralization after the repeated flights in comparison with the dynamics of the readaptation period after the first flight.

ACKNOWLEDGMENTS

The work was carried out within the framework of the basic theme of the Russian Academy of Sciences 65.3.

Keywords: space flight, proteomics of cosmonauts' blood, repeated flights, bone tissue readaptation

REFERENCES

Kashirina, D.N., Percy, A.J., Pastushkova, L.Kh., Borchers, C.H., Kireev, K.S., Ivanisenko, V.A., Kononikhin, A.S., Nikolaev, E.N., Larina, I.M. (2019). The molecular mechanisms driving physiological changes after long duration space flights revealed by quantitative analysis of human blood proteins. BMC Medical Genomics. 12 (Supplement 2), 97-105. doi : 10.1186/s12920-019-0490-y

Larina, I.M., Percy, A.J., Borchers, C.H., Nosovsky, A.M., Grigoriev, A.I., Nikolaev, E.N. (2017). Protein expression changes caused by spaceflight as measured for 18 Russian cosmonauts. Scientific reports. 7(1):8142. doi: 10.1038/s41598-017-08432-w

Oganov, V.S., Bogomolov, V.V., Bakulin, A.V. et al. (2010). Comparative analysis of changes in the skeleton of cosmonauts in long-term orbital flights and the possibilities of prediction for interplanetary missions. Human Physiology. 36, 282-289. doi: 10.1134/S0362119710030059

Siller, A.F., Whyte, M.P. (2018). Alkaline phosphatase: discovery and naming of our favorite enzyme. J. Bone Miner. Res. 33, 362–364. doi: 10.1002/jbmr.3225

The influence of altered-gravity on bimanual force coordination

Deanna M. Kennedy[1]*, Madison M. Davis[1], Renee Woodruff[2], Yiyu Wang[1], Traver Wright[1], Bonnie J. Dunbar[2], Ana Diaz-Artiles[1,2]

[1]*Department of Health and Kinesiology, Texas A&M University, College Station, USA*
[2]*Department of Aerospace Engineering, Texas A&M University, College Station, USA*
**hpedmk@tamu.edu*

INTRODUCTION

Many of the activities associated with spaceflight require individuals to coordinate actions between the limbs (e.g., controlling a rover, landing a spacecraft). However, much of the research investigating the effects of gravity on manual control have examined unimanual rather than bimanual performance (e.g., Rosenberg et al. 2018). Bimanual tasks are characterized by precise spatio-temporal relationships between the limbs and are described using variables that reflect the spatial and/or timing relationship between the limbs (e.g., relative phase, frequency relationship). A large body of research has focused on how bimanual coordination patterns emerge, stabilize, and transition in normal gravity environments (e.g., Kelso 1994). The results have identified only two inherently stable bimanual coordination patterns, in-phase (0°) and anti-phase (180°) with in-phase more stable than anti-phase. Other phase (e.g., 90°) and frequency (e.g., 1:2) relationships have proved difficult or near impossible to perform without significant training (e.g., Summers et al. 1993).

The difficulties associated with producing bimanual tasks such as 90° relative phase and 1:2 multi-frequency relationships have been attributed to both inherent and incidental constraints. Inherent constraints are associated with the structure of the neuromuscular system (e.g., Swinnen 2002), whereas incidental constraints are associated with specific perceptual, cognitive, and/or attentional features of the task or task environment (Shea et al. 2016). The objective of our project is to understand the neurophysiological and psychological constraints that influence coordination dynamics in altered-gravity environments. To achieve this goal, a series of experiments in altered-gravity using a tilt paradigm, a short radius centrifuge, and a parabolic flight have been designed. The purpose of the current experiment was to determine an individuals' ability to adapt to altered-gravity environments when performing simple (1:1) and complex (1:2) bimanual force tasks in an altered-gravity environment using a tilt paradigm.

MATERIAL AND METHODS

A tilt table was used to simulate gravity on Earth (90° Head Up Tilt or HUT), Mars (22.3° HUT), the Moon (9.5° HUT), and in microgravity (-6° Head Down Tilt or HDT) (see Figure 1). Right arm dominant participants (N=12) were required to produce rhythmical 1:1 and 1:2 bimanual coordination patterns by producing a pattern of isometric forces with their left arm that was coordinated to a pattern of isometric forces produced with their right arm (see Figure 2). The 1:1 task required participants to produce simultaneous patterns of force with their two arms while the 1:2 task required participants

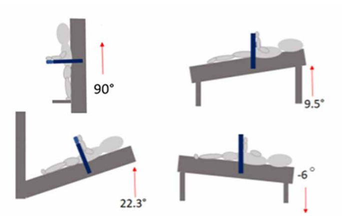

FIGURE 1: Illustration depicting the experimental arrangement for the gravity conditions (**a**), Earth (90° HUT) (**b**), Mars (22.3° HUT) (**c**), Moon (9.5° HUT) (**d**), Microgravity (-6° HDT).

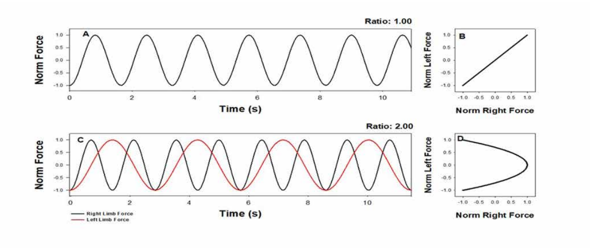

FIGURE 2: Simulated goal coordination pattern and corresponding Lissajous template for the 1:1 (a,b) and 1:2 (c,d) tasks.

to produced two patterns of force with the right arm for each pattern of force produced by the left arm. Lissajous feedback information was provided to guide performance. The Lissajous displays consisted of a goal template and a cursor indicating the forces produced by the two arms. The cursor moved from left-to-right as force was produced with the left arm and from bottom-to-top as force was produced by the right arm. The template illustrated the specific pattern of force requirements needed to produce the goal coordination patterns. Participants performed 14 practice trials for each coordination pattern at 90° HUT (Earth). Following a 30-minute rest period, participants performed 2 retention trials (Earth) followed by two transfer trials for the two coordination patterns at each simulated gravity environment (Mars, Moon, microgravity) in a counterbalanced order. All trials were 30 s.

Performance was assessed using both unimanual and bimanual measures. Unimanual measures included: inter-peak interval (provides information regarding the rate of performance), standard deviation (STD) of the inter-peak interval (provides information regarding the variability in the rate of performance), phase angle velocity (provides information regarding the rate of performance), harmonicity (quantifies the harmonic nature of the action - an h-index of 0 indicates that the movement time series is inharmonic and that one or more adjustments or perturbations have impacted the action produced by the limb, whereas an h-index of 1 indicates an harmonic time series in which subtle adjustments or perturbations are not evident), peak force, and mean force. The bimanual measures included: inter-peak interval ratio (provides information regarding the accuracy in timing the goal bimanual coordination pattern), inter-peak ratio error (provides information regarding the accuracy of the goal pattern), and phase angle slope ratio (provides information regarding accuracy in timing).

RESULTS

Figure 3 provides the results for inter-peak interval ratio. Note, that the goal inter-peak interval ratio for the 1:1 task is 1.0 while the goal ratio for the 1:2 task is 2.0. The results indicated that participants could perform the required bimanual patterns (1:1, 1:2) in all four environments (Earth, Mars, Moon, microgravity). Similar results were observed for the phase angle slope ratio indicating that participants were able to effectively time the goal bimanual tasks. Furthermore, the performance curve, illustrating the error of the IPI

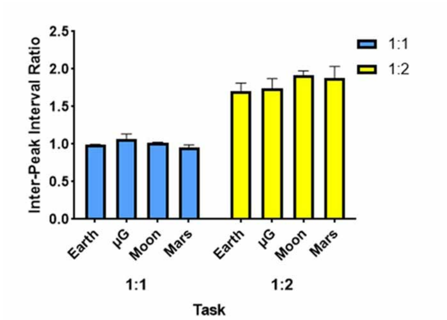

FIGURE 3: Mean inter-peak interval ratio by gravity condition. Error bars represents standard errors. The results indicate the participants performed the required bimanual patterns in all gravity environments.

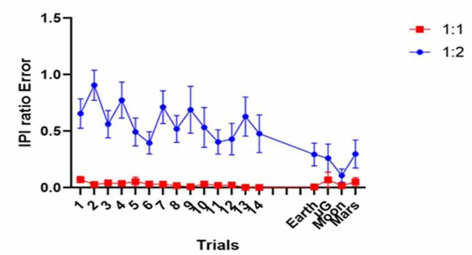

FIGURE 4: Performance Curve for the 1:1 and 1:2 Inter-Peak Interval Error. Participants performed 14 training trials. After 30 minute delay period participants performed retention (Earth) and transfer (microgravity, Moon, Mars) tests.

ratio between left and right limb (see Figure 4), indicated that performance for the 1:2 task improved with training and participants were able to maintain performance after the delay period and transfer training to the altered-gravity environments.

Although no differences between conditions were observed for measures associated with the timing of the task (inter-peak interval ratio, phase angle slope ratio), differences in measures associated with force production (harmonicity, mean force, STD of force) were observed. Results also indicated differences between Earth and the altered-gravity environments for the left limb mean force and STD of force during the 1:1 task (see Figure 5).

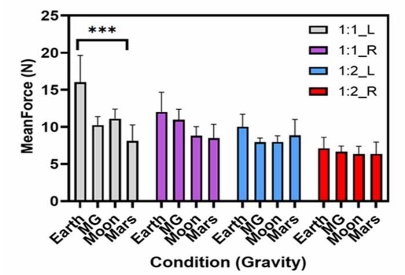

FIGURE 5: Mean Force by gravity condition. Error bars represents standard errors, ** indicates a significance level less than 0.01.

DISCUSSION

On Earth's gravity, several recent investigations have demonstrated that a variety of complex bimanual coordination patterns, that were once thought difficult or near impossible to perform without extensive training, could be quickly and effectively performed with Lissajous information and movement templates (e.g., Kovacs et al. 2020; Wang et al. 2021). The results of the current experiment extend these findings to include altered-gravity environments. The ability to quickly and effectively coordinate patterns of isometric forces in the altered-gravity environments provide additional evidence for the robust utility of integrated feedback displays in facilitating complex patterns of coordination.

The ability to coordinate complex bimanual tasks when provided Lissajous displays suggest that the detrimental effects associated with poor bimanual control may be due to attentional, cognitive, and/or perceptual constraints associated with the task or task environment (Shea et al. 2016). This may be particularly noteworthy in altered-gravity environments given the increased psychological demands associated with spaceflight (e.g., Friedl-Werner et al. 2021). Our results suggest that feedback information that reduces the attentional demands of the task may prove an effective countermeasure for the manual control performance decrements often associated with altered-gravity (e.g., Paloski et al. 2008). Future research should further explore this possibility.

Despite participants' ability to quickly and effectively time their bimanual actions in altered-gravity environments, differences in measures associated with the control of force were observed between Earth and the altered-gravity conditions (see Figure 5). The results indicated differences between Earth and the altered-gravity environments for the left limb mean force and STD of force during the 1:1 task. Given that 1:1 coordination task is considered to be the brains default coordination mode, differences with gravity suggest that the coordination landscape differs between Earth and altered-gravity environments. We will continue to explore constraints that facilitate or interfere with bimanual coordination in altered-gravitational environments using HUT/HDT paradigms, parabolic flight, and short-radius centrifugation. In addition, we will examine factors such as the impact of motion sickness medication on coordination dynamics and use additional tools such as electromyography.

CONCLUSION

The results of the current investigation indicate that participants can quickly and effectively coordinate complex patterns of force when provided Lissajous information and movement templates in altered-gravity environments. In addition, the results suggest that training on Earth with Lissajous information can be transferred to altered-gravity environments.

ACKNOWLEDGMENTS

Work Supported by NASA 80NSSC20K1499

Keywords: bimanual coordination, manual control, coordination dynamics, altered-gravity

REFERENCES

Friedl-Werner, A., Machado, M. L., Balestra, C., Liegard, Y., Philoxene, B., Brauns, K., Stahn, A. C., Hitier, M., & Besnard, S. (2021). Impaired Attentional Processing During Parabolic Flight. Front. Physiol. 12, 675426.

Kelso, J.A.S (1994). The informational character of self-organized coordination dynamics. Hum. Mov. Sc.i 13, 393-413.

Kovacs, A.J., Wang, Y., Kennedy, D.M. (2020). Accessing interpersonal and intrapersonal coordination dynamics. Exp. Brain Res. 238, 17–27.

Paloski, W.H., Oman, C.M., Bloomberg, J.J., Reschke, M.F., Wood, S.J., ...Stone, L.S. (2008). Risk of sensory-motor performance failures affecting vehicle control during space missions: A review of the evidence. J. Gravit. Physiol. 15, 1-29.

Rosenberg, M.J., Galvan-Garza, R.C., Clark, T.K., Sherwood, D.P., Young, L.R., Karmali, F. (2018). Human manual control precision depends on vestibular sensory precision and gravitational magnitude J. Neurophysiol. 120, 3187–3197.

Shea, C.H., Buchanan, J.J., Kennedy, D.M. (2016). Perception and action influences on discrete and reciprocal bimanual coordination. Psychon. Bull. Rev. 23, 361–386.

Summers, J.J, Todd, J.A, Kim, Y.H. (1993). The influence of perceptual and motor factors on bimanual coordination in a polyrhythmic tapping task. Psychol. Res. 55, 107-115.

Swinnen, S.P. (2002). Intermanual coordination: From behavioural principles to neural-network interactions. Nature Rev. 3, 350-361.

Wang, Y., Neto, O.P., Davis, M.M., Kennedy, D.M. (2021). The effects of inherent and incidental constraints on bimanual and social coordination. Exp. Brain Res., 239, 2089-2105.

A review of ambulation energy expenditure in hypogravity analogs

Logan Kluis[1], Collette Gillaspie[1], Ana Diaz Artiles[1,2]*

[1]*Department of Aerospace Engineering, Texas A&M University, College Station, TX, USA*
[2]*Department of Health and Kinesiology, Texas A&M University, College Station, TX, USA*
**adartiles@tamu.edu*

INTRODUCTION

Future missions to the Moon and Mars further humanity's trek into space and simultaneously relay groundbreaking knowledge back to Earth. Equipment deployment, sustainable outpost construction, geological sampling, and mission-facilitating resource discovery are the key tasks involved in this trajectory and result in a substantial increase in the number and complexity of extravehicular activities (EVAs). In particular, planetary EVAs will be more complex than those conducted on the International Space Station due to the required ambulation between work sites on the surface [Mars Architecture Steering Group, 2009]. Gas-pressurized spacesuits, such as the current Exploration Extravehicular Mobility Unit (xEMU), can be cumbersome. High pressure, improper fit, significant mass penalties, and movement-induced volume fluctuations inhibit astronaut performance and negatively impact mission success [Anderson *et al*., 2013, Scheuring *et al*., 2009, Belobrajdic *et al*., 2021, and Kluis *et al*., 2021]. To mitigate these operational shortcomings and support mission planning, a robust metabolic model for planetary ambulation is advantageous [Márquez et al., 2008]. An accurate model for EVA ambulation will require a robust energy expenditure model for walking in hypogravity (i.e., $0 < g < 1$) environments. Unfortunately, current metabolic models for walking in Earth gravity vary widely in predictive performance and poorly account for changes in gravity level, if at all [Norcross *et al*., 2010, Carr *et al*., 2009, Márquez, 2007, Givoni *et al*., 1971, and Bobbert, 1960].

While there is an abundance of physiological, biomechanical, and computational information available regarding ambulation under gravitational acceleration equal to 1-*g*, very little is known about human movement in sustained hypogravity. In addition to comparing three hypogravity analogs, this study presents a plan to investigate ambulation in a partial gravity environment and proposes an approach to evaluate experimental and open-source data.

COMPUTATIONAL FRAMEWORK & COMPARISON

A robust metabolic model for partial gravity ambulation is a valuable tool for future EVA planning, Lunar and Martian mission operations, and spacesuit performance measurements [Sainz Ubide *et al.*, 2020]. A metabolic model aids in identifying the key contributing factors to overall energy expenditure and helps determine designs and methodologies for reducing an astronaut's total metabolic cost.

Hypogravity analogs form the basis for which the computational framework is validated. A comparison can be made between the following hypogravity analogs: body weight support systems [Farley *et al.*, 1992, Wortz *et al.*, 1966, and Hazard, 1965], water immersion [Margaria *et* al., 1957 and Ferguson *et al.*, 1963], and Lower Body Positive Pressure (LBPP) [Cutuk *et al.*, 2006]. Each analog has advantages and disadvantages in the context of modeling human ambulation in partial gravity. Recognizing the key features of each will allow for a more precise and complete understanding of their contributions to the field.

The mechanical nature of body weight support systems engenders their simplistic usage. These mechanisms are typically used in conjunction with a treadmill to assess metabolic rates, gait patterns, kinetics, and general biomechanics. However, body harnesses typically used with this hypogravity analog might cause an uneven distribution of vertical force, impacting a subject's gait pattern [Mignardot *et al.*, 2017]. The NASA Active Response Gravity Offload System (ARGOS) uses a body weight support system to test and evaluate spacesuits. This device is shown in Figure 1 [Bekdash *et al.*, 2020]. Simpler devices may also be used for unsuited hypogravity tests, such as the "*Moonwalker III*" simulator at the Massachusetts Institute of Technology [Harvey, 2020].

Hypogravity can also be simulated with buoyant forces. Complete and partial water immersion exploits buoyant forces to offload the subject to simulate hypogravity. Unfortunately, water immersion studies entail complex testing and machinery. Additionally, the water surrounding the subject induces resistance to movement, although hydrodynamic studies have indicated that the impact of water resistance on metabolic rate may contribute as little as 6% [Newman *et al.*, 1994]. NASA uses water immersion analogs for

FIGURE 1: Spacesuit testing with NASA's body weight support system ARGOS.

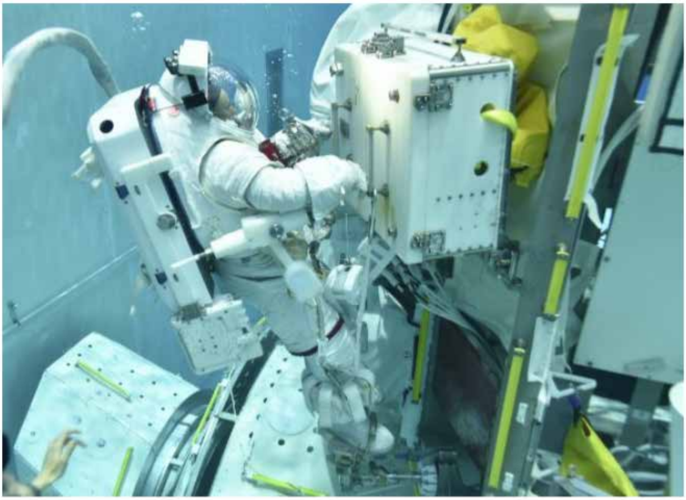

FIGURE 2: Astronaut training in the neutral buoyancy laboratory (NBL) where microgravity conditions can be simulated.

EVA training (Figure 2) [Davis *et al*., 2019], and the University of Maryland uses water immersion analogs for biomechanics testing [Mirvis, 2011].

Another analog, LBPP, increases air pressure on the lower portion of a subject, creating a lifting force with minimal disturbances to gait mechanics [Tajino *et al*., 2019]. While the positive pressure creates an even distribution of force across the lower body of the subject, there are concerns in using the device due to the high-pressure differences between upper and lower halves of the body. In addition, these systems are complex; unintended horizontal forces can arise from poor interfaces between the human and the device [Cutuk *et al*., 2006 and Grabowski *et al*., 2008]. The device used by Cutuk *et al*. capitalizes on a rigid structure with a flexible seal while the device used by Gabrowski and Kram employs a flexible pressurized tent.

FUTURE WORK

To enhance current metabolic models for partial gravity ambulation, body weight support tests will be completed on a treadmill to simulate multiple hypogravity environments. Twelve subjects between the ages of 18 and 45 will be offloaded using a crane and harness mechanism. Subject heights, weights, and leg lengths will be measured prior to testing. Each subject will walk at speeds ranging from 1 to 4 mph at gravity levels ranging from 0.12-*g* to 1-*g*. A portion of the 1-*g* trials will include walking with the addition of 25 and 50 pounds. Throughout these tests, the COSMED K5 wearable metabolic system will collect gas calorimetry data while a VICON motion capture system will collect kinematic data. In addition, ground reaction forces will be sampled with force plates located in the treadmill. The data and results from these tests will be integrated into a larger pool of metabolic data for ambulation in a variety of gravity levels, speeds, suited conditions, and hypogravity analogs. Models will then be created from this data using multiple methods including classical multivariate regression and machine learning techniques such as recurrent neural networks. These models will help with future spacesuit designs and the integration of new technologies [Kluis *et al*., 2021 and Kluis *et al*., 2021].

ACKNOWLEDGMENTS

The researchers would like to thank the Texas A&M Triads for Transformation (T3) program for funding this research effort.

Keywords: Hypogravity analog, extravehicular activity, physiological response, metabolic modeling

REFERENCES

Mars Architecture Steering Group. (2009). "Human Exploration of Mars Design Reference Architecture 5.0." *NASA-SP-2009-566*.

Anderson, A. P., Diaz, A., Kracik, M., Trotti, G., Hoffman, J., and Newman, D. J. (2013). "Understanding Human-Spacesuit Interaction to Prevent Injury during Extravehicular Activity." *NASA Human Research Program Investigator's Workshop*.

Scheuring, R. A., Mathers, C. H., Jones, J. A., and Wear, M. L. (2009). "Musculoskeletal Injuries and Minor Trauma in Space: Incidence and Injury Mechanisms in U.S. Astronauts." *Aviation, Space, and Environmental Medicine*, Vol. 80, No. 2, pp. 117–124. https://doi.org/10.3357/ASEM.2270.2009.

Belobrajdic, B., Melone, K., and Diaz Artiles, A. (2021). "Planetary Extravehicular Activity (EVA) Risk Mitigation Strategies for Long-Duration Space Missions." *NPJ Microgravity.* 16. Volume 7. https://doi.org/10.1038/s41526-021-00144-w.

Márquez, J. J., and Cummings, M. L. (2008). "Design and Evaluation of Path Planning Decision Support for Planetary Surface Exploration." *Journal of Aerospace Computing, Information and Communication*, Vol. 5, No. 3, pp. 57–71. https://doi.org/10.2514/1.26248.

Norcross, J. R., Clowers, K. G., Clark, T., Harvill, L., Morency, R. M., Stroud, L. C., Desantis, L., Vos, J. R., and Gernhardt, M. L. (2010). "Metabolic Costs and Biomechanics of Level Ambulation in a Planetary Suit." *NASA Technical Report*.

Carr, C. E., and McGee, J. (2009). "The Apollo Number: Space Suits, Self-Support, and the Walk-Run Transition." *PLoS ONE*, Vol. 4, No. 8. https://doi.org/10.1371/journal.pone.0006614.

Márquez, J. J. (2007). *Human-Automation Collaboration: Decision Support for Lunar and Planetary Exploration*. Massachusetts Institute of Technology. Ph.D. Thesis.

Givoni, B., and Goldman R. F. (1971). "Predicting metabolic energy cost." *Journal of Applied Physiology*, Vol. 30, No. 3, pp. 429–433.

Bobbert, A. C. (1960). "Energy expenditure in level and grade walking." *Journal of Applied Physiology*, Vol. 15, pp. 1015–1021.

Farley, C. T., McMahon, and T. A. (1992). "Energetics of walking and running: insights from simulated reduced-gravity experiments." *Journal of Applied Physiology*, Vol. 73, No. 6, pp. 2709–2712.

Wortz, E. C., and Prescott, E. J. (1966). "Effects of subgravity traction simulation on the energy costs of walking." *Aerospace Medicine*. Vol. 37, No. 12, pp. 1217–1222.

Margaria, R., Gualtierotti, T., and Spinelli, D. (1957). "Protection against acceleration forces in animals by immersion in water." *Journal of Aviation Medicine*, Vol. 22, No. 6, pp. 433–437.

Ferguson, J. C., and Randall, M. C. (1963). *Psychological Aspects of Water Immersion Studies*. USN: NADC MA-63281 N 6115755.

Hazard, A. B. (1965). "Results of Preliminary Physiological Testing Under Simulated Lunar and Martian Gravity Conditions." *AIAA 4th Manned Space Flight Meeting*.

Cutuk, A., Groppo, E. R., Quigley, E. J., White, K. W., Pedowitz, R. A., and Hargens, A. R. (2006). "Ambulation in simulated fractional gravity using lower body positive pressure: cardiovascular safety and gait analyses." *Journal of Applied Physiology*, Vol. 101, pp. 771–777.

Mignardot, J. B., Le Goff, C. G., van den Brand, R., Capogrosso, M., Fumeaux, N., Vallery, H., *et al*. (2017). "A multidirectional gravity-assist algorithm that enhances locomotor control in patients with stroke or spinal cord injury." *Science Translational Medicine*, Vol. 19.

Davis, K., and Meginnis, I. (2019). "Testing of the NASA Exploration Extravehicular Mobility Unit Demonstration (XEMU Demo) Architecture at the Neutral Buoyancy Laboratory (NBL)." *International Conference on Environmental Systems*.

Mirvis, A. D. (2011). *A Dynamics-Based Fidelity Assessment of Partial Gravity Gait Simulation Using Underwater Body Segment Ballasting*. University of Maryland. M.S. Thesis.

Tajino, J., Ito, A., Torii, Y., Tsuchimoto, K., Iijima, H., Zhang, X., Tanima, M., Yamaguchi, S., Ieki, H., Kakinoki, R., and Kuroki, H. (2019). "Lower-body positive pressure diminishes surface blood flow reactivity during treadmill walking." *BMC Res Notes*, Vol. 12, No. 733.

Grabowski, A. M., and Kram, R. (2008). "Effects of Velocity and Weight Support on Ground Reaction Forces and Metabolic Power during Running." *Journal of Applied Biomechanics*, Vol. 24, No. 3.

Bekdash, O., Valle, P., Kim, K., Jarvis, S., Norcoss, J., Dunn, J., and Ambercromby, A. (2020). "Development and Evaluation of the Active Response Gravity Offload System as a Lunar and Martian EVA Simulation Environment." *International Conference on Environmental Systems*.

Harvey, A. D. (2020). *Partial Gravity Simulators, Harness Design, and an Examination of Gait Transitions in Partial Gravity*. Massachusetts Institute of Technology. M.S. Thesis.

Newman, D.J. Alexander, H.L. (1993). "Human Locomotion and Workload for Simulated Lunar and Martian Environments." *Acta Astronautica*. Vol. 29, No. 8. 613–620. https://doi.org/10.1016/0094-5765(93)90078-B.

Kluis, L., Keller, N., Iyengar, N., Bai, H., Shepherd, R., Diaz Artiles, A. (2021). "An Overview of the SmartSuit Architecture" *International Conference on Environmental Systems*.

Kluis, L., Keller, N., Iyengar, N., Bai, H., Shepherd, R., Diaz Artiles, A. (2021). "Reducing Metabolic Cost During Planetary Ambulation Using Robotic Actuation." *Journal of Aerospace Medicine and Human Performance*, Vol. 92, No. 7. pp. 570–579.

Sainz Ubide, V., Diaz Artiles, A., and Casas Piedrafita, J. O. (2020). *Metabolic Cost of Traverses on Future Planetary Extra Vehicular Activities*. Universitat Politècnica de Catalunya. B.S. Thesis.

Kluis, L., and Diaz-Artiles, A. (2021). "Revisiting Decompression Sickness Risk and Mobility in the Context of the SmartSuit, a Hybrid Planetary Spacesuit." *NPJ Microgravity*. (Under Review).

Morphological and functional changes in the murine intestine during 30-day Hindlimb unloading and recovery

Evgeniya Lagereva[1]*, Mikhail Mashkin[1], Alexander Andreev-Andrievskiy[1, 2]

[1]*Animal phenotyping laboratory, Institute of Biomedical Problem of Russian Academy of Science, Moscow, Russia*
[2]*Biology faculty, M.V. Lomonosov Moscow State University, Moscow, Russia*
**e.lagereva@gmail.com*

INTRODUCTION

The digestive system is the only way of nutrients entry into the body and one of the first to appear evolutionally. At rest, it receives roughly 25 % of the cardiac output. The gastrointestinal tract (GIT) hosts the commensal bacteria, which help to extract or synthesize nutrients, interact with the immune system, and affect diverse physiological functions via their metabolites. Despite plenty of studies of GIT function on the ground, much less is known about GIT adaptation to the conditions of spaceflight.

Microgravity and other spaceflight factors exert a complex action on the gastrointestinal system (Yang et al., 2020) and the mesenteric vasculature (Behnke et al., 2013), which might lead to gastrointestinal disorders, especially in long-term flights. Interpretation of human data is complicated by heterogeneity of the subjects, diet, and the use of countermeasures, while analysis of gastrointestinal function in space-flown animals is often limited to *in vitro* tests. Thus, animal studies in the standard laboratory setting are needed to investigate microgravity effects on GIT. Hindlimb unloading is used to simulate microgravity effects in rodents. Here we report the dynamics of functional and morphological changes in the murine intestine over 30-days of hindlimb unloading and 7-day recovery.

MATERIAL AND METHODS

Male BALB/c mice were subject to 30 days of hindlimb unloading (HLU) or attachment (ATT) with subsequent 7-day recovery. Transit time and GIT permeability to FITC-inulin were measured repeatedly *in vivo* (13 HLU and 15 ATT mice) before (d-3), on unloading days 3, 7, 14, 30, and after 7 days of reloading (d30+7). Contractility, Blue No1 permeation, and intestinal morphology were investigated *in vitro*, using 6-12 HLU mice per time point before (d0), on unloading days 3, 10, 30, and after 3 days of reloading (d30+3). All the procedures complied with the EU Directive 2010/63/EU for animal experiments.

Total transit time (TT) was measured as an integrative *in vivo* estimate of intestinal function. After 12h food deprivation mice were refed 2 h before administration of 50 mg/kg carmine red by oral gavage. TT was estimated by the appearance of the dyed fecal pellet.

Intestinal contractility was investigated in isolated jejunum and distal colon segments. The 8 mm segments were incubated in aerated Krebs solution (pH=7.2, 37°C). Isometric contractions were measured with FT03 force transducer (Grass) and Power Lab, and analyzed using Lab Chart 8.1.17 (AD Instruments) software. After 1 h preincubation, the amplitude and frequency of spontaneous jejunum contractions were recorded. Next, the effects of phenylephrine (PE; $1*10^{-6}$M), histamine ($1*10^{-7}$– $3*10^{-6}$ M), and nifedipine ($1*10^{-11}$ to $1*10^{-7}$M) were studies (fig. 2A). In the colon segments, after 1 h equilibration, the effects of PE ($1*10^{-6}$M) and carbachol (CCh; $1*10^{-8}$ to $3*10^{-4}$M) were recorded (fig. 2D). Preparations were double washed and equilibrated for 20 min between the drugs

To assess intestinal permeability *in vivo*, 1 hour after oral administration of 260 mg/kg FITC-inulin (4 kDa) a 100 µl blood sample was drawn. Plasma was analyzed fluorometrically using Anthos Zenith 3000 plate reader (Biochrom). Intestinal permeability to Blue No1 dye (0.8 kDa) was assessed *in vitro* in jejunum everted sac preparations (2.5 cm). The sacs were incubated for 45 min in aerated Krebs solution (pH=7.2, 37°C) containing 2.5 µg/ml Blue No1. The dye concentration in the sac contents was measured spectrophotometrically (Plate Screen, Hospitex).

Intestinal wall morphology was studied in hematoxylin-eosin histological sections of the proximal, distal, and medial small intestine segments (fig. 4A). The villus height, crypt depth, and muscle layer thickness were measured using ImageJ software (NIH).

The data were analyzed using two-way (group, time) or one-way (time) ANOVA followed with Sidak's or Tukey's post-test using Prism (v. 9.0, GraphPad, USA). The differences were considered significant at p < 0.05. The data is presented as mean ± s.e.m.

RESULTS

Total transit time in HLU mice increased during the first 10 days of unloading peaking +70 % as compared to ATT animals (fig. 1). The differences subsided by HLU d30. While spontaneous contractions of the isolated jejunum segments were unchanged (not shown), their sensitivity to inhibition with L-type calcium channel blocker nifedipine was transiently enhanced on HLU d10 (fig. 2C). PE induced relaxation of the jejunum segments gradually decreased over 30 days of unloading (fig. 2B). Colon segments displayed increased sensitivity (EC_{50}) to carbachol starting from HLU d 14 (fig. 2F) and increased

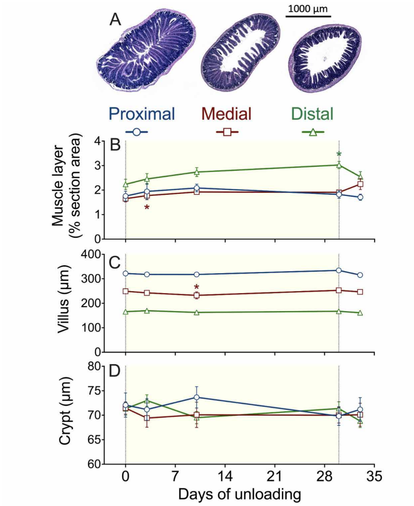

FIGURE 1: Total transit time in hindlimb-unloaded (HLU) and control (attached, ATT) mice over 30 days on unloading and 7-day recovery. Total transit time (TT) was measured *in vivo* by the appearance of the first dyed fecal pellet following oral gavage of 2% nonabsorbable carmine red 4 ml/kg. TT in HLU animals increased gradually peaking at +70 % compared to ATT counterparts by HLU d10 ($F_{(3.356,\ 87.26)}$=9.343, p<.0001; Unloading: $F_{(1,\ 26)}$=1.519, p=0.2288; Time **X** Unloading: $F_{(6,\ 156)}$=1.613, p=0.1470). The TT differences subsided by HLU d30. Statistics: * – p<0.05, Sidak's post-test.

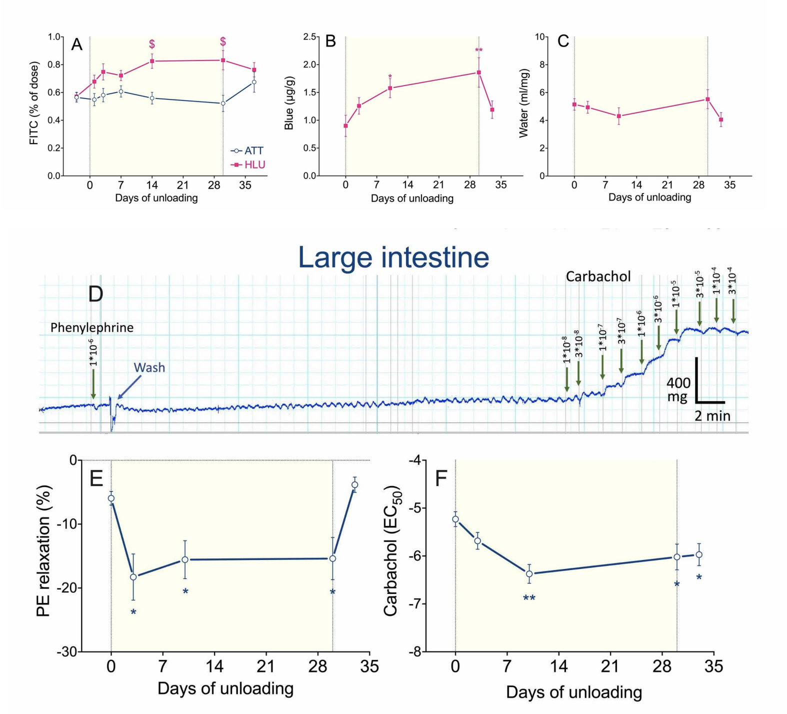

FIGURE 2: (**A**) Isometric contractions of jejunum segments were studied *ex vivo*. After 1 h equilibration in aerated Krebs solution at 37 °C, first, the spontaneous contractions were recorded, next phenylephrine (PE, $1*10^{-6}$ M), histamine ($1*10^{-7}$– $3*10^{-6}$ M), and nifedipine ($1*10^{-11}$ to $1*10^{-7}$M) were applied with appropriate washes and equilibration periods between the drugs. (**B**) PE-induced relaxation of the jejunal segments was gradually inhibited over 30 days of HLU ($F_{(4, 40)}$=3.62, p=0.0132). (**C**) Sensitivity of the jejunal segments to L-type Ca-channel blocker nifedipine expressed as IC_{50} increased on HLU d10 and recovered by the end of HLU ($F_{(1, 162)}$=14.33, p=0.0002). (**D**) In colon segments, after 1 h equilibration in aerated Krebs solution at 37 °C, the responses to PE ($1*10^{-6}$ M) and carbachol (CCh; $1*10^{-8}$ to $3*10^{-4}$M) were studied. (**E**) PE-induced relaxation of colon segments was enhanced as soon as HLU d3 and recovered quickly after reloading ($F_{(4, 53)}$=5.27, p=0.0012). F. Sensitivity to cholinomimetic carbachol increased by HLU d10 and plateaued thereafter ($F_{(4, 42)}$=4.33, p=0.0050). Statistics: * – p<0.05, Sidak's post-test.

response to adrenoreceptor agonist phenylephrine as soon as d 3 of HLU (fig. 2E).

The intestinal permeability to FITC-inulin increased by 30% by HLU d14 and remained elevated thereafter (fig. 3A). Similarly, permeability to Blue No1 in the isolated jejunum segments increased by 2 weeks of suspension and remained elevated till prompt recovery after reloading (fig. 3B). The rate of water absorption in the same preparations did not change (fig. 3C). The intestinal wall muscle layer thickness gradually increased in the medial, distal, but not the proximal part of the small intestine (fig. 4B). The villus height, crypt depth, and their ratio in the small intestine of hindlimb unloaded mice were largely unaffected, except for decreased villus height in the medial segment on d10 of unloading (fig. 4C).

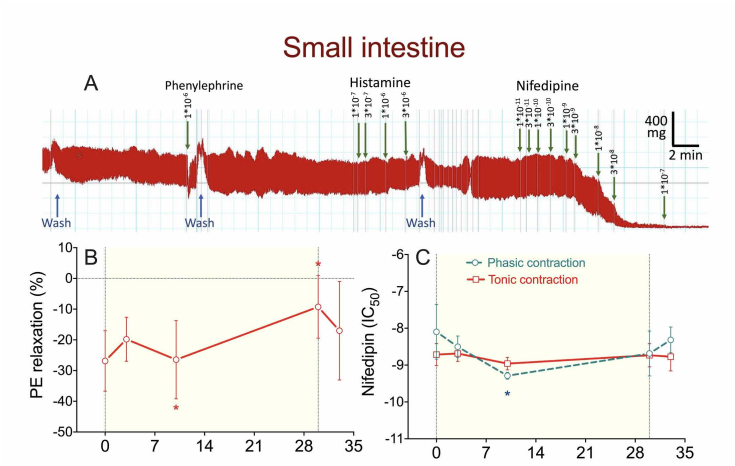

FIGURE 3: (**A**) Intestinal permeability to FITC-labelled inulin measured *in vivo* from plasma dye concentration 1 h after oral gavage of 260 mg/kg FITC-inulin (≈4 kDa), was increased in HLU mice starting from HLU d14 till reloading. Time: $F_{(3.435, 77.28)}=3.48$, p=0.0155; Unloading: $F_{(1, 24)}=10.18$, p=0.0039; Time x Unloading: $F_{(6, 135)}=3.38$, p=0.0039 (**B**) *In vitro*, permeability of everted sac jejunal preparations to Blue No1 (≈0.8 kDa) was also increased from HLU d10 till the end of unloading ($F_{(4, 47)}=4.14$, p=0.0059). (**C**) Water absorption in the same isolated jejunum segments was not affected ($F_{(4, 48)}=1.25$, p=0.3044). Statistics: * – p<0.05 vs. ATT, $ – p<0.05 vs. d0, Sidak's post-test.

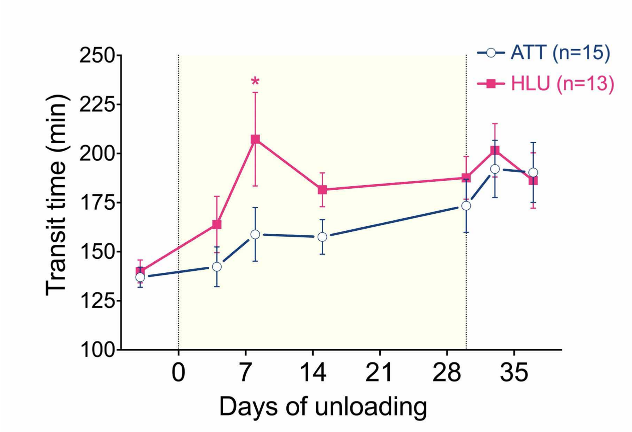

FIGURE 4: (**A**) Intestinal morphology was investigated in hematoxylin-eosin stained sections of the proximal, medial and distal segments of small intestine during 30 days of unloading and after 7-day recovery. (**B**) The tunica muscularis thickness was increased in the distal and medial, but not the proximal intestinal segment (Time: $F_{(4, 54)} = 1.35$, p=0.2644; Segment: $F_{(1.869, 94.38)}=37.63$, p<0.0001; Time x Segment: $F_{(8, 101)} = 2.44$, p=0.0189). (**C**) Villus height was not affected (Time: $F_{(4, 54)}=6.12$, p=0.0004; Segment: $F_{(1.783, 95.41)} = 167.9$, p<0.0001; Time x Segment: $F_{(8, 107)} = 0.67$, p=0.7146). (**D**) Crypt depth was not affected by HLU (Time: $F_{(4, 159)}=0.34$, p=0.8508; Segment: $F_{(2, 159)}=0.66$, p=0.5182; Time x Segment: $F_{(8, 159)}=0.57$, p=0.8046). Statistics: * – p<0.05 vs. ATT, Sidak's post-test.

DISCUSSION

Physical analysis of gastrointestinal transport identifies gravity as one of the leading forces affecting the digesta movement (Amidon et al., 1991; ARUN, 2004). Indeed, elongation of gastrointestinal transport is reported in humans in spaceflight or on-ground simulations (Afonin and Sedova, 2009). Here we show that transit time is increased in tail-suspended mice, disregarding the dramatic differences in body size or body position between the diminutive quadruped mice and biped humans.

To investigate the reasons for TT elongation we have evaluated the isolated intestinal segments contractility and gut morphology. While the jejunum segments' spontaneous contractions were minimally affected by 30-days of HLU, the smooth muscle SM sensitivity to L-type calcium channel blocker, nifedipine, was increased. As of now, there is no data on electrophysiology, Ca-sensitivity, or molecular changes of the intestinal smooth muscles (ISM) under microgravity conditions, except for an isolated report of increased ROCK expression in the intestinal mucosa of HLU rats (Wang et al., 2021). Thus, it is not possible to identify the reason for enhanced sensitivity to the VDCC blocker.

We found no difference in jejunal response to histamine. The predominant histamine effect is SM contraction mediated by H1-receptors and IP3, but upon H1-receptors blockade, relaxation is unmasked, which is mediated via H2-receptors, cAMP, and PKA (Kim et al., 2011). The absence of differences in responses to histamine suggests these pathways were not affected by HLU.

Relaxation induced with α1-agonist phenylephrine in the jejunum decreased gradually over 30 days of unloading, while in the colon PE-induced relaxation was enhanced. α1-agonists inhibit spontaneous contractions of murine ISM independently of enteric nerves by activating small conductance K-channels in the interstitial cells of Cajal, thus inhibiting their depolarization and initiation of contraction. The heterogeneous distribution of adrenoreceptor subtypes along the GIT explains the regional differences in PE sensitivity we report here. But what are the reasons for PE sensitivity shifts in HLU animals?

Fight experiments evidence altered catecholamine turnover in several rat tissues, including elevated plasma adrenaline, presumably, due to the stresses of landing and gravity reloading (Kwetniansky and Tigranian, 1981; Macho et al., 2001). However, a similar increase is reported in the unloading model, where no landing stress is present (Aviles et al., 2005; Feng et al., 2016). In line with increased circulating adrenaline levels, SM sensitivity to adrenaline is decreased in different regions (Tarasova et al., 2016). The mesenteric vessels were reported to have either enhanced or attenuated sensitivity to adrenergic agonists (Behnke et al., 2013). Our findings are in line with the idea of adrenoreceptors desensitization over 30 days of unloading due to either increased blood adrenaline or higher sympathetic activity in the intestines of HLU animals (Bouzeghrane et al., 1999). However, in our hands the adrenal weights and plasma corticosterone concentrations were not elevated in male or female mice after 30 days of HLU, thus excluding the possibility of stress governing the contractility changes.

Carbachol IC_{50} in colon segments decreased over the first 10 days of unloading and plateaued for the rest of the study. Muscarinic agonists induce intestinal SM contraction by activating M3 receptors and IP3-mediated increase in

Ca_i. Activation of the more abundant M2-receptor plays an auxiliary role by inhibiting cAMP production. The signaling complexity prevents speculations on the possible reasons for enhanced carbachol sensitivity. Previous studies report no changes in intestinal sensitivity to acetylcholine, possibly, due to species or timing differences (Salvatore et al., 2004). The changes in intestinal contractility peaked around HLU d10 and subsided by HLU d30. The increase of tunica muscularis thickness by HLU d30 can underlie intestinal contractility normalization at this period.

Differential permeability and barrier functions are critical for absorption of nutrients and defense of the host. We have found increased absorption of FITC-labelled inulin *in vivo* and the matching increase in Blue No1 accumulation *ex vivo*. These data are in concord with previous reports (Belay et al., 2002; Chen et al., 2011). The lack of villus or crypt length change, similar to previous reports in space-flown rats (Sawyer et al., 1992), excludes higher absorptive surface area as a reason for higher dyes absorption. Considering that inulin and Blue No1 permeate the intestinal mucosa paracellularly, the epithelial layer tightness could be decreased. Indeed, the decrease in several tight-junction proteins has been reported in hindlimb unloaded rats (Jin et al., 2018). Noticeably, 7 d after reloading permeability to both molecules returned to pre-suspension levels, matching the 3-5 days required for the villus regeneration (Kaunitz and Akiba, 2019). Intestinal absorption relies on adequate blood flow; thus the remodeling of mesenteric arterial supply and vascular outflow could contribute to the intestinal permeability increase we report here. Finally, microgravity exposure alters the intestinal microbiota (Voorhies and Lorenzi, 2016). The altered production of short-chain fatty acids or other metabolites by commensal microbiota could contribute to shifts in intestinal contractility. Recent findings of TLR4-mediated changes in intestinal contractility (Anitha et al., 2012) provide another link between the microbiota and the changes in intestinal function (Obata et al., 2020).

CONCLUSION

We conclude that the changes of intestinal contractility, morphology, and transit time in HLU mice are an adaptation to the change of gravity direction relative to the body axis. The increased intestinal wall permeability might have negative implications for the health of the subject by facilitating bacterial invasion.

ACKNOWLEDGMENTS

The work was performed according to the Plan for Fundamental research of SRC RF -Institute for Biomedical Problems RAS.

Keywords: Intestine, contractility, permeability, microgravity, hindlimb-unloaded mice

REFERENCES

Afonin, B. V., and Sedova, E. A. (2009). Digestive system functioning during simulation of the microgravity effects on humans by immersion. *Aviakosmicheskaia Ekologicheskaia Meditsina Aerosp Environ Medicine* 43, 48–52.

Amidon, G. L., DeBrincat, G. A., and Najib, N. (1991). Effects of Gravity on Gastric Emptying, Intestinal Transit, and Drug Absorption. *J Clin Pharmacol* 31, 968–973. doi:10.1002/j.1552-4604.1991.tb03658.x.

Anitha, M., Vijay–Kumar, M., Sitaraman, S. V., Gewirtz, A. T., and Srinivasan, S. (2012). Gut Microbial Products Regulate Murine Gastrointestinal Motility via Toll-Like Receptor 4 Signaling. *Gastroenterology* 143, 1006-1016.e4. doi:10.1053/j.gastro.2012.06.034.

ARUN, C. P. (2004). The Importance of Being Asymmetric: The Physiology of Digesta Propulsion on Earth and in Space. *Ann Ny Acad Sci* 1027, 74–84. doi:10.1196/annals.1324.008.

Aviles, H., Belay, T., Vance, M., and Sonnenfeld, G. (2005). Effects of Space Flight Conditions on the Function of the Immune System and Catecholamine Production Simulated in a Rodent Model of Hindlimb Unloading. *Neuroimmunomodulat* 12, 173–181. doi:10.1159/000084850.

Behnke, B. J., Stabley, J. N., McCullough, D. J., III, R. T. D., II, J. M. D., Muller–Delp, J. M., et al. (2013). Effects of spaceflight and ground recovery on mesenteric artery and vein constrictor properties in mice. *Faseb J* 27, 399–409. doi:10.1096/fj.12-218503.

Belay, T., Aviles, H., Vance, M., Fountain, K., and Sonnenfeld, G. (2002). Effects of the hindlimb-unloading model of spaceflight conditions on resistance of mice to infection with Klebsiella pneumoniae. *J Allergy Clin Immun* 110, 262–268. doi:10.1067/mai.2002.126459.

Bouzeghrane, F., Somody, L., Gallo-Bona, N., Gauquelin-Koch, G., Gharib, C., and Fagette, S. (1999). Effect of a 14-day hindlimb suspension on β-adrenoreceptors in rats. *Comp Biochem Physiology Part C Pharmacol Toxicol Endocrinol* 123, 95–102. doi:10.1016/s0742-8413(99)00015-8.

Chen, Y., Yang, C., Mao, G., Liu, Q., and Guo, M. (2011). Effects of simulated weightlessness on the intestinal mucosal barrier of rats. *Adv Space Res-series* 48, 395–402. doi:10.1016/j.asr.2011.03.031.

Feng, L., Liu, X., Cao, F., Wang, L., Chen, Y., Pan, R., et al. (2016). Anti-stress effects of ginseng total saponins on hindlimb-unloaded rats assessed by a metabolomics study. *J Ethnopharmacol* 188, 39–47. doi:10.1016/j.jep.2016.04.028.

Jin, M., Zhang, H., Zhao, K., Xu, C., Shao, D., Huang, Q., et al. (2018). Responses of Intestinal Mucosal Barrier Functions of Rats to Simulated Weightlessness. *Front Physiol* 9, 729. doi:10.3389/fphys.2018.00729.

Kaunitz, J. D., and Akiba, Y. (2019). Control of Intestinal Epithelial Proliferation and Differentiation: The Microbiome, Enteroendocrine L Cells, Telocytes, Enteric Nerves, and GLP, Too. *Digest Dis Sci* 64, 2709–2716. doi:10.1007/s10620-019-05778-1.

Kim, H., Dwyer, L., Song, J. H., Martin-Cano, F. E., Bahney, J., Peri, L., et al. (2011). Identification of histamine receptors and effects of histamine on murine and simian colonic excitability. *Neurogastroenterol Motil* 23, 949-e409. doi:10.1111/j.1365-2982.2011.01760.x.

Kwetniansky, R., and Tigranian, R. A. (1981). Catecholamines and their metabolic enzymes in the rat myocardium after prolonged space flight. *Kosmicheskaia Biologiia Aviakosmicheskaia Meditsina* 15, 45–7.

Macho, L., Kvetnansky, R., Fickova, M., Popova, I. A., and Grigoriev, A. (2001). Effects of exposure to space flight on endocrine regulations in experimental animals. *Endocr Regul* 35, 101–14.

Obata, Y., Castaño, Á., Boeing, S., Bon-Frauches, A. C., Fung, C., Fallesen, T., et al. (2020). Neuronal programming by microbiota regulates intestinal physiology. *Nature* 578, 284–289. doi:10.1038/s41586-020-1975-8.

Salvatore, G. D., Desaphy, J. -F., Piepoli, A. L., Natale, L., Salvia, M. A. D., Mitolo, C. I., et al. (2004). Functional alterations of mesenteric vascular bed, vas deferens and intestinal tracts in a rat hindlimb unloading model of microgravity. *Autonomic Autacoid Pharmacol* 24, 45–54. doi:10.1111/j.1474-8673.2004.00315.x.

Sawyer, H. R., Moeller, C. L., Phillips, R. W., and Smirnov, K. L. (1992). Proliferation of jejunal mucosal cells in rats flown in space. *J Appl Physiol* 73, S148–S150. doi:10.1152/jappl.1992.73.2.s148.

Tarasova, O. S., Sofronova, S. I., .Borzykh, A. A., Gaynullina, D. K., Vinogradova, O. L., and Delp, M. D. (2016). Influence of space flight conditions on vasomotor reactions of small arteries of different organs. *Space scientific project "Bion-M1" biomedical experiments and research,* 310–317.

Voorhies, A. A., and Lorenzi, H. A. (2016). The Challenge of Maintaining a Healthy Microbiome during Long-Duration Space Missions. *Frontiers Astronomy Space Sci* 3, 23. doi:10.3389/fspas.2016.00023.

Wang, S., Wang, R., Li, G. Q., Cho, J.-L., Deng, Y., and Li, Y. (2021). Myosin light chain kinase mediates intestinal barrier dysfunction following simulated microgravity based on proteomic strategy. *J Proteomics* 231, 104001. doi:10.1016/j.jprot.2020.104001.

Yang, J.-Q., Jiang, N., Li, Z.-P., Guo, S., Chen, Z.-Y., Li, B.-B., et al. (2020). State and functions of the major digestive organs under microgravity. *Life Sci Space Res* 27, 74–82. doi:10.1016/j.lssr.2020.07.009.

Resolution of inflammation is altered under simulated microgravity conditions

Alessandro Leuti[1,2], Marina Fava[2,3], Niccolò Pellegrini[1], Federico Fanti[3], Eleonora Oliva[3], Manuel Sergi[3], Dario Compagnone[3], Mauro Maccarrone[2,4]*

[1]*Department of Medicine, Campus Bio-Medico University of Rome, Via Alvaro del Portillo Rome, Italy*
[2]*European Center for Brain Research/IRCCS Santa Lucia Foundation, Via del Fosso di Fiorano Rome, Italy*
[3]*Faculty of Biosciences and Technology for Food Agriculture and Environment, University of Teramo, Via R. Balzarini, Teramo, Italy*
[4]*Department of Biotechnological and Applied Clinical and Sciences, University of L'Aquila, L'Aquila, Italy*
**mauro.maccarrone@univaq.it*

INTRODUCTION

One of the earliest discoveries in Space was that astronauts exposed to microgravity exhibit symptoms of altered immune response and inflammatory homeostasis (Hughes-Fulford, 2011). Indeed, seminal studies have clearly demonstrated that both innate and adaptive immune cells, such as lymphocytes and monocytes/macrophages, are significantly influenced by both simulated and authentic weightlessness; also their differentiation, activation, and ability to produce immune mediators such as cytokines and bioactive lipids is strongly compromised. Among the several mediators controlling immune response that seem to be influenced by microgravity, endogenous lipids that control several elements of the inflammatory reaction have been recently investigated (Fava et al., 2020). In the last 20 years a new group of endogenous lipids has been identified that plays a crucial role in inflammation and avoids aberrant or misdirected inflammatory events that might lead to tissue damage and acute or chronic pathologies. These molecules, termed specialized pro-resolving mediators (SPMs), are produced by – and act on – healthy immune cells starting from polyunsaturated fatty acids (e.g., arachidonic, eicosapentaenoic and docosahexaenoic acid), and include four main classes of molecules such as resolvins (Rv), maresins (MaR), protectins and lipoxins (LX) (Serhan and Levy, 2018). Of note, a growing number of studies in the past ten years have strongly suggested that the pathogenesis of virtually all diseases implying inflammation, either as a main source or as a secondary element, can be tracked down to impaired resolution by SPMs

(Chiurchiù et al., 2018; Leuti et al., 2020). To date, these molecules have not been investigated yet under microgravity conditions.

Here, we interrogated possible alterations of the resolution system in human peripheral blood mononuclear cells (PBMCs) that underwent rotary cell culture system (RCCS)-simulated microgravity for 48 hours.

MATERIALS AND METHODS

Cell isolation and culture

PBMCs were isolated after venous puncture from healthy volunteers and were separated by density gradient over Ficoll-Paque (GE Healthcare) as previously reported (Chiurchiù et al., 2016). Briefly: the blood sample was diluted 1:1 volume ratio with Dulbecco's Phosphate Buffered Saline (DPBS) (Gibco®-Life Sciences™). It was gently layered on top of the Ficoll- Paque and separated by centrifugation at 300 x g for 25' and the PMBC were collected from the buffy coat strata. The harvested cells were washed in DPBS and centrifuged at 300 x g for 25'. The cells were then resuspended at the concentration of 10^6 cells/ml in RPMI 10%FBS and kept for 48h at 1g (earth gravity) or RCCS-simulated microgravity (PBMCs were cultured in 10ml disposable vessel from Synthecon and left rotate at 7.6 rpm for 48h). After 48h, a cell aliquote ($5x10^5$) was harvested to extract mRNA. Remaining cells were left untreated or stimulated for 6h with PMA [50ng/ml], Ionomicin[1ug/ml] .

RNA extraction

Total RNA was extracted with the The ReliaPrep™ RNA Miniprep Systems (Promega) and SensiFAST cDNA Synthesis Kit was used for complementary DNA synthesis.

Transcripts were quantified by qRT-PCR on an ABI PRISM 7900 sequence detector (Applied Biosystems) with Applied Biosystems predesigned TaqMan Gene Expression Assays.

The following probes were used (Applied Biosystems; assay identification numbers are in parentheses): ALX (Hs02759175_s1); ChemR23 (Hs01081979_s1); GPR18 (Hs01921463_s1); GPR32 (Hs00265986_s1); LGR6 (Hs00663887_m1).

Analyses were performed on each sample in duplicate, using 5 ng of cDNA per well. In order to calculate the relative fold gene expression of samples was used the 2-ΔCt method, using the β-actin house-keeping gene for normalization.

Lipid extraction and HPLC-MS/MS analysis

Cells stimulated with PMA/Ionomicin ($5x10^6$ cells) were collected and processed as recently reported (Fanti et al., 2021); briefly, cells are resuspended in 1 mL of MeOH with 1 ng/mL of ISs and sonicated in ice for 3 cycles of 30 s with ultrasonic tips set at 60 % of power (60 W); the sample was added to 1 mL of 25 mM acetate buffer pH 4 and 2 mL of CHCl3 then vortexed for 1 min and centrifuged for 5 min 2000 rpm. After centrifuge, CHCl3 portion was collected and dried. Sample was resuspended in 100 L of 25 mM acetate buffer at pH 4: methanol (90:10, v/v), then µSPE clean-up was processed The HPLC-MSMS analysis were perfomed by an Nexera LC20 pump system from Shimadzu (Tokyo, Japan) equipped with a Kinetex C18 polar column coupled with a Qtrap 4500 mass spectrometer from Sciex (Toronto, ON, Canada) as reported previously (Fanti et al., 2021).

RESULTS

RCCS-simulated microgravity modulates expression of SPM receptors

Both authentic and simulated weightlessness have been previously demonstrated to affect immune response, as well as on signalling networks controlled by lipids (Fava et al., 2020); however, SPMs have never been investigated in this paradigm. Thus, we sought to understand whether simulated microgravity was able to exert an effect over the resolution system, especially on the expression of the main SPM receptors such as those engaging D/E-series Rvs, protectins, MaRs and LXs. We found that PMA/Ionomicin-stimulated PBMCs that underwent 48h of RCCS-simulated microgravity displayed a significant increase in the relative amount of GPR32, ChemR23 and GPR18 mRNAs, in respect with their 1g counterpart (Fig 1A).

RCCS-simulated microgravity abates the synthesis of RvD1

In light of the observed up-regulation of the aforementioned receptors, we sought to understand if this rearrangement of the SPM-related receptor repertoire, associated with prolonged weightlessness, is accompanied by a change

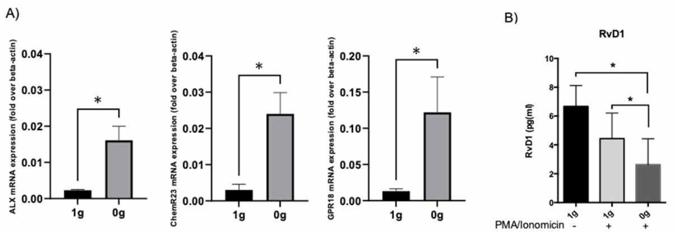

FIGURE 1: Alteration of the resolution system in human PBMCs that underwent 48h of microgravity: PBMCs (5x106 per plate) were kept for 48h at 1g or RCCS-simulated microgravity. After 48h, a cell aliquote (5x105) was harvested to extract mRNA and assay the expression of SPM-engaging receptors by means of qRT-PCR (**A**). Remaining cells were left untreated or stimulated with PMA/Ionomycin for 6 hours, before harvesting the cells, which were later used to assay the presence of RvD1 by means of LC-MS/MS (**B**). Data are shown as means ± SEM of four independent experiments. *p<0.05 (Mann-Whitney (A) or one-way ANOVA (B)).

in the production of the main SPMs. LC-MS/MS analysis showed a significant reduction in the RvD1 produced by PMA/Ionomicin- stimulated PBMCs that underwent 48h simulated microgravity, in respect with the same cells that remained at 1g (Fig 1B).

DISCUSSION

Microgravity-induced alterations of the immune and inflammatory response represent a main mechanism behind the pathologies associated to Space travel. So far, several elements have been associated to pathophysiological dysfunctions triggered by microgravity, including cytokines/chemokines and – relevant to our results – bioactive lipids metabolism (Fava et al., 2020). Indeed, 1-LOX has been suggested to act as a "gravity sensor", in that weightlessness enhances the affinity for its substrates (i.e., fatty acids) (Maccarrone and Finazzi-Agrò, 2001). Microgravity also enhances cyclooxygenase-2 (COX-2) activity (Maccarrone et al., 2000) as well as it induces 5-LOX-dependent apoptosis in immune cells (Maccarrone et al., 2003; Battista et al., 2012;

Gasperi et al., 2014). Endocannabinoids too have consistently been demonstrated to be altered by both authentic and simulated weightlessness (Fava et al., 2020). These data strongly suggests that metabolism and signalling of bioactive lipids might be altered during Space travel. However, SPMs have never been investigated in respect with their involvement in microgravity-induced inflammatory alterations. RvDs have been consistently demonstrated to act on immune cells (Chiurchiù et al., 2016; Serhan and Levy, 2018), and their functional impairment is involved on several chronic inflammatory pathologies (Leuti et al., 2020). The reduction in RvD1 production exerted by microgravity might be connected to both exacerbated inflammation and delay of pathogen clearance that microgravity has been demonstrated to exert on astronauts. Indeed, insufficient production of SPMs is also associated with delayed resolution of infective inflammation due to impaired pathogen clearance (Serhan and Levy, 2018). The observed up-regulation of pivotal SPM- related receptors (i.e., ALX, ChemR23 and GPR18) might represent a compensatory mechanism in response to the alteration of tonic SPM production during inflammatory challenges.

CONCLUSIONS

Taken together, our preliminary results represent the first attempt at investigating the effect of microgravity on the resolution system and demonstrates an effect of weightlessness conditions on the synthesis and signalling of SPMs.

ACKNOWLEDGEMENTS

Financial support by the Italian Space Agency (Agenzia Spaziale Italiana, ASI) (SERiSM Mission - Role of the Endocannabinoid System in Reprogramming human pluripotent Stem cells under Microgravity, under the contract N. 2016-5-U.o to M.M.) is gratefully acknowledged.

Keywords: Resolution of inflammation, inflammation, D-series resolvins, specialized pro-resolving mediators, microgravity

REFERENCES

Battista, N., Meloni, M. A., Bari, M., Mastrangelo, N., Galleri, G., Rapino, C., et al. (2012). 5-Lipoxygenase-dependent apoptosis of human lymphocytes in the International Space Station: data from the ROALD experiment. *The FASEB Journal* 26, 1791–1798. doi:10.1096/fj.11-199406.

Chiurchiù, V., Leuti, A., Dalli, J., Jacobsson, A., Battistini, L., Maccarrone, M., et al. (2016). Proresolving lipid mediators resolvin D1, resolvin D2, and maresin 1 are critical in modulating T cell responses. *Sci Transl Med* 8, 353ra111. doi:10.1126/scitranslmed.aaf7483.

Chiurchiù, V., Leuti, A., and Maccarrone, M. (2018). Bioactive Lipids and Chronic Inflammation: Managing the Fire Within. Front *Immunol* 9, 38. doi:10.3389/fimmu.2018.00038.

Fanti, F., Oliva, E., Tortolani, D., Di Meo, C., Fava, M., Leuti, A., et al. (2021). µSPE followed by HPLC-MS/MS for the determination of series D and E resolvins in biological matrices. *J Pharm Biomed* Anal 203, 114181. doi:10.1016/j.jpba.2021.114181.

Fava, M., Leuti, A., and Maccarrone, M. (2020). Lipid Signalling in Human Immune Response and Bone Remodelling under Microgravity. *Applied Sciences* 10, 4309. doi:10.3390/app10124309.

Gasperi, V., Rapino, C., Battista, N., Bari, M., Mastrangelo, N., Angeletti, S., et al. (2014). A Functional Interplay between 5-Lipoxygenase and µ-Calpain Affects Survival and Cytokine Profile of Human Jurkat T Lymphocyte Exposed to Simulated Microgravity. *BioMed Research International* 2014, e782390. doi:10.1155/2014/782390.

Hughes-Fulford, M. (2011). To infinity ... and beyond! Human spaceflight and life science.

The FASEB Journal 25, 2858–2864. doi:10.1096/fj.11-0902ufm.

Leuti, A., Fazio, D., Fava, M., Piccoli, A., Oddi, S., and Maccarrone, M. (2020). Bioactive lipids, inflammation and chronic diseases. *Adv Drug Deliv Rev* 159, 133–169. doi:10.1016/j.addr.2020.06.028.

Maccarrone, M., Bari, M., Lorenzon, T., and Finazzi-Agrò, A. (2000). Altered gravity modulates prostaglandin H synthase in human K562 cells. *J Gravit Physiol* 7, P61-62.

Maccarrone, M., Battista, N., Meloni, M., Bari, M., Galleri, G., Pippia, P., et al. (2003). Creating conditions similar to those that occur during exposure of cells to microgravity induces apoptosis in human lymphocytes by 5-lipoxygenase-mediated mitochondrial uncoupling and cytochrome *c release. Journal of Leukocyte Biology* 73, 472–481. doi:10.1189/jlb.0602295.

Maccarrone, M., and Finazzi-Agrò, A. (2001). Microgravity increases the affinity of lipoxygenases for free fatty acids. *FEBS Letters* 489, 283–283. doi:10.1016/S0014- 5793(00)02327-9.

Serhan, C. N., and Levy, B. D. (2018). Resolvins in inflammation: emergence of the pro- resolving superfamily of mediators. *J Clin Invest* 128, 2657–2669. doi:10.1172/JCI97943.

Stimulus-Reaction tasks in subjects with Parkinson's disease under repetitive sessions of "dry" immersion: Issues of rehabilitation and modeling of interplanetary missions

Alexander Meigal[1,2]*, Liudmila Gerasimova-Meigal[1,2]

[1]Department of Human and Animal Physiology, Pathophysiology, Petrozavodsk State University, Petrozavodsk, Russia
[2]Laboratory for Novel methods in Physiology, Institute of Higher Biomedical Technologies, Petrozavodsk State University, Petrozavodsk, Russia
**meigal@petrsu.ru*

INTRODUCTION

There are several reasons to study Parkinson's disease (PD) under the conditions of microgravity. First, PD is characterized by gradual course, and its symptoms are easily quantified clinimentrically and instrumentally, and mathematically readily modeled. Next, PD is suitable to apply science-intensive instrumental methods and therefore increasingly becomes a kind of a "model disease" for novel approaches in diagnostics and rehabilitation (Pasluosta et al., 2015). Then, muscle rigidity and tremor in PD were shown to improve after a single session of dry immersion (DI) and a program of immersions (Meigal et al., 2018, Miroshnichenko et al., 2018). Also, PD represents a unique and promising model to study cognition detriment under hazardous conditions of long duration space mission (LDSM) (Cucinotta, Cacao, 2020). Finally, PD patients represent older people, which already take their share of space commercial traveling, e.g. Richard Bronson at VSS Unity vehicle.

Besides classic motor symptoms, PD is characterized by subtle, not readily seen cognition deficits, such as impaired time processing, increased reaction time (RT) to stimuli, and general slowdown of cognition. Tasks for RT are 1) instrumentally feasible, 2) they are linked to specific brain circuitries, and therefore 3) allow evaluating specific cognitive functions, such as signal detection, decision-making, categorization, attention, inhibition of unwanted reaction (go/no-go tasks). Reaction time tasks are widely used to evaluate sensorimotor integration at varied environmental conditions. Earlier we have shown that in subjects with PD, the RT tests have improved in a "dose of cognition-reaction" manner under the program of analog microgravity modeled with "dry" immersion (DI) (Meigal et al., 2021).

Besides classic RT tasks, there is a group of manual target interception tasks (MTI), in which man reacts with manual motion to hit or catch an object (target) (Merchant et al., 2009). This task can also be performed with PC-based set-up where man reacts with pushing or releasing a button to stop moving object right at the interception zone (stationary target). Thus, interception task lies within the paradigm of Time-to-Contact tasks (López-Moliner, Bonnet, 2002, Tresilian, 1999). In the most general sense, MTI can be regarded as a class of RT tasks loaded with time processing. The ultimate goal of interception is to make effector (hand, cursor) and object (target) meet (collide) at the same location and time (to match spatially and temporally) (Merchant, 2009).

In everyday life, MTI is important as it allows to interact with varied actively (people, cars, animals, etc.) or passively (displaced with external forces) moving objects in the gravity field of Earth (1G), by reaching/intercepting desirable objects or, instead, avoiding unwanted collision, for example, with moving car or another human, predicting collisions with other people or furniture when walking on crowded streets or in a room. Therefore, for older people and subjects with brain diseases correct MTI is vitally important.

In the pre-existing study, execution of choice and discrimination RT tasks in PD subjects were improved across the program of DI sessions (Meigal *et al.*, 2021). Given that, we admit that MTI time would also have improved under the program of DI sessions. To test this working hypothesis, subjects with PD were tested with help of a MTI task across the program of seven 45-min DI sessions.

METHODS

The groups of PD subjects with (n=10) and without DI (n=5) were exactly same with our earlier study (Meigal *et al.*, 2021). The DI procedure during a single session, inclusion and no-inclusion criteria, the program of the DI sessions, measures to control the condition of subjects during DI are in-detail presented in our earlier study (Meigal *et al.*, 2021). In brief, seven 45-min DI sessions were applied (altogether 5 hours, 15 min of DI) within 25-30 days. Four study points were used to assess the effect of the program of the DI sessions: before (preDI) and right after the DI program (postDI), 2 weeks (DI2w) and 2 months after it (DI2m).

The MTI appeared as a PC-based task which required to intercept circularly moving in clockwise direction target, represented as smoothly growing red-colored sector, by pushing the button on the operating panel strictly when the sector reached the contact marker (a green-colored radius) on the clock face (90 mm in diameter, circumference 283 mm). The background was light gray-blue by color. The circular velocity of the red sector growing was 180°s^{-1}. Thus, 1°s^{-1} corresponded to a time period of 5.6 ms and to distance of 0.79 mm on the circumference of the clock face. As soon as the button is pushed, the target immediately stopped, and the contact marker instantly re-appeared in a new unpredictable position. Then, the target began to circularly grow again from where it has previously stopped. 30 serial trials were assigned within the time period of 40 s. Precise interceptions (hits, %) served as the main metric. Hit meant for an interception within ±33 ms, what corresponded to ±3.0° apart (before or behind the radius marker). Also, % of "early" (-34--66 ms, E), "very early" (<-67 ms, EE), "late" (34-66 ms, L), and "very late" (>67 ms, LL) errant interceptions. Thus, late and very late errant interceptions constituted the majority of trials. The time range (ms) within 25-75% (central 50%) of trials were considered.

The analysis was executed with IBM SPSS Statistics 21.0 (SPSS, IBM Company, Chicago, IL, USA). Data are presented as mean±SD. The variables were preliminarily tested for normality with Shapiro-Wilk test. It has been found that most of variables were not normally distributed. Therefore, the SPSS Friedman test with further *post hoc* comparisons (the Newman-Keuls test) was applied to find difference between the RT variables along study points. In the DI group, the study point "DI2m" was excluded from the analysis because 4 individual data of 10 were missing.

RESULTS

Before the DI program, hits constituted 44.1±10.0% of interception trials, and it did not change neither by the end of the DI program (46.9±9.0%), nor 2 weeks after the program (48.0±9.3%, p>0.05, Friedman test) (Figure 1). The time range within 25-75% of trials was 85.3±20.0, 80.6±16.4, and 76.4±25.8 ms, respectively (p>0.05) (Figure 2). Before the DI program, EE trials accounted for 9.6±7.7, E - 10.7±4.9, L - 17.0±8.9, and LL trials - 18.9±13.1, and this proportion did not modify along the study (see Figure 1). In the control group, all studied parameters were similar with the study group by values, and remained also unchanged along the study period.

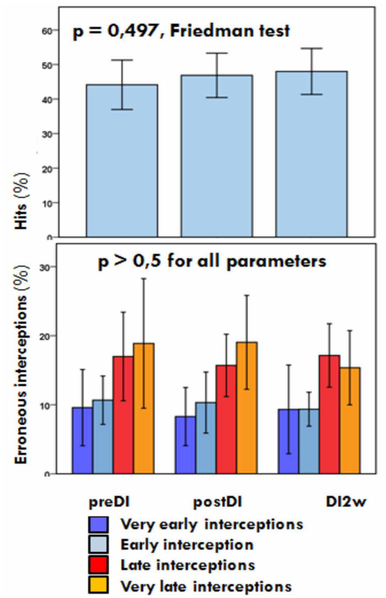

FIGURE 1: Percent of hits (upper panel) and errant interceptions (bottom panel) in the MTI task across the program of DI sessions in PD subjects.

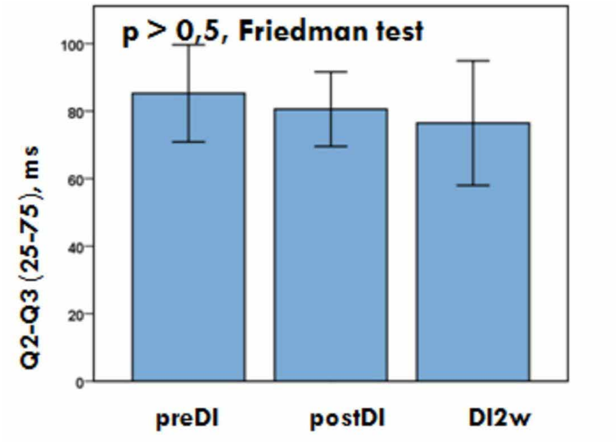

FIGURE 2: Time range of central 50% (25-75%) interceptions in the MTI task across the program of DI sessions in PD subjects.

DISCUSSION

Thus, unlike the cognition-loaded RT tasks, performance of the MTI task in subjects with PD did not change along the program of 45-min DI sessions, though there was slight tendency to increase hit proportion and decrease the time range of central 50% of trials. Such result prompts that time processing, the visual-motor and temporal-spatial integration in CNS are not improved by the program of DI sessions in PD subjects. Two lines of discussion can be figured out to explain that result. First, MTI tasks have much in common with simple RT, as both kinds of tasks are based on pre-programming strategy without inference of visual feedback (Tresilian, 2005), and with discriminative RT tasks as it uses go/nogo strategy (postponing the motor response until the appropriate moment to act) (Lungu *et al.*, 2016). Simple RT has not change under the program of DI sessions, and discriminative RT has improved only by 8% (Meigal et al. 2021). Therefore, MTI is probably just "not enough cognition-loaded" to be modified with the conditions of modeled microgravity. Second, the function of timing (time processing) probably stood unaffected by DI in PD subjects. We suppose that timing (time production, time reproduction), which is specifically affected in PD subjects, would be interesting to further evaluate under the conditions of DI.

From the other side, we did not find signs of decrement of MTI in PD subjects under a program of short-term DI what looks promising for future space tourism in the group of older subjects and the LDSM. Taken together with our earlier study on RT under DI in PD (Meigal *et al.,* 2021), we could conclude that:

1. The visual-motor and temporal-spatial integration in CNS in PD did not response to the program of DI sessions.

2. Ground-based models of microgravity in a form of DI seem promising as a novel measure for mental rehabilitation in PD.

3. Microgravity, under hazardous conditions of LDSM, would have speculatively exerted modest beneficial effect on cognitive functions in older humans.

ACKNOWLEDGMENTS

The research was financially supported by Ministry of Science and Higher Education of the Russian Federation (No 0752-2020-0007).

Keywords: Analogue microgravity, "Dry" immersion, Parkinson's disease, Reaction time, Manual target interception

REFERENCES

Cuccinota, F.A., Cacao E. (2020). Predictions of cognitive detriments from galactic cosmic ray exposures to astronauts on exploration missions. Life Sciences in Space Research. 25, 129–135.

López-Moliner, J., Bonnet, C. (2002). Speed of response initiation in a time-to-contact discrimination task reflects the use of eta. Vision Res. 42, 2419-2430.

Lungu, O.V., Bares, M., Liu, T., Gomez, C.M., Cechova, I., Ashe, J. (2016). Trial-to-trial adaptation: parsing out the roles of cerebellum and bg in predictive motor timing. J. Cogn. Neurosci. 28, 920-934.

Meigal, A., Gerasimova-Meigal, L., Saenko, I., and Subbotina, N. (2018). Dry immersion as a novel physical therapeutic intervention for rehabilitation of Parkinson's disease patients: a feasibility study. Phys. Med. Rehab. Kuror. 28, 275-281.

Meigal, A.Y., Tretjakova, O.G., Gerasimova-Meigal, L.I., Sayenko, I.V. (2021). Program of 7 45-min dry immersion sessions improves choice reaction time in Parkinson's disease. Front. Physiol. 11:621198, doi 10.3389/fphys.2020.621198.

Merchant, H., Zarco, W, Prado, L., Perez, O. (2009). Behavioral and neurophysiological aspects of target interception. Progress in Motor Control, Sternad (ed.), 201-220. DOI 10.1007/978-0-387-77064-2.

Miroshnichenko, G.G., Meigal, A.Y., Saenko, I.V., Gerasimova-Meigal, L.I., Chernikova, L.A., Subbotina, N.S., et al. (2018). Parameters of surface electromyogram suggest that dry immersion relieves motor symptoms in patients with parkinsonism. Front Neurosci. 12:667. doi: 10.3389/fnins.2018.00667.

Pasluosta, C.F., Gassner, H., Winkler, J. Klucken, J., Eskofier, B. (2015). Parkinson's disease as a working model for global healthcare restructuration: The Internet of Things and Wearables Technologies. *MOBIHEALTH. 14-16.10.2015.* doi: 10.4108/eai.14-10-2015.2261705.

Tresilian, J.R. (2004). The accuracy of interceptive action in time and space. Exerc. Sport Sci. Rev. 32, 167-173.

Dynamics of functional performance indicators under conditions of a one-year wintering at the Antarctic station Vostok

Nikolay Osetskiy*, Elena Tomilovskaya, Kirill Gordienko, Evgeniy Ilyin

Institute of Biomedical Problem of Russian Academy of Sciences, Moscow, Russia
**n.osetskiy@gmail.com*

Due to extreme environmental factors, a long stay at polar scientific stations and the territories of Central Antarctica requires the participants of polar expeditions to maintain a high level of physical performance.

Within the framework of the comprehensive scientific program of the Institute of Biomedical Problems, compiled for implementation in the 64th Russian Antarctic Expedition, Antarctica was considered as a ground model of extraterrestrial colonization. The habitat conditions for polar explorers at Vostok station in Antarctica, such as unstable electromagnetic background, hypobaric hypoxia, hypodynamia, isolation in a confined space, artificial lighting are similar to the factors of the artificial habitat of a spacecraft or an alien base, and this makes it possible to use human functional stability in relation to tasks of medical service of flights into deep space. Our institute conducted a study of the state of general human functional capacity during the annual wintering. The aim was to obtain new objective data on the state of the functional working capacity of the human body at various stages of being in the extreme conditions of Central Antarctica. The study involved 6 male polar explorers aged from 33 to 65 years. The state of functional performance was assessed using the Harvard step test, which is a simple and effective way to assess this parameter. Analysis of indicators of systolic blood pressure, diastolic blood pressure, as well as SpO_2 demonstrates the high adaptability of the mechanisms of blood circulation autoregulation.

INTRODUCTION

Due to extreme environmental conditions, a long-term stay at polar scientific stations is considered to be a good ground-based model of long-term space flight or extraterrestrial colonization (Ilyin, 2020). Not only prolonged exposure to an isolated, confined and extreme (ICE) environment such as Antarctica is associated with a wide range of psychological and physiological problems for the crew, it also requires the participants of polar expeditions to maintain a high level of physical performance (Strewe.,et al., 2018). The habitat conditions for polar explorers at Vostok station in Antarctica, such as unstable electromagnetic background, hypobaric hypoxia, hypodynamia, isolation in a confined space, artificial lighting are similar to the factors of the artificial habitat of a spacecraft or an extraterrestrial colony, and this makes it possible to use human functional stability in relation to tasks of medical service of flights into deep space (Sandal, G. M., et al., 2018). Thus, wintering in Antarctica provides an opportunity to fully explore the changes and possible impairments that take place in such an environment(Chen, N., et al., 2016). Within the framework of the comprehensive scientific program of the Institute of Biomedical Problems, compiled for implementation in the 64th Russian Antarctic Expedition, the study of the state of general human functional capacity during the annual wintering at Vostok station was performed (Van Ombergen et al., 2021).

The aim of this study was to obtain new objective data on the state of the functional performance capacity of the human body at various stages of exposure to the extreme conditions of Central Antarctica.

MATERIALS AND METHODS

The study involved 6 male polar expeditioners aged from 33 to 65 years. The state of functional performance was assessed using the Harvard step test, which is a simple and effective way to assess this parameter (Montoye, H.J., 1953). A study was carried out to determine the indicators of heart rate, blood pressure and blood oxygen saturation, conduct the main stage of the test, perform oneself ascending a step with a height of 30 cm with frequency of 30 times per minute. One ascent and descent consists of four motor components: the subject gets up on the step with one foot, the subject gets up on the step with two feet, strictly upright position, the subject puts the leg with which he started the ascent back on the floor, the subject set his leg on the floor. During ascent and descent the arms perform the normal movements - lifting and lowering. During the test, the subject could change the leg with which the ascent began several times. A metronome was used for strict dosing of the schemes of ascent and descent from it, the frequency of which was set equal to 120 beats/min. In this case, each movement would correspond to one beat of the metronome (Bohannon, Crouch, 2019).

The experimental sessions were planned before reaching the Vostok station (BDC), in January 2019, and three times on the station - in May 2019 (the 4th month) (AM1), August 2019 (7th month) (AM2) and November 2019 (the 10th month)(AM3). Due to the fact that it was impossible to maintain the planned cadence at the May data collection point (AM1) due to rapid fatigue of the test takers, the point was not taken. Data collection points in August and November have been completed in full.

RESULTS

Statistical processing of the obtained data did not reveal any significant changesin the measurements taken, but nevertheless, there is a tendency to a decrease in diastolic blood pressure(Figure 1) and systolic blood pressure (Figure 2) in AM2 point. It is interesting that there was no further tendency of diastolic and systolic blood pressure decrease in AM3.

The SpO_2 parameter has decreased by 10 % (p=0.076) in AM2 data collection point and then slightly increased by 3% approximately in AM3 data collection point (p=0.076) (Figure 3).

The physical fitness index (PFI) hasdecreased in AM2 compared to BDC level (p=0.0313) while AM3 value showed an increase compared to AM2 (Figure 4).

The values of the analyzed parameters are presented as median (Me) and interquartile range (IQR). Comparison of parameter values at different stages of observation was carried out using Friedman's test, Wilcoxon's test with Benjamini-Yekutili's correction for multiple comparisons. Statistical tests were performed using STATISTICA 10 softwareand GraphPad Prism 9.

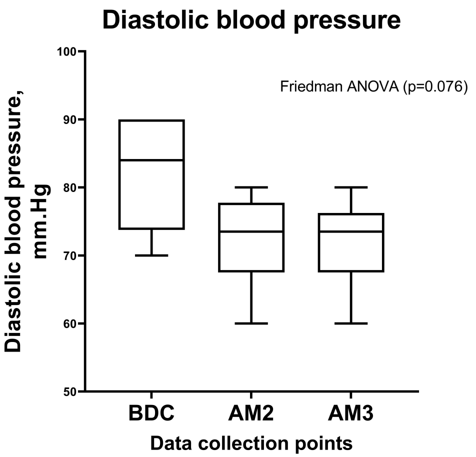

FIGURE 1: The level of diastolic pressure in subjects measured in millimeters Hg (mm.Hg) throughout the data collection points, n=6. Comparison of parameter values at different stages of observation was carried out using Friedman's test, p=0.076.

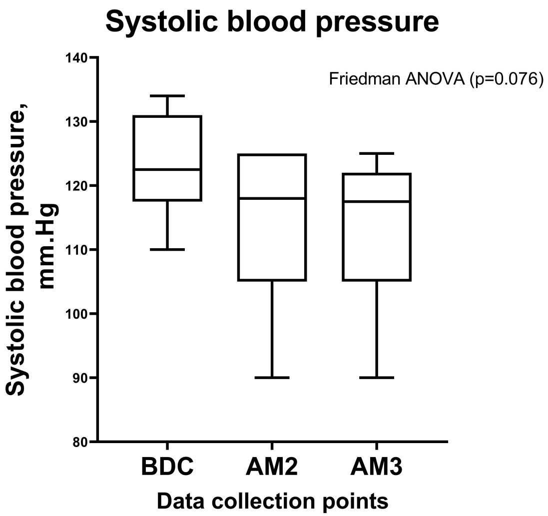

FIGURE 2: The level of systolic pressure in subjects measured in millimeters Hg (mm.Hg) throughout the data collection points, n=6. Comparison of parameter values at different stages of observation was carried out using Friedman's test, p=0.076.

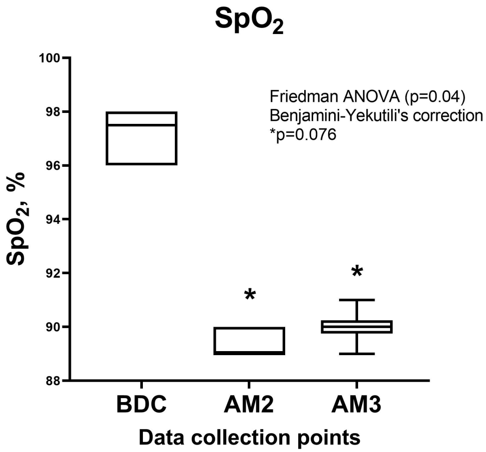

FIGURE 3: The SpO_2 parameter level was measured throughout all the data collection points, n=6. * - values at AM2 and AM3 show a tendency to decrease compared to BDC value. Comparison of parameter values at different stages of observation was carried out using Wilcoxon's test with Benjamini-Yekutili's correction, p = 0.076.

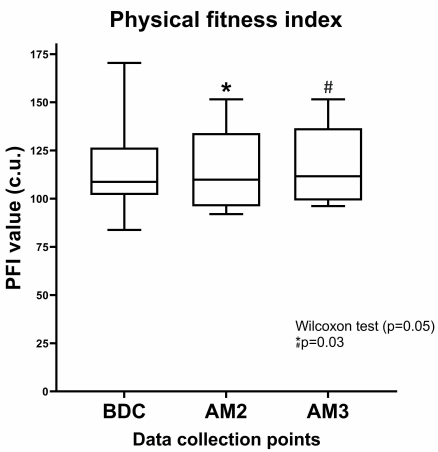

FIGURE 4: The physical fitness index (PFI) level throughout the data collection points, n=6. * - the physical fitness index (PFI) has decreased in AM2 compared to BDC level (p=0.03); # - AM3 value showed an increase in PFI compared to AM2 value (p=0.03). Comparison of parameter values at different stages of observation was carried out using Wilcoxon's test, p=0.03.

DISCUSSION

Analysis of indicators of systolic blood pressure, diastolic blood pressure, as well as SpO_2 demonstrates the high adaptability of the mechanisms of blood circulation autoregulation. The main part of the impairment processes takes place in the first 4 months of stay in the extreme conditions of Central Antarctica(Porcelli, S., Marzorati, M., et al., 2017). Unfortunately, due to the fact that we were unable to collect data at the AM1 point (4 months), we could not witness a statistically significant decrease, but only a tendency to decrease of systolic and diastolic blood pressure at AM2 (7 months) and AM3(10 months) after the compensatory mechanisms already began to work. But the decrease of SpO_2 by 10% after 7 months of wintering was, in fact, significant, as was the slight increase 3 months later, which also means the compensatory mechanisms, took on. At the AM1 point no experimental data has been collected due to the fact that on the initial phase of performing the test the subject's heart rate rose up to 180 bpm so the point session had to be cancelled. We presume that it took place due to relatively high intensity of physical load while performing the test as the subject had to maintain the pace of 30 steps per minute while the level of adaptation to the hypoxia conditions has not been quite effective yet unlike during the following sessions.

As for the physical fitness index it is obvious that the maximum values of physical performance capacity have decreased after 7 and 10 months of wintering and the minimum values increased, which is why the mean value remained unchanged. One of the explanations may be that,even though the expeditioners were involved into certain physical activity while maintaining the Vostok station grounds (e.g. snow removal by shovels), those who were initially the strongest suffered from functional impairments due to the environment extreme conditions. Those who had lowest PFI results in the beginning probably do not engage in physical activity in their everyday life, which is why their functional performance increased during overwinter as they simply trained more than they usually did back home.

CONCLUSION

Blood circulation autoregulation is a highly adaptable system. Even though 7 months of wintering decreased blood circulation parameters such as diastolic and systolic blood pressure and SpO_2, there is evidence of compensatory mechanisms activation due to the observed increase of these parameters after 10 months of wintering.

The mean PFI values have decreased during overwintering. There is a hypothesis that the values of the most trained individuals decreased due to the exposition in ICE environment, while the values of the most detrained increased, probably due to the elevation of physical activity compared to their home regime.

ACKNOWLEDGMENTS

The study is supported by the Russian Academy of Sciences (64.1).

Keywords: Antarctica, physical fitness, blood autoregulation, hypoxia

REFERENCES

Montoye, H.J. (1953) The Harvard step test and work capacity. ReviewsofCanadianBiology, 11, 491-499.

Ilyin, E.A., Levando, K.K. (2020) Some results of biomedical research at Vostok station. Russian Polar Research, №3 2020, 37-39.

Van Ombergen, Angelique & Rossiter, Andrea & Ngo-Anh, Thu. (2020). "White Mars" – nearly two decades of biomedical research at the Antarctic Concordia station. Experimental Physiology. 106. 10.1113/ep088352.

Strewe, C., Thieme, D., Dangoisse, C., Fiedel, B., van den Berg, F., Bauer, H., Salam, A. P., Gössmann-Lang, P., Campolongo, P., Moser, D., Quintens, R., Moreels, M., Baatout, S., Kohlberg, E., Schelling, G., Choukèr, A., & Feuerecker, M. (2018). Modulations of Neuroendocrine stress responses during confinement in Antarctica and the role of Hypobaric Hypoxia. Frontiers in physiology, 9, 1647. https://doi.org/10.3389/fphys.2018.01647.

Bohannon, R. W., & Crouch, R. H. (2019). Two-Minute Step Test of Exercise Capacity: Systematic Review of Procedures, Performance, and Clinimetric Properties. Journal of geriatric physical therapy (2001), 42(2), 105–112. https://doi.org/10.1519/JPT.0000000000000164

Sandal, G. M., van deVijver, F., & Smith, N. (2018). Psychological Hibernation in Antarctica. Frontiers in psychology, 9, 2235. https://doi.org/10.3389/fpsyg.2018.02235

Chen, N., Wu, Q., Li, H., Zhang, T., & Xu, C. (2016). Different adaptations of Chinese winter-over expeditioners during prolonged Antarctic and sub-Antarctic residence. International journal of biometeorology, 60(5), 737–747. https://doi.org/10.1007/s00484-015-1069-8

Maciejczyk, M., Araźny, A., &Opyrchał, M. (2017). Changes in aerobic performance, body composition, and physical activity in polar explorers during a year-long stay at the polar station in the Arctic. International journal of biometeorology, 61(4), 669–675. https://doi.org/10.1007/s00484-016-1244-6

Porcelli, S., Marzorati, M., Healey, B., Terraneo, L., Vezzoli, A., Bella, S. D., Dicasillati, R., & Samaja, M. (2017). Lack of acclimatization to chronic hypoxia in humans in the Antarctica. Scientific reports, 7(1), 18090. https://doi.org/10.1038/s41598-017-18212-1

The role of microgravity in the onset of atrial fibrillation during long-term space missions

Roberto Parisi[1,2]*

[1]*Department of Medicine, MD student, Surgery and Dentistry, Scuola Medica Salernitana, University of Salerno, Baronissi (Salerno), Italy*
[2]*Visiting Scholar, Blue Marble Space Institute of Science, Seattle, WA, USA*
**roberto.parisi@bmsis.org*

INTRODUCTION

Although several past space programs offer evidence of alterations of the natural cardiac rhythm, there is still little knowledge about the potential link between cardiac adaptation to weightlessness and the onset of severe arrythmias. It is known that different factors might play a pivotal role in the cardiac physiology during space missions (e.g., ionizing radiation, genetic conditions, electrolyte imbalance) and this work aims to analyze the correlation between cardiac arrhythmias and exposure to microgravity, proposing the introduction of genetic screenings as a viable method to improve the selection processes of candidate astronauts.

MATERIAL AND METHODS

A systematic review of different past space missions, from the Mercury Program (1961-1963) to the NASA-Mir Partnership Program (1993-1998) was conducted to collect evidence of peculiar ECG changes, potentially relevant in terms of astronauts' health.

A particular attention was paid to atrial fibrillation, a heart condition with a high prevalence in global population, and its onset during space missions after exposure to long-term weightlessness.

Table 1: Data collected from past space programs

Space program	Relevant cardiac changes
Mercury Program	- No significant arrythmia (except PAC/PVC before flight)
Apollo Program	- 22-beat nodal bigeminal rhythm (Apollo 15) - Premature atrial beats (Apollo 15)
Skylab Program	- Premature ventricular/supraventricular beats
Nasa-Mir Program	- Atrioventricular junction ectopic rhythms - Tachycardia (max. 215 bpm)

RESULTS

Relevant data (Table 1) were collected from the analysis of reports about past space missions. During the Mercury Program, no significant arrythmia was detected, besides rare premature atrial (PACs) and ventricular (PVCs) contractions during pre-flight operations (Lee *et al.*, 2017). One Apollo 15 crewmember developed a 22-beat nodal bigeminal rhythm and a PAC during the space mission and was later diagnosed with coronary artery disease and myocardial infarction (Johnston *et al.*, 1975). During the Skylab Program, premature ventricular and supraventricular beats were recorded along with nodal arrythmias, apparently during extravehicular activities (EVAs) and the use of chambers for lower body negative pressure (Johnston *et al.*, 1977). During the NASA-Mir program, both atrial and ventricular arrythmias were detected in 10 of 19 crewmembers at rest, during exercise and during EVAs, revealing a case of 14-beat ventricular tachycardia with a maximum heart rate of 215 bpm (Fritsch-Yelle *et al.*, 1998).

DISCUSSION

During space missions, microgravity can cause a generalized cephaloid fluid shift, strongly impacting on the physiological hemodynamics (Thornton *et* *al.*, 1987). The antigravitational characteristics of space environment enhance a reduced blood stasis in ventricular chambers and an increased volumetric accumulation of blood in apical structures, that are the atrial chambers. From literature it is known that the volumetric enlargement of atrial chambers represents an important risk factor for the onset of atrial fibrillation (Seko *et al.*, 2018). It could be speculated that the increased heart rate is a cardiovascular adaptive mechanism to weightlessness for which there is a compensation of the reduced stroke volume and a restoration of the homeostatic value for cardiac output. There is evidence of ECG changes in astronauts after a 6-months spaceflight, such as prolongated P waves, clinical marker of altered cardiomyoelectric conduction, and a reduction in the root mean square of ECG voltages during the whole space mission except for the landing day when it has been hypothesized that the sympathetic branch of the autonomous nervous system significantly alters the atrial electrophysiology (Khine *et al.*, 2018).

Important ECG changes, such as atrial fibrillation, might represent a valid medical criterion for candidates' disqualification. By way of example, ESA requires a health certificate, known as JAR-FCL 3 Class 2, characterized by several medical examinations, to proceed with the candidature processes. Therefore, it is crucial to prematurely diagnose cardiac pathologies in potential candidates since long-term exposure to space environment can increase the risk of atrial fibrillation whose paroxysmal variant might be triggered by sudden hemodynamic changes and fluid shifts induced by microgravity (Barr *et al.*, 2010). As already suggested in literature (Anzai *et al.*, 2014), an innovative method to improve selection processes for astronauts and avert potential dangerous clinical situations during spaceflight might be represented by the implementation of genetic tests, evaluating specific polymorphisms which are commonly associated with congenital cardiac arrythmias.

To propose a first cluster of the most significant genetic polymorphisms (Table 2) involved in atrial fibrillation, a cut-off of 1.5 was arbitrarily applied to odds ratios statistically derived from a genome-wide association study (GWAS) focused on atrial fibrillation (Paludan-Müller *et al.*, 2016). Four gene polymorphisms showed the highest odds ratio scores, that are *KCNN3* (rs13376333), *PITX2* (rs2200733/rs6843082), *KCNH2* (rs2968863) and *TGF-β1* (rs1800489). rs13376333 (OR=1.58) is located in 1q21, close to *KCNN3* gene, encoding for a calcium-activated potassium channel whose overexpression has been

Table 2: Significant gene polymorphisms involved in atrial fibrillation

Gene	Polymorphism	OR score	Locus	Gene function
KCNH2	rs2968863	2.4	7q36	Voltage-activated potassium channel
PITX2	rs6843082	2.03	4q25	Homeobox transcription factor
	rs2200733	1.84		
KCNN3	rs13376333	1.58	1q21	Calcium-activated potassium channel
TGF-β1	rs1800489	1.5	19q13	Secreted ligand of TGF-beta

correlated with an increased risk of cardiac arrythmias (Mahida *et al.*, 2014); rs2200733 (OR=1.84) and rs6843082 (OR=2.03) are located in 4q25, close to the *PITX2* gene, encoding for a homeobox transcription factor whose deletion during embryogenesis is correlated with congenital cardiac diseases (Franco *et al.,* 2017); rs2968863 (OR=2.4) is located in 7q36, close to the *KCNH2* gene, encoding for a voltage-activated potassium channel whose mutations have been associated in literature with long QT syndromes (Zamorano-León *et al.,* 2012); rs1800489 (OR=1.5) is located in 19q13, close to the *TGF-β1* gene, encoding for a secreted ligand of the TGF-beta whose dysregulation is involved in cardiac fibrosis, remodeling and failure (Liu *et al.,* 2017).

CONCLUSION

Nowadays, atrial fibrillation represents one of the most common cardiac pathologies in western countries (Kornej *et al.,* 2020) and could turn into a dangerous clinical condition to treat during long-term spaceflights. Considering the eventuality of inherited cardiomyoelectric pathologies which increase the susceptibility to the onset of cardiac arrythmias, this work aims at suggesting the implementation of specific genetic tests, which could help clinicians choose the best candidates for long-term spaceflights along with standard ECG interpretations.

Keywords: arrythmias, microgravity, genetic screening, atrial fibrillation

REFERENCES

Anzai T., Frey M. A., Nogami A. (2014). Cardiac arrhythmias during long-duration spaceflights. Journal of Arrhythmia, 30:3, 139-149. doi:10.1016/j.joa.2013.07.009.

Barr Y.R., Watkins S.D., Polk J.D. (2010). Atrial arrhythmia summit: summary report NASA/TP-2010-216124. Washington, DC: NASA.

Franco D., Sedmera D., Lozano-Velasco E. (2017). Multiple Roles of Pitx2 in Cardiac Development and Disease. J Cardiovasc Dev Dis. Oct 11;4(4):16. doi:10.3390/jcdd4040016

Fritsch-Yelle J.M., Leuenberger U.A., D'Aunno D.S., Rossum A.C., Brown T. E., Wood M. L., Josephson M. E., Goldberger A. L. (1998). An episode of ventricular tachycardia during long-duration spaceflight. Am J Cardiol, 81:1391-2. doi: 10.1016/S0002-9149(98)00179-9

Johnston R.S., Dietlein L.F., Berry C.A. (1975). Biomedical Results of Apollo. Washington, DC: U.S. Government Printing Office; 43-81.

Johnston R.S., Dietlein L.F. (1977). Biomedical results from SkyLab, SP-377. Washington, DC: NASA; 313–23.

Khine, H. W., Steding-Ehrenborg, K., Hastings, J. L., Kowal, J., Daniels, J. D., Page, R. L., Goldberger, J. J., Ng, J., Adams-Huet, B., Bungo, M. W., Levine, B. D. (2018). Effects of Prolonged Spaceflight on Atrial Size, Atrial Electrophysiology, and Risk of Atrial Fibrillation. Circulation. Arrhythmia and electrophysiology, 11:5. doi:10.1161/CIRCEP.117.005959

Kornej, J., Börschel, C. S., Benjamin, E. J., Schnabel, R. B. (2020). Epidemiology of Atrial Fibrillation in the 21st Century: Novel Methods and New Insights. Circulation research, 127 :1, 4–20. doi:10.1161/CIRCRESAHA.120.316340

Lee M.C. Stuart, Stenger B. Michael, Laurie S. Steven, Macias R. Brandon (2017). Evidence Report: Risk of Cardiac Rhythm Problems during Space Flight. Washington, DC: NASA.

Liu G., Ma C., Yang H., Zhang P.Y. (2017). Transforming growth factor β and its role in heart disease. Exp Ther Med. 2017.13:5, 2123-2128. doi:10.3892/etm.2017.4246

Mahida S., Mills R.W., Tucker N.R., Simonson B., Macri V., Lemoine M.D., Das S., Milan D.J., Ellinor P.T. (2014). Overexpression of KCNN3 results in sudden cardiac death. Cardiovasc Res. Feb 1;101(2), 326-34. doi:10.1093/cvr/cvt269

Paludan-Müller C., Svendsen J. H., Olesen M. S. (2016). The role of common genetic variants in atrial fibrillation, Journal of Electrocardiology, 49:6, 864-870. doi:10.1016/j.jelectrocard.2016.08.012

Seko Y., Kato T., Haruna T., Izumi T., Miyamoto S., Nakane E., Inoko M. (2018). Association between atrial fibrillation, atrial enlargement, and left ventricular geometric remodeling. Sci Rep 8, 6366. doi: 10.1038/s41598-018-24875-1

Thornton W.E., Moore T.P., Pool S.L. (1987). Fluid shifts in weightlessness. Aviat Space Environ Med 58:A86-90.

Zamorano-León J.J., Yañez R., Jaime G., Rodriguez-Sierra P., Calatrava-Ledrado L., Alvarez-Granada R.R., Mateos-Cáceres P.J., Macaya C., López-Farré A.J. (2012). KCNH2 gene mutation: a potential link between epilepsy and long QT-2 syndrome. J Neurogenet. Sep;26(3-4), 382-6. doi:10.3109/01677063.2012.674993

Cardiovascular and fluid changes induced by the acute phase of dry-immersion

Adrien Robin[1,2]*, Bernard Degryse[3], Ronan Murphy[3], Françoise Larcher[4], Marie-Pierre Bareille[5], Claude Gharib[6], Guillemette Gauquelin-Koch[7], Marc-Antoine Custaud[1,2], Nastassia Navasiolava[1, 2]

[1]*Centre de Recherche Clinique, CHU d'Angers, Angers, France*
[2]*MitoVasc UMR INSERM CNRS, Université d'Angers, Angers, France*
[3]*School of Health and Human Performance, Dublin City University, Dublin, Ireland*
[4]*Laboratoire de Biochimie, CHU d'Angers, Angers, France*
[5]*MEDES, Toulouse, France*
[6]*Faculté de Médecine Lyon-Est, Institut NeuroMyoGène, Université de Lyon, Lyon, France*
[7]*Centre National d'Études Spatiales, Paris, France*
**adrien.robin@univ-angers.fr*

INTRODUCTION

Venoconstrictive Thigh Cuffs are used by cosmonauts to improve symptoms associated with cephalad fluid shift and have been implemented and employed as a standard countermeasure since 1990 (Arbeille *et al.*,1999). Testing countermeasures against fluid transfer is a priority in preparation of deep space missions, to fight not only cardiovascular deconditioning, but also Spaceflight-Associated-Neuro-Ocular-Syndrome (SANS). The dry-immersion (DI) model is particularly well adapted for a rapid evaluation of countermeasures against fluid transfer and its consequences. Our aim was to investigate the effects of the acute phase of DI (first 8h) and Thigh Cuffs countermeasures on body fluid changes, as well as on cardiovascular deconditioning.

MATERIAL AND METHODS

Eighteen healthy men (25-43 years), randomly divided into two groups (Control: Ctrl group or with Thigh Cuffs worn 10 h/day: Cuffs group), underwent 5-day strict DI at MEDES (Toulouse, France) from 19/11/2018 to 23/03/2019. Heart rate (with R-R interval) and blood pressure (BP) were continuously recorded by a cuffless beat-by-beat recording device SOMNOtouch™ (SOMNOmedics®, Randersacker, Germany) during the first day of DI (DI1). The SOMNOtouch™

provides an estimation of BP through the calculation of the pulse wave velocity following every heartbeat (Figure 1). It is composed with a 3 leads ECG, a SPO_2 finger sensor, and an accelerometer.

Body fluid changes were assessed by bio-impedance Bodystat QuadScan 4000 (Bodystat Ltd., Isle of Man, United Kingdom) and hormonal assay in the morning and the evening of DI1; plasma volume evolution was estimated using Dill and Costill method (hematocrit and hemoglobin formula; data shown previously: Robin *et al*., 2020).

Some results have already been published by Robin and coworkers (Robin *et al*., 2020), this extended abstract focus on the acute phase of dry-immersion.

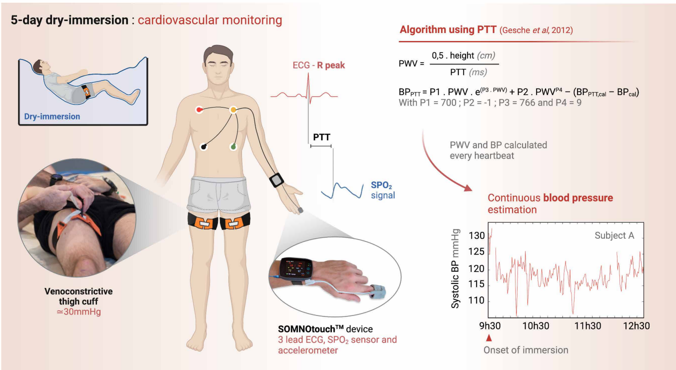

FIGURE 1: Venoconstrictive thigh cuffs and SOMNOtouch™ under dry-immersion. Thigh cuffs applied about 30mmHg to limit the venous return under 5-day dry-immersion. The SOMNOtouch™ device estimates the blood pressure with the pulse wave velocity (PWV) calculated from the pulse transit time (PTT) and included in an algorithm (Gesche *et al*, 2012). *Created with BioRender.com*

The experimental protocol conformed to the standards set by the Declaration of Helsinki and was approved by the local Ethic Committee (CPP Est III: October 2, 2018, n° ID RCB 2018-A01470-55) and French Health Authorities (ANSM: August 13, 2018). ClinicalTrials.gov Identifier: NCT03915457.

RESULTS

Before dry-immersion, there was no significant difference in general characteristics between groups (**Table 1**).

During the acute phase of DI, Thigh Cuffs limited the loss in total body water (-2.9% in Ctrl vs. -0.9% in Cuffs), and tended to limit the loss in calf volume, extracellular volume and plasma volume during the acute phase of DI (**Figure 2a, b, c**).

Thigh Cuffs limited the increase in N-terminal prohormone of brain natriuretic peptide (NT-proBNP: +21.2ng.L^{-1} in Ctrl vs. -1.0 ng.L^{-1} in Cuffs) (**Figure 3a**) and the decrease in renin (-9.3ng.L^{-1} in Ctrl vs. -2.9ng.L^{-1} in Cuffs) (**Figure 3b**).

Table 1: Baseline group characteristics before dry-immersion (B-2)

	Age (year)	**Height (cm)**	**Weight (kg)**	**BMI (kg/m²)**	**VO_2peak (ml/min/kg)**
Control (n = 9)	33.9 ± 7.1	176 ± 6	73.9 ± 7.5	23.9 ± 1.7	46.5 ± 8.1
Cuffs (n = 9)	34.1 ± 3.7	180 ± 4	74.3 ± 8.8	22.7 ± 1.8	46.9 ± 5.8

Values are mean ± SD. Unpaired T-test did not reveal significant differences between groups.

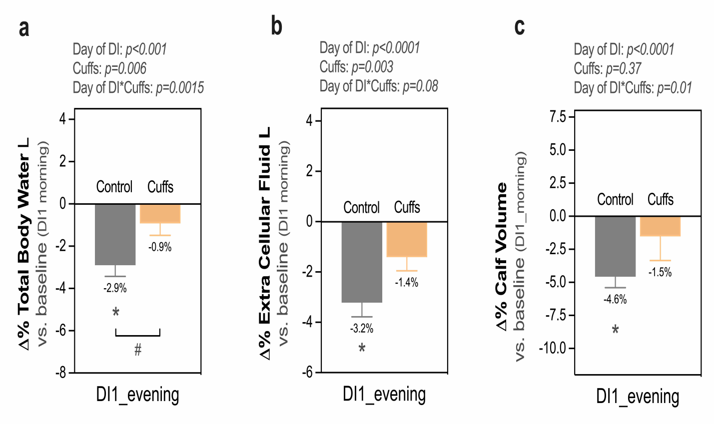

FIGURE 2: Body fluid changes at the evening of the first day of dry-immersion compared to baseline. Sample size in n=9/control and n=9/cuffs. Values are mean ± SEM *p<0.05 vs.baseline and #p<0.05 vs. Control.

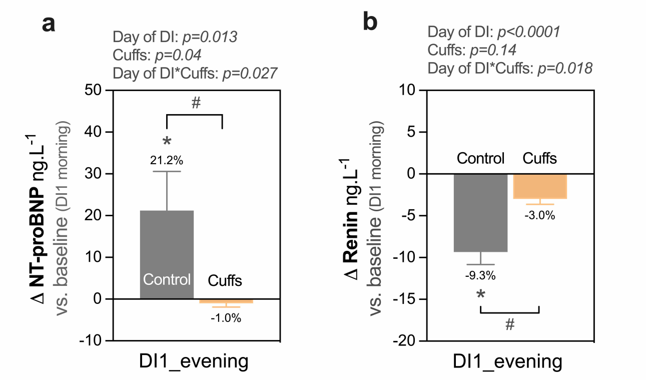

FIGURE 3: Hormones changes at the evening of the first day of dry-immersion compared to baseline. Sample size in *n*=9/control and *n*=9/cuffs. Values are mean ± SEM *p<0.05 vs.baseline and #p<0.05 vs. Control.

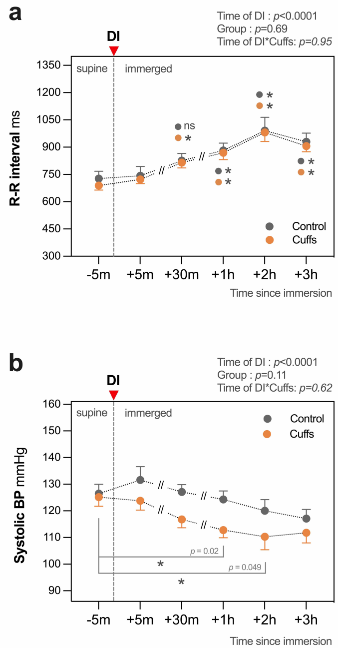

FIGURE 4: R-R interval (**a**) and systolic blood pressure (**b**) evolution during the first hours following the onset of dry-immersion. Sample size in *n*=9/control and *n*=9/cuffs. Values are mean ± SEM *p<0.05 vs. -5min (5min bedrest supine before being immerged).

Finally, Thigh Cuffs tended to limit the increase in systolic BP (after 2 hours: from 126 to 120mmHg in Ctrl, ns; and from 125 to 110mmHg in Cuffs, *p*=0.049) (**Figure 4b**) but do not have any effects on R-R interval (**Figure 4a**).

DISCUSSION

The changes observed in hormones and water repartition are induced by the fluidshift (liquids transfer toward the thoraco-cephalic area) during the acute phase of dry immersion (**Figure 2 & 3**). Such alterations are expected at the beginning of immersion, when, with hydrostatic compression and increased water and sodium excretion, body fluids decrease, especially in the plasma and extracellular compartments (Leach Huntoon *et al*., 1998; Navasiolava *et al*., 2011; Coupe *et al*., 2013). The slowing heart rate is due to the fluid centralization in addition with acute inactivity, and the decrease of systolic blood pressure might be induced by vasodilation (**Figure 4b**).

Thigh cuffs lightened these initial alterations by sequestrating fluids in lower limbs (Arbeille *et al*., 1999). The fluid sequestration by the Thigh Cuffs is stronger than the DI effect, that is why this countermeasure limited hormones changes and loss of total body water (**Figure 2**). The systolic blood pressure decreased more in the Thigh Cuffs group (**Figure 4b**), probably due to a less circulating blood volume and a resetted gain of the baroreflex.

CONCLUSION

Thigh Cuffs had a beneficial effect during the first hours of dry-immersion, by limiting the negative effect of fluidshift, despite the increase in hydrostatic pressure in the lower limbs induced by the immersion model.

ACKNOWLEDGMENTS

We thank the volunteers and the staff of MEDES for participation in this protocol at the MEDES space clinic in 2018–2019. This study was funded by CNES. Adrien Robin received a PhD grant from « CNES » and « Région des Pays de la Loire ».

Keywords: simulated microgravity, thigh cuffs, countermeasure, fluid shift, volemia

REFERENCES

Arbeille, P., Herault, S., Fomina, G., Roumy, J., Alferova, I., and Gharib, C. (1999). Influences of thigh cuffs on the cardiovascular system during 7-day head-down bed rest. J. Appl. Physiol. 87, 2168–2176. doi: 10.1152/jappl.1999.87.6.2168

Coupe, M., Tomilovskaya, E., Larcher, F., Diquet, B., Pastushkova, L., Kozlovskaya, I., et al. (2013). Body fluid changes, cardiovascular deconditioning and metabolic impairment are reversed 24 hours after a 5-day dry immersion. Open J. Nephrol. 3, 13–24. doi: 10.4236/ojneph.2013.31004

Gesche, H., Grosskurth, D., Küchler, G., & Patzak, A. (2012). Continuous blood pressure measurement by using the pulse transit time: comparison to a cuff-based method. European journal of applied physiology, 112(1), 309–315. doi: 10.1007/s00421-011-1983-3

Leach Huntoon, C.S., Grigoriev, A.I., and Natochin, Y.V.(eds) (1998). Fluid and electrolyte regulation in spaceflight. San Diego, CA: American Astronautical Society, vol 94.

Navasiolava, N. M., Custaud, M. A., Tomilovskaya, E. S., Larina, I. M., Mano, T., Gauquelin Koch, G., et al. (2011). Long-term dry immersion: review and prospects. Eur. J. Appl. Physiol. 111, 1235–1260. doi: 10.1007/s00421-010- 1750-x

Robin, A., Auvinet, A., Degryse, B., Murphy, R., Bareille, M. P., Beck, A., Gharib, C., Gauquelin-Koch, G., Daviet, A., Larcher, F., Custaud, M. A., & Navasiolava, N. (2020). DI-5 CUFFS: Venoconstrictive Thigh Cuffs Limit Body Fluid Changes but Not Orthostatic Intolerance Induced by a 5-Day Dry Immersion. Frontiers in physiology, 11, 383. doi: 10.3389/fphys.2020.00383

Molecular basis of hypergravity-induced wheat root growth phenotype

Malarvizhi Sathasivam, Basavalingayya K Swamy, Ravikumar Hosamani*

Department of Biotechnology, University of Agricultural Sciences, Dharwad (UAS-D), Karnataka, India
**hosamanirr@uasd.in*

INTRODUCTION

Hypergravity being an evolutionarily novel environment is reported to influence plant growth and morphogenesis. Recently, we have reported wheat seeds (variety - UAS-375) exposed to hypergravity at 10g for 12 hrs, and sown in greenhouse induced significant increase in root length (21.93%, p=0.000), root volume (27.91%, p=0.004), and root dry weight (18.09%, p=0.040). Besides, 10g for 12hrs positively influenced various physio-biochemical parameters such as chlorophyll content, RuBisCo expression in leaf, and various stress hormones in the root (Basavalingayya, 2020). In the present study, we investigated the molecular basis of this enhanced root phenotype through a 45-days-old-root transcriptome. The resultant data enables us to identify candidate genes, and provide an insight into the molecular basis of enhanced root growth phenotype in hypergravity condition.

MATERIAL AND METHODS

Hypergravity treatment, plant material, RNA isolation, library preparation and sequencing

Wheat seeds (variety UAS-375) were exposed to 10g for 12 hrs and later sown in greenhouse condition with total of 12 sets. The experiment was laid out in CRD with seven internal replications for each treatment group. From 45-days-old plant roots, RNA was extracted using Quick-RNA Plant Miniprep Plus kit. The RNA-Seq paired end sequencing libraries were prepared using Illumina TruSeq Stranded mRNA sample Prep kit. After purification, mRNA quality was checked by using a 4200 tape station with D1000 screen tape. The QC passed libraries were sequenced on Illumina NextSeq500 platform using 2 x 150 bp chemistry.

Quality filtering and assembly

The raw reads were trimmed, adapter removal and quality checking was done by Fastp (v.0.20) with a minimum Phred score of 30 (Chen et al., 2018). De Novo assembly was performed using Trinity with 5X average depth and 70% coverage.

Differential expression analysis

Annotation was performed using BLASTX against NCBI Ref sequence protein databases in BioBamOmicsbox (v1.3) (Gotz et al., 2008). Differential expression analysis (Robinson et al., 2010) with cut off of $\geq$ 2-fold change and FDR $\leq$ 0.05, and gene ontology enrichment of differentially expressed genes was performed. Pathway analysis was performed using Plant Reactome for the identification of significant pathways altered under hypergravity condition.

RESULTS

Raw reads, final assembly statistics and sequence length distribution of transcripts

The average percentage of high quality reads after processing of Control and Treatment sample reads were 98.9 and 99.1% respectively. Final assembly statistics after de novo transcript assembly were as follows: Total number of transcripts after assembly – 147,297, total number of bases – 186,251,628 bp, minimum sequence length of transcripts - 483 bp, maximum sequence length – 16,909 bp, average sequence length - 998, N50 length – 1,459 bp and percent of GC content - 47.86.

Differential gene expression (DEG) analysis and Gene ontology (GO)

Among the 147297 annotated transcripts, transcripts exhibiting differential expression in Control v/s Treatment pairwise comparison resulted in a total of 4632 up-regulated genes and 2976 down-regulated genes in response to hypergravity (Figure 1). Gene ontology terms such as regulation of auxin biosynthetic process, actin filament depolymerization, plant-type primary cell-wall biosynthesis, trehalose biosynthetic process were enriched in up-regulated genes. In case of down-regulated genes, response to Jasmonic acid, salicylic acid, positive regulation of abscisic acid biosynthetic process, and auxin homeostasis were significantly enriched.

Putative genes associated with hypergravity-induced root growth phenotype

Reactome pathway analysis revealed root elongation, primary root development, auxin biosynthesis, cellulose synthase, ABA, and jasmonic acid signalling pathways were significantly affected in response to hypergravity (Figure 2). Interestingly, all these pathways positively correlate with the enhanced root

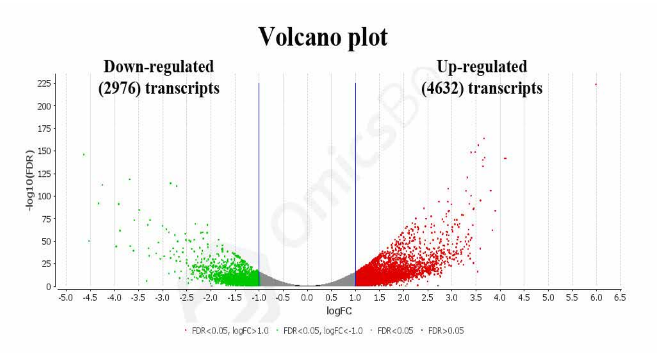

FIGURE 1: Differential gene expression analysis - Volcano plot indicating the significantly up (4632) and down-regulated (2976) transcripts with the minimum cut off of fold change ≥ 2 and q-value ≤ 0.05.

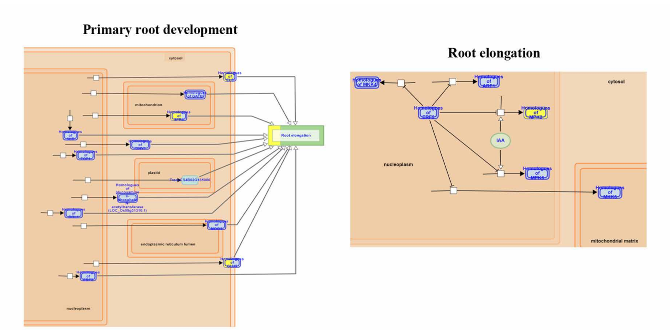

FIGURE 2: Primary root development and root elongation pathways (generated using Plant Reactome) with associated genes affected due to hypergravity (yellow highlighted).

length phenotype suggesting auxin driven cell division leading to high demand of cell-wall constituents due to increased root growth. Further, the candidate genes identified are listed in the Table 1.

Table 1: Candidate genes identified for enhanced root growth phenotype in response to hypergravity

Transcripts	Uniprot ID	Description	log2 Fold Change	q-value
Auxin biosynthesis				
TRINITY_DN4013_c0_g1_i14	P49572	indole-3-glycerol phosphate synthase, chloroplastic-like isoform X1	1.03993	0.02295
TRINITY_DN4013_c0_g1_i6			0.01697	
TRINITY_DN4013_c0_g1_i16		1.05927 1.06232	0.01972	
TRINITY_DN4013_c0_g1_i1		1.31368	0.00073	
Cell division				
TRINITY_DN51301_c0_g1_i12	Q9SD82	PREDICTED: replication protein A 70 kDa DNA-binding subunit C-like	1.32424	0.02409
TRINITY_DN51301_c0_g1_i14		PREDICTED: replication protein A 70 kDa DNA-binding subunit C-like	1.33823	0.02124

TRINITY_DN46428_c0_g1_i1	P34149	cdc42 homolog	1.39095	0.00902
TRINITY_DN2778_c0_g2_i2	Q9SZA4	cell division cycle 20.2, cofactor of APC complex-like	1.20507	0.00688
TRINITY_DN70789_c0_g1_i1	Q54TK8	cell division control protein 25-like	1.41861	0.01691
TRINITY_DN20916_c0_g1_i1	P54774	cell division cycle protein 48 homolog	1.6379	3.6E-05
Cell number regulator				
TRINITY_DN50_c0_g1_i2	D9HP26	cell number regulator 2-like	-1.3999	0.00050
TRINITY_DN50_c0_g4_i1		cell number regulator 2	-1.1521	0.04147
ABA degradation				
TRINITY_DN1734_c0_g1_i5	Q09J79	abscisic acid 8′-hydroxylase 1	1.08208	0.00781
TRINITY_DN1734_c0_g1_i4			1.25004	0.00336
TRINITY_DN60843_c0_g1_i2	F1SY99	abscisic acid 8′-hydroxylase CYP707A2	1.36392	0.00657

Table 1 (Contd)...

ABA receptor				
TRINITY_DN3981_c0_g1_i2	Q9FLB1	abscisic acid receptor PYL4-like	-1.1528	0.02391
TRINITY_DN3981_c0_g1_i1			-1.376	0.0025
TRINITY_DN2863_c0_g1_i2	O80920		-1.2865	0.00108
TRINITY_DN14720_c1_g1_i1	Q7XBY6	abscisic acid receptor PYR1-like	-1.2627	0.03697
TRINITY_DN37259_c0_g1_i8	Q6I5C3	abscisic acid receptor PYL9-like	-1.6912	4E-05
Jasmonic acid				
TRINITY_DN20936_c0_g2_i1	Q5NAZ7	jasmonic acid-amido synthetase JAR2-like	-1.3916	0.01244
Cell wall (cellulose synthase)				
TRINITY_DN5875_c0_g1_i7	A2Y0X2	cellulose synthase-1	1.15984	0.00174
TRINITY_DN17995_c0_g1_i2	A2WV32	cellulose synthase A catalytic subunit 4 [UDP-forming]	1.24595	0.00177
TRINITY_DN11219_c0_g1_i1	Q9LHZ7	cellulose synthase-like protein D2	1.22321	0.00109
TRINITY_DN36556_c0_g1_i1			1.03457	0.04801
TRINITY_DN1437_c0_g1_i12			1.38909	0.00018
TRINITY_DN1437_c0_g1_i5			1.42678	0.00018
TRINITY_DN1437_c0_g1_i9	A2YU42		1.31685	0.00028

TRINITY_DN3616_c0_g2_i1	Q651X6	cellulose synthase-like protein E6	1.46105	8E-05
TRINITY_DN51709_c0_g1_i1			1.50801	0.00037
TRINITY_DN3616_c0_g3_i2			1.72465	1.9E-05

DISCUSSION

Transcriptome study revealed putative candidate genes and pathways associated with hypergravity induced root growth phenotype. The gene products for auxin biosynthesis, cell division and/or proliferation, cellulose synthase were found to be significantly up-regulated in response to hypergravity. Generally, tryptophan-dependent/independent auxin biosynthesis pathways require the key intermediate product – Indole-3-glycerol phosphate (IGP) (Wright et al., 1991; Normanly et al., 1993). In the present study, Indole-3-glycerol phosphate synthase gene was found to be significantly up-regulated in response to hypergravity indicating the increased auxin level leading to the enhanced root growth. Genes involved in cell division RPA, Cell division cycle 42 (CDC42) Homolog and Cell division control protein 25-like (CDC25-like) were found to be highly expressed in the hypergravity treatment group implying mitotic cell division is highly up-regulated in response to hypergravity. Coupled with this, down-regulation of isoform level expression of a negative regulator of cell division gene – Cell number regulator 2 further supports the hypergravity-influence on cell division. As a consequence of cell division (number or cell size), there was necessity of higher demand for cell-wall constituents in hypergravity treated samples. In line with this, current study showed genes associated with UDP formation leading to cellulose synthesis were found to be highly expressed as evident from cellulose biosynthesis pathway analysis. Similarly, multiple researches reported up-regulation of cellulose synthase gene upon or under hypergravity treatment (Martzivanou and Hampp, 20003; Tamaoki et al., 2009). Further, the contribution of UDP-glucose to the synthesis of cell wall polysaccharides in plants was well documented (Verbanci et al., 2017).

A significant role of phytohormones in root growth is recently reported. Specifically, ABA was reported to negatively regulate maize root growth (Mega et al., 2015). Multiple shreds of evidence indicate that high concentrations of ABA not only inhibit cell division in the apical meristems but also repress cell expansion in the elongation zone in roots (Takatsuka and Umeda, 2014; Bai et al., 2009; Yang et al., 2014). Specifically, ABA hydroxylase reported to degrade ABA (Gillard and Walton, 1976; Krochko et al., 1998), thus, reducing the concentration of ABA and facilitating root growth. Consistent with this data, ABA hydroxylase was significantly up-regulated, and in contrast, ABA receptor PYL-4 like was significantly down-regulated in response to hyper-gravity. Another interesting hormone Jasmonic acid was also reported to play an inhibitory role in primary root growth (Gasperini et al., 2015). The repression of JA level was mediated by JAZ proteins which further recruits MYCs (Chini et al., 2007; Thines et al., 2007; Yan et al., 2007), co-repressor TPL (Shyu et al., 2012), or NINJA adaptor proteins (Pauwels et al., 2010) and facilitate root growth. In line with this, we found up-regulation of JAZ repressor complex relevant transcripts and downregulation of Jasmonic acid-amido synthetase JAR2-like gene suggesting hypergravity induced suppression of JA levels, thus, contributing to enhanced root growth phenotype.

CONCLUSION

Collectively, this investigation was able to identify putative genes or pathways associated with hypergravity-induced enhanced root phenotype. This study also provides an insight into the molecular changes underlying wheat root growth phenotype in response to hypergravity.

ACKNOWLEDGMENTS

The first author (MS) and Basavalingayya K Swamy (BKS) acknowledge the DBT-JNU, Govt. of India for the fellowship. The corresponding author, Ravikumar Hosamani (RH) acknowledges DST-SERB for awarding research grant of which this publication is part.

Keywords: Hypergravity, Wheat, Root transcriptome

REFERENCES

Bai, L., Zhang, G.Z., Zhou, Y., Zhang, Z.P., Wang, W., Du, Y.Y., Wu, Z.Y., Song, C.P. (2009). Plasma membrane-associated proline-rich extensin-like receptor kinase 4, a novel regulator of Ca^{2+} signalling, is required for abscisic acid responses in Arabidopsis thaliana. Plant J. 60, 314–327.

Basavalingayya (2020). Hypergravity-induced phenotypic, hormonal, and temporal protein changes in wheat (Triticum aestivum L.). [Masters' Thesis]. [Dharwad]: University of Agricultural Sciences (India).

Chen, S., Zhou, Y., Chen, Y., Gu, J. (2018). Fastp: an ultra-fast all-in-one FASTQ pre-processor. Bioinformatics 34:17, i884–i890.

Chini, A., Fonseca, S., Fernandez, G., Adie, B., Chico, J.M., Lorenzo, O., Garcia-Casado, G., Lopez-Vidriero, I., Lozano, F.M., Ponce, M.R., Micol, J.L., Solano, R. (2007). The JAZ family of repressors is the missing link in jasmonate signalling. Nature 448, 666–671.

Gasperini, D., Chetelat, A., Acosta, I.F., Goossens, J., Pauwels, L., Goossens, A., Dreos, R., Alfonso, E., Farmer, E.E. (2015) Multilayered organization of jasmonate signalling in the regulation of root growth. PLoS Genet. 11:6, e1005300. doi: 10.1371/journal.pgen.1005300

Gillard, D.F., Walton, D.C. (1976). Abscisic acid metabolism by a cell-free preparation from Echinocystis lobata liquid endosperm. Plant Physiol. 58, 790–795.

Gotz, S., Garcia-Gomez, J.M., Terol, J., Williams, T.D., Nagaraj, S.H., Nueda, M.J., Robles, M., Talon, M., Dopazo, J., Conesa, A. (2008). High-throughput functional annotation and data mining with the Blast2GO suite. Nucleic acids research 36:10, 3420-35.

Krochko, J.E., Abrams, G.D., Loewen, M.K., Abrams, S.R., Cutler, A.J. (1998). (+)-Abscisic acid 8′-hydroxylase is a cytochrome P450 monooxygenase. Plant Physiol. 118, 849–860.

Martzivanou, M., Hampp, R. (2003). Hyper-gravity effects on the Arabidopsis transcriptome. Physiologia Plantarum 118, 221–231.

Mega, R., Meguro-Maoka, A., Endo, A., Shimosaka, E., Murayama, S., Nambara, E., Seo, M., Kanno, Y., Suzanne, R., Sato, Y. (2015). Sustained low abscisic acid levels increase seedling vigor under cold stress in rice (Oryza sativa L.). Scientific Rep. 5, 813-829.

Normanly, J., Cohen, J.D., Fink, G.R. (1993). Arabidopsis thaliana auxotrophs reveal a tryptophan-independent biosynthetic pathway for indole-3-acetic acid. Proc. Natl. Acad. Sci. 90, 10355–10359.

Pauwels, L., Barbero, G.F., Geerinck, J., Tilleman, S., Grunewald, W., Perez, A.C., Chico, J.M., Bossche, R.V., Sewell, J., Gil, E., Casado, G.G., Witters, E., Inze, D., Long, J.A., Jaeger, G.D., Solano, R., Goossens, A. (2010). NINJA connects the co-repressor TOPLESS to jasmonate signalling. Nature 464, 788–791.

Robinson, M.D., McCarthy, D.J., Smyth, G.K. (2010). edgeR: a Bioconductor package for differential expression analysis of digital gene expression data. Bioinformatics 26:1, 139-40.

Shyu, C., Figueroa, P., DePew, C.L., Cooke, T.F., Sheard, L.B., Moreno, J.E., Katsir, L., Zheng, N., Browse, J., Howe, G.A. (2012). JAZ8 lacks a canonical degron and has an EAR motif that mediates transcriptional repression of jasmonate responses in Arabidopsis. Plant Cell 24, 536–550.

Takatsuka, H., and Umeda, M. (2014). Hormonal control of cell division and elongation along differentiation trajectories in roots. J. Exp Bot. 65, 2633–2643.

Tamaoki, D., Karahara, I., Nishiuchi, T., Oliveira, S.D., Schreiber, L., Wakasugi, T., Yamada, K., Yamaguchi, K., Kamisaka, S. (2009). Transcriptome profiling in Arabidopsis inflorescence stems grown under hypergravity in terms of cell walls and plant hormones. Adv. Space Res. 44, 245–253.

Thines, B., Katsir, L., Melotto, M., Niu, Y., Mandaokar, A., Liu, G., Nomura, K., He, S.Y., Howe, G.A., Browse, J. (2007). JAZ repressor proteins are targets of the SCFCOI1 complex during jasmonate signalling. Nature 448, 661–665.

Verbanci, J., Lunn, J.E., Stitt, M., Persson, S. (2017). Carbon Supply and the Regulation of Cell Wall Synthesis. Molecular Plant. 11, 75–94.

Wright, A.D., Sampson, M.B., Neuffer, M.G., Michalczuk, L., Slovin, J.P., Cohen, J.D. (1991). Indole-3-acetic acid biosynthesis in the mutant maize orange pericarp, a tryptophan auxotroph. Science 254, 998–1000.

Yan, Y., Stolz, S., Chetelat, A., Reymond, P., Pagni, M., Dubugnon, L., Farmer, E.E. (2007). A down-stream mediator in the growth repression limb of the jasmonate pathway. Plant Cell 19, 2470–2483.

Yang, L., Zhang, J., He, J., Qin, Y., Hua, D., Duan, Y., Chen, Z., Gong, Z. (2014). ABA-mediated ROS in mitochondria regulate root meristem activity by controlling PLETHORA expression in *Arabidopsis*. PLoS Genet. 10, e1004791.

Assessment of the relationship between the cardiovascular system during 6-degrees head-down tilt using conditional entropy: A terrestrial based microgravity study

Vishwajeet Shankhwar[1]*, Dilbag Singh[1], K K Deepak[2]

[1]*Department of Instrumentation and Control Engineering, Dr B R Ambedkar National Institute of Technology, Jalandhar, Punjab, India*

[2]*Department of Physiology, All India Institute of Medical Science, New Delhi, India*

**vishwajeet915@gmail.com*

INTRODUCTION

Gravity is essential for the cardiovascular system to operate accurately. In the absence of gravity, cardiac muscles deconditioned that leads to multisystem failure upon reintroduction of gravity (Hargens et al., 2013; Shankhwar et al., 2021b, 2021a) Due to the lack of use, muscles weaken and play a vital role in cardiac muscle deconditioning during microgravity exposure (Waldie and Newman, 2011).

Analogues are available to replicate the effects of microgravity on Earth using head-down tilt (HDT) (Haider et al., 2013; Hargens and Vico, 2016; Shankhwar et al., 2021c). The 6-degree HDT model is extensively used in microgravity simulations. This HDT causes a shift in blood volume from the lower body to the thoracic cavity. The cardiovascular system responses are investigated via the linear domain analyses (time and frequency domain) (Billman, 2011; Vishwajeet et al., 2020)the beat-to-beat variation in either heart rate or the duration of the R-R interval - the heart period, has become a popular clinical and investigational tool. The temporal fluctuations in heart rate exhibit a marked synchrony with respiration (increasing during inspiration and decreasing during expiration - the so called respiratory sinus arrhythmia, RSA. Interestingly, various techniques for detecting and quantifying information flow between time-series data have been documented. Cross-correlation in the time domain and coherence analysis in the frequency domain are the most prominent mechanisms for analysis. However, they are insufficient to quantify the coupling and information flow between two biological systems. Based on conditional entropy, a novel approach for analyzing coupling indices has been developed (CE). It is used to assess the directionality of connection between time-series signals (Nollo et al., 2005; Faes et al., 2011; Porta et al., 2011).

It's also used to anticipate the behavior of a time series signal based on previous data while interacting causally with another series (Eichler, 2013). Directional coupling occurs between two-time series A and B: A→B and B→A. Whereas indirect coupling was observed due to one mutual C series in between two-time (A, B) series. Direct coupling indicates A→B and B→C, and indirect coupling is A→C mediated by B. The coupling between and within the signal is required to gain a better understanding of how a system works (Javorka et al., 2017).

The cardiovascular system is a closed-loop system with a feedback mechanism for resolving issues (Porta et al., 1998) but it is able to increase when no robust statistic can be performed as a result of a limited amount of available samples. As a consequence of the minimisation procedure, the proposed index is obtained without an a-priori definition of the pattern length (i.e. of the embedding dimension of the reconstructed phase space. In the present study, 5-minute of 6-degree HDT was used to replicate immediate microgravity effects. With the aid of conditional entropy, the interaction between the cardiovascular, cardiorespiratory, and vasculorespiratory systems during HDT and supine posture was investigated. To the best of the author's knowledge, this is the first study to use directional coupling analysis to assess the 6-degree HDT response with the simultaneous recording of electrocardiography (ECG), blood pressure (BP), and respiration.

MATERIAL AND METHODS

Twenty young male individuals participated and their averaged age, height and weight was 25.3 ± 6.14yr, 169.3 ± 6.94cm and 62.5 ± 12.31Kg respectively (mean ± standard deviation). All subjects signed a consent form before participating in the study. Subjects having a history of cardiovascular, psychological, hypertensive or medical problems were excluded from the study. Subjects were told not to take any medicine for at least 24 hours and not to drink tea or eat anything for at least 3 hours before being recorded. After receiving clearance from the institute's ethical committee, the investigation was carried out in the institute's biomedical instrumentation laboratory.

The recording was carried out in a controlled room environment (controlled temperature and comfortable light), ECG was recorded using a Biopac MP100 data acquisition system (Biopac Services, Inc., Goleta, CA). The non-invasive tonometric blood pressure monitor NIBP 100B Biopac Systems (FUSION) was used to monitor the blood pressure. The Biopac SS5LB respiratory transducer belt was used to record respiration (in mV). All of the signals were collected at 1,000 Hz and saved on a computer to be analyzed with MATLAB 2018b.

The participant was advised to rest in the supine position on the tilt table. After that, electrodes for ECG recording were placed. To get the BP signal, a BP radial artery sensor was positioned. An adjustable nylon strap integrated transducer was used over the thorax to record variations during breathing. After 20 minutes of resting phase, a baseline recording in the supine position for 5 minutes was taken. The participant was tilted to 6-degree HDT for 5 minutes after the baseline recording. In addition, the individual was told to breathe regularly (12-15 breath cycles per minute). A detailed schematic study protocol is shown in Figure 1.

Conditional entropy (CE) analysis, which is based on the information domain method and computes the information contained in time series was utilized. Based on Shannon entropy, it has also shown the amount of information transmission across time series. By removing the mean and dividing by the standard deviation, all time series utilized for analysis were normalized. The CE technique proposed by Faes et al. 2015 has been used in the present study for the calculation of interaction index. The interaction among electrocardiograph (RRI), systolic blood pressure (SBP) and respiratory (RSP) signal was investigated. The conditioning vector depends on the interaction used the study such as SBP to RRI, RRI to SBP, RSP to RRI, RRI to RSP, RSP to SBP and SBP to RSP. Source and target series was based on the selected interaction.

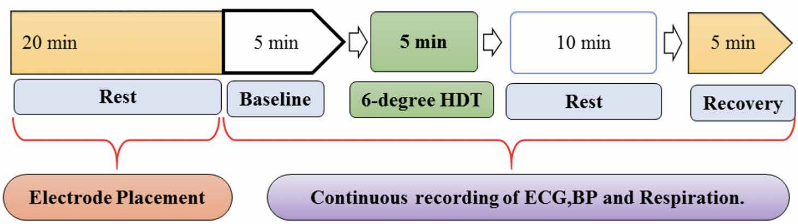

FIGURE 1:. Schematic representation of the study protocol followed by each subject.

To evaluate the interaction from SBP to RRI, the SBP taken as source and RRI as target series.

RESULTS

RRI was derived from ECG, SBP derived from raw BP and ECG-R peaks were used to locate the respiration amplitude. Three hundred simultaneous samples of RRI, SBP, and RSP time series are taken from each subject during baseline and 6-degree HDT. Table 1 shows the coupling index of cardiovascular, cardiorespiratory and vasculorespiratory interaction. The cardiovascular interaction values reveals that the effect of SBP on RRI increased significantly during 6-degree HDT as compared to baseline. Whereas, the RRI's effect decreases significantly for the same. The cardiorespiratory and vasculorespiratory interaction values shows no significant variations between baseline and 6-degree HDT (Figure 2).

Table 1: Information transfer (coupling) between RRI, SBP and RSP time series for baseline and 6-degree HDT

Interaction **(Coupling Index)**		**0-degree (Baseline)**	**6-degree HDT**
Cardiovascular		0.19 ± 0.04	0.21 ± 0.04$^{\$\#}$
(ECG ↔ BP)		0.06 ± 0.01	0.02 ± 0.01$^{\$}$
Cardiorespiratory		0.16 ± 0.04	0.17 ± 0.02
(ECG ↔ Respiration)		0.00 ± 0.00	0.00 ± 0.01
Vasculorespiratory		0.09 ± 0.01	0.10 ± 0.03
(BP ↔ Respiration)		0.00 ± 0.02	0.00 ± 0.00

Note: n=20 '$C_{A\rightarrow B}$', indicates A's effect on B; Values are given as mean ± SD; Significance test: $^{\$}p<0.05$ Baseline vs 6-degree HDT; $^{\#}p<0.05$ $C_{SBP\rightarrow RRI}$ vs $C_{RRI\rightarrow SBP}$ or $C_{RSP\rightarrow RRI}$ vs $C_{RRI\rightarrow RSP}$ or $C_{RSP\rightarrow SBP}$ vs $C_{SBP\rightarrow RSP}$ (Paired student t-test).

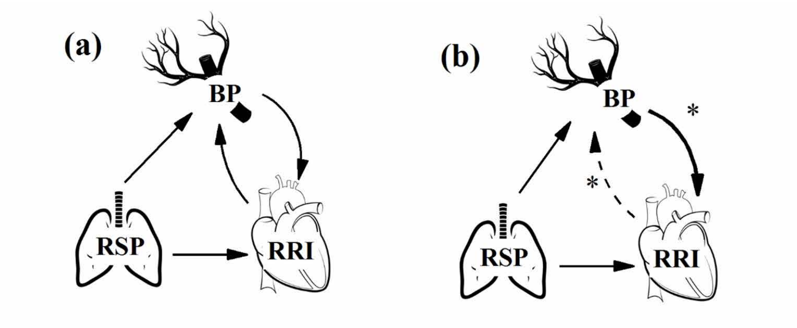

FIGURE 2: Graphical representation of the results of information flow analysis in two conditions: (**a**) supine position (baseline) and (**b**) head down tilt position. Arrows between two systems are present when the coupling index is non-zero between two systems. The style of the arrow is arranged so that to reflect the information flow between them. (i.e., the coupling is significantly increased for bold arrows and decreased for dashed arrows, and for solid arrows, no changes were observed). Further, the statistical significance between baseline and HDT (i.e., the significance of the coupling index) is indicated by '*'

DISCUSSION

The present study deals with an information domain technique, which has been used to evaluated the relationship between cardiac, vascular, and respiratory responses for 6-degree HDT. At 6-degree HDT, the results of this investigation demonstrate a considerable increase in information flow from SBP to RRI. The cardiovascular system has a feedforward and feedback mechanism, it is a closed-loop system. These processes naturally control the variations in the cardiovascular system that occur in the human body. The parasympathetic system is activated by an increase in blood pressure perceived by baroreflex receptors, which results in reduction of heart rate. The arterial baroreflex is one of the mechanisms for maintaining blood pressure by causing a change in heart rate. During a 6-degree head-down tilt, the heart rate was regulated according to the SBP measured. Because of the baroreflex system, the effect of RRI on SBP was reduced during 6-degree HDT. This baroreflex mechanism keeps blood pressures stable without affecting RRI. The mechanical feed-forward system is another name for this mechanism. This mechanism decreases its effect because the information transfer was decreased from RRI to SBP. In contrast to this, effect of SBP on RRI was increased by homeostasis mechanism. This correction mechanism may have narrowed the vessel in order to preserve the appropriate functioning of the human body. The CE method aided in a better understanding of HDT cardiac, vascular, and respiratory responses, as well as determining the system's dominance during HDT microgravity analogue.

CONCLUSION

A CE technique based on the information domain method was used to assess the interaction between the cardiac, vascular, and respiratory subsystems. The CE approach was used to determine the coupling index and the effect of one system on another. During a 6-degree HDT, the parasympathetic nervous system was activated, and the influence of vascular on heart function was enhanced. The results derived from the CE approach are in line with the physiological mechanisms described for cardiovascular change for HDT.

ACKNOWLEDGMENTS

Mr. Vishwajeet Shankhwar is thankful to the Ministry of Human Resource Development (MHRD), New Delhi for providing fellowship.

Keywords: Microgravity, Conditional entropy, Cardiovascular, Cardiorespiratory, Vasculorespiratory, Coupling index

REFERENCES

Billman, G. E. (2011). Heart rate variability - A historical perspective. Front. Physiol. 2 NOV, 1–13. doi:10.3389/fphys.2011.00086.

Eichler, M. (2013). Causal inference with multiple time series: Principles and problems. Philos. Trans. R. Soc. A Math. Phys. Eng. Sci. 371. doi:10.1098/rsta.2011.0613.

Faes, L., Nollo, G., and Porta, A. (2011). Information domain approach to the investigation of cardio-vascular, cardio-pulmonary, and vasculo-pulmonary causal couplings. Front. Physiol. 2 NOV, 1–13. doi:10.3389/fphys.2011.00080.

Faes, L., Porta, A., and Nollo, G. (2015). Information decomposition in bivariate systems: Theory and application to cardiorespiratory dynamics. Entropy 17, 277–303. doi:10.3390/e17010277.

Haider, T., Gunga, H. C., Matteucci-Gothe, R., Sottara, E., Griesmacher, A., Belavý, D. L., et al. (2013). Effects of long-term head-down-tilt bed rest and different training regimes on the coagulation system of healthy men. Physiol. Rep. 1, 1–13. doi:10.1002/phy2.135.

Hargens, A. R., Bhattacharya, R., and Schneider, S. M. (2013). Space physiology VI: Exercise, artificial gravity, and countermeasure development for prolonged space flight. Eur. J. Appl. Physiol. 113, 2183–2192. doi:10.1007/s00421-012-2523-5.

Hargens, A. R., and Vico, L. (2016). Long-duration bed rest as an analog to microgravity. J. Appl. Physiol. 120, 891–903. doi:10.1152/japplphysiol.00935.2015.

Javorka, M., Czippelova, B., Turianikova, Z., Lazarova, Z., Tonhajzerova, I., and Faes, L. (2017). Causal analysis of short-term cardiovascular variability: state-dependent contribution of feedback and feedforward mechanisms. Med. Biol. Eng. Comput. 55, 179–190. doi:10.1007/s11517-016-1492-y.

Nollo, G., Faes, L., Porta, A., Antolini, R., and Ravelli, F. (2005). Exploring directionality in spontaneous heart period and systolic pressure variability interactions in humans: Implications in the evaluation of baroreflex gain. Am. J. Physiol. - Hear. Circ. Physiol. 288, 1777–1785. doi:10.1152/ajpheart.00594.2004.

Porta, A., Baselli, G., Liberati, D., Montano, N., Cogliati, C., Gnecchi-Ruscone, T., et al. (1998). Measuring regularity by means of a corrected conditional entropy in sympathetic outflow. Biol. Cybern. 78, 71–78. doi:10.1007/s004220050414.

Porta, A., Catai, A. M., Takahashi, A. C. M., Magagnin, V., Bassani, T., Tobaldini, E., et al. (2011). Causal relationships between heart period and systolic arterial pressure during graded head-up tilt. Am. J. Physiol. - Regul. Integr. Comp. Physiol. 300, 378–386. doi:10.1152/ajpregu.00553.2010.

Shankhwar, V., Singh, D., and Deepak, K. K. (2021a). Characterization of Electromyographical Signals from Biceps and Rectus Femoris Muscles to Evaluate the Performance of Squats Coupled with Countermeasure Gravitational Load Modulating Bodygear. Microgravity Sci. Technol. 33:49, 1–11. doi:10.1007/s12217-021-09899-z.

Shankhwar, V., Singh, D., and Deepak, K. K. (2021b). Effect of Novel Designed Bodygear on Gastrocnemius and Soleus Muscles during Stepping in Human Body. Microgravity Sci. Technol. 33:29, 1–10. doi:10.1007/s12217-021-09870-y.

Shankhwar, V., Singh, D., and Deepak, K. K. (2021c). Immediate changes in cardiac autonomic tone and stroke volume during microgravity simulation using head-down tilt. 65, 86–93.

Vishwajeet, Singh, D., and Deepak, K. K. (2020). "Investigation of heart rate variability with the help of welch periodogram in indian young adults based on body physique," in Smart Healthcare for Disease Diagnosis and Prevention (Elsevier), 51–57. doi:10.1016/B978-0-12-817913-0.00008-0.

Waldie, J. M., and Newman, D. J. (2011). A gravity loading countermeasure skinsuit. Acta Astronaut. 68, 722–730. doi:10.1016/j.actaastro.2010.07.022.

Computationally modeling the effect of curcumin on cancer and healthy breast cells under ionizing radiation and microgravity conditions

Siddhant Sharma[1,2]*, Busra Elkatmis[1,3], Brooke Carruthers[1,4], Anjali Sharma[2], Jéssica Carneiro[1,5], Garrett Campion[1], Kendall Godwin[6]

[1]*Blue Marble Space Institute of Science, Seattle, Washington, United States*
[2]*Department of Biochemistry, University of Delhi, New Delhi, India*
[3]*Cluster of Excellence on Plant Science, Heinrich-Heine-Universität Düsseldorf, Germany*
[4]*University of Arizona, Tucson, Arizona United States*
[5]*Institute of Sea Studies Admiral Paulo Moreira, Arraial do Cabo, Brazil*
[6]*Penn State University, University Park, Pennsylvania, United States*
**siddhaantsharma.ss@gmail.com*

INTRODUCTION

Earth is conducive for the origins of life in part due to its reduced exposure to cosmic radiation relative to open space. Radiation can induce tumorous growth formation but treatment with radiotherapy in breast cancer cell lines such as MCF-7 have demonstrated a reduction in cancer cells (Lagadec *et al.,* 2012; Haussman *et al.,* 2020). Similarly, bioactive compounds such as curcumin have been shown to slow the development of breast cancer (Liu & Ho 2018). Being an easily accessible molecule, it is an alternative route in the treatment of various types of cancer; both as an isolated molecule and in conjunction with antineoplastic agents (Giordano & Tommonaro 2019; Zoi *et al*., 2021). Curcumin exerts chemopreventive and antiproliferative activities, inhibiting the growth and proliferation of cancer cells.

In this study, we review the current biochemical understanding of curcumin as it pertains to the breast cancer treatment and propose a computational model to predict and elucidate the effects of curcumin on cancer and healthy breast cell lines under conditions induced by ionizing radiation (Nassef *et al.,* 2020) and microgravity. In our proposed model, we will utilize computational modeling to analyze the expression of WTH3 (GAN *et al.,* 2015), a gene known to inhibit cell proliferation via the activation of tumor suppressor genes which is known to be differentially expressed in cancer and normal breast tissue. Curcumin presents an attractive target for our analysis owing to its known therapeutic properties to human health, wide availability, and non-prohibitive cost. The aim of this work is to compare the level of expression of the WTH3 gene in healthy cancer cells and MCF-7 under ionizing radiation conditions, such as those on other potentially habitable regions for future space colonization efforts.

METHODS

The SMILES (Simplified molecular-input line-entry system) for curcumin was collected from PubChem Database (https://pubchem.ncbi.nlm.nih.gov/). We utilized OMIM database (Stelzer *et al.,* 2011) to gather disease-associated targets (Breast Cancer) and WTH3 gene interactions. The curated targets of breast cancer were imported into the Uniprot database (https://www.uniprot.org/) to gather gene-related information. STRING (Search Tool for the Retrieval of Interacting Genes) (Szklarczyk *et al.,* 2018) was used to construct a PPI network of interacting related genes. Estimates of gene expression, interaction, and sub-cellular locations were done through Human Protein Atlas (Uhlen *et al.,* 2017). The pharmacokinetic properties of curcumin were screened through the pkCSM package (Pires *et al.,* 2015). We utilized the pdCSM package suite (Al-Jarf *et al.,* 2021) to validate our results using state of the art graph-based signature approaches; screening curcumin as a potent bioactive compound for MCF-7 breast cancer cell lines and exploring its use as a small molecule kinase inhibitor. Prediction of ADME (Absorption, Distribution, Metabolism, and Excretion) parameters and druglike nature was done through SwissADME (Daina *et al.,* 2017) and macromolecular target prediction was achieved through SwissTargetPrediction (Daina *et al.,* 2019), for bioactive curcumin to enable small molecule drug discovery. The data and results of pkCSM, pdCSM, SwissADME and SwissTargetPrediction are provided in the supporting information of this study.

For the analysis of differential gene expression between the MCF-7 cell lines and under the ionizing radiation conditions, we propose the use of RNA-Seq to observe the up or down regulation of WTH3 gene expression within our proposed workflow. We wish to employ the SCDE package (Kharchenko *et al.,* 2014) coupled to PangaloDB (Franzén *et al.,* 2019) for exploration of the differential gene expression and RNA-Seq data, and NetworkAnalyst (Zhou *et al.,* 2019) for visualization of the said data generated. Ease of Access RNA-Seq workflows will be preferred for quick analysis of the resulting data using the proposed workflow in our study (Melsted *et al.,* 2019). The resulting interacting biological networks will be parsed and processed with BioNetComp (Carvalho *et al.*, 2021) to enable more insights into differential gene expression of WTH3 under varying curcumin concentrations.

Computational modeling of a multicellular system to simulate the radiation flow in culture systems of 3D cells will be done by employing the use of open-source radiation transport packages, Geant4 (Agostinelli et al., 2003) and EGSnrc (Kawrakow *et al.*, 2017). The *in-silico* modeling of cancer cells will be done via established NEATG cell-modelling methods (Pantziarka 2016). We wish to further employ the cell modeling methods used in a similar study (Cheng *et al.* 2020) to predict the anticancer properties of curcumin. The LIDE.Space (https://lide.space/) platform will be used to collect real experimental microgravity data for the wet-lab experiments in our study on a competitive basis.

RESULTS AND DISCUSSION

The pdCSM results are elucidated in Figure 1. and they support the interaction of curcumin with MCF-7 breast cancer cell lines. The BOILED-EGG (Daina & Zoete 2016) depiction from SwissADME is shown in Figure 2. A), confirming

SMILES	General Anticancer Activity	Breast BT_549	Breast HS_578T	Breast MCF7
COC1=C(C=CC(=C1)C=CC(=O)CC(=O)C=CC2=CC(=C(C=C2)O)OC)O	Active	5.274 ✓	5.071 ✓	5.493 ✓

FIGURE 1: The pdCSM result supports the interaction of curcumin with MCF-7 breast cancer cell lines.

the Human Intestinal Absorption of bioactive curcumin. The pie-chart of the results from SwissTargetPrediction analysis is shown in Figure 2. B), providing a comprehensive list of probable macromolecular drug targets. The SwissTargetPrediction results show the top promising targets are Family B G protein and kinases. The graphical representation of RNA-Seq workflow to be employed in our study is shown in Figure 3.

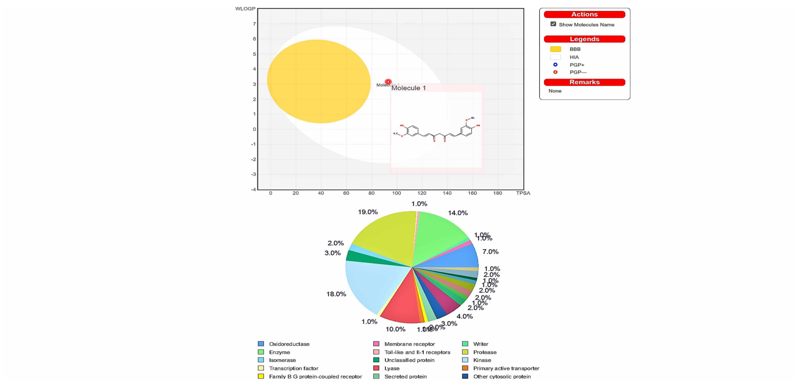

FIGURE 2: (**A**) Schematic showing the BOILED-EGG (Daina & Zoete 2016) depiction from SwissADME, confirming the Human Intestinal Absorption of bioactive curcumin. (**B**) Results from SwissTargetPrediction analysis.

FIGURE 3: Graphical representation of the RNA-Seq workflow to be employed in our study.

We aim to analyze the effect of application of curcumin on the WTH3 expression level under ionizing radiation conditions. We hypothesize that In order to prevent the formation of cancer in the body caused by radiation in harsh space conditions, the level of WTH3 should be increased as in healthy cells. The WTH3 promoters are upregulated with increased activity of tumor suppressor genes such as p53 in the curcumin added samples. We expect to see a decrease in the number of cancer cells with an increased expression of WTH3 when cancer cells such as MCF - 7 when exposed to curcumin treatment.

Analogous to the results that will be obtained through our proposed workflow and computational model, biological products based on the bioactive curcumin may be applied to astronauts in space environments to solve the problems associated with ionizing surface radiation in future space travel and establishment missions. This study may direct the development of potent novel bioactive supplements for the future human colonization missions.

SUPPORTING INFORMATION

The supplementary information containing the results and data of predictions is provided online on GitHub and can be obtained from: https://github.com/ssiddhantsharma/ISGP_Study_Data

ACKNOWLEDGMENTS

The authors would like to thank the Blue Marble Space Institute of Science (BMSIS) for organizing the YSP2020 program (SS, BE, BC, JC, GC) and for providing an active medium of collaboration. The authors acknowledge the discussions on the subject with Roberto Parisi. The authors would also like to thank the organizers for the invitation to submit to this issue.

Keywords: Surface Radiation, Computational Simulations, Bioactive Curcumin, Cancer Growth, Microgravity Simulations

REFERENCES

Lagadec, C., Vlashi, E., Della Donna, L., Dekmezian, C., & Pajonk, F. (2012). Radiation-Induced Reprogramming of Breast Cancer Cells. STEM CELLS, 30(5), 833–844. https://doi.org/10.1002/stem.1058

Haussmann, J., Corradini, S., Nestle-Kraemling, C., Bölke, E., Njanang, F. J. D., Tamaskovics, B., Orth, K., Ruckhaeberle, E., Fehm, T., Mohrmann, S., Simiantonakis, I., Budach, W., & Matuschek, C. (2020). Recent advances in radiotherapy of breast cancer. Radiation Oncology, 15(1). https://doi.org/10.1186/s13014-020-01501-x

Liu, H.-T., & Ho, Y.-S. (2018). Anticancer effect of curcumin on breast cancer and stem cells. Food Science and Human Wellness, 7(2), 134–137. https://doi.org/10.1016/j.fshw.2018.06.001

Zoi, V., Galani, V., Lianos, G. D., Voulgaris, S., Kyritsis, A. P., & Alexiou, G. A. (2021). The Role of Curcumin in Cancer Treatment. Biomedicines, 9(9), 1086. https://doi.org/10.3390/biomedicines9091086

Sueth-Santiago, V., Mendes-Silva, G. P., Decoté-Ricardo, D., & Lima, M. E. F. D. (2015). Curcumin, the golden powder from turmeric: Insights into chemical and biological activities. Química Nova, 38(4), 538-552.https://doi.org/10.5935/0100-4042.20150035

Giordano, A., & Tommonaro, G. (2019). Curcumin and cancer. Nutrients, 11(10), 2376.https://doi.org/10.3390/biomedicines9091086

Nassef, M. Z., Melnik, D., Kopp, S., Sahana, J., Infanger, M., Lützenberg, R., Relja, B., Wehland, M., Grimm, D., & Krüger, M. (2020). Breast Cancer Cells in Microgravity: New Aspects for Cancer Research. International Journal of Molecular Sciences, 21(19), 7345. https://doi.org/10.3390/ijms21197345

GAN, L., ZUO, G., WANG, T., MIN, J., WANG, Y., WANG, Y., & LV, G. (2015). Expression of WTH3 in breast cancer tissue and the effects on the biological behavior of breast cancer cells. Experimental and Therapeutic Medicine, 10(1), 154–158. https://doi.org/10.3892/etm.2015.2458

Stelzer, G., Dalah, I., Stein, T.I. et al. In-silico human genomics with GeneCards. Hum Genomics 5, 709 (2011). https://doi.org/10.1186/1479-7364-5-6-709

Szklarczyk, D., Gable, A. L., Lyon, D., Junge, A., Wyder, S., Huerta-Cepas, J., Simonovic, M., Doncheva, N. T., Morris, J. H., Bork, P., Jensen, L. J., & Mering, C. von. (2018). STRING v11: protein–protein association networks with increased coverage, supporting functional discovery in genome-wide experimental datasets. Nucleic Acids Research, 47(D1), D607–D613. https://doi.org/10.1093/nar/gky1131

Uhlen, M., Zhang, C., Lee, S., Sjöstedt, E., Fagerberg, L., Bidkhori, G., Benfeitas, R., Arif, M., Liu, Z., Edfors, F., Sanli, K., von Feilitzen, K., Oksvold, P., Lundberg, E., Hober, S., Nilsson, P., Mattsson, J., Schwenk, J. M., Brunnström, H., ... Ponten, F. (2017). A pathology atlas of the human cancer transcriptome. Science, 357(6352), eaan2507. https://doi.org/10.1126/science.aan2507

Pires, D. E. V., Blundell, T. L., & Ascher, D. B. (2015). pkCSM: Predicting Small-Molecule Pharmacokinetic and Toxicity Properties Using Graph-Based Signatures. Journal of Medicinal Chemistry, 58(9), 4066–4072. https://doi.org/10.1021/acs.jmedchem.5b00104

Al-Jarf, R., de Sá, A. G. C., Pires, D. E. V., & Ascher, D. B. (2021). pdCSM-cancer: Using Graph-Based Signatures to Identify Small Molecules with Anticancer Properties. Journal of Chemical Information and Modeling, 61(7), 3314–3322. https://doi.org/10.1021/acs.jcim.1c00168

Daina, A., Michielin, O. & Zoete, V. SwissADME: a free web tool to evaluate pharmacokinetics, drug-likeness and medicinal chemistry friendliness of small molecules. Sci Rep 7, 42717 (2017). https://doi.org/10.1038/srep42717

Daina, A., Michielin, O., & Zoete, V. (2019). SwissTargetPrediction: updated data and new features for efficient prediction of protein targets of small molecules. Nucleic Acids Research, 47(W1), W357–W364. https://doi.org/10.1093/nar/gkz382

Kharchenko, P., Silberstein, L. & Scadden, D. Bayesian approach to single-cell differential expression analysis. Nat Methods 11, 740–742 (2014). https://doi.org/10.1038/nmeth.2967

Franzén, O., Gan, L.-M., & Björkegren, J. L. M. (2019). PanglaoDB: a web server for exploration of mouse and human single-cell RNA sequencing data. Database, 2019. https://doi.org/10.1093/database/baz046

Zhou, G., Soufan, O., Ewald, J., Hancock, R. E. W., Basu, N., & Xia, J. (2019). NetworkAnalyst 3.0: a visual analytics platform for comprehensive gene expression profiling and meta-analysis. Nucleic Acids Research, 47(W1), W234–W241. https://doi.org/10.1093/nar/gkz240

Melsted, P., Booeshaghi, A. S., Gao, F., Beltrame, E., Lu, L., Hjorleifsson, K. E., Gehring, J., & Pachter, L. (2019). Modular and efficient pre-processing of single-cell RNA-seq. Cold Spring Harbor Laboratory. https://doi.org/10.1101/673285

Carvalho, L. M. (2021). BioNetComp: a Python package for biological network development and comparison. Cold Spring Harbor Laboratory. https://doi.org/10.1101/2021.04.14.439897

I Kawrakow, E Mainegra-Hing, DWO Rogers, F Tessier, BRB Walters. The EGSnrc Code System: Monte Carlo simulation of electron and photon transport. Technical Report PIRS-701, National Research Council Canada (2017).

Agostinelli, S., Allison, J., Amako, K., Apostolakis, J., Araujo, H., Arce, P., Asai, M., Axen, D., Banerjee, S., Barrand, G., Behner, F., Bellagamba, L., Boudreau, J., Broglia, L., Brunengo, A., Burkhardt, H., Chauvie, S., Chuma, J., Chytracek, R., … Zschiesche, D. (2003). Geant4—a simulation toolkit. Nuclear Instruments and Methods in Physics Research Section A: Accelerators, Spectrometers, Detectors and Associated Equipment, 506(3), 250–303. https://doi.org/10.1016/s0168-9002(03)01368-8

Pantziarka, P. (2016). Emergent properties of a computational model of tumour growth. PeerJ, 4, e2176. https://doi.org/10.7717/peerj.2176

Cheng, L., Majumdar, A., Stover, D., Wu, S., Lu, Y., & Li, L. (2020). Computational Cancer Cell Models to Guide Precision Breast Cancer Medicine. Genes, 11(3), 263. https://doi.org/10.3390/genes11030263

Daina, A., & Zoete, V. (2016). A BOILED-Egg To Predict Gastrointestinal Absorption and Brain Penetration of Small Molecules. ChemMedChem, 11(11), 1117–1121. https://doi.org/10.1002/cmdc.201600182

Effect of 21-day support unloading on the characteristics of postural correction responses

Nikita Shishkin*, Nelly Abu Sheli, Vladimir Kitov, Liubov Amirova, Elena Tomilovskaya

Institute of Biomedical Problems, Russian Academy of Sciences, Moscow, Russia
**chachaturan@yandex.ru*

INTRODUCTION

The decrease in postural stability after space flights still remains the most important problem of aerospace medicine. For a number of reasons, it is difficult to study a person's balance immediately after landing, but it is possible to fully perform this in ground-based model experiments. It is known that after Dry Immersion (DI) – one of the models reproducing the effects of weightlessness - the slow-to-fast muscle fibers transformation is observed (Nemirovskaya 1999, Shenkman 2016), the activity of small tonic motor units of the leg extensor muscles decreases (Shigueva 2013), which can adversely affect the function of postural muscles designed to hold long-term tension, and as a result, the capabilities of postural stability control systems deteriorate (Shigueva, 2020).

One of the tests that assess the vertical balance under external disturbing influences is a test with the presentation of mechanical stimuli – chest pushes that cause postural correction responses (PCR). It is shown that the characteristics of the PCR change after the 6-hour DI (Sayenko, 2016). In previous studies, the changes occurring in the postural stability system after short periods (up to 7 days) of support unloading were well studied, but no studies of the human posture after long term immersion exposure were conducted. Based on the data of earlier studies, it can be assumed that exposure to 21-day DI will lead to significant changes in human postural stability.

METHODS

The study involved 10 healthy male volunteers without visible pathologies of the musculoskeletal system. The protocol of 21-day Dry Immersion is described in detail in the article (Tomilovskaya 2020). All participants were familiarized with the conditions of the experiment and gave written informed consent to participate in it.

The examination was started from a stand on a stable platform with eyes open (EO) and closed (EC) for 60 seconds. Next the subjects performed a stand with EC on an unstable platform (a foam cushion 20 cm thick) for 40 seconds. As disturbing perturbations in the conditions of a stand with EC on a stable platform, 15-20 pushes of various strengths were applied to the chest of the subjects, while recording PCR using the stabilographic platform "Stabilan-01" (OKB Ritm, Russia). Figure 1 shows a schematic image of the test and an example of a PCR.

Testing was performed three times before the start of DI and 1 hour after its completion.

The following parameters were analyzed:

- the Romberg coefficient (RC), which characterizes the contribution of vision to maintaining a vertical stance. RC was calculated as the

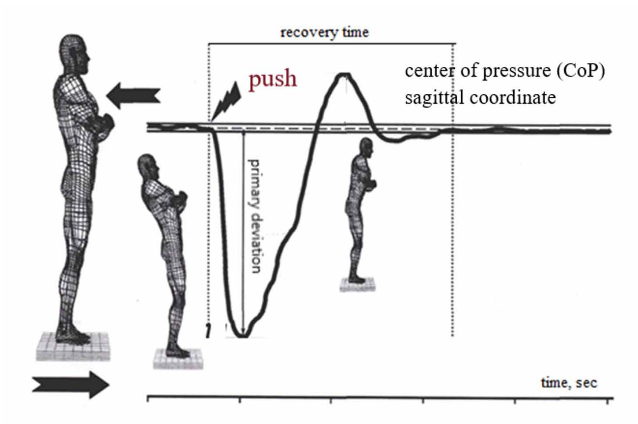

FIGURE 1: Schematic representation of the test with the application of disturbing pushes to the chest in the conditions of a stand on a solid platform with closed eyes. The line shows an example of a sagittal stabilogram. The recovery time is the time during which the fluctuations of the CoP return to the values recorded before the push (calculated according to the method described in (Halbach, 2007)).

percentage ratio of the amplitude of the range of CoP oscillations at the EO stance to the range of oscillations at the EC stance .

- the ratio of the range of oscillations on the unstable platform with EC after the end of the immersion exposure to the same parameter registered before DI - characterizes the change in postural stability without extraneous perturbations.

The specific recovery time was calculated from the sagittal stabilogram of PCR. Recovery time is the time during which the fluctuations of the CoP return to the values recorded before the push (calculated according to the method described in (Halbach, 2007): when standing with EC on stable platform, the standard deviation (SD) of CoP velocity is calculated for a period of 4 seconds. After each push, a period of duration is determined, during which the average CoP velocity remains within the range of 3 SD. The time from the moment of the push to the start of this segment was considered as the recovery time. The ratio of this time to the push force (s/kg) was taken as the specific recovery time.

RESULTS

When analyzing the results, a slight increase in the specific recovery time after DI completion was revealed, while no changes in the Romberg coefficient were observed (Figure 2).

However, when calculating the RC in the sessions before DI, it turned out that the subjects were divided equally into 2 groups (5 people each) according to the type of reaction to the elimination of visual feedback (Figure 3). In the group 1, the range of the CoP oscillations increased in the absence of visual control, in the 2nd group - decreased. At the same time, in the group 1, the range of the CoP oscillations on the unstable platform after immersion exposure did not change, and in group 2 it increased by 11% ($p=0.0516$). Next, we will consider these groups separately.

While analyzing the specific recovery time in 2 groups of volunteers, a different direction of changes was found (Figure 4). In group 1, there was an increase in this parameter after the end of immersion exposure compared to the pre-DI results, from 0.327 ± 0.045 to 0.400 ± 0.018 s/kg. In group 2, we do

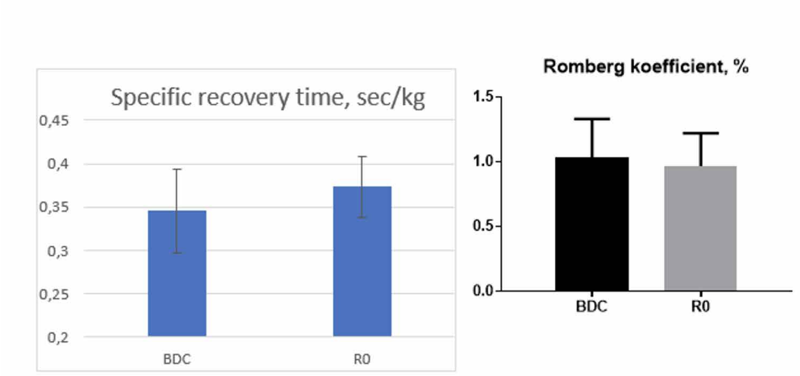

FIGURE 2: Specific recovery time (left) and Romberg coefficient (right) before and after 21-day immersion exposure. BDC - studies conducted before immersion exposure, R0 - 60 minutes after the end of DI.

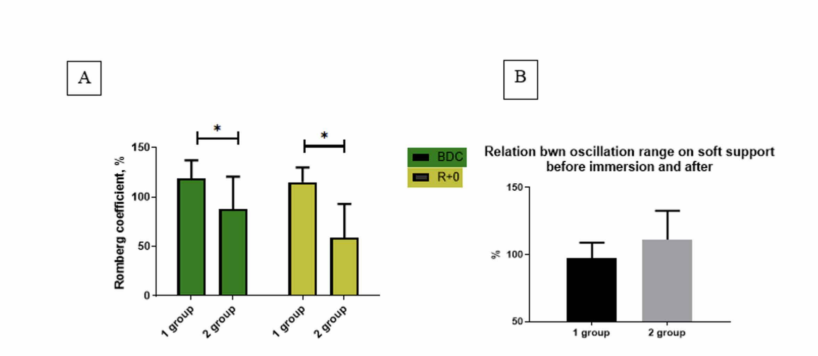

FIGURE 3: (**A**) Average values of the Romberg coefficient (RC) in 2 groups of subjects. * - significant differences (p<0.05, Mann-Whitney test) between the groups. (**B**) The ratio of the fluctuations of the central nervous system on a soft support with closed eyes before and after immersion exposure.

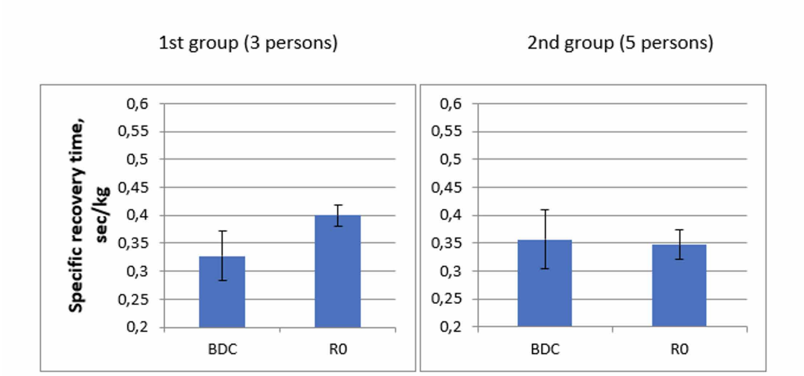

FIGURE 4: Specific recovery time after pushes in the chest in two groups of volunteers (the division into groups is described in Figure 3). BDC - studies conducted before immersion exposure, R0 - 60 minutes after the end of DI.

not observe any changes in the specific recovery time after DI completion compared to the initial values. However, it should be clarified that due to the difficulties of conducting an immersion experiment in group 1 it was possible to obtain PCR data only from 3 volunteers. Based on this, it can be assumed that the specific recovery time of vertical equilibrium after chest pushes in people with RC < 1 does not change after 21-day immersion exposure.

DISCUSSION

There are known studies in which the value of the Romberg coefficient less than 100% was observed in people with neurological disorders (Nikityuk, 2016). It is assumed that with the complication of the task of maintaining balance in volunteers with a deficit of somatosensory information, visual signals can destabilize the posture (Kim, 2017). There are also studies that registered a similar ratio in elderly people without neurological disorders (Fujita, 2017). It can be assumed that the subjects of the group 2 are more focused on vision and less - on the information coming from internal receptors. Normally, people have the excess of sensory information about the position of the body in space (Paolucci 2018, Tjernström 2015). However, even if this excess is absent, in condition with open eyes and stable platform this absence may not manifest itself in any way. At the same time, when presenting complex tests for equilibrium, the existing afferent flow may not be enough, which, apparently, leads to a change in the strategy of maintaining equilibrium (Alexandrov 2001) to a more energy-consuming, but more effective one, which is expressed in a decrease in the range of oscillations when eyes are closed.

CONCLUSION

Immersion exposure led to different changes in the studied characteristics in 2 groups of volunteers. At first glance, it may seems that the invariability of the specific recovery time indicates the greater vertical equilibrium of people with a Romberg coefficient < 1 after immersion exposure. However, an increase in the range of oscillations while standing on the unstable platform indicates an objective decrease in their stability in this test, which, however, is not observed in group 1. We attribute this to the likely change in the movement strategy when the sensory environment changes – when the eyes are closed, unstable platform, etc. (Horak 1986, Alexandrov 2001). The inverted Romberg coefficient can indicate an internal psychophysiological tension (Ryzhov 2013, Kanbara 2004) that a person experiences when closing his eyes, as a result of which he can subconsciously reduce the range of fluctuations. This hypothesis can be verified by studies of the electromyographic activity of postural muscles during the test with open and closed eyes (Kanbara 2004). As a result, when considering a group with a Romberg coefficient > 1 after prolonged immersion exposure, a significant increase in the specific recovery time after chest pushes is observed.

FUNDING

The research was supported by the Russian Science Foundation project No. 19-15-00435.

ACKNOWLEDGMENTS

The authors remember and honour the contribution of Prof. Inessa Kozlovskaya's contribution in researching of sensory-motor systems.

keywords: Romberg coefficient, posturology, postural correction responses, "dry" immersion

REFERENCES

Nemirovskaya T.L., Shenkman B.S. (1999). Influence of single hindlimb support on fiber characteristics of unloaded skeletal muscle. J. of Gravit. Physiol.: a Journal of the International Society for Gravitational Physiology. 6.(1).

Shenkman B.S. (2016). From slow to fast: hypogravity-induced remodeling of muscle fiber myosin phenotype. Acta Naturae, 8(4), 47-59.

Shigueva T.A., Zakirova A.Z., Tomilovskaya E.S., Kozlovskaya I.B. (2013). Effect of support deprivation on the sequence of motor units recruiting. Aviakosm Ekolog Med, 47(3), 50-53

Shigueva T.A., Kitov V.V., Tomilovskaya E.S., Kozlovskaya I.B. (2020). Characteristics of precise motor control in human under microgravity conditions. International journal of applied and fundamental research, 2, 34-39.

Sayenko D.G., Miller T.F., Melnik K.A. (2016). Acute effects of dry immersion on kinematic characteristics of postural corrective responses. Acta Astronaut, 121, 110–115.

Halbach P.S., Slobounov S.M., Slobounova E.S., Newell K.M. (2007). Aging and time-to-postural stability following a visual perturbation. Aging Clin Exp Res, 19(6), 438 – 443.

Tomilovskaya E.S., Rukavishnikov I.V., Amirova L.E., Shigueva T.A., Saveko A.A., Kitov V.V., Vassilieva G.YU., Ponomarev S.A., Smirnova T.A., Kozlovskaya I.B., Orlov O.I. (2020). 21-day Dry Immersion: design and primary results. Aviakosm. i ekolog. med., (54)4, 5-14.

Halbach P.S., Slobounov S.M., Slobounova E.S., Newell K.M. (2007). Aging and time-to-postural stability following a visual perturbation. Aging Clin Exp Res, 19(6), 438 – 443.

Nikityuk I.E., Vissarionov S.V., Umnov V.V., Rozhdestvenskii V.Y., Moshonkina T.R., Shcherbakova N.A., Gerasimenko Y.P. (2016). Effect of locomotor training and functional electrical stimulation on postural function in children with severe cerebral palsy. Human Physiology, 42(3), 262-270.

Kim K.M., Kim J.S., Grooms D.R. (2017). Stroboscopic Vision to Induce Sensory Reweighting During Postural Control. J Sport Rehabil, 1-11.

Fujita T., Nakamura S., Ohue M., Fujii Y., Miyauchi A., Takagi Y., Tsugeno H. (2005). Effect of age on body sway assessed by computerized posturography. J Bone Miner Metab, (23)2, 152-156.

Paolucci T., Fratte M.D., Saraceni V.M., Iosa M., Morone G., Paolucci S., Villani C. (2018). Romberg ratio coefficient in quiet stance and postural control in Parkinson's disease. Neurol. Sci., 39(8), 1355–1360.

Tjernström F., Björklund M., Malmström E.M. (2015). Romberg ratio in quiet stance posturography – test to retest reliability. Gait Posture, 42(1), 27–31.

Alexandrov A.V., Frolov A.A., Massion J. (2001). Biomechanical analysis of movement strategies in human forward trunk bending. II. experimental study. Biological Cybernetics, (84)6, 435-443.

Horak F. B., Nashner L. M. (1986). Central programming of postural movements: adaptation to altered support-surface configurations. J Neurophysiol, 55(6), 1369-81.

Ryzhov B. N. (2013). System psychometrics of tension. Systems psychology and sociology, 7, 5-25.

Kanbara K., Mitani Y., Fukunaga M., Ishino S., Takebayashi N., Nakai Y. (2004). Paradoxical Results of Psychophysiological Stress Profile in Functional Somatic Syndrome: Correlation Between Subjective Tension Score and Objective Stress Response. Applied Psychophysiology and Biofeedback, 29(4), 255-68.

Hypergravity-induced enhanced root growth phenotype and associated physio-biochemical parameters in wheat

Basavalingayya K Swamy, Malarvizhi Sathasivam, Ravikumar Hosamani*

Department of Biotechnology, University of Agricultural Sciences, Dharwad (UAS-D), Karnataka, India
**hosamanirr@uasd.in*

INTRODUCTION

Gravity is the only constant fundamental force throughout the evolution of the Earth (Raff, 1996). Hence, all the living organisms are evolutionarily adapted to Earth's gravity of 1*g*. Any deviation from Earth's gravity (1*g*) to either hypergravity or hypogravity causes a fundamental shift in physiology, structure, function, and behaviour of organisms including plants (Merkys and Laurinavicius, 1991). In plants, few studies reported that a hypergravity treatment can impart phenotypic, physiological, and structural benefits to plants, and interestingly some physiological traits were significantly altered due to hypergravity. For instance, rocket (*Eruca sativa*) and carrot seeds exposed to hypergravity (7*g*) significantly increased their germination rate, seedling growth and photosynthesis (Santos *et al.,* 2012). Similarly, chronic hypergravity (at 10*g* for 8 weeks) was reported to enhance the photosynthesis rate by increasing chloroplast size in *Physcomitrella patens* (Takemura *et al.,* 2017). These studies suggest that hypergravity can effectively induce variability among desired traits. In this context, the present study evaluated the hypergravity-induced phenotypic and biochemical changes in wheat seedlings.

METHODOLOGY

Hypergravity treatments were carried out using table-top centrifuges with tube holders to accommodate small seeds. These centrifuges can create the desired range of hypergravity environments by precisely regulating acceleration due to gravity. Briefly, tubes containing a minimum of 100 wheat seeds (UAS-375 genotype) were subjected to hypergravity treatment (10*g* for 12 and 24 hrs) and evaluated for seedling vigour and plant growth parameters in the laboratory and greenhouse conditions. Later the associated biochemical changes such as seed enzyme activity – α-amylase and total dehydrogenase, seed protein profile, total chlorophyll content and endogenous phytohormones levels at different stages of vegetative growth were estimated using standard protocols (Swamy *et al.,* 2021).

RESULTS

Wheat seeds exposed to 10*g* for 12 hrs exhibited a significant increase in root length, shoot length, seedling dry weight and seedling vigour index by 19.58%, 9.15%, 10.52% and 13.73% respectively at 10*g* for 12 hrs only compared to control. At 10*g* for 24 hrs time point no significant change in any of the tested parameters was observed on the 8th day (final count of the seedling stage). However, these phenotypic changes were slightly decreased when compared to 10*g* 12 hrs treated seeds. Inconsistent with 8th-day plant growth phenotypes, on the 45th day also, root length and root-associated parameters were significantly enhanced in response to 10*g*, for 12 hrs only. In specific, at 10*g*, for 12 hrs, root length, root dry weight and root volume were significantly enhanced by 21.93%, 18.09% and 27.91% respectively when compared to control root. In contrast, at 24 hrs, no such significant change in root length and its associated parameters were observed (Figure 1 and Table 1).

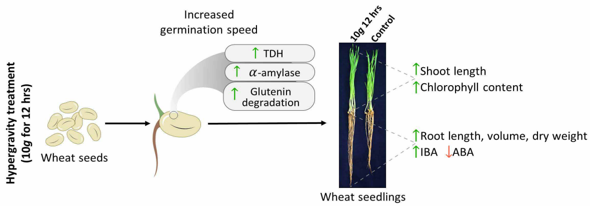

FIGURE 1: Hypergravity treatment (10*g* for 12 hrs) induced changes in seed biochemical activities, and root phenotypes in wheat.

Table 1: Hypergravity-induced changes in wheat growth parameters recorded on the final count of wheat seedlings (8th day) and at the beginning of the reproductive phase (45th day) in greenhouse conditions **(Tab. F (5%) = 3.555)**

	Hyper *g* treatment	Mean ± S. Em	% change over control	P ≤ 0.05	Cal. F	CD (5%)	CV (%)
8th DAY	**Root length (cm)**						
	Control (1*g*)	14.76 ± 0.401					
	10*g* 12 hrs	17.65 ± 0.371	19.58	0.000*	11.83	1.268	7.032
	24 hrs	15.78 ± 0.497	6.91	0.235			
	Shoot length (cm)						
	Control (1*g*)	15.19 ± 0.350					
	10*g* 12 hrs	16.58 ± 0.302	9.15	0.032*	4.059	1.057	5.892
	24 hrs	16.18 ± 0.406	6.52	0.149			
	Seedling vigour index						
	Control (1*g*)	2374 ± 86.44					
	10*g* 12 hrs	2700 ± 88.01	13.73	0.027*	4.593	240.3	8.324
	24 hrs	2638 ± 66.43	11.12	0.080			
45th DAY	**Root length (cm)**						
	Control (1*g*)	39.17 ± 2.097					
	10*g* 12 hrs	47.76 ± 2.982	21.93	0.000*	17.25	3.512	13.43
	24 hrs	39.34 ± 1.421	4.07	0.995			
	Shoot length (cm)						
	Control (1*g*)	43.21 ± 2.407					
	10*g* 12 hrs	48.24 ± 2.202	11.64	0.012*	18.94	1.410	12.76
	24 hrs	44.97 ± 2.684	4.10	0.083			
	Root volume (cm^3)						
	Control (1*g*)	0.86 ± 0.045					
	10*g* 12 hrs	1.10 ± 0.050	27.91	0.004*	7.883	0.130	12.11
	24 hrs	0.93 ± 0.037	8.14	0.549			
	Root dry weight (mg)						
	Control (1*g*)	157.3 ± 6.422					
	10*g* 12 hrs	185.8 ± 7.193	18.09	0.040*	4.641	20.69	10.91
	24 hrs	163.4 ± 8.809	3.87	1.000			

Since seedling vigour was significantly enhanced in response to hypergravity, we decided to investigate the underlying biochemical basis in terms of α-amylase and TDH activity and protein profile, specifically in seeds, post hypergravity exposure. In response to hypergravity (10*g* for 12 hrs) treatment, α-amylase activity was significantly enhanced by 13.57% when compared to untreated seeds. However, at 24 hrs, no significant change was observed. Similarly, TDH activity was also significantly enhanced by 22.4% at 10*g*, for 12 hrs only, with no significant change at 24 hrs when compared to control seeds (Figure 1). The SDS-PAGE analysis showed a marginal increase in the total number of wheat seed protein bands in response to hypergravity. In addition, the total chlorophyll content was estimated on the 8^{th} and 45^{th}-day growth stages. We found significantly enhanced total chlorophyll content by 16.65% in response to 10*g* for 12 hrs on the 8^{th} day only. Further, the endogenous phytohormone levels relevant to root growth such as indole-3-butyric acid (IBA) and Abscisic acid (ABA) were quantified using the LCMS-MS method on both 8^{th} and 45^{th}-day growth stages. We found a significant increase in IBA level by 21.2% and 28.91%, and a decrease in ABA level by 24.59% and 86.82% in response to 10*g* for 12 hrs both at 8^{th} and 45^{th} day respectively (Table 2).

Table 2: Hypergravity elicits robust phytohormones dynamics in the root, profiled on the 8^{th} day and 45^{th} day grown in greenhouse conditions **(Tab.t = 4.303)**

8^{th} DAY	**3-Indole butyric acid (IBA)**					
	Control (1*g*)	09.68 ± 0.128				
	10*g* 12 hrs	11.73 ± 0.454	21.20	0.57	6.29	0.024*
	24 hrs	13.21 ± 0.864	36.51	1.72	4.55	0.071
	Abscisic acid (ABA)					
	Control (1g)	0.152 ± 0.016				
	10*g* 12 hrs	0.115 ± 0.003	-24.59	0.022	2.88	0.021*
	24 hrs	0.032 ± 0.005	-79.02	0.019	10.7	0.009*
45^{th} DAY	**3-Indole butyric acid (IBA)**					
	Control (1*g*)	51.13 ± 0.915				
	10*g* 12 hrs	65.92 ± 3.57	28.91	4.61	5.54	0.031*
	24 hrs	51.11 ± 0.025	-0.03	1.54	0.02	0.984
	Abscisic acid (ABA)					
	Control (1*g*)	0.277 ± 0.019				
	10*g* 12 hrs	0.036 ± 0.004	-86.82	0.025	16.33	0.004*
	24 hrs	0.042 ± 0.001	-84.66	0.036	11.12	0.008*

DISCUSSION

The present study explores the possibility of hypergravity treatment for inducing beneficial crop improvement traits both at seedling and vegetative growth stages of the wheat crop in laboratory and greenhouse conditions. Resultant data revealed that hypergravity treatment (10*g* for 12 hrs) significantly enhanced root length, root volume, and root biomass in response to hypergravity. Enhanced root length, root volume, and root biomass phenotype in wheat have significant relevance in crop improvement, in specific, for drought avoidance or tolerance through better water usage management mechanisms (Pfeifer *et al.,* 2015). The enhanced root length could aid plants in establishing robust growth and development. Lengthy roots can assist the plants in penetrating deep into the soil and absorb water efficiently during drought conditions. Interestingly, the observed physio-biochemical changes such as increased α-amylase and TDH enzyme activities and reduced concentration of seed gluten proteins were attributed to the robust seedling growth phenotype in response to hypergravity (10*g* for 12 hrs). Similarly, elevated total chlorophyll content across different stages of vegetative growth in response to hypergravity may impart physiological benefits to wheat growth (Swamy *et al.,* 2021). Furthermore, the hypergravity elicited robust endogenous phytohormones (IBA and ABA) dynamics in root signifying altered phenotype/s (Epstein *et al.,* 1993; Kaur *et al.,* 2014).

CONCLUSION

In summary, the present study investigated hypergravity treatment (10*g* for 12 hrs) induced significant changes in root and shoot phenotypes and associated biochemical changes in wheat seeds and seedlings, these changes suggest the robust seedling vigour phenotype in response to hypergravity. Collectively, this study for the first time describes the utility of hypergravity as a novel tool in inducing reliable root phenotype that could be potentially exploited for improving wheat varieties for better water usage management and thus, helps in terrestrial agriculture.

ACKNOWLEDGEMENTS

First author (BKS) and Malarvizhi S acknowledge the DBT-JNU, Govt. of India for the fellowship. The corresponding author (Ravikumar Hosamani) acknowledges DST-SERB for awarding a research grant of which this publication is part of.

Keywords: Hypergravity, wheat, seedling vigour, chlorophyll content

REFERENCES

Raff, M. C. (1996). Size control: the regulation of cell numbers in animal development. Cell. 86, 173–175.

Merkys, A. and Laurinavicius, R. (1991). Development of higher plants under altered gravitational conditions. Adv. Space Biol. Med. 1, 155-181.

Santos, M. A., Fachel, F. N. S., Nava, M. J. A., *et al.* (2012). Effect of hypergravity simulation on carrot germination and growth. Aviat. Space Environ Med., 83, 1011–1012.

Takemura K, Kamachi H, Kume A, *et al.* (2017a). A hypergravity environment increases chloroplast size, photosynthesis, and plant growth in the moss *Physcomitrella patens*. J. Plant Res. 130, 181–192.

Swamy BK, Hosamani R, Sathasivam M, *et al.* (2021). Novel hypergravity treatment enhances root phenotype and positively influences physio-biochemical parameters in bread wheat (*Triticum aestivum* L.). Sci. Rep. 11, 15303.

Pfeifer, J., Kirchgessner, N., Colombi, T. (2015). Rapid phenotyping of crop root systems in undisturbed field soils using X-ray computed tomography. Plant Methods. 11, 41.

Epstein, E. and Ludwig-Muller, J. Indole-3-butyric acid in plants: Occurrence, biosynthesis, metabolism, and transport. Physiol. Plant 88, 382–389 (1993).

Kaur, L., Gupta, A. K. and Zhawar, V. K. (2014). ABA improvement of antioxidant metabolism under water stress in two wheat cultivars contrasting in drought tolerance. Indian J. Plant Physiol. 19, 189–196.

Cervical, thoracic, and lumbar myofascial properties and pain development during five days of dry immersion: DI-5-Cuffs

Plé Camille[1]*, Zuj Kathryn[2], Gauquelin-Koch Guillemette[3], Gharib Claude[4], Treffel Loïc[1,4]

[1]*Institut Toulousain d'Ostéopathie, Institut de recherche Franc'Ostéo iRF'O, Toulouse, France*
[2]*Faculty of Applied Health Sciences, University of Waterloo, Waterloo, ON, Canada*
[3]*Centre National d'Études Spatiales, CNES Paris, France*
[4]*Faculté de Médecine Lyon-Est, Institut NeuroMyoGène, Lyon, France*
**moving.studies@gmail.com*

INTRODUCTION

In microgravity, the muscular effort required to maintain posture and perform daily activities is greatly reduced (Vernikos and Schneider, 2010). Adaptation to this reduced level of physical activity results in whole body deconditioning (Demangel et al., 2017). Postural muscles undergo deconditioning consisting of atrophy, changes in muscle fiber composition, and reduced contraction strength (Berry et al., 1993) with the greatest loss of muscle mass occurring in the first few days of hypoactivity (Akima et al., 2004; Pagano, 2016). Spinal deconditioning also occurs resulting in a loss of curvature, development of back pain, and an increased risk of intervertebral disc herniation (Buckey, 2006; Kerstman et al., 2012; Belavy et al., 2016).

Dry immersion (DI), used as a model of microgravity exposure (Tomilovskaya et al, 2019), alters the force of gravity on the human body and results in muscle atrophy, reduced muscle tone, spinal dysfunction, and back pain (De Abreu et al., 2017; Demangel et al., 2017; Treffel et al., 2017). The purpose of this study was to determine changes in core myofascial properties with exposure to DI and to investigate a potential relationship between the development of back pain and changes in myofascial properties after three days of dry immersion. It was hypothesised that DI would result in a stiffening of core muscles and that these changes would relate to the development of back pain.

METHODS

The study was conducted at the Institute of Space Medicine and Physiology (MEDES-IMPS) in Toulouse, France with data collected from 18 male participants (35 ± 6 years of age). Each participant completed five days of DI as previously described (De Abreu et al., 2017; Treffel et al., 2017; Tomilovskaya et al., 2019). Participants were randomly assigned to either a control condition or an experimental group (10 participants) where thigh cuffs were used as a countermeasure against fluid shift (Custaud et al., 2020). All assessments were conducted before dry immersion (BDC), on the third day of immersion (DI-3), and after 5 days of immersion (R+0).

Participants were asked to rate their levels of pain using a visual analogue scale of 0 to 10 where 0 represents no pain and 10 is unbearable pain. For each pain assessment, participants provided a rating for four different regions: cervical, posterior thoracic, abdominal, and lumbar.

Myofascial tissue properties were evaluated using the MyotonPro system (Gavronski et al., 2007). This system provided real-time calculations of dynamic stiffness (N/m), frequency of oscillation (Hz), and stress relaxation time (ms). The system was used in multi-scan mode where five measures were performed at each measurement location (Aird et al., 2012; Chuang et al., 2012; Dietsch et al., 2014). Four different muscles were evaluated corresponding to the four regions used for the assessment of pain: superior trapezius (cervical), longissimus (posterior thoracic), rectus abdominus (abdominal), and erector spinae (lumbar). Measurements were made on both the left and right sides of the body and averaged to provide a single measure for each muscle at each time point.

Preliminary analysis did not find an effect of the thigh cuff countermeasure; therefore, all participants were pooled for the analysis (n=18). Effects of DI were determined using paired t-tests. Linear regressions were then used to determine potential relationships between the change in back pain, muscle properties at rest, and the change in muscle properties with DI. Significance was set at $p<0.05$ with results presented as mean ± SD.

RESULTS

With DI, there was a significant increase in pain from BCD levels in all four regions (Figure 1). Pain in the cervical, posterior thoracic, abdominal, and lumbar regions increased by 1.5±1.7, 0.8±1.5, 2.0±2.7, and 3.1±2.4 respectively. Pain levels in all regions retuned to BDC levels on R+0.

Assessment of myofascial tissue properties found significant effects of dry immersion (Table 1). Oscillation frequency and stiffness of the superior trapezius and longissimus muscles were increased with DI with reduced relaxation times. The rectus abdominus muscle decreased stiffness on DI-3 with no changes in oscillation frequency or relaxation time. No effects of DI were found for the erector spinae muscle. Post DI, all values returned to BDC levels.

Linear regression analysis was used to determine if the change in muscle properties with DI or resting properties before DI exposure (BDC) related to the development of back pain during DI. Therefore, superior trapezius properties

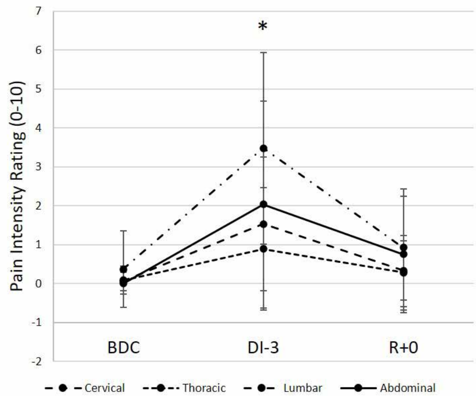

FIGURE 1: Participant pain intensity ratings before (BDC), during (DI-3), and after (R+0) dry immersion (mean ± SD). Pain was significantly increased in all regions during DI (* $p<0.05$).

Table 1: Myofascial properties

		Superior Trapezius	Longissi-mus	Rectus Abdominus	Erector Spinae
Frequency (Hz)	BDC	15.01 ± 1.58	17.10 ± 2.39	15.45 ± 1.73	18.73 ± 2.33
	DI-3	17.70 ± 2.21*	17.98 ± 3.09*	14.96 ± 1.93	18.37 ± 2.41
	R+0	15.35 ± 1.35	17.31 ± 2.39	15.14 ± 1.65	18.43 ± 1.49
Stiffness (N/m)	BDC	251.37 ± 40.55	344.40 ± 89.82	274.98 ± 41.48	358.38 ± 41.06
	DI-3	312.33 ± 57.40*	391.01 ± 114.25*	255.46 ± 43.23*	370.45 ± 53.84
	R+0	257.23 ± 32.27	354.79 ± 90.39	264.43 ± 35.83	358.19 ± 36.96
Relaxation (ms)	BDC	20.88 ± 3.10	15.51 ± 3.38	19.56 ± 2.53	14.96 ± 1.74
	DI-3	16.84 ± 3.24*	14.33 ± 3.78*	20.77 ± 2.96	14.88 ± 2.14
	R+0	20.18 ± 2.33	15.31 ± 3.65	20.33 ± 2.34	15.12 ± 1.61

Values (mean ± SD) of myofascial properties assess at rest (BDC), on day three of dry immersion (DI-3), and after three days of dry immersion (R+0). Values that are different from the respective BDC value are indicated by * ($p<0.05$).

were compared to the change in cervical pain, longissimus properties to the change in posterior thoracic pain, rectus abdominus properties to the change in abdominal pain, and erector spinae properties to the change in lumbar pain. Results of this analysis (Table 2) did not find a strong correlation between any of the variables assessed.

Table 2: Regression analysis results

		Cervical (Superior Trapezius)	Posterior Thoracic (Longissimus)	Abdominal (Rectus Abdominus)	Lumbar (Erector Spinae)
BDC	Frequency	0.001	0.000	0.018	0.108
	Stiffness	0.037	0.000	0.001	0.132
	Relaxation	0.016	0.003	0.006	0.141
DI Change	Frequency	0.038	0.088	0.040	0.098
	Stiffness	0.031	0.089	0.018	0.001
	Relaxation	0.027	0.066	0.024	0.000

Values of R squared from the regression analysis comparing the change in perceived pain with DI to the respective muscle properties at rest (BDC) and the change in muscle properties with DI (DI Change). None of the assessed relationships reached the threshold for statistical significance ($p>0.05$).

DISCUSSION

The purpose of the study was to assess back pain and myofascial properties of core muscles before, during, and after exposure to simulated microgravity using dry immersion. Consistent with the hypothesis, DI resulted in increased back pain and changes in muscle properties. However, contrary to the hypothesis, the change in back pain was not correlated to muscle properties at rest or to the change in muscle properties with DI exposure.

Dry immersion has been used as a model of simulated microgravity exposure showing fluid shifts and muscle adaptations similar to those observed during spaceflight (Tomilovskaya et al., 2019). During DI, individuals are suspended in a water bath which reduces the gravitational load on the spine resulting in spinal deconditioning as seen by reduced curvature, intervertebral disc swelling, and increased back pain (Treffel et al., 2017). The current study also found increased back pain with DI and changes in myofascial properties.

The greatest increase in pain with DI occurred in the lumbar region; however, properties of the erector spinae muscle were not different with DI. This indicates that factors other than myofascial properties, such as intervertebral disk swelling and a reduction in lumbar curvature which were also noted in this study population (Treffel et al., 2020), are likely contributing to pain development in this region during DI.

Tension in the longissimus muscle was increased with DI whereas rectus abdominis muscle tone decreased. This allowed for spinal flexion during DI potentially leading to an increase in abdominal wall tension and compression of the abdominal viscera contributing to abdominal pain and dorsal thoracic pain.

Although the head and arms are not submerged during DI and are still subjected to the effects of gravity, a significant increase in cervical pain and increased superior trapezius stiffness were found. The positioning maintained during DI required the participants shoulders to be raised for daily activities which likely contributed to the observed results rather than unloading of the cervical spine due to simulated microgravity.

While the development of back pain in various regions was associated with changes in muscle properties, the magnitude pain did not correlate to resting muscle properties or the degree of change with DI. This could suggest that other variables, such as intervertebral disc swelling and changes in spinal curvature have a greater influence on pain development during DI or individual variability exists for the relationship between myofascial property changes and the manifestation of pain. Additionally, the lack of relationship between pain and resting muscle properties indicates that resting values of the muscles assessed are not a good predictor of pain development during DI.

CONCLUSION

The dry immersion analogue of microgravity exposure results in spinal deconditioning. Myofascial changes with DI exposure were observed along with the development of back pain. A linear correlation was not found between pain and myofascial properties suggesting the contribution of other factors to the development of back pain or individual variability in responses. However, as muscle changes were observed during DI, these changes need to be considered in future investigations of spinal deconditioning with microgravity exposure.

ACKNOWLEDGMENTS

We thank the MEDES-IMPS team, the Medical Imaging Service of Rangueil Hospital in Toulouse, France, and all the subjects for their participation in the study.

Keywords: vertebral deconditioning, MyotonPro, microgravity, dry immersion, DI5-Cuffs, back pain

REFERENCES

Aird, L., Samuel, D., and Stokes, M. (2012). Quadriceps muscle tone, elasticity and stiffness in older males: Reliability and symmetry using the MyotonPRO. Arch. Gerontol. Geriatr. 55, e31–e39. doi:10.1016/j.archger.2012.03.005.

Akima, H., Takahashi, H., Kuno, S., and Katsuta, S. (2004). Coactivation pattern in human quadriceps during isokinetic knee-extension by muscle functional MRI. Eur. J. Appl. Physiol. 91, 7–14. doi:10.1007/s00421-003-0942-z.

Belavy, D. L., Adams, M., Brisby, H., Cagnie, B., Danneels, L., Fairbank, J., et al. (2016). Disc herniations in astronauts: What causes them, and what does it tell us about herniation on earth? Eur. Spine J. Off. Publ. Eur. Spine Soc. Eur. Spinal Deform. Soc. Eur. Sect. Cerv. Spine Res. Soc. 25, 144–154. doi:10.1007/s00586-015-3917-y.

Berry, P., Berry, I., Manelfe, C. (1993). Magnetic resonance imaging evaluation of lower limb muscles during bed rest--a microgravity simulation model. Aviat Space Env. Med, 212–8.

Buckey, J. C. (2006). Space Physiology. Oxford, New York: Oxford University Press.

Chuang, L.-L., Lin, K.-C., Wu, C.-Y., Chang, C.-W., Chen, H.-C., Yin, H.-P., et al. (2013). Relative and Absolute Reliabilities of the Myotonometric Measurements of Hemiparetic Arms in Patients With Stroke. Arch. Phys. Med. Rehabil. 94, 459–466. doi:10.1016/j.apmr.2012.08.212.

Custaud, M.-A., Blanc, S., Gauquelin-Koch, G., Gharib, C. (2020). L'humain & l'espace - Ses adaptations physiologiques -. BoD-Books on Demand.

De Abreu, S., Amirova, L., Murphy, R., Wallace, R., Twomey, L., Gauquelin-Koch, G., et al. (2017). Multi-System Deconditioning in 3-Day Dry Immersion without Daily Raise. Front. Physiol. 8, 799. doi:10.3389/fphys.2017.00799.

Demangel, R., Treffel, L., Py, G., Brioche, T., Pagano, A. F., Bareille, M.-P., et al. (2017). Early structural and functional signature of 3-day human skeletal muscle disuse using the dry immersion model: Short-term muscle deconditioning. J. Physiol. 595, 4301–4315. doi:10.1113/JP273895.

Dietsch, A. M., Solomon, N. P., Sharkey, L. A., Duffy, J. R., Strand, E. A., and Clark, H. M. (2014). Perceptual and instrumental assessments of orofacial muscle tone in dysarthric and normal speakers. J. Rehabil. Res. Dev. 51, 1127–1142. doi:10.1682/JRRD.2013.07.0167.

Gavronski, G., Veraksitš, A., Vasar, E., and Maaroos, J. (2007). Evaluation of viscoelastic parameters of the skeletal muscles in junior triathletes. Physiol. Meas. 28, 625–637. doi:10.1088/0967-3334/28/6/002.

Kerstman, E. L., Scheuring, R. A., Barnes, M. G., DeKorse, T. B., and Saile, L. G. (2012). Space Adaptation Back Pain: A Retrospective Study. doi:info:doi/10.3357/ASEM.2876.2012.

Pagano, A. (2016). Déconditionnement et régénération du muscle strié squelettique: rôle du niveau d'activité contractile sur le développement d'infiltrations graisseuses. Available at: https://tel.archives-ouvertes.fr/tel-01510485.

Tomilovskaya, E., Shigueva, T., Sayenko, D., Rukavishnikov, I., and Kozlovskaya, I. (2019). Dry Immersion as a Ground-Based Model of Microgravity Physiological Effects. Front. Physiol. 10, 284. doi:10.3389/fphys.2019.00284.

Treffel, L., Massabuau, N., Zuj, K., Custaud, M.-A., Gauquelin-Koch, G., Blanc, S., et al. (2017). Pain and Vertebral Dysfunction in Dry Immersion: A Model of Microgravity Simulation Different from Bed Rest Studies. Pain Res. Manag. 2017, 1–10. doi:10.1155/2017/9602131.

Treffel, L., Navasiolava, N., Mkhitaryan, K., Jouan, E., Zuj, K., Gauquelin-Koch, G., et al. (2020). DI-5-Cuffs: Lumbar Intervertebral Disc Proteoglycan and Water Content Changes in Humans after Five Days of Dry Immersion to Simulate Microgravity. Int. J. Mol. Sci. 21, E3748. doi:10.3390/ijms21113748.

Vernikos, J., and Schneider, V. S. (2010). Space, Gravity and the Physiology of Aging: Parallel or Convergent Disciplines? A Mini-Review. Gerontology 56, 157–166. doi:10.1159/000252852.

Integrated feedback displays to facilitate bimanual coordination in simulated gravity

Yiyu Wang[1], Madison M. Davis[1]*, Renee Woodruff[2], Tray Wright[1], Bonnie J. Dunbar[2], Ana Diaz-Artiles[2], Deanna Kennedy[1]

[1]*Department of Health and Kinesiology, Texas A&M University, College Station, US*
[2]*Department of Aerospace Engineering, Texas A&M University, College Station, US*
**ydavidw@tamu.edu*

INTRODUCTION

The ability to coordinate actions between the limbs is important for many activities associated with spaceflight. For example, tasks such as controlling a rover or piloting a spacecraft often involve some type of coordination between the limbs. Numerous ground studies have demonstrated that bimanual tasks that require phase relationships other than 1:1 in-phase (0°) or anti-phase (180°) are difficult or near impossible without extensive training (Lee et al., 1995;Fontaine et al., 1997;Swinnen et al., 1997). The difficulty associated with producing complex relative phase patterns, such as 90°, have been traditionally attributed to inherent constraints associated with the structure of the neuromuscular system (Schoner and Kelso, 1988). It is important to note, however, that auditory and/or visual metronomes were typically used to pace bimanual performance in these experiments (Zanone and Kelso, 1992).

More recent research, however, has indicated that complex coordination patterns (e.g., 90° relative phase) could be performed quite well within a few minutes of training when provided integrated feedback information and other attentional distractions were minimized (e.g., metronomes, vison of the limbs) (Kovacs et al., 2010;Kennedy et al., 2015). One type of integrated feedback that has proved successful in facilitating complex modes of coordination is Lissajous displays (Figure 1). Lissajous displays provide a goal template along with on-line integrated information regarding the position of two individual points (e.g., limbs) as a single point (e.g., cursor). The general results of experiments using Lissajous displays have indicated that this type of feedback information allowed participants to quickly and effectively produce a wide range of complex bimanual tasks. (Kovacs et al., 2009a;Kovacs et al., 2009b;Kennedy et al., 2016;Kovacs et al., 2020).

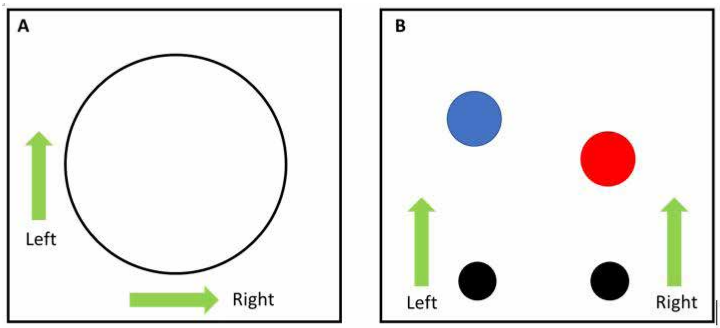

FIGURE 1: Illustration depicting Lissajous plot of 90 degrees relative phase (**A**), and visual metronome (**B**) feedback conditions.

In a recent experiment directly comparing bimanual performance with Lissajous displays to visual metronomes, Kovacs et al. 2020 demonstrated that participants could produce a wide variety of relative phase patterns after only 6 minutes of practice whereas participants were not able to produce the same relative phase patterns with visual metronome. The ability to coordinate complex bimanual tasks with the limbs when provided integrated feedback information suggest that the detrimental effects associated with complex bimanual coordination tasks may be due to attentional, perceptual, and or cognitive constraints associated with the task or environment (Shea et al., 2016). It is believed that Lissajous displays provide the CNS system an opportunity to override the perceptual and/or neurophysiological constraints acting on the system However, producing complex bimanual coordination in altered-gravity environments may be even more challenging for the CNS due to the increased attentional, perceptual, and cognitive demands associated with spaceflight and altered gravity environments (Friedl-Werner et al., 2021). As such, it is not clear whether individuals can use Lissajous displays to coordinate complex bimanual coordination patterns in altered-gravity environments similar to ground studies. Therefore, the purpose of the current study is to determine if individuals can coordinate a complex pattern of force (90°) in simulated microgravity similar to performance on Earth and to compare performance between the two types of feedback information (Lissajous plots vs. visual metronome).

METHOD

A head-up tilt (HUT)/head-down tilt (HDT) paradigm was used to compare microgravity and Earth. Earth (90° HUT) and microgravity (-6° head-down HDT) environments were simulated with a tilt table (Figure 2). Right limb dominant participants (N= 8) attempted to produce a continuous 1:1 bimanual force pattern with a 90° relative phase offset paced with a visual metronome or Lissajous displays. The metronome consisted of two separate targets, one for each limb, with a 90° phase offset moving at 1 Hz from bottom-to-top (Figure 1B). Participants produced force with each limb to match the pattern paced by the metronome. The Lissajous display consisted of a goal template and a cursor indicating the forces produced by the two arms (Figure 1A). For the Lissajous condition, participants' movement were self-paced to meet a goal frequency of 1 Hz. Participants were asked to speed up or slow down when their movements frequency was slower or faster than 1 Hz. The cursor moved from left-to-right as force was produced with the right arm and from bottom-to-top as force was produced by the left arm. The template illustrated the specific pattern of force needed to produce the 90° goal coordination pattern. Participants performed 14 trials for each feedback (metronome, Lissajous) and gravity (Earth, microgravity) condition, counterbalanced across conditions. Each trial was 30 s. Absolute error (AE) of the continuous relative phase was used a measure of the degree to which the required goal relative phase was achieved. Variability of error (VE) and constant error (CE) were used as measures of stability and bias of the 90° coordination pattern.

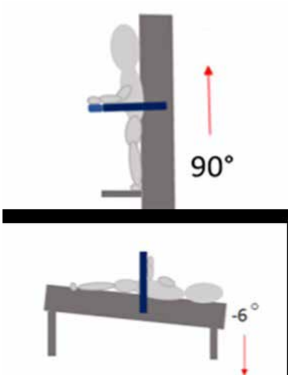

FIGURE 2: Illustration depicting the experimental arrangement for the gravity conditions (**a**), Earth (90° HUT) (**b**), Microgravity (-6° HDT).

All force signals were processed by using MATLAB, and the two-way repeated measure of variances analysis (Feedback × Gravity) for the variables AE, VE and CE was performed by SPSS 27.0.

RESULTS

Results indicated significantly lower AE with Lissajous displays compared to visual metronomes (P= .03) (Figure 3). However, participants were not able to tune-in the goal coordination pattern (high AE and VE) within the 6 minutes of practice with the metronomes and performance was biased (CE) toward the anti-phase coordination pattern (180°).

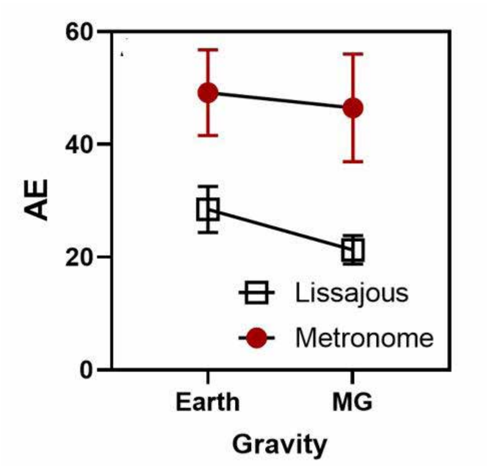

FIGURE 3: Mean absolute error (AE) by feedback condition. The results indicate that participants were more accurate with Lissajous displays than metronomes for both Earth and microgravity conditions.

DISCUSSION

The results of the current investigation indicate that participants were able to effectively (low AE) produce the 90° relative phase bimanual force pattern within the 6 minutes of training when provided Lissajous displays. This result is similar with a number of ground studies demonstrating that complex bimanual coordination patterns could be performed following relatively little training when provided integrated feedback information (Shea et al. 2016; Kovacs et al. 2020; Wang et al. 2021). Extending this line of research to microgravity environments provides further evidence for the robust utility of Lissajous displays in facilitating complex bimanual coordination tasks (Shea et al. 2016).

The Lissajous displays provided a goal template of the 90° relative phase pattern along with on-line feedback information regarding the position of the position of the two limbs as a single point. Participants were able to use this information, regardless of the gravity condition, to produce the goal pattern within a few minutes of practice. Given that participants were able to perform the goal in microgravity is particularly impressive considering the increased attentional, cognitive, and perceptual demands associated with spaceflight and altered-gravity environments (Friedl-Werner et al. 2021).

Participants were not able to tune-in the goal coordination pattern (high AE and VE) within the 6 minutes of practice when provided metronomes to pace performance. In addition, performance was biased (CE) toward the anti-phase coordination pattern (180°). This result is consistent with the Haken, Kelso, and Bunz (HKB) model. A feature of the HKB model is that both in-phase and anti-phase coordination patterns are modeled as stable fixed-point attractors. Other phases (e.g., 90°) act as repellers in the coordination landscape which may result in a phase transition to a fixed-point attractor (i.e., 0°, 180°). It is believed that Lissajous displays provide the system an opportunity to override the perceptual and/or neurophysiological constraints acting on the system. It appears this type of feedback is also effective in overcoming constraints imposed by microgravity. Research should further explore Lissajous displays as a countermeasure to the detrimental performance effects often associated with altered-gravity (e.g., Clark et al. 2015).

CONCLUSIONS

Results indicated that participants were able to effectively produce (low AE) a complex 90° relative phase when provided Lissajous displays in microgravity similar to Earth. This result provides additional evidence regarding the robust nature of Lissajous displays in facilitating complex bimanual performance.

ACKNOWLEDGMENTS

Work Supported by NASA 80NSSC20K1499

Keywords: bimanual coordination, altered-gravity, visual feedback

REFERENCES

Clark, T.K., Newman, M.C., Merfeld, D.M., Oman, C.M., Young, L.R. (2015). Human manual control performance in hyper-gravity. Exp. Brain. Res. 233, 1409–1420.

Fontaine, R.J., Lee, T.D., and Swinnen, S.P. (1997). Learning a new bimanual coordination pattern: reciprocal influences of intrinsic and to-be-learned patterns. Can. J. Exp. Psychol. 51, 1-9.doi: 10.1037/1196-1961.51.1.1

Friedl-Werner, A., Machado, M.L., Balestra, C., Liegard, Y., Philoxene, B., Brauns, K., Stahn, A.C., Hitier, M., and Besnard, S. (2021). Impaired Attentional Processing During Parabolic Flight. Front. Physiol. 12, 675426.10.3389/fphys.2021.675426

Gentili, R., Cahouet, V., and Papaxanthis, C. (2007). Motor planning of arm movements is direction-dependent in the gravity field. Neuroscience 145, 20-32.doi: 10.1016/j.neuroscience.2006.11.035

Kennedy, D.M., Boyle, J.B., Rhee, J., and Shea, C.H. (2015). Rhythmical bimanual force production: homologous and non-homologous muscles. Exp. Brain Res. 233, 181-195.doi: 10.1007/s00221-014-4102-y

Kennedy, D.M., Wang, C., Panzer, S., and Shea, C.H. (2016). Continuous scanning trials:Transitioning through the attractor landscape. Neurosci. Lett. 610, 66-72.doi: 10.1016/j.neulet.2015.10.073

Kovacs, A.J., Buchanan, J.J., and Shea, C.H. (2009a). Using scanning trials to assess intrinsic coordination dynamics. Neurosci. Lett. 455, 162-167.doi: 10.1016/j.neulet.2009.02.046

Kovacs, A.J., Buchanan, J.J., and Shea, C.H. (2010). Impossible is nothing: 5:3 and 4:3 multi-frequency bimanual coordination. Exp. Brain Res. 201, 249-259.doi: 10.1007/s00221-009-2031-y

Kovacs, A.J., Han, D.W., and Shea, C.H. (2009b). Representation of movement sequences is related to task characteristics. Acta Psychol. (Amst.) 132, 54-61.doi: 10.1016/j.actpsy.2009.06.007

Kovacs, A.J., Wang, Y., and Kennedy, D.M. (2020). Accessing interpersonal and intrapersonal coordination dynamics. Exp. Brain Res. 238, 17-27.doi: 10.1007/s00221-019-05676-y

Lee, T.D., Swinnen, S.P., and Verschueren, S. (1995). Relative Phase Alterations During Bimanual Skill Acquisition. J Mot Behav 27, 263-274.doi: 10.1080/00222895.1995.9941716

Schoner, G., and Kelso, J.A. (1988). Dynamic pattern generation in behavioral and neural systems. Science 239, 1513-1520.doi: 10.1126/science.3281253

Shea, C.H., Buchanan, J.J., and Kennedy, D.M. (2016). Perception and action influences on discrete and reciprocal bimanual coordination. Psychon Bull Rev 23, 361-386.doi: 10.3758/s13423-015-0915-3

Swinnen, S.P., Van Langendonk, L., Verschueren, S., Peeters, G., Dom, R., and De Weerdt, W. (1997). Interlimb coordination deficits in patients with Parkinson's disease during the production of two-joint oscillations in the sagittal plane. Mov. Disord. 12, 958-968.doi: 10.1002/mds.870120619

Zanone, P.G., and Kelso, J.A. (1992). Evolution of behavioral attractors with learning: non-equilibrium phase transitions. J. Exp. Psychol. Hum. Percept. Perform. 18, 403-421.doi: 10.1037//0096-1523.18.2.403

Acute gravitational dose-response curves in hemodynamic and ocular variables induced by tilt

Richard S. Whittle[1]*, Nathan Keller[2], Lindsay M. Stapleton[1], Eric A. Hall[3], Bonnie J. Dunbar[1], Ana Diaz-Artiles[1,2]

[1]*Department of Aerospace Engineering, Texas A&M University, College Station, TX, USA*
[2]*Department of Health and Kinesiology, Texas A&M University, College Station, TX, USA*
[3]*Department of Biomedical Engineering, Texas A&M University, College Station, TX, USA*
**rswhittle@tamu.edu*

INTRODUCTION

Exposure to microgravity causes the removal of hydrostatic pressure gradients and a permanent cephalad fluid shift, leading to a redistribution of blood. This has been potentially linked to a collection of neuro-ocular and functional changes developed in some astronauts, collectively known as Spaceflight Associated Neuro-Ocular Syndrome (SANS) (Marshall-Goebel *et al.*, 2017). Chronic fluid redistribution affecting intravascular, interstitial, and cerebrospinal fluids and pressures is widely hypothesized to be a contributing factor to SANS; however, the exact mechanisms are currently unknown. Additionally, recently demonstrated stagnant and retrograde blood flow and venous thrombosis in the left internal jugular vein during spaceflight could also be associated with sustained headward blood and tissue fluid shift (Marshall-Goebel *et al.*, 2019).

The objective of this ground-based research effort is to generate acute gravitational dose-response curves of cardiovascular (CV) and ocular variables due to changes in the gravitational vector induced by tilt. These dose-response curves inform us of the specific physiological response to a particular gravity level (or "dose"), leading to a greater understanding of hemodynamics and fluid shifts in both the eye and systemic circulation, deepening understanding of the etiology of SANS.

MATERIAL AND METHODS

Eight male subjects (from a total of 12 subjects to be included in the study) were rotated from 45° head up tilt (HUT) to 45° head down tilt (HDT) in 15° increments. Subjects were tested in both prone and supine postures on two different days, in a counterbalanced design. After a 5-min rest period in each position, a range of cardiovascular and ocular variables were collected including: CV hemodynamics (Finapres NOVA, Finapres Medical Systems), cardiac output (Innocor, Cosmed), heart rate variability and other various autonomic indices (Finapres NOVA), intraocular pressure (IOP, iCare), internal jugular vein (IJV) and common carotid artery cross-sectional areas (Vscan Extend Ultrasound, GE Healthcare), and IJV pressure (VeinPress, VeinPress GmbH).

RESULTS

Preliminary results from eight subjects show cardiac output increasing from 4.2±0.3 l/min to 6.2±0.3 l/min, from 45° HUT to 45° HDT, mostly due to an increase in stroke volume from 49.2±3.3 ml/beat to 91.0±5.8 ml/beat, blunted by a decrease in heart rate from 85.4±2.6 bpm to 70.0±2.8 bpm (Figure 1). Cardiac output in prone position (e.g., 4.9±0.3 l/min at 0°) was lower than in supine position (5.6±0.4 l/min at 0°). With tilt, there was a marked increase in IJV pressure (11.7±1.5 mmHg in 45° HUT to 57.9±2.6 mmHg in

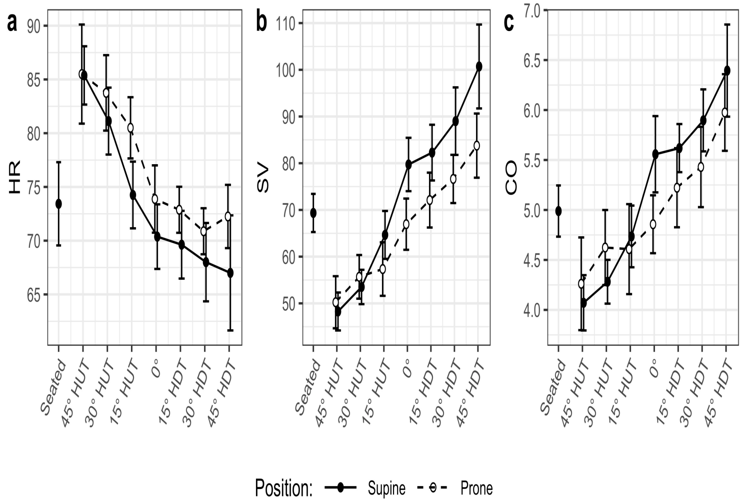

FIGURE 1: (**a**) Heart rate, (**b**) stroke volume, and (**c**) cardiac output of eight subjects tilted from 45° head up tilt (HUT) to 45° head down tilt (HDT). Solid line: supine (face up); dashed line: prone (face down). Data presented as mean and standard error.

45° HDT) (Figure 2). Heart rate variability also increased in multiple metrics with increasing HDT (Figure 3).

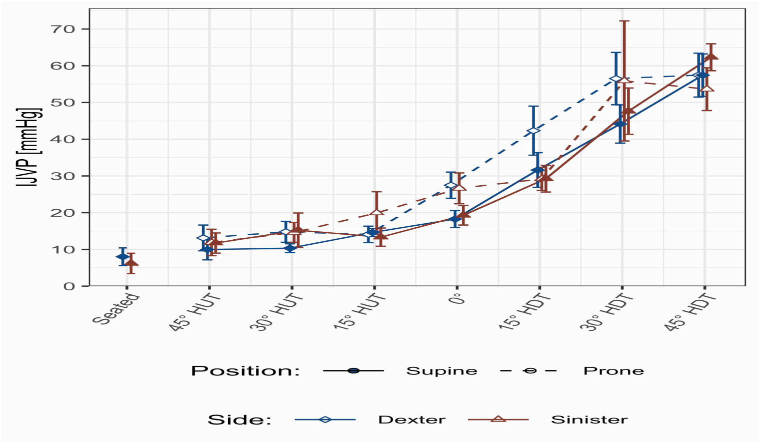

FIGURE 2: Internal jugular vein pressure (IJVP) of eight subjects tilted from 45° head up tilt (HUT) to 45° head down tilt (HUT). Solid line: supine (face up); dashed line: prone (face down); blue: dexter (right) side; red: sinister (left) side. Data presented as mean and standard error.

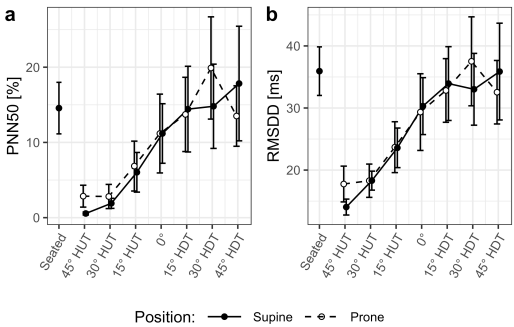

FIGURE 3: Heart rate variability of eight subjects tilted from 45° head up tilt (HUT) to 45° head down tilt (HDT). (**a**) PNN(50) represents the percentage of NN intervals that change by more than 50 ms between successive beats. (**b**) RMSDD is the root mean square of direct differences between successive NN intervals. Solid line: supine (face up); dashed line: prone (face down). Data presented as mean and standard error.

DISCUSSION

Increasing head down tilt alters the effective gravitational vector in the head to foot direction (Diaz-Artiles *et al.*, 2019b). –6° HDT is often used as an analog for microgravity. The increase in cardiac output, together with increased stroke volume and reduced heart rate with increasing HDT agrees with both experimental studies and computational models of reduced gravity simulations (Diaz Artiles *et al.*, 2016; Whittle *et al.*, 2021) due to stimulation of the baroreceptors and enhanced venous return increasing preload. The finding that prone positioning reduces cardiac function has also been previously documented (Dharmavaram *et al.*, 2006) and is a result of reduced venous return and ventricular compliance compared with the supine position.

The cephalad fluid shift induced by HDT results in increasing IJV pressure. These findings match those found by multiple studies including Marshall-Goebel *et al.* (2017) up to –18° HDT and continue to increase all the way up to –45° HDT. We do not see any significant difference between left- and right-side pressures. However, it was noted that some subjects presented a clear asymmetry between their left and right IJV pressures (i.e., one side being significantly higher than the other side). Further investigation is required to examine the relationship between venous dominance, IJVP, and other measures of cephalad fluid shift (e.g., IJV cross-sectional area, IOP) in relation to outflow through different sides of the venous drainage pathways.

Finally, the two metrics of heart rate variability considered give some insight into the function of the autonomic nervous system during tilt. Both RMSDD (the root mean square of the direct differences in NN interval) and PNN(50) (the percentage of NN intervals that change by more than 50 ms between successive beats) are closely correlated with parasympathetic nervous system activity (Shaffer *et al.*, 2017). Hence, an increase matches the finding of a reduction in heart rate.

CONCLUSION

The results of this study generate dose-response curves across a range of gravitational conditions in a number of different CV and ocular variables. Consideration of these curves leads to a greater understanding of the gravitational thresholds for different physiological parameters, e.g., where do the parameters depart from clinically permissible ranges. This is the first experiment of a larger study that will also consider the effect of countermeasures focused on producing hydrostatic gradients or reducing the microgravity-induced fluid shift, such as lower body negative pressure (LBNP) or centrifugation (Diaz *et al.*, 2015a; Diaz *et al.*, 2015b; Diaz Artiles *et al.*, 2018). Thus, in future experiments, we plan to test the same 12 subjects in a range of LBNP and artificial gravity conditions on the Texas A&M Aerospace Engineering Centrifuge. We are simultaneously developing a numerical framework to predict these CV and ocular responses to altered-gravity environments (Diaz-Artiles *et al.*, 2019a; Whittle *et al.*, 2020). Results from this investigation will inform current and future countermeasure development and in-flight prescriptions.

ACKNOWLEDGMENTS

This work is supported by the NASA Human Research Program (HRP), Grant 80NSSC20K1521.

Keywords: Dose response, Tilt, Hemodynamics, Ocular, SANS

REFERENCES

Dharmavaram, S., Jellish, W.S., Nockels, R.P., Mehmood, R., Ghanayem, A., Kleinman, B., Jacobs, W. (2006). Effect of prone positioning systems on hemodynamic and cardiac function during lumbar spine surgery: an echocardiographic study. Spine 31, 1388-1393.

Diaz, A., Heldt, T., Young, L.R.(2015a). Cardiovascular responses under artificial gravity combined with exercise. 2015 IEEE Aerosp Conf. doi: 10.1109/AERO.2015.7118969

Diaz, A., Trigg, C., Young, L.R. (2015b). Combining ergometer exercise and artificial gravity in a compact-radius centrifuge. Acta Astronautica 113, 80-88.

Diaz Artiles, A., Heldt, T., Young, L.R. (2016). Effects of artificial gravity on the cardiovascular system: computational approach. Acta Astronautica 126, 395-410.

Diaz Artiles, A., Heldt, T., Young, L.R. (2018). Short-term cardiovascular response to short-radius centrifugation with and without ergometer exercise. Front Physiol. 9, 1492.

Diaz-Artiles, A., Heldt, T., Young, L.R. (2019a). Computational model of cardiovascular response to centrifugation and lower body cycling exercise. J Appl Physiol 127, 1453-1468.

Diaz-Artiles, A., Navarro Tichel, P., Perez, F. (2019b). Cardiopulmonary Responses to Sub-Maximal Ergometer Exercise in a Hypo-Gravity Analog Using Head-Down Tilt & Head-Up Tilt. Front Physiol 10, 720.

Marshall-Goebel, K., Mulder, E., Bershad, E., Laing, C., Eklund, C., Malm, J., Stern, C., Rittweger, J. (2017). Intracranial and intraocular pressure during various degrees of head-down tilt. Aerosp Med Hum Perform 88, 10-16.

Marshall-Goebel, K., Laurie, S.S., Alferova, I.V., Arbeille, P., Auñon-Chancellor, S.M., Elbert, D.J., Lee, S.M.C., Macias, B.R., Martin, D.S., Pattarini, J.M., Ploutz-Snyder, R., Ribeiro, L.C., Tarver, W.J., Dulchavsky, S.A., Hargens, A.R., Stenger, M.B. (2019). Assessment of jugular venous blood flow stasis and thrombosis during spaceflight. JAMA Netw Open 2, e1915011.

Shaffer, F., Ginsberg, J.P. (2017). An overview of heart rate variability metrics and norms. Front Public Health 5, 258.

Whittle, R.S., Diaz-Artiles, A. (2020). Metabolic modeling in altered gravity. 2020 IEEE Aerosp Conf. doi: 10.1109/AERO47225.2020.9172582

Whittle, R.S., and Diaz-Artiles, A. (2021). Modeling individual differences in cardiovascular response to gravitational stress using a sensitivity analysis. J Appl Physiol 130, 1983-2001.

Effect of centrifuge generated altered-gravity on bimanual coordination

Renee Woodruff[1]*, Madison M. Davis[2], Yiyu Wang[2], Traver Wright[2], Bonnie J. Dunbar[1], Deanna Kennedy[2], Ana Diaz-Artiles[1,2]

[1]Department of Aerospace Engineering, Texas A&M University, College Station, US
[2]Department of Health and Kinesiology, Texas A&M University, College Station, US
renee.woodruff@tamu.edu

INTRODUCTION

Space exploration missions subject astronauts to extreme environments that can adversely affect physiological function. Consequently, this can jeopardize performance and mission operations (Buckey, 2006). Although we make continuous progress understanding how human physiology is affected by various stimuli, we still do not know the range of gravity levels that maintain nominal physiological function. By investigating and determining the relationship between gravity level (i.e., gravity dose) and physiological response, we can then predict physiological responses at Martian and Lunar gravity and define what range of gravity levels elicits an "Earth-like response" (Galvan-Garza, 2018). Sensorimotor function in altered gravity has been somewhat explored, and findings have shown performance decrements in manual control tasks accompanied by adaptation in hyper-gravity environments (Rosenburg et al, 2018; Clark et al, 2015). However, these investigations primarily focused on unimanual control tasks, and there are many space mission relevant tasks (e.g., rover teleoperation or landing a spacecraft) that require the use and coordination of two limbs while in an altered gravity environment or during periods of rapid gravity level transitions. Thus, to address this gap, this research will specifically investigate the effect of altered gravity on bimanual coordination.

AIMS AND OBJECTIVES

The four main objectives of this research are to 1) generate gravity dose-response relationships between bimanual coordination operational variables as a function of gravity level in a centrifuge setting, 2) determine the G-thresholds that result in decrements in bimanual coordination performance, 3) investigate if bimanual coordination adaptation occurs after repeated exposure to altered gravity environments in a centrifuge setting, and 4) compare findings to results generated from other altered gravity analogs.

MATERIAL AND METHODS

Performance during two different bimanual control tasks will be compared across six simulated gravity levels. Altered gravity levels of 0, 0.25, 0.50, 0.75, 1, and 1.8 G will be delivered via a short-arm centrifuge located on the Texas A&M University campus (see Figure 1). Subjects will lay supine, feet facing radially outward, and rotated at an angular velocity that results in the desired gravity level at the subject's center of gravity in the head-to-toe direction. During

FIGURE 1: Short Radius Centrifuge, located on the Texas A&M University Campus at the Human Clinical Research Facility. Subjects will perform a bimanual movement or force coordination task at 0, 0.25, 0.5, 0.75, 1, and 1.8 G.

the experiment, subjects will perform either a bimanual force coordination task or bimanual movement coordination task (see Figure 2).

For the force task, participants must coordinate forces produced with their triceps muscles for in-phase (1:1) and multi-frequency (1:2) bimanual force patterns. Subjects, with their upper arms parallel to the ground and elbows at 90° angles, will rest their forearms on force transducers. A Lissajous plot template and a black cursor, controlled by the triceps forces produced, will be displayed on a screen for the subject. The subject must trace the template with the cursor by producing and coordinating forces between their right and left arms (i.e., the cursor moves bottom to top as force is produced with the left arm whereas the cursor moves left to right as force is produced with the right arm). The movement coordination task will require subjects to

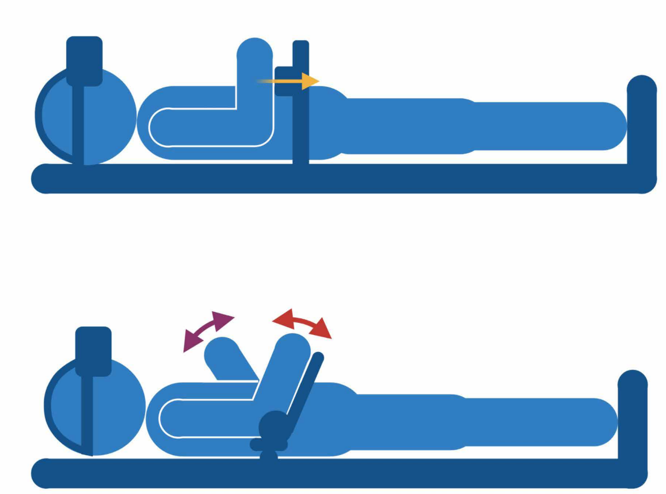

FIGURE 2: Bimanual coordination tasks setup on the short radius centrifuge. For both tasks, subjects will lay supine with their feet pointing out radially. Top: Force task configuration with the subject's forearms resting on force transducers. Subjects must produce an isometric force with their triceps and coordinate these forces to follow the Lissajous template provided on the headset display. Bottom: Movement task configuration with the subject's forearms positioned on rotating levers. The subject must coordinate their arm movements to follow the guide template provided on the headset display.

coordinate their right and left limb movements in a pattern that continuously changes from 0 ° to 180 °. Subjects will lay in the supine position with their forearms on custom levers and elbows limited to flexion-extension in the vertical plane. In a similar method as the force task, participants will be asked to trace a template on a screen by controlling a cursor's horizontal movement with one arm and vertical movement with the other arm. Potentiometers at the pivot point of the levers will monitor the movement of the subject's arms. For both the force and movement coordination tasks, wireless EMG sensors will be placed on the subject's triceps muscles to monitor muscle activation patterns. Subjects will complete the force coordination task in the 1:1 and 1:2 patterns and the movement coordination task for all 6 gravity levels. Dependent variables investigated include interpeak interval ratio, standard deviation of interpeak interval, harmonicity, peak force, peak force bias, mean force, phase angle slope ratio, EMG-EMG coherence, phase angle velocity, absolute error, constant error, and error variability.

DISCUSSION AND CONCLUSION

Determining a gravity dose-response relationship and the G-thresholds at which bimanual coordination is adversely affected will allow us to predict how physiological function is affected in relevant altered gravity conditions such as at lunar or Martian gravity levels. Moreover, while previous studies have indicated that sensorimotor function performance can adapt to new gravity levels within a few minutes (Clark et al, 2015), this was only investigated in hyper-gravity and not in hypo-gravity environments. Determining the presence or absence of adaptation to partial gravity levels will further expand our understanding of physiology and coordination dynamics for the context of human spaceflight. With this knowledge, we can make more informed decisions when developing astronaut training to better prepare them for future missions.

This research is part of a larger effort to investigate bimanual coordination in altered gravity environments. Current testing is using a tilt-table analog to simulate gravity levels ranging from 0 to 1 G (Kennedy, 2021; Davis, 2021; Wang, 2021). These research efforts will culminate in a set of experiments conducted during parabolic flight simulating 0, 0.25, 0.50, and 0.75 G (Diaz-Artiles, 2021). Gravity-dose response curves will be generated for each of the three analogs (tilt-table, centrifuge, parabolic flight) and then compared to each other to inform recommendations on the relationship between dose-response curves and the chosen altered gravity analogs. These results will provide further insight into the relationship between each analog and its associated dose-response curve. Additionally, this research as a whole will further develop our understanding of human neurophysiology in altered gravity environments.

ACKNOWLEDGMENTS

Work Supported by NASA 80NSSC20K1499

Keywords: bimanual coordination, altered-gravity, centrifuge, coordination dynamics

REFERENCES

Buckey, J.C. (2006). Space Physiology. Oxford University Press.

Galvan-Garza, R.C., Clark T.K., Sherwood D., Diaz-Artiles A., Rosenberg M.J., Natapoff A., Karmali F., Oman C.M., Young L.R. (2018). Human Perception of Whole-Body Roll Tilt Orientation in a Hypo-Gravity Analog: Underestimation and Adaptation. J. Neurophysiol. 120:6, 3110-3121. doi: 10.1152/jn.00140.2018.

Rosenberg, M.J., Galvan-Garza, R.C., Clark, T.K., Sherwood, D.P., Young, L.R., Karmali, F. (2018). Human manual control precision depends on vestibular sensory precision and gravitational magnitude J. Neurophysiol. 120:6. doi: 10.1152/jn.00565.2018

Clark, T.K., Newman, M.C., Merfeld, D.M., Oman, C.M., Young, L.R. (2015). Human manual control performance in hyper-gravity. Exp. Brain Res. 233, 1409-1420.

Kennedy D.M., Davis M.M., Woodruff R., Wang Y., Wright, T., Dunbar B.J., Diaz-Artiles A. (2021). The influence of Altered-Gravity on Bimanual Force Coordination (extended abstract). ISGP.

Davis M.M., Wang Y., Woodruff R., Wright, T., Dunbar B.J., Diaz-Artiles A., Kennedy D.M. (2021). The influence of perceptual constraints on bimanual force coordination in microgravity (extended abstract). ISGP.

Wang Y., Davis M.M., Woodruff R., Wright, T., Dunbar B.J., Diaz-Artiles A., Kennedy D.M. (2021). Integrated Feedback Displays to Facilitate Bimanual Coordination in Simulated Gravity (extended abstract). ISGP.

Diaz-Artiles A., Woodruff R., Davis M.M., Wang Y., Dunbar B.J., Kennedy D.M. (2021). Bimanual Coordination in Altered Gravity during Parabolic Flight (abstract and short presentation). NASA Human Research Program Investigators' Workshop.

Advantages of publishing in Frontiers

OPEN ACCESS
Articles are free to read for greatest visibility and readership

FAST PUBLICATION
Around 90 days from submission to decision

HIGH QUALITY PEER-REVIEW
Rigorous, collaborative, and constructive peer-review

TRANSPARENT PEER-REVIEW
Editors and reviewers acknowledged by name on published articles

Frontiers
Avenue du Tribunal-Fédéral 34
1005 Lausanne | Switzerland

Visit us: www.frontiersin.org
Contact us: info@frontiersin.org | +41 21 510 17 00

REPRODUCIBILITY OF RESEARCH
Support open data and methods to enhance research reproducibility

DIGITAL PUBLISHING
Articles designed for optimal readership across devices

FOLLOW US
@frontiersin

IMPACT METRICS
Advanced article metrics track visibility across digital media

EXTENSIVE PROMOTION
Marketing and promotion of impactful research

LOOP RESEARCH NETWORK
Our network increases your article's readership